



National Library  
of Canada

Bibliothèque nationale  
du Canada

Canadian Theses Service

Services des thèses canadiennes

Ottawa, Canada  
K1A 0N4

## CANADIAN THESES

## THÈSES CANADIENNES

### NOTICE

The quality of this microfiche is heavily dependent upon the quality of the original thesis submitted for microfilming. Every effort has been made to ensure the highest quality of reproduction possible.

If pages are missing, contact the university which granted the degree.

Some pages may have indistinct print especially if the original pages were typed with a poor typewriter ribbon or if the university sent us an inferior photocopy.

Previously copyrighted materials (journal articles, published tests, etc.) are not filmed.

Reproduction in full or in part of this film is governed by the Canadian Copyright Act, R.S.C. 1970, c. C-30.

**THIS DISSERTATION  
HAS BEEN MICROFILMED  
EXACTLY AS RECEIVED**

### AVIS

La qualité de cette microfiche dépend grandement de la qualité de la thèse soumise au microfilmage. Nous avons tout fait pour assurer une qualité supérieure de reproduction.

S'il manque des pages, veuillez communiquer avec l'université qui a conféré le grade.

La qualité d'impression de certaines pages peut laisser à désirer, surtout si les pages originales ont été dactylographiées à l'aide d'un ruban usé ou si l'université nous a fait parvenir une photocopie de qualité inférieure.

Les documents qui font déjà l'objet d'un droit d'auteur (articles de revue, examens publiés, etc.) ne sont pas microfilmés.

La reproduction, même partielle, de ce microfilm est soumise à la Loi canadienne sur le droit d'auteur, SRC 1970, c. C-30.

**LA THÈSE A ÉTÉ  
MICROFILMÉE TELLE QUE  
NOUS L'AVONS REÇUE**

SOLUBILITY OF GASES IN LIQUIDS

BY

HARUKI ASATANI

Thesis Submitted to the School of Graduate Studies  
as Partial Fulfillment of the Requirements for the  
Degree of Ph.D. in Chemical Engineering

UNIVERSITY OF OTTAWA

OTTAWA, CANADA, 1986

© Haruki Asatani, Ottawa, Canada, 1986.

Permission has been granted to the National Library of Canada to microfilm this thesis and to lend or sell copies of the film.

The author (copyright owner) has reserved other publication rights, and neither the thesis nor extensive extracts from it may be printed or otherwise reproduced without his/her written permission.

L'autorisation a été accordée à la Bibliothèque nationale du Canada de microfilmer cette thèse et de prêter ou de vendre des exemplaires du film.

L'auteur (titulaire du droit d'auteur) se réserve les autres droits de publication; ni la thèse ni de longs extraits de celle-ci ne doivent être imprimés ou autrement reproduits sans son autorisation écrite.

ISBN 0-315-36464-5



UNIVERSITÉ D'OTTAWA  
UNIVERSITY OF OTTAWA

ABSTRACT

Solubilities of propene, isobutene, n-butane and isobutane were measured at atmospheric pressure in the solvents n-octane, chlorobenzene and n-butanol. The experiments were conducted at temperatures of 298.15 K, 323.15 K and 343.15 K. The apparatus used for the measurements at atmospheric pressure was similar in type to that used by a number of researchers at the University of Ottawa but was modified for the gases of high solubility that were to be investigated.

A method of interpolating and extrapolating gas solubilities that are available at atmospheric pressure to other temperatures is presented. Two-parameter equations are used to describe the solubility behavior in systems composed of non-polar or slightly polar solvents and various solute gases, including hydrogen and helium gases.

Solubilities of highly soluble gases, measured at atmospheric pressure in a number of polar and associating solvents including n-butanol were used to illustrate a means of correlating solubility data using hydrogen-bonding factors. This method, based on a limited amount of solubility data in polar and associating solvents, is expected to be useful for the prediction of solubilities of other highly soluble gases in similar polar and associating solvents.

Solubilities of propane and isobutene were measured in the solvents n-octane, chlorobenzene and n-butanol at elevated pressures up to 1.93 MPa utilizing a volumetric

solubility apparatus developed in this investigation. The experiments were conducted at temperatures of 298.15 K, 323.15 K and 343.15 K. For the determination of the gas solubilities at elevated pressures, a knowledge of the densities of the gas-saturated solutions was required. Therefore the densities of the gas-saturated solutions were measured under pressure for the same gas-solvent systems. The apparatus used for the solution density measurements involved the use of a new equilibration technique and the use of an Anton Paar density meter for high pressures. A knowledge of the solution densities permitted the accurate determination of solubilities at elevated pressures.

In order to check the consistency of the solubility measurements at elevated pressures, gas chromatographic analyses of the gas-saturated solutions were performed. The resulting good agreement between the results obtained by the volumetric measurement and those obtained by the gas chromatographic analysis indicated that the solubility measurements were consistent. As a result it was considered that the solubility apparatus developed in this investigation was suitable for investigating the solubility behaviour of gases at elevated pressures.

Finally, solubilities obtained at elevated pressures were compared with those predicted by utilizing the SRK equation of state and the UNIFAC method. Good agreement between the experimental and predicted solubilities was obtained for the systems involving n-octane as the solvent,

but large deviations between the experimental and predicted solubilities were observed for the systems containing n-butanol as the solvent.

ACKNOWLEDGEMENTS

The author wishes to express his gratitude to Dr. Walter Hayduk, Professor of Chemical Engineering, for his kind encouragement and invaluable guidance throughout the course of this investigation.

The author is also grateful to Professor Benjamin C.-Y. Lu, Dr. Kazumari Ohgaki and Dr. Yoshinori Adachi for their kind advice and helpful discussion.

The author also wishes to thank Dr. Masahiro Yorizane, Emeritus Professor at Hiroshima University, Professor Shoshin Yoshimura, Professor Hirokatsu Masuoka, and Dr. Yoshimori Miyano for their kind encouragement to study abroad.

The author is also indebted to Dr. Akira Kudo, Dr. Kei Miyamoto and other members of Japanese Researcher's Association of Ottawa for their personal encouragement and meaningful discussion concerning science and engineering.

Special thanks are due to Mr. J. Gasperetti and his staff for their technical aid in constructing the equipment used in this investigation.

For financial aid the author wishes to thank the Rotary Foundation of Rotary International, the Department of Chemical Engineering, Professor W. Hayduk and the Graduate School of the University of Ottawa.

Gratitude is also extended to Mr. R. Huish for proof reading the manuscript and to Miss Andrée Mainville and Francine Pétrin for their skillful typing.

v

TABLE OF CONTENTS

	<u>Page</u>
ABSTRACT .....	i
ACKNOWLEDGEMENTS .....	iv
NOMENCLATURE .....	xx
LIST OF SYMBOLS .....	xx
GREEK LETTERS .....	xxii
SUPERSCRIPTS .....	xxiii
SUBSCRIPTS .....	xxiii
CHAPTER I INTRODUCTION .....	1
CHAPTER II LITERATURE SURVEY .....	5
2.1 Experimental Techniques .....	7
2.1.1 Classification of Methods for Experimental Determination of Gas solubility .....	7
2.1.2 Solvent Degassing Techniques .....	9
2.1.3 Equilibration Techniques for Gas-Liquid Systems .....	11
2.2 Prediction and Correlation of Gas Solubility in Liquids .....	15
CHAPTER III DEVELOPMENT OF A GAS SOLUBILITY CORRELATION .....	22
CHAPTER IV PROPERTIES OF MATERIALS .....	38

CHAPTER V	EXPERIMENTAL EQUIPMENT	
	AND PROCÉDURES.....	45
5.1	Apparatus and Operating Procedure for Density Measurements of Pure Solvents at Atmospheric Pressure.....	46
5.2	Apparatus and Operating Procedure for Measurement of Gas Solubility at Atmospheric Pressure.....	48
5.3	Treatment of Data for Gas Solubility at Atmospheric Pressure.....	55
5.4	Apparatus and Operating Procedure for the Determination of Gas-Saturated Solution Density.....	57
5.5	Calibration of the High Pressure Density Meter.....	62
5.6	Apparatus and Operating Procedure for Measurement of Gas Solubility at Elevated Pressures.....	68
5.7	Treatment of Data for Gas Solubility at Elevated Pressures.....	76
5.8	Apparatus and Operating Procedure for Gas Chromatographic Analysis of Gas-Saturated Solutions.....	79

	<u>Page</u>
CHAPTER VI RESULTS AND DISCUSSION .....	86
6.1 Solvent Density and Gas Solubility	
Measurements at Atmospheric Pressure .....	87
6.2 Density of Gas-Saturated Solutions	
at Elevated Pressures .....	116
6.2.1 Prediction of Density of	
Gas-saturated Solutions at	
Elevated Pressures .....	116
6.2.2 Measured Densities of Gas-Saturated	
Solutions at Elevated Pressures .....	134
6.3 Gas Solubility at Elevated Pressures .....	150
6.3.1 Gas Solubility Prediction by the	
UNIFAC Method .....	151
6.3.2 Solubility Results at Elevated	
Pressures .....	161
6.4 Results of Solubility Measurements	
Based on Gas Chromatographic	
Analysis of Gas-Saturated Solutions .....	182
6.5 Development of a Correlation for	
Interpolation or Extrapolation of	
Gas Solubilities at Atmospheric	
Pressure .....	185
CHAPTER VII CONCLUSIONS .....	191
REFERENCES .....	196

	<u>Page</u>
APPENDIX A Diagrams for the Correlated Solu- bilities Measured at Atmospheric Pressure .....	206
APPENDIX B Sample Calculation for the Determination of Gas Solubility Measured at Atmospheric Pressure .....	216
APPENDIX C Densities of Gas-Saturated Solutions as a Function of Pressure .....	219
APPENDIX D Experimental and Predicted Densities of Gas-Saturated Solutions .....	232
APPENDIX E Sample Calculation for the determi- nation of Gas Solubility on the Basis of Gas Chromatographic Analysis of Gas-Saturated Solutions .....	250
APPENDIX F Estimated Precision for the Measurements Conducted in this Investigation .....	253

LIST OF TABLES

<u>Table</u>	<u>Page</u>
3-1 Source of gas solubility data used for the correlation .....	23
3-2 Summary of correlation results for gas solubilities in various solvents.....	28
4-1 Physical properties of the solvents used in this investigation.....	39
4-2 Physical properties of solute gases used in this investigation.....	39
4-3 Constants of Equation (4-1) to calculate second virial coefficients.....	41
4-4 Constants required for the saturated vapor pressure calculation.....	43
4-5 Densities at reference temperature used in Gunn and Yamada equation.....	44
5-1 Densities of water at temperatures of 298.15 K, 323.15 K and 343.15 K at elevated pressures.....	66
5-2 Comparison of molar volumes of nitrogen available in Din's table with those calculated by Pitzer-Curl method.....	67
5-3 Calibration constants for high pressure density meter and the second virial coefficients for nitrogen.....	67
6-1 Densities of n-octane, chlorobenzene and n-butanol at atmospheric pressure.....	88
6-2 Densities of n-octane at atmospheric pressure by Chappelow, Winnick et al.....	88
6-3 Solubilities of Propene measured at atmospheric pressure in the solvents, n-octane, chlorobenzene and n-butanol.....	91
6-4 Solubilities of Isobutene measured at atmospheric pressure in the solvents, n-octane, chlorobenzene and n-butanol.....	91

<u>Table</u>	<u>Page</u>
6-5 Solubilities of n-Butane measured at atmospheric pressure in the solvents, n-octane, chlorobenzene and n-butanol.....	92
6-6 Solubilities of Isobutane measured at atmospheric pressure in the solvents, n-octane, chlorobenzene and n-butanol.....	92
6-7 Gas solubilities for a gas partial pressure of 101.325 kPa.....	94
6-8 A comparison of gas solubilities measured in this work with those reported for a gas partial pressure of 101.325 kPa.....	96
6-9 Hydrogen-bonding factors in polar and associating solvents at 298.15 K.....	108
6-10 Values for $Q_{ai}$ and $Q_{bi}$ of the SRK equation of state for solutes and solvents.....	123
6-11 Values of $k_{12}$ for solvent-solute systems when the SRK equation of state is utilized.....	126
6-12 Solution densities predicted by the SRK equation of state for the (1)n-octane-(2)propene system at elevated pressures.....	128
6-13 Solution densities predicted by the SRK equation of state for the (1)chlorobenzene-(2)propene system at elevated pressures.....	129
6-14 Solution densities predicted by the SRK equation of state for the (1)n-butanol-(2)propene system at elevated pressures.....	130
6-15 Solution densities predicted by the SRK equation of state for the (1)n-octane-(2)isobutene system at elevated pressures.....	131
6-16 Solution densities predicted by the SRK equation of state for the (1)chlorobenzene-(2)isobutene system at elevated pressures.....	132
6-17 Solution densities predicted by the SRK equation of state for the (1)n-butanol-(2)isobutene system at elevated pressure.....	133
6-18 Solution densities measured at elevated pressures for the (1)n-octane-(2)propene system.....	135

<u>Table</u>	<u>Page</u>
6-19 Solution densities measured at elevated pressures for the (1)chlorobenzene-(2)propene system.....	135
6-20 Solution densities measured at elevated pressures for the (1)n-butanol-(2)propene system.....	136
6-21 Solution densities measured at elevated pressures for the (1)n-octane-(2)isobutene system.....	136
6-22 Solution densities measured at elevated pressures for the (1)chlorobenzene-(2)isobutene system.....	137
6-23 Solution densities measured at elevated pressures for the (1)n-butanol-(2)isobutene system.....	137
6-24 Results of vapor-liquid equilibrium calculation utilizing the UNIFAC method for the (1)n-octane- (2)propene system.....	159
6-25 Results of vapor-liquid equilibrium calculation utilizing the UNIFAC method for the (1)n-butanol- (2)propene system.....	159
6-26 Results of vapor-liquid equilibrium calculation utilizing the UNIFAC method for the (1)n-octane- (2)isobutene system.....	160
6-27 Results of vapor-liquid equilibrium calculation utilizing the UNIFAC method for the (1)n-butanol- (2)isobutene system.....	160
6-28 Solubilities of propene in n-octane at elevated pressures.....	165
6-29 Solubilities of propene in chlorobenzene at elevated pressures.....	165
6-30 Solubilities of propene in n-butanol at elevated pressures.....	166
6-31 Solubilities of isobutene in n-octane at elevated pressures.....	166
6-32 Solubilities of isobutene in chlorobenzene at elevated pressures.....	167
6-33 Solubilities of isobutene in n-butanol at elevated pressures.....	167

<u>Table</u>	<u>Page</u>
6-34 Comparison of gas solubilities obtained by the volumetric measurements with those obtained by the gas chromatographic analysis for the (1)n-octane-(2)propene system.....	184
6-35 Comparison of gas solubilities obtained by the volumetric measurements with those obtained by the gas chromatographic analysis for the (1)n-octane-(2)isobutene system.....	184

LIST OF FIGURES

<u>Figure</u>	<u>Page</u>
3-1	Partial molar entropy change of the solute for n-hexadecane as a function of the logarithm of absolute temperature..... 26
3-2	Flow chart for the calculation to determine $x_{Cl}^{exp}$ ..... 29
3-3	Correlated gas solubilities in n-heptane ..... 33
5-1	Degassing apparatus used for the solubility measurements at atmospheric pressure ..... 50
5-2	Solubility apparatus for the measurements of gas solubilities at atmospheric pressure ..... 51
5-3	Equilibration cell used for the measurements of gas-saturated solution densities ..... 59
5-4	Schematic diagram of the apparatus used for the density measurements of gas-saturated solutions ..... 61
5-5	Schematic diagram of the volumetric apparatus used for the measurements of gas solubilities at elevated pressures ..... 73
5-6	Equilibration cell used for the measurements of gas solubilities at elevated pressures ..... 74
5-7	Schematic diagram of the apparatus used for the gas chromatographic analysis of gas-saturated solutions ..... 80
5-8	Calibration line used for the gas chromatographic analysis for propene-saturated n-octane solutions ..... 83
5-9	Calibration line used for the gas chromatographic analysis for isobutene-saturated n-octane solutions ..... 84
6-1	Densities of n-octane at atmospheric pressure as a function of the absolute temperature ..... 89
6-2	Gas solubilities in n-octane measured at atmospheric pressure ..... 98
6-3	Gas solubilities in chlorobenzene measured at atmospheric pressure ..... 99

<u>Figure</u>	<u>Page</u>
6-4 Gas solubilities in n-butanol measured at atmospheric pressure .....	100
6-5 Solubilities of propene in the solvents, n-octane, chlorobenzene and n-butanol .....	103
6-6 Solubilities of isobutene in the solvents, n-octane, chlorobenzene and n-butanol .....	104
6-7 Solubilities of n-butane in the solvents, n-octane, chlorobenzene and n-butanol .....	105
6-8 Solubilities of isobutane in the solvents, n-octane, chlorobenzene and n-butanol .....	106
6-9 Hydrogen-bonding factors at 298.15 K in methanol and ethylene glycol as a function of H-bonding factors in n-butanol .....	109
6-10 Gas solubilities and hydrogen-bonding factors at 298.15 K in methanol and n-butanol .....	111
6-11 Hydrogen-bonding factors at 298.15 K in ethanol as a function of H-bonding factors in n-butanol .....	113
6-12 Hydrogen-bonding factors at 298.15 K in methyl acetate and ethyl acetate as a function of H-bonding factors in n-butanol .....	114
6-13 Hydrogen-bonding factors at 298.15 K in acetonitrile as a function of H-bonding factors in n-butanol .....	115
6-14 Flow chart for the determination of $Q_{ai}$ and $Q_{bi}$ for solutes and solvents when the SRK equation of state is used .....	122
6-15 Flow chart for the determination of $k_{12}$ for specific solute-solvent systems when the SRK equation of state is utilized .....	125
6-16 Flow chart for the calculation of solution density and solution composition when the SRK equation of state is utilized .....	127
6-17 Densities of propene-saturated solutions under pressure .....	138
6-18 Densities of isobutene-saturated solution under pressure .....	139

<u>Figure</u>	<u>Page</u>
6-19	Experimental and predicted densities of propene-saturated n-octane solutions at 298.15 K as a function of pressure ..... 142
6-20	Experimental and predicted densities of propene-saturated n-octane solutions at 323.15 K as a function of pressure ..... 143
6-21	Experimental and predicted densities of propene-saturated n-octane solutions at 343.15 K as a function of pressure ..... 144
6-22	Experimental and predicted densities of propene-saturated chlorobenzene solutions at 323.15 K as a function of pressure ..... 145
6-23	Experimental and predicted densities of propene-saturated n-butanol solutions at 298.15 K as a function of pressure ..... 147
6-24	Experimental and predicted densities of propene-saturated n-butanol solutions at 323.15 K as a function of pressure ..... 148
6-25	Experimental and predicted densities of propene-saturated n-butanol solutions at 343.15 K as a function of pressure ..... 149
6-26	Flow chart for the vapor-liquid equilibrium calculation utilizing the UNIFAC method ..... 158
6-27	Volumes of propene used for the solubility measurements at 323.15 K and elevated pressures as a function of the volumes of n-octane supplied to the equilibrium cell ... 162
6-28	Volumes of propene saturated n-octane solutions at 323.15 K formed in the equilibration cell as a function of the volumes of n-octane supplied to the cell ..... 163
6-29	Experimental and predicted solubilities of propene in n-octane at elevated pressures ... 168
6-30	Experimental and predicted solubilities of propene in chlorobenzene at elevated pressures ..... 169
6-31	Experimental and predicted solubilities of propene in n-butanol at elevated pressures .. 170

<u>Figure</u>	<u>Page</u>
6-32	Experimental and predicted solubilities of isobutene in n-octane at elevated pressures ...171
6-33	Experimental and predicted solubilities of isobutene in chlorobenzene at elevated pressures .....172
6-34	Experimental and predicted solubilities of isobutene in n-butanol at elevated pressures .. 173
6-35	Experimental and predicted densities of propene-saturated n-octane solutions at 323.15 K as a function of mole fraction of propene in the solution ..... 177
6-36	Densities of propene-saturated n-octane solutions at 323.15 K as a function of volume fraction of propene in the solution ... 178
6-37	Densities of propene-saturated chlorobenzene solutions at 323.15 K as a function of volume fraction of propene in the solution ..... 180
6-38	Densities of propene-saturated n-butanol solutions at 323.15 K as a function of volume fraction of propene in the solution ..... 181
A-1	Correlated gas solubilities in carbon disulfide ..... 207
A-2	Correlated gas solubilities in carbon tetrachloride ..... 208
A-3	Correlated gas solubilities in benzene ..... 209
A-4	Correlated gas solubilities in toluene ..... 210
A-5	Correlated gas solubilities in cyclohexane ... 211
A-6	Correlated gas solubilities in n-octane ..... 212
A-7	Correlated gas solubilities in isooctane ..... 213
A-8	Correlated gas solubilities in n-hexadecane .. 214
A-9	Correlated gas solubilities in perfluoroheptane ..... 215
C-1	Experimental and predicted densities of propene-saturated chlorobenzene solutions at 298.15 K as a function of pressure ..... 221

<u>Figure</u>	<u>Page</u>
C-2	Experimental and predicted densities of propene-saturated chlorobenzene solutions at 343.15 K as a function of pressure..... 222
C-3	Experimental and predicted densities of isobutene-saturated n-octane solutions at 298.15 K as a function of pressure..... 223
C-4	Experimental and predicted densities of isobutene-saturated n-octane solutions at 323.15 K as a function of pressure..... 224
C-5	Experimental and predicted densities of isobutene-saturated chlorobenzene solutions at 343.15 K as a function of pressure..... 225
C-6	Experimental and predicted densities of isobutene-saturated chlorobenzene solutions at 298.15 K as a function of pressure..... 226
C-7	Experimental and predicted densities of isobutene-saturated chlorobenzene solutions at 323.15 K as a function of pressure..... 227
C-8	Experimental and predicted densities of isobutene-saturated chlorobenzene solutions at 343.15 K as a function of pressure..... 228
C-9	Experimental and predicted densities of isobutene-saturated n-butanol solutions at 298.15 K as a function of pressure..... 229
C-10	Experimental and predicted densities of isobutene-saturated n-butanol solutions at 323.15 K as a function of pressure..... 230
C-11	Experimental and predicted densities of isobutene-saturated n-butanol solutions at 343.15 K as a function of pressure..... 231
D-1	Experimental and predicted densities of propene-saturated n-octane solutions at 298.15 K as a function of mole fraction of propene in the solution..... 233
D-2	Experimental and predicted densities of propene-saturated n-octane solutions at 343.15 K as a function of mole fraction of propene in the solution..... 234

<u>Figure</u>		<u>Page</u>
D-3	Experimental and predicted densities of propene-saturated chlorobenzene solutions at 298.15 K as a function of mole fraction of propene in the solution.....	235
D-4	Experimental and predicted densities of propene-saturated chlorobenzene solutions at 323.15 K as a function of mole fraction of propene in the solution.....	236
D-5	Experimental and predicted densities of propene-saturated chlorobenzene solutions at 343.15 K as a function of mole fraction of propene in the solution.....	237
D-6	Experimental and predicted densities of propene-saturated n-butanol solutions at 298.15 K as a function of mole fraction of propene in the solution.....	238
D-7	Experimental and predicted densities of propene-saturated n-butanol solutions at 323.15 K as a function of mole fraction of propene in the solution.....	239
D-8	Experimental and predicted densities of propene-saturated n-butanol solutions at 343.15 K as a function of mole fraction of propene in the solution.....	240
D-9	Experimental and predicted densities of isobutene-saturated n-octane solutions at 298.15 K as a function of mole fraction of isobutene in the solution.....	241
D-10	Experimental and predicted densities of isobutene-saturated n-octane solutions at 323.15 K as a function of mole fraction of isobutene in the solution.....	242
D-11	Experimental and predicted densities of isobutene-saturated n-octane solutions at 343.15 K as a function of mole fraction of isobutene in the solution.....	243
D-12	Experimental and predicted densities of isobutene-saturated chlorobenzene solutions at 298.15 K as a function of mole fraction of isobutene in the solution.....	244

<u>Figure</u>		<u>Page</u>
D-13	Experimental and predicted densities of isobutene-saturated chlorobenzene solutions at 323.15 K as a function of mole fraction of isobutene in the solution.....	245
D-14	Experimental and predicted densities of isobutene-saturated chlorobenzene solutions at 343.15 K as a function of mole fraction of isobutene in the solution.....	246
D-15	Experimental and predicted densities of isobutene-saturated n-butanol solutions at 298.15 K as a function of mole fraction of isobutene in the solution.....	247
D-16	Experimental and predicted densities of isobutene-saturated n-butanol solutions at 323.15 K as a function of mole fraction of isobutene in the solution.....	248
D-17	Experimental and predicted densities of isobutene-saturated n-butanol solutions at 343.15 K as a function of mole fraction of isobutene in the solution.....	249

NOMENCLATURELIST OF SYMBOLS

<u>a, b, c, d</u>	universal constants in Equation (3-11) $a = 1.1480 \times 10^3$ $b = -6.7833 \times 10$ $c = 2.0006 \times 10^{-2}$ $d = -1.3813 \times 10^{-5}$
<u>a, b, a<sub>ii</sub>, b<sub>i</sub></u>	coefficients in Equations (6-1), (6-4), and (6-6)
<u>a<sub>ij</sub></u>	cross coefficient in Equation (6-3)
<u>A</u>	calibration constant in Equation (5-11)
<u>A<sub>1</sub>, A<sub>2</sub></u>	constants in Equation (3-4)
<u>A, B, C</u>	constants in Equation (4-8)
<u>B</u>	second virial coefficient in Equations (3-7) to (3-10), (4-1), (4-3), (4-4), and (6-25) to (6-28)
<u>B<sup>0</sup>, B<sup>1</sup></u>	constants defined by Equations (6-29) and (6-30)
<u>C<sub>1</sub>, C<sub>2</sub></u>	constants in Equation (3-2)
<u>e, f</u>	constants in Equation (4-3)
<u>g, h</u>	constants in Equation (4-1)
<u>k<sub>12</sub></u>	binary interaction parameter
<u>k<sub>1</sub>, k<sub>2</sub></u>	constants in Equation (5-9)
<u>K</u>	equilibrium constant
<u>l<sub>1</sub></u>	constant defined by Equation (6-15)
<u>m</u>	constant in Equation (4-7)

$m_i$	constant defined by Equation (6-5)
M	molecular weight
(MD)	molar density
P	pressure
q	molecular surface area
Q	periods of oscillation in Equations (5-1) and (5-2)
$Q_k$	parameter characteristic of functional group k
r	measure of molecular volume
R	gas constant
$R_k$	parameter characteristic of functional group k
$\Delta S_2$	partial molar entropy change of solute
(SP)	slope used in Equations (5-4) and (5-16)
T	absolute temperature
V	molar volume
$V_r^{(0)}$	parameter in Equation (4-9)
W, W'	weight of sample tube
x	mole fraction in liquid phase
$X_m$	mole fraction of group m in the mixture
Y	mole fraction in vapor phase
Z	compressibility factor

GREEK LETTERS

$\alpha$	density derivative with respect to temperature in Equation (3-14)
$\beta, \gamma$	constants in Equation (4-7)
$\gamma$	activity coefficient
$\Gamma$	constant defined by Equation (4-12)
$\Gamma_k$	activity coefficient of group k
$n^{(0)}, n^{(1)}$	constants defined by Equations (4-5) and (4-6)
$\theta$	area fraction
$v_k^{(i)}$	number of group k in molecule (i)
$\rho$	density
$\sigma_{12}$	constant defined by Equation (6-27)
$\phi$	fugacity coefficient
$\phi_i$	segment fraction of molecule i
$\phi_1, \phi_2$	constants defined by Equations (6-25) and (6-26)
$\tau_{mn}$	group interaction parameter defined by Equation (6-23)
$w$	acentric factor
$\Omega_a, \Omega_b$	parameters in Equations (6-4) and (6-7)

SUPERSCRIPTS

C	combinatorial
cor	correlated
exp	experimental
GC	gas chromatographic
ideal	ideal
l	liquid phase
M	model
R	residual
s	saturated
v	vapor phase
∞	infinitely diluted
°	initial value

SUBSCRIPTS

1	solvent
2	solute
c1	solvent at critical point
c12	mixture at critical point
ci	component i at critical point
i, j	component identification
ij	i-j pair
J-K	Jonah and King
k, m, n	group identification
km, nm	k-m pair and n-m pair
r	reduced property

## CHAPTER I

### INTRODUCTION

A knowledge of equilibrium gas solubility is essential for the design of absorption or desorption equipment for chemical processes. If we have the information that some component of a gas mixture is much more soluble in a particular solvent than are the other gases present, we can use that solvent as an absorption medium for that gas. As a specific example, in the separation and purification process of  $C_3$  and  $C_4$  hydrocarbons which include propane, propene, 1,3-butadiene, trans-2-butene, cis-2-butene, isobutene, n-butane and isobutane, which may be obtained as a result of a fractional distillation of a hydrocarbon mixture, a combination of absorption and extractive distillation may be utilized for the separation of the components involved. For such a process the precise information concerning the equilibrium gas solubilities is required for the design of the separation equipment.

It is of particular interest that the solubilities of  $C_3$  and  $C_4$  hydrocarbons at atmospheric pressure in many hydrocarbon solvents are very high (1,2,3,4). Usually the terminology "gas solubility" is reserved for solubilities in which the dissolved gas concentration in the solvent is about 5 mole %. However, those of  $C_3$  and  $C_4$  hydrocarbons often exceed 30 mole % and especially at low temperatures gas solubilities sometimes exceed 80 mole %. This fact

indicates that there is no clear dividing line between gas solubility and vapor-liquid equilibria.

This investigation involved firstly, the precise measurement of gas solubilities at atmospheric pressure as well as at elevated pressures for highly soluble gases and secondly, an attempt to extend the knowledge concerning the solubility phenomena of highly soluble gases. As a starting point for our discussion we may consider, for example, that when gas solubilities are plotted as a function of the absolute temperature on a log scale it is confirmed that the gas solubilities approach unity when the solubility relations are extrapolated to the boiling points of solute gases. Experimental observations for solutions of highly soluble gases agree with the characteristic relationship for ideal gas solubility in which the mole fraction solubility depends on the solute gas vapor pressure as follows:

$$x_2^{\text{ideal}} = \frac{101.325}{P_2^S} \quad (1-1)$$

In the above expression when  $P_2^S$  is the saturated vapor pressure with units of kPa for the solute component, at the boiling point of the solute gas the ideal gas solubility becomes unity.

The aim of this investigation was to engage in a systematic study of gas solubility behavior including that of highly soluble gases. This investigation involved the measurement of the gas solubilities of propene, isobutene, n-butane and isobutane in the solvents, n-octane, chloroben-

zene and butanol at atmospheric pressure and for pressures to 2 MPa (300 psia) over a wide temperature range. The experiments were performed using a dynamic or solvent flow-type of gas solubility apparatus which was designed and constructed for moderate pressures. An apparatus for measuring the density of gas-saturated solutions under pressure was also developed because this property was useful for precisely determining gas solubilities at high pressure. Also developed was a method for gas chromatographic analysis of gas-saturated solutions. Good agreement between the results from the volumetric determinations using the solubility apparatus and those from gas chromatographic analysis was obtained, indicating a high degree of consistency between the two methods.

This investigation also involved the development of a correlation for gas solubility in non-polar solvents at atmospheric pressure. The correlation developed was intended for the extrapolation and interpolation of gas solubilities to other temperatures using one or two known values of solubility. It has been confirmed that the correlation developed permits the extrapolation or interpolation of gas solubilities to other temperatures with good accuracy for the solvents, carbon disulfide, carbon tetrachloride, benzene, toluene, cyclohexane, n-heptane, n-octane, isooctane, hexadecane and perfluoroheptane. It is considered to be applicable for other non-polar solvents.

This thesis is presented in seven chapters, the first

being the introduction itself. The second chapter gives a brief review of the literature that is relevant to this investigation. In the third chapter the development of the correlation for gas solubilities measured at atmospheric pressure is discussed. The properties of the chemicals used in this investigation are presented in Chapter 4. The details of the experimental equipment and the operating techniques involved are described in Chapter 5. The results and discussion of this investigation are presented in Chapter 6 and the conclusions drawn are presented in Chapter 7.

CHAPTER II  
LITERATURE SURVEY

This chapter contains a brief review of the literature that is relevant to this investigation. This chapter has been separated into two sections. The first section deals with the development of experimental techniques involved in the measurement of gas solubility in liquids at atmospheric and elevated pressures. Important considerations required for the successful measurement of gas solubilities are reviewed. In this section the broad classification of gas solubility apparatuses is discussed and the critical techniques involved are reviewed. In the second section the literature concerning gas solubility correlations and predictions is reviewed. Both theoretical and empirical approaches describing gas-liquid solubility equilibria are quoted and discussed.

Comprehensive reviews related to the subject of gas solubility in liquids are available including those of Markham and Kobe (5), Clever and Battino (6, 7), Katayama (8), and Wilhelm, Battino and Wilcock (9). These reviews describe many different methods for determining the solubility of gases in liquids.

It is understood from the literature survey that in the experimental measurement of gas solubility some apparatuses are simple in construction and easy to use, and others are complex and difficult. Some methods are available only for

pressures near atmospheric pressure and temperatures near ambient temperature, but others are useful for wide ranges of pressure and temperature. Some methods are appropriate for high solubility systems, but others are not. Also, some methods promise high accuracy for the results and others provide just approximate values of gas solubility. It is apparent that the choice of solubility equipment depends upon the systems to be examined, the measurement conditions desired, and the ease of measurement and accuracy required. There are several original theoretical models for the prediction or correlation of gas solubilities in liquids. These include the regular solution theory developed by Hildebrand (10, 11) and the scaled particle theory introduced by Pierotti (12) to explain the phenomena of gas-liquid solubility equilibria. In many cases the prediction and correlation methods reported to date utilize these major ideas as a basis, but the original theories are modified when they are applied to specific problems involving particular gas-liquid systems. It is noted that for predictions and correlations involving gases of high solubility, the methods for describing vapor-liquid equilibria may also be applicable. For example, there are methods for the prediction of vapor-liquid equilibria utilizing equations of state, and methods utilizing liquid phase activity coefficients. It is appropriate to say that no general or widely applicable method for predicting and correlating gas solubilities in liquids has yet appeared except perhaps for those

partially successful original studies which were previously mentioned.

## 2.1 EXPERIMENTAL TECHNIQUES

Various types of equipment for the measurement of gas solubility in liquids have been reported depending upon specific needs and applications. It is seen, however, that there are large discrepancies between published values for gas solubilities which are obtained using different experimental devices. This fact indicates that each apparatus has more or less its own drawbacks. Cook and Hanson (13) pointed out the factors which lead to errors in solubility measurements. These factors include failure to completely degas the solvent, failure to attain equilibrium, and failure to ascertain the true amount of gas dissolved. These three important factors need to be considered in the design of equipment for measuring gas solubilities. Following the classification of gas solubility equipment, the solvent degassing techniques and equilibration techniques appearing in the literature are reviewed.

### 2.1.1 CLASSIFICATION OF METHODS FOR EXPERIMENTAL DETERMINATION OF GAS SOLUBILITY

The methods for the determination of gas solubility may be largely divided into two broad classifications: physical methods wherein the amounts of gas and liquid required for the solubility equilibrium are determined by means of purely

physical analysis, and next, chemical methods wherein the composition is determined by chemical reaction. The latter methods (14, 15, 16) are naturally limited to specific gas-liquid systems in which a quantitative determination of solute gas concentration can be made by means of an appropriate chemical reaction. Those solute gases are usually expected to have either acid, base, or redox properties for the purpose of chemical analysis.

Physical methods are used more frequently for determining gas solubility because of their wide applicability. These methods include volumetric methods, mass spectrometric methods, and gas chromatographic methods.

Volumetric methods (13, 17, 18, 19, 20, 32) are among the most precise available. These methods involve the measurement of volumes of gas and liquid required for the gas-liquid solubility equilibrium. The volume measurement for the liquid required is relatively easy, while that for the gas is generally difficult because the gas is compressible. Special techniques are required for the quantitative measurement of gas volume dissolved in a known volume of liquid. For example, these techniques may involve a method to replace the gas dissolved in the solvent using mercury (20), a method to count the number of soap bubbles created in the gas burette as the gas expands, a method utilizing a gas-tight piston keeping the pressure constant and finally, a method to determine the change in the gas volume by observing the pressure change in the gas reservoir of known

volume (41).

Mass spectrometric methods (21, 22, 23) for solubility determinations involve first the quantitative degassing of a gas-saturated liquid solution and then the entrapment of the gas for analysis by mass spectrometry. These methods have been used, for example, for the solubility of argon in liquid ammonia and various gases in blood (120).

Gas chromatographic methods (24, 25, 26, 27) usually involve passing a carrier gas through a known volume of gas-saturated liquid to separate the solute gas from the solvent, and then analyzing for both components by gas chromatography.

#### 2.1.2 SOLVENT DEGASSING TECHNIQUES

The complete removal of gas, usually air, from a liquid prior to a solubility determination is essential for the precise measurement of gas solubility in liquids. Cook and Hanson (13) mentioned that incomplete degassing of solvent is one of the factors which leads to erroneous solubility measurements. Gas solubilities obtained tend to be lower than the actual solubilities because of the tendency of the gas or air originally present in the solvent to contaminate the gas phase during the solubility determination. As a result, the partial pressure of the dissolving gas is reduced and solubility obtained is erroneously low.

The most frequently used method for degassing a liquid is to boil away a portion of it under vacuum. This method

is effective especially when heat, in addition to vacuum, is applied to the liquid. However, the loss of the liquid is usually significant, being approximately 10 to 20% of that initially charged.

In order to prevent the loss of solvent during degassing, another degassing method was developed. This method (28) employs a procedure of "pumping on" the frozen solvent which involves subjecting the frozen solvent to a high vacuum. It produces effective degassing with little loss of the solvent, but it also requires more time for degassing since the process of gas removal out of the solid solvent is much slower than from the liquid solvent. Usually this method must be repeated a number of times, alternately freezing and thawing the solvent, and is not appropriate when a large amount of solvent is to be degassed.

Another method (29, 30) of degassing the liquid utilizes a fine nozzle through which the liquid is sprayed into an evacuated flask. It is found that rapid and complete degassing is obtained by this technique, but it is also accompanied by a considerable loss of solvent.

A successful method for degassing liquids while minimizing the loss of solvent was employed by Battino and coworkers (31). The apparatus is made from a suction flask but is equipped with a condenser to minimize solvent loss. The vigorous stirring of the liquid by means of a magnetically-driven stirrer in the flask enhances the rate of degassing.

### 2.1.3 EQUILIBRATION TECHNIQUES FOR GAS-LIQUID SYSTEMS

For the determination of gas solubility, the attainment of equilibrium is of prime importance. Failure to attain equilibrium may result in large errors between the apparent solubilities and the true values. Many attempts have been made to ensure that equilibrium is established at the experimental temperature and pressure, and accordingly various equilibration techniques have been proposed.

Cook and Hanson (13) provided a means for shaking the whole apparatus such that equilibrium was enhanced in the container where the gas and liquid were in contact. The whole apparatus was mounted on a steel plate which was shaken at a frequency of about 170 cycles/min, and at an amplitude of about 3/8 inches. The direction of the shaking was horizontal to minimize pressure disturbances resulting from the vertical acceleration of mercury present in the apparatus. The entire apparatus was housed in an air thermostat controlled to within 0.1 C. The reproducibility was claimed to be better than 0.1%.

Morrison and Billet (32) utilized a gas-filled glass absorption spiral through which the liquid flowed forming a thin film. In their method, solvent is allowed to drip slowly into the absorption spiral and by the time the liquid arrives at the lower end, gas-liquid equilibrium is established. Several modifications have been made to this type of apparatus. One of these is an apparatus described by Battino et al. (33). They provided a storage spiral for

degassed solvent at the top of the regular absorption spiral, and also equipped a container to draw off saturated solvent for the measurement of solubilities for gases of low solubility. They claimed a precision of less than 1.0%. Hayduk and Chang (20) also utilized an apparatus based on the Morrison-Billet method of equilibration. They used a motor-driven syringe to provide degassed solvent into the absorption spiral to avoid the irregular rate of dissolution of solute gas caused by the dropwise supply of solvent. The motor-driven syringe is calibrated prior to the measurement and therefore, the solvent flow rate in the absorption spiral is known. After passing through the absorption spiral, the saturated solvent stagnates momentarily in a small U-tube manometer so that the pressure inside the absorption spiral can be compared with atmospheric pressure. The precision claimed is about 1.0%.

Dymond and Hildebrand (34) utilized a solubility apparatus in which the gas-liquid equilibrium was achieved by spraying slugs of solvent into the gas, resulting in good contact as the solvent ran down the container walls as a thin film. The solvent was circulated through the gas to promote the attainment of equilibrium. The apparatus was claimed to provide solubilities which had a precision of about 0.5%.

Gerrard (35) utilized a solubility apparatus which contained a bubbling tube. It consisted of an absorption vessel with a capacity of about 20 to 25 cm<sup>3</sup>, fitted with

two glass taps, one at either end. The first was connected to a cone and the other to a socket. Solute gas was introduced through the socket to the bottom of the bubbling vessel containing the solvent to be saturated. In this method for the determination of solubility, a bubbling process for the gas in the liquid was considered to enhance equilibration. The excess gas and vapor of the solvent were passed into a cone where the pressure was measured by means of a manometer. The solubility was based on an increase in the mass of the gas-saturated solution which was obtained by closing the taps, removing the bubbling tube, and then weighing it.

Equilibration techniques for the measurement of gas solubility at pressures higher than atmospheric involve more difficulty than those designed for atmospheric pressure. Adequate mixing of both gas and liquid phases is essential during the process of measuring solubility to ensure that equilibrium is established. The precise control of temperature and pressure is also required to maintain the desired conditions during the operation.

Wieb, Gaddy and Coworkers (36, 37, 38) utilized equipment which involved the continuous bubbling of compressed gas through a liquid to establish the equilibrium. The excess gas was allowed to escape to the atmosphere, and the gas-saturated solution was sampled and analyzed. It was considered possible to use this equilibration method even for high pressures (to 10 MPa). A disadvantage is that it

is limited to systems in which inexpensive, nontoxic, and nonflammable gases are used as solutes, because they are simply vented to the atmosphere.

Gardiner and Smith (39) modified the apparatus developed by ~~Wise~~ et al. by installing a magnetically-driven flat-bladed, turbine stirrer that disperses gas bubbles in the liquid. The equilibration was enhanced since the gas was drawn into the liquid through the hollow turbine shaft provided for that purpose. Because of the partial vacuum, the gas was dispersed in the liquid and mixed by the turbine blades.

Pray et al. (40) used an apparatus in which equilibrium was established by placing the gas-liquid equilibrium cell in a rocking autoclave that could be set in motion during operation. A disadvantage of this equilibration technique is that a long period of time is required for establishing equilibrium.

Koonce and Kobayashi (41) used a solubility apparatus with a ball bearing mixer that was magnetically activated to provide a reciprocating motion in the equilibrium vessel. A 5/8 inch diameter ball bearing was placed within the cylindrical vessel of nonmagnetic stainless steel that was 3/4 inch in diameter and 18 inches in length. The ball bearing inside the vessel was raised and lowered in accordance with the reciprocating motion of a strong horseshoe magnet fitted directly around the cylinder body. This motion resulted in good mixing of the gas and liquid, thereby enhancing equilibration.

## 2.2 PREDICTION AND CORRELATION OF GAS SOLUBILITY IN LIQUIDS

Since the emergence of the regular solution theory of Hildebrand (10, 11) attempts have been made to predict or correlate gas solubilities in liquids based on this theory. This simple and yet successful theory for non-polar solvent-solute systems utilizes solubility parameters as a measure of the intermolecular forces. Solubility parameters may be evaluated for most volatile substances and are defined as the energy of vaporization per unit volume raised to the one-half power. Some of the attempts for predicting solubility have involved modification to the nature of the solubility parameters themselves. Gjaldbaek and Anderson (42) introduced the dipole interaction to polar solvents. Lachowicz and Weale (43) introduced a solute gas-solvent interaction parameter to replace the solubility parameter. Gjaldbaek and Nieman (44) treated the solubility parameter as a function of the dielectric constant of the solvent and the polarizability of the solute gas. Despite such modifications to the solubility parameter, however, predictions for gas solubility were not significantly improved.

Prausnitz and Shair (45) proposed a gas solubility prediction method also based on the regular solution theory. They divided the gas dissolution process into two steps, the first being the condensation of the solute gas to a hypothetical state having a liquid-like volume, and the second being the dissolution of the hypothetical liquid-like fluid

in the solvent. The sum of the Gibbs free energy for the two-step dissolution process was then equated to zero because of the establishment of equilibrium. The activity coefficient involved in the second step was determined by means of the regular solution theory. Although somewhat complex, their correlation proved to be more useful for the prediction of gas solubilities for non-polar systems than the regular solution theory itself.

Yen and Mcketta (46) developed a correlation utilizing a similar idea to that of Prausnitz and Shair. They modified the regular solution theory for application to polar liquids by employing the Stockmayer potential function to describe solvent-solvent molecular interactions and the Lennard-Jones potential function for solute-solute interactions. The average deviation between experimental and calculated gas solubilities in polar nonassociated liquids is reported to be about 16%.

Another approach to gas solubility prediction and correlation was the use of equations of state which are capable of describing vapor-liquid equilibrium with good accuracy. The advantage for the use of equations of state is that they are applicable for the prediction or correlation of solubilities even for mixed solvents and over wide ranges of temperature and pressure. A difficulty involved in the use of equations of state is that a binary interaction parameter, characteristic of each pair of components and each equation of state, has to be determined precisely to be

useful for other conditions or compositions. Although there are some correlations for binary interaction parameters (47,48,49,50), the best determination of these parameters usually requires accurate vapor-liquid equilibrium data. In this sense equations of state do not provide an independent method for the prediction of gas solubility.

Sazamoto et al. (51) incorporated an equation of state based on the liquid phase activity coefficients obtained from the regular solution theory in order to predict gas solubilities at high pressure. The equations of state employed were the Redlich-Kwong (52) equation of state and the Benedict-Webb-Rubin (53, 54) equation of state. The prediction results for gas solubilities obtained by means of the equations of state were both satisfactory, but it was found that even minor changes in the values of binary interaction parameters greatly affected the prediction results.

Sagara et al. (55) also utilized Benedict-Webb-Rubin equations of state along with the regular solution theory to predict Henry's law constants for binary hydrocarbon systems and hydrogen-hydrocarbon systems. They proposed equations to estimate hypothetical liquid properties of solute and obtained satisfactory results for the systems examined.

Chu and Lu (56) applied a modified Redlich-Kwong equation of state to predict gas solubilities and phase equilibria of normal fluid mixtures with one supercritical component. They obtained results by their methods which agreed

well with the experimental results found in the literature.

Preston and Prausnitz (57) derived a generalized thermodynamic expression for Henry's law constants based on the two fluid theory of Scott (58) and utilizing the Strobridge-Gosman (59) equation of state. The general equation obtained was successful in correlating Henry's law constants for non-polar systems. This method was extended for systems involving polar solvents by Cysewski and Prausnitz (60). They applied the Carnahan and Starling (61) equation of state instead of the Strobridge-Gosman equation of state. However, the results were subject to large errors.

Moyson et al. (62) utilized the Soave-Redlich-Kwong (63) and Peng-Robinson (64) equations of state to predict the solubility of hydrogen in hydrocarbon solvents. The binary interaction parameters were determined so that the predicted gas solubilities agreed with those experimentally obtained, and a correlation for the binary interaction parameters was developed. They confirmed that both equations of state could be used to predict hydrogen solubilities in hydrocarbon solvents.

There are several other reports (64, 66, 67, 68) that also describe methods utilizing equations of state to predict or correlate gas solubilities in liquids. It should be realized, however, that equations of state are often unsuccessful for describing equilibria of systems involving polar substances.

Yet another approach for the prediction and correlation of gas solubilities involves the concept of a molecular model in which cavities are considered to exist in the liquid structure for possible locations of dissolved solute as proposed first by Uhlig (69) and subsequently extended by Pierotti (12, 70). In this approach it is considered that a hole or cavity is created in the solvent and that the gas molecule is then inserted into the cavity. The solubility is determined by calculating the work required for cavity formation and the interaction energy between the solute gas and solvent molecules. Pierotti introduced a Lennard-Jones (6-12) pairwise potential to calculate the solute gas-solvent interaction energy. The agreement between the experimental and predicted gas solubilities was quite satisfactory for the non-polar systems considered.

There are also other approaches available to predict or correlate gas solubilities and Henry's law constants. For example, there are methods based on classical thermodynamics (71, 72, 73, 74), those based on statistical thermodynamics (75, 76, 77, 78, 79) and those based on the prediction of the activity coefficient, which include the ASOG method (80) and the UNIFAC method (81). These methods, as well as many of those mentioned above, however, are usually not successful, if applicable, for the prediction or correlation of gas solubilities at atmospheric pressure. Part of the difficulty in describing solubility phenomena may be related to the range of solubilities involved. Gas solubilities at atmos-

spheric pressure given in mole fraction vary in magnitude from the order of  $10^{-1}$  to that of  $10^{-5}$  depending upon the solute and solvent. Because of this extremely large range in solubility, the prediction and correlation for gas solubility at atmospheric pressure based on empirical or semi-empirical equations rather than theoretical approaches appear to be more practical and useful at present.

A semiempirical correlation for gas solubility in non-polar solvents, intended for engineering applications, was proposed by Katayama et al. (82, 83). They chose benzene as a reference solvent and developed a correlation by considering the difference in solubilities of a gas in benzene and in other solvents. With the correlation, the solubility prediction is also possible for systems for which there is no data available. They estimated that prediction errors usually fell within 15%.

Himmelblau (84) presented a fourth order empirical equation for correlating the temperature variation of the Henry's law constant for non-polar gases in water. The proposed correlation requires at least one value of the Henry's law constant at one temperature before it is employed for the estimation of the constant at other temperatures. The temperature variation of the Henry's law constant for simple permanent gases is claimed to be represented to within 3%.

Hayduk and Laudie (85) proposed an empirical correlation for the solubility of gases in water and other associated

solvents based on the "hydrogen-bonding factor", which was defined by them as the ratio of actual gas solubility to ideal gas solubility. They considered that a large reduction in solubility from the ideal gas solubility was attributed to strong hydrogen-bonds in the solvent, and successfully correlated hydrogen-bonding factors of a gas in a polar liquid to that of the same gas in other associated liquids. It is claimed that semiquantitative predictions of solubilities in associated solvents are possible with their correlation, in many cases with good accuracy.

CHAPTER III

DEVELOPMENT OF A GAS SOLUBILITY CORRELATION

Hayduk and Buckley (100) reported that the extrapolated gas solubilities of many solutes in any solvent had a tendency to approach some constant solubility at the solvent critical temperature. This solubility, unique to a solvent, was referred to as the "reference solubility". Beutier and Renon (106), and subsequently Schotte (107), thermodynamically justified such a limiting law of gas solubilities in liquids and suggested that any theory or correlation for gas solubilities in liquids should consider the limiting behavior. A gas solubility correlation developed in this investigation is based on the concept of the reference solubility and intended for practical engineering applications.

For the purpose of developing the correlation, gas solubility data were collected from the literature. Four criteria for choosing solute gas-solvent systems were considered: the first was that the solubility data should be those measured at low pressures, the second was that the solvent should be non-polar or slightly polar, the third was that the solvent should be one in which gas solubilities of many solute gases were measured, and the fourth was that the solubilities should be available for at least three different temperatures. All the solubility data utilized for the development of the solubility correlation are tabulated in Table 3-1.

Table 3-1. Source of gas solubility data used for the correlation.

Solvent	Solute gas, source of data
CS <sub>2</sub>	N <sub>2</sub> O(86), CO <sub>2</sub> (87), CH <sub>4</sub> (87), SF(87), Ar(88), N <sub>2</sub> (87), CF <sub>4</sub> (89), D <sub>2</sub> (90), H <sub>2</sub> (90)
CCl <sub>4</sub>	C <sub>3</sub> H <sub>8</sub> (1), N <sub>2</sub> O(86), C <sub>2</sub> H <sub>4</sub> (102), SF <sub>6</sub> (89), Ar(88), CF <sub>4</sub> (89), D <sub>2</sub> (93), H <sub>2</sub> (93), N <sub>2</sub> (92), O <sub>2</sub> (02), CO(92), CH <sub>4</sub> (92), C <sub>2</sub> H <sub>6</sub> (92), C <sub>2</sub> H <sub>2</sub> (92)
C <sub>6</sub> H <sub>6</sub>	C <sub>2</sub> H <sub>2</sub> (96), N <sub>2</sub> O(86), Xe(95), Kr(94), SF <sub>5</sub> (89), Ar(94), CF <sub>4</sub> (89), D <sub>2</sub> (93), H <sub>2</sub> (93), Ne(94), He(94).
C <sub>6</sub> H <sub>5</sub> CH <sub>3</sub>	C <sub>2</sub> H <sub>2</sub> (96), Ar(97), D <sub>2</sub> (93), H <sub>2</sub> (93), Ne(97), He(97)
cyclo-C <sub>6</sub> H <sub>12</sub>	C <sub>3</sub> H <sub>8</sub> (98), C <sub>2</sub> H <sub>6</sub> (99), cyclo-C <sub>4</sub> F <sub>8</sub> (98), Xe(99), CClF <sub>3</sub> (98), CO <sub>2</sub> (99), C <sub>3</sub> F <sub>8</sub> (98), SF <sub>6</sub> (89), Kr(99), C <sub>2</sub> F <sub>6</sub> (98), Ar(99), CF <sub>4</sub> (89), N <sub>2</sub> (99), H <sub>2</sub> (99), Ne(99)
n-C <sub>7</sub> H <sub>16</sub>	C <sub>2</sub> H <sub>5</sub> (20), C <sub>2</sub> H <sub>4</sub> (102), N <sub>2</sub> O(86), CO <sub>2</sub> (101), SF <sub>6</sub> (89), Kr(94), CH <sub>4</sub> (100), Ar(94), CF <sub>4</sub> (89), D <sub>2</sub> (93), H <sub>2</sub> (93), Ne(94), He(94)

Solvent	Solute gas, source of data
n-C <sub>8</sub> H <sub>18</sub>	Kr(94), CH <sub>4</sub> (100), Ar(94), D <sub>2</sub> (93), H <sub>2</sub> (93), Ne(94), He(94)
iso-C <sub>8</sub> H <sub>18</sub>	C <sub>2</sub> H <sub>6</sub> (87), Xe(95), N <sub>2</sub> O(86), SF <sub>6</sub> (87), CO <sub>2</sub> (103), CH <sub>4</sub> (103), CF <sub>4</sub> (89), O <sub>2</sub> (104), D <sub>2</sub> (93), H <sub>2</sub> (93)
n-C <sub>16</sub> H <sub>34</sub>	C <sub>2</sub> H <sub>6</sub> (130), SO <sub>2</sub> (131), H <sub>2</sub> S(131), NH <sub>3</sub> (131), CO <sub>2</sub> (131), CH <sub>4</sub> (91.130), CO(131), N <sub>2</sub> (131)
n-C <sub>7</sub> F <sub>14</sub>	SF <sub>6</sub> (87), CO <sub>2</sub> (87), CH <sub>4</sub> (87), N <sub>2</sub> (105) D <sub>2</sub> (93), H <sub>2</sub> (93), He(87)

The development of the correlation will now be detailed. It was expressed by Hildebrand and Scott (11) that the temperature coefficient is related to the partial molar entropy change of the solute during dissolution:

$$\left(\frac{\partial \ln x_2}{\partial \ln T}\right)_P = \Delta \bar{S}_2/R \quad (3-1)$$

where  $x_2$ ,  $T$ ,  $P$ ,  $\Delta \bar{S}_2$ , and  $R$  are mole fraction solubility, absolute temperature, total pressure, partial molar entropy change and the gas constant, respectively.

It was found in this study that the change in partial molar entropy for dissolution is well represented by the equation of the following form:

$$\Delta \bar{S}_2/R = C_1 + C_2 \ln T \quad (3-2)$$

In the above equation  $C_1$  and  $C_2$  are the constants specific to a solvent and solute gas system. In Figure 3-1 the partial molar entropy change is plotted as a function of the logarithm of absolute temperature for the four solute gases, sulfur dioxide, carbon dioxide, carbon monoxide and nitrogen, in hexadecane. It is evident from the figure that for all these gases the partial molar entropy is linear with the logarithm of absolute temperature.

The observation by Hayduk and Buckley that extrapolated gas solubilities go through a reference solubility characteristic of a solvent at the solvent critical temperature is

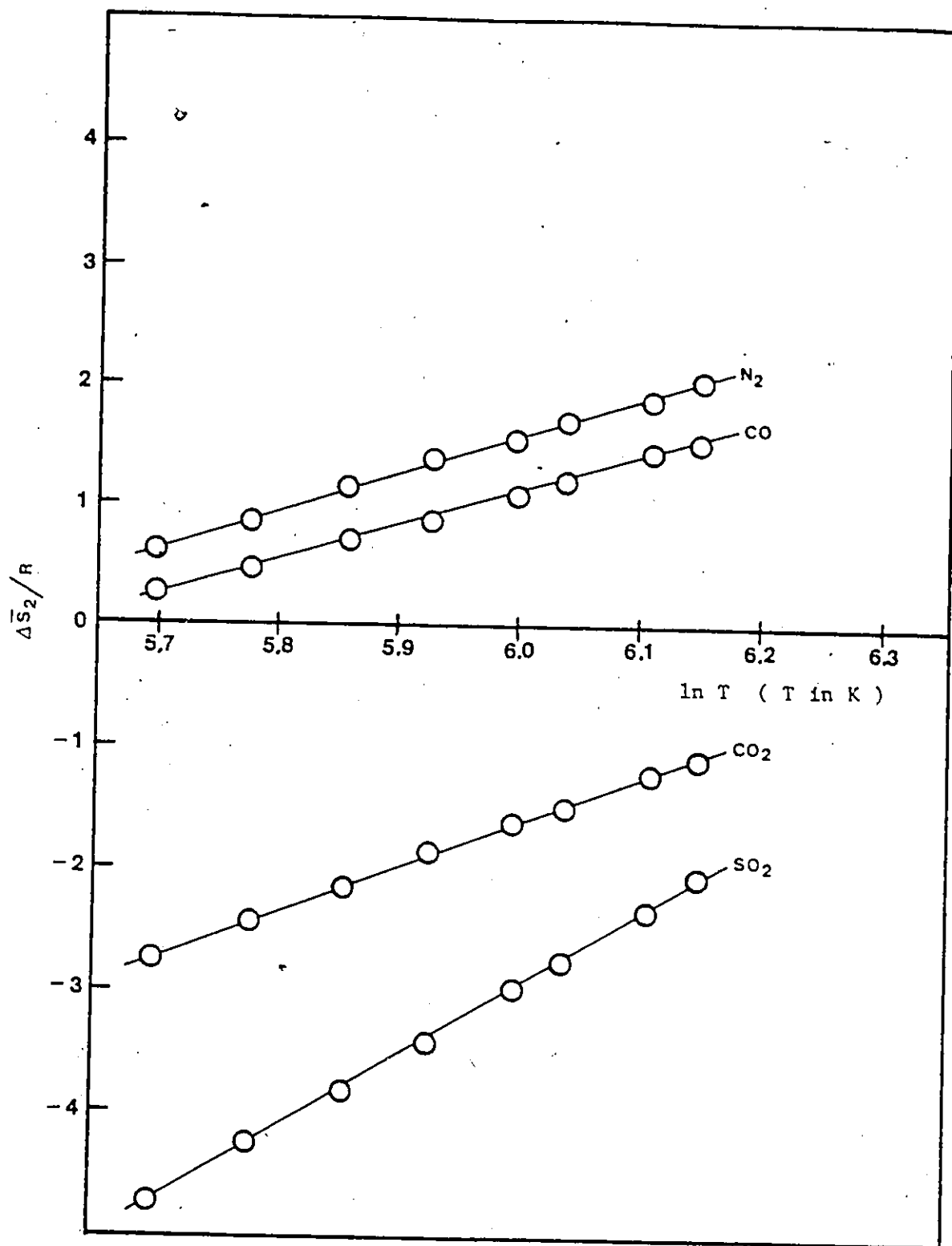


Figure 3-1 Partial molar entropy change of the solute for n-hexadecane as a function of the logarithm of absolute temperature.

expressed mathematically by:

$$x_2 = x_{cl} \quad \text{at } T = T_{cl} \quad (3-3)$$

In the above expression,  $x_{cl}$ , and  $T_{cl}$ , are the reference solubility of a solvent, and the critical temperature of the solvent, respectively.

The combination of Equations (3-1) and (3-2) with the condition given by Equation (3-3) results in:

$$\ln \frac{x_2}{x_{cl}} = A_1 \ln \frac{T}{T_{cl}} + A_2 \left( \ln \frac{T}{T_{cl}} \right)^2 \quad (3-4)$$

In the above equation  $A_1$  and  $A_2$  are constants specific to each solute gas-solvent system. Equation (3-4) was used as the model equation for the solubility correlation developed in this study.

Because the reference solubility,  $x_{cl}$ , is considered unique to a solvent, an  $x_{cl}$  value was obtained for each solvent. The best value of the reference solubility was determined on the basis that the summation of all the percent deviations between the experimental gas solubilities and those obtained using the model equation was minimized. The  $x_{cl}$  values thus obtained are listed in column (3) of Table 3-2. The flow chart for this calculation utilizing the computer (IBM 370) is shown in Figure 3-2.

Further on in the development of the correlation, it was necessary to relate the reference solubilities of a number

Table 3-2. Summary of correlation results for gas solubilities in various solvents.

Col.(1)	Col.(2)	Col.(3)	Col.(4)	Col.(5)	Col.(6)	Col.(7)
Solvent	No. of Solutes	$x_{cl}^{exp}$	$x_{cl}^{cor}$	Avg. % Dev.	Avg. % Dev.	Avg. % Dev.
CS <sub>2</sub>	9	7.75x10 <sup>-4</sup>	7.62x10 <sup>-4</sup>	0.46	1.05	2.5
CC <sub>14</sub>	14	1.13x10 <sup>-3</sup>	2.23x10 <sup>-3</sup>	0.76	1.67	4.5
C <sub>6</sub> H <sub>6</sub>	11	1.32x10 <sup>-3</sup>	2.07x10 <sup>-3</sup>	0.71	1.69	3.0
C <sub>6</sub> H <sub>5</sub> CH <sub>3</sub>	6	1.42x10 <sup>-3</sup>	2.28x10 <sup>-3</sup>	0.59	1.06	5.5
cyclo-C <sub>6</sub> H <sub>12</sub>	15	1.70x10 <sup>-3</sup>	2.42x10 <sup>-3</sup>	0.29	0.63	1.9
n-C <sub>7</sub> H <sub>16</sub>	13	1.79x10 <sup>-3</sup>	2.42x10 <sup>-3</sup>	0.46	1.01	3.3
n-C <sub>8</sub> H <sub>18</sub>	7	1.85x10 <sup>-3</sup>	2.20x10 <sup>-3</sup>	0.34	0.81	1.9
iso-C <sub>8</sub> H <sub>18</sub>	10	1.69x10 <sup>-3</sup>	2.28x10 <sup>-3</sup>	0.29	0.60	5.2
n-C <sub>16</sub> H <sub>34</sub>	8	7.43x10 <sup>-3</sup>	7.85x10 <sup>-3</sup>	1.37	3.84	16.7
perf-C <sub>7</sub> F <sub>16</sub>	7	3.55x10 <sup>-3</sup>	2.87x10 <sup>-3</sup>	0.28	0.58	3.4

Read all the experimental solubilities and  
critical temperature of solvent

Assume  $x_{cl}^{exp}$  at  $T_{cl}$

↓  
Fit Model Eqn. to experimental  
gas solubilities to obtain  $x^M$ 's

↓  
Calculate  $\Sigma \frac{x^M - x^{exp}}{x^{exp}} \times 100$

↓  
Check if  $\Sigma \frac{x^M - x^{exp}}{x^{exp}} \times 100$  is minimum  
No  $x_{cl}^{exp}$

↓ Yes

Print  $x_{cl}^{exp}$

Figure 3-2 Flow chart for the calculation to determine  
 $x_{cl}^{exp}$ .

of solvents to other appropriate variables. It was considered that for up to moderate pressures, gas solubilities for a solute partial pressure equal to one atmosphere, are expressed by Henry's law:

$$x_2 = \frac{1}{H_{21}(T, P_1^S)} \quad (3-5)$$

In the above equation,  $H_{21}(T, P_1^S)$  is the Henry's law constant at temperature  $T$  and the solvent vapor pressure  $P_1^S$ .

Henry's law is also expressed by the following equation:

$$H_{21}(T, P_1^S) = \lim_{x_2 \rightarrow 0} \left( \frac{P y_2 \phi_2^V}{x_2} \right) \quad (3-6)$$

In the above equation,  $\phi_2^V$ ,  $P$ ,  $y_2$  and  $x_2$  are, respectively, the fugacity coefficient of the solute gas in the vapor phase, the total pressure, the solute gas mole fraction in the vapor phase and the solute mole fraction in the liquid phase.

The  $\phi_2^{V, \infty}$ , which is the fugacity coefficient of the solute gas at infinite dilution in the vapor phase is expressed in terms of the cross virial coefficient:

$$\phi_2^{V, \infty} = \exp \left( \frac{2B_{12}}{V_1^V} - \ln Z_1^V \right) \quad (3-7)$$

In the above expression,  $B_{12}$ ,  $V_1^V$  and  $Z_1^V$  are the cross virial

coefficient, the molar volume of solvent vapor, and the compressibility factor for the solvent vapor, respectively. The combination of Equations (3-5), (3-6) and (3-7) results in:

$$x_2 = \frac{\lim_{x_2 \rightarrow 0} \left( \frac{x_2}{Y_2} \right)}{P_1^s \exp \left( \frac{2B_{12}}{V_1^v} - \ln Z_1^v \right)} \quad (3-8)$$

It is assumed that Equation (3-8) is valid for temperatures increasing to the critical temperature of the solvent. Then Equation (3-8) may be written in terms of a relationship,  $\lim_{x_2 \rightarrow 0} (x_2/Y_2) = 1$  derived by Hala (108):

$$x_{cl} = \frac{1}{P_{cl} \exp \left( \frac{2B_{c12}}{V_{cl}} - \ln Z_{cl} \right)} \quad (3-9)$$

In Equation (3-9),  $P_{cl}$ ,  $V_{cl}$ ,  $Z_{cl}$  and  $B_{c12}$  are the critical pressure, the critical volume, the critical compressibility factor of a solvent and the critical virial coefficient at the critical temperature of the solvent, respectively.

In order to make the reference solubility a function only of the solvent properties, the term  $2B_{c12}$  in Equation (3-9) was expressed as a polynomial in  $V_{cl}$ :

$$2B_{c_{12}} = a + bV_{c1} + cV_{c1}^2 + dV_{c1}^3 \quad (3-10)$$

It was observed in the above equation that a, b, c and d could be universal constants regardless of the solvent. The substitution of Equation (3-10) into (3-9) thus results in:

$$x_{c1} = \frac{1}{P_{c1} \exp\left\{\left(\frac{a + bV_{c1} + cV_{c1}^2 + dV_{c1}^3}{V_{c1}}\right) - \ln Z_{c1}\right\}} \quad (3-11)$$

The constants a, b, c and d were determined so that Equation (3-11) adequately expressed  $x_{c1}$  values. For this calculation, Equation (3-11) was reduced to a linearized form of the equation and the constants were estimated by means of the least squares method utilizing the computer. The values of a, b, c and d obtained are listed in the Nomenclature. In column (4) of Table 3-2, the  $x_{c1}$  values calculated by means of Equations (3-11) are listed. Also listed in column (5) of the same table are the average percent deviations for each solvent. The deviations indicated are those between experimental solubilities and those calculated by the model equation (3-4) with  $x_{c1}$  determined using Equation (3-11). It is observed that Equation (3-4), when used with the correlated reference solubility, fits the experimental solubilities very well; the maximum average percent deviation being 1.37%.

In Figure 3.3 are shown the solubilities in n-heptane, along with the fitted curves which pass through the refer-

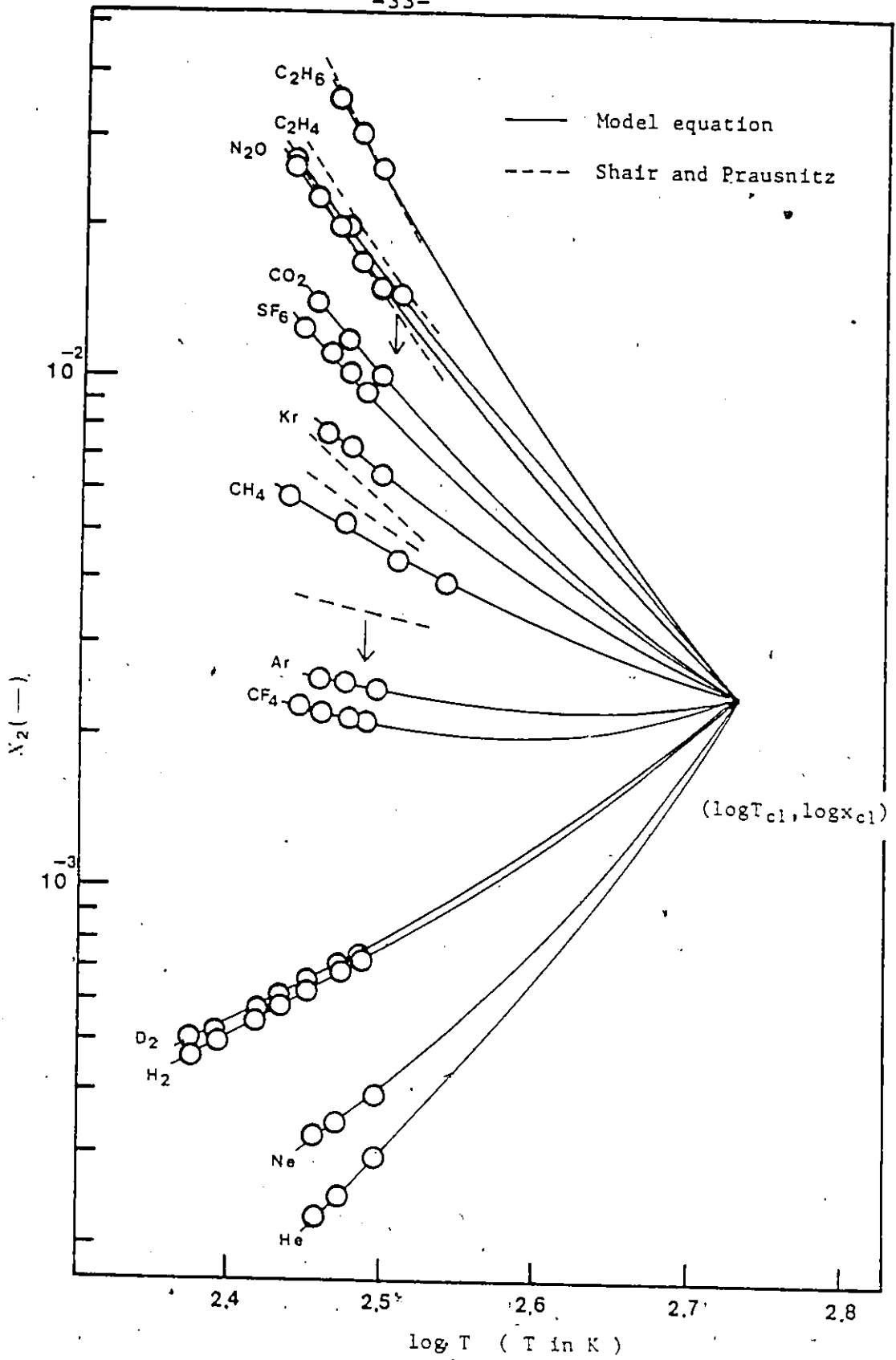


Figure 3-3 Correlated gas solubilities in n-heptane.

ence solubility determined by Equation (3-11). The dotted line in the same diagram represents the gas solubilities predicted by the method proposed by Shair and Prausnitz. Only those predicted solubilities which are relatively close to experimental solubilities are shown. Those not shown in the figure have deviations well over 100%. Such a situation implies that truly successful prediction methods for gas solubilities are yet to be developed. It is noted therefore that interpolation and extrapolation of gas solubilities based on a minimum amount of gas solubility data are much more likely to be accurate than prediction methods themselves. Similar diagrams for other solvent systems are shown in Appendix A.

Attempts were made to interpolate and extrapolate gas solubilities with changing temperature using Equation (3-4). It involves two constants,  $A_1$  and  $A_2$ ; therefore, if two values of gas solubility at different temperatures are available,  $A_1$  and  $A_2$  can be estimated analytically. If only a single value of gas solubility is available, it is necessary to introduce another equation for evaluation of the two characteristic constants.

When two gas solubilities at different temperatures are available:  $(x_{21}, T_1)$  and  $(x_{22}, T_2)$ , the two constants,  $A_1$  and  $A_2$  in the model Equation (3-4), are expressed analytically as follows:

$$A_1 = \frac{(\ln \frac{T_1}{T_{cl}})^2 (\ln \frac{x_{22}}{x_{cl}}) - (\ln \frac{x_{21}}{x_{cl}}) (\ln \frac{T_2}{T_{cl}})}{(\ln \frac{T_1}{T_{cl}})^2 (\ln \frac{T_2}{T_{cl}}) - (\ln \frac{T_1}{T_{cl}}) (\ln \frac{T_2}{T_{cl}})^2} \quad (3-12)$$

$$A_2 = \frac{(\ln \frac{T_2}{T_{cl}}) (\ln \frac{x_{21}}{x_{cl}}) - (\ln \frac{x_{22}}{x_{cl}}) (\ln \frac{T_1}{T_{cl}})}{(\ln \frac{T_2}{T_{cl}})^2 (\ln \frac{T_1}{T_{cl}}) - (\ln \frac{T_1}{T_{cl}}) (\ln \frac{T_2}{T_{cl}})^2} \quad (3-13)$$

The constants were evaluated utilizing solubilities at the highest and lowest temperatures in each solvent. Using the constants obtained, average percent deviations between experimental and estimated gas solubilities were calculated for all the solubilities in this study. The results are shown in column (6) of Table 3-2.

For the case when only a single value of gas solubility was assumed available at a certain temperature, another approach was taken. It was reported by Jonah and King (109) that the temperature coefficient is suitably expressed by the following equation:

$$\left(\frac{\partial \ln x_2}{\partial \ln T}\right)_{J-K} = -2 + \alpha T - (1 + \alpha T) \left(\ln \frac{RTx_2}{V}\right) \quad (3-14)$$

In the above equation  $V$ ,  $\alpha$ ,  $R$  and  $T$  are the molar volume of the solvent, the derivative of the logarithm of  $V$  with respect to temperature, gas constant and absolute temperature, respectively. It was considered that Equation (3-14) enables one to predict the temperature coefficient for

common solvents at temperatures corresponding to a solvent reduced temperature between 0.5 and 0.65. On the other hand, the temperature coefficient for Equation (3-4) is obtained for comparison by differentiation as follows:

$$\left(\frac{\partial \ln x_2}{\partial \ln T}\right)_M = A_1 + 2A_2 \left(\ln \frac{T}{T_{cl}}\right) \quad (3-15)$$

To estimate constants  $A_1$  and  $A_2$  in the model equation using a single known value of gas solubility at some temperature, the temperature coefficient is first calculated by means of Equation (3-14). Then the temperature coefficient so obtained is substituted into Equation (3-15) by setting:

$$\left(\frac{\partial \ln x_2}{\partial \ln T}\right)_{J-K} = \left(\frac{\partial \ln x_2}{\partial \ln T}\right)_M \quad (3-16)$$

The constants  $A_1$  and  $A_2$  are estimated by equating Equations (3-4) and (3-15). The resulting equations for the two constants in this case are:

$$A_1 = - \frac{\left(\frac{\partial \ln x_2}{\partial \ln T}\right)_{J-K} \left(\ln \frac{T_1}{T_{cl}}\right) + \left(\ln \frac{x_{21}}{x_{cl}}\right)}{\left(\ln \frac{T_1}{T_{cl}}\right)} \quad (3-17)$$

$$A_2 = \frac{\left(\frac{\partial \ln x_2}{\partial \ln T}\right)_{J-K} \left(\ln \frac{T_1}{T_{cl}}\right) - \left(\ln \frac{x_{21}}{x_{cl}}\right)}{\left(\ln \frac{T_1}{T_{cl}}\right)} \quad (3-18)$$

In the above expression,  $x_{21}$  is the gas solubility at the temperature  $T_1$ . In column (7) of Table 3-2, the percent deviations between experimental and estimated gas solubilities are listed for the solvents used in this study based on a single solubility value. In this calculation, the single gas solubility value was always the experimental one measured at the lowest temperature. In these calculations, it was also necessary to estimate the saturated liquid density and its temperature dependence. The method proposed by Yamada and Gunn (110) was utilized for this purpose.

CHAPTER IV  
PROPERTIES OF MATERIALS

The materials used in this investigation were obtained from different companies. The solute gases, propene, isobutene, n-butane and isobutane were purchased from Air Products. The specified minimum purities of these gases were 99.0, 99.0, 99.5 and 99.0%, respectively. Of the three solvents used in this investigation, chlorobenzene and n-butanol were purchased from J.T. Baker, and n-octane was supplied by the Aldrich Chemical Company. The claimed purities of these solvents were 99.8, 99.8 and 99.0 +%, respectively. The physical properties of the solvents and solute gases that were required in this investigation are listed in Tables 4-1 and 4-2.

Molar densities of solute gases were calculated by means of the second virial coefficient. For the solute gases, propene (111), n-butane (112) and isobutane (113), the experimental data for the second virial coefficient were available and were fitted by the following equation:

$$B = eT^f \quad (4-1)$$

In the equation above, B is the second virial coefficient, e and f are the constants characteristic of the substance, and T is the absolute temperature. The constants, e and f for propene, n-butane and isobutane, which were determined by

Table 4-1. Physical properties of the solvents used in this investigation (115).

Property (*)	n-Octane	Chlorobenzene	n-Butanol
M.W.	114.232	112.559	74.123
B.P.	398.8	404.9	390.9
F.P.	216.4	227.6	183.9
Tc	568.8	632.4	562.9
Pc	24.5	44.6	43.6
Vc	492.	308.	274.
Zc	0.259	0.265	0.259
$\omega$	0.394	0.249	0.59

Table 4-2. Physical properties of the solute gases used in this investigation (115).

Property (*)	Propene	Isobutene	n-Butane	Isobutane
M.W.	42.081	56.108	58.124	58.124
B.P.	225.4	266.3	272.7	261.3
Tc	365.0	417.9	425.2	408.1
Pc	45.6	39.5	37.5	36.0
Vc	181.	239.	255.	263.
Zc	0.275	0.275	0.274	0.283
$\omega$	0.148	0.190	0.193	0.176

(\*) M.W.: molecular weight in g/mol, B.P.: normal boiling point in K, F.P.: normal freezing point in K, Tc: critical temperature in K, Pc: critical pressure in atm, Vc: critical volume in (cm<sup>3</sup>/mol), Zc: critical compressibility,  $\omega$ : Pitzer's acentric factor.

the optimization techniques utilizing the computer, are listed in Table 4-3.

The virial coefficient obtained by Equation (4-1) was then substituted into the truncated form of the virial equation of state:

$$PV/(RT) = 1 + B/V \quad (4-2)$$

In the above equation, P, V, R and T are the pressure, the molar volume, the gas constant and the absolute temperature. The molar density, (MD), which is the inverse of molar volume, V, was obtained by the transformation of Equation (4-2) as:

$$(MD) = \{0.5D + 0.5 (D^2 + 4BD)^{0.5}\}^{-1} \quad (4-3)$$

In the above expression,  $D = RT/P$ . For the molar densities of isobutene, the second virial coefficient was predicted by the method proposed by Pitzer and Curl (114). This method requires the following equations: -

$$\frac{BP_c}{RT_c} = \eta^{(0)}(T_r) + \omega \eta^{(1)}(T_r) \quad (4-4)$$

$$\eta^{(0)} = 0.1445 - 0.330/T_r - 0.1385/T_r^2 - 0.0121/T_r^3 \quad (4-5)$$

$$\eta^{(1)} = 0.073 + 0.46/T_r - 0.5/T_r^2 - 0.097/T_r^3 - 0.0073/T_r^8 \quad (4-6)$$

Table 4-3. Constants of Equation (4-1) to calculate second virial coefficient.

Constant	Propene	n-Butane	Isobutane
e	$-1.012 \times 10^8$	$-7.985 \times 10^8$	$-1.403 \times 10^9$
f	-2.209	-2.436	-2.542

In the equation above,  $T_c$ ,  $P_c$ ,  $\omega$  and  $T_r$  are the critical temperature, the critical pressure, the acentric factor and the reduced temperature. The second virial coefficient calculated by means of Equations (4-4) to (4-6) was also substituted in Equation (4-3), and the molar densities of isobutene were obtained.

Saturated vapor pressures of all the solvents and solute gases were calculated by the Antoine equation (115) and the equation proposed by Gomez-Nieto and Thodos (116). For each substance, the constants required in these equations are listed in Table 4-4.

Saturated liquid densities of these gases, propene and isobutene, which were used as references in the density measurements at elevated pressures, were predicted by the equation proposed by Gunn and Yamada (118). The saturated densities at the reference temperature required for the density calculation are shown in Table 4-5 along with the proposed equation.

Densities of all the solvents used in this investigation were measured at atmospheric pressure. Therefore, the method utilized in the measurement of solubilities and densities and the results are presented in Chapters 5 and 6.

Table 4-4. Constants required for the saturated vapor pressure calculation.

n-Octane (*)	Chlorobenzene (**)	n-Butanol (**)
$\beta = 4,41938$	$A = 16.0676$	$A = 17,2160$
$\gamma = 0,17823$	$B = 3295.12$	$B = 3137,02$
$m = 1,47145$	$C = -55.60$	$C = -94.43$

Propene (*)	Isobutene (**)	n-Butane (*)	Isobutane (*)
$\beta = -4.22339$	$A = 15.7528$	$\beta = -4.42382$	$\beta = -4.11217$
$\gamma = 0.15757$	$B = 2125.75$	$\gamma = 0.14194$	$\gamma = 0.19181$
$m = 1.29720$	$C = -33.15$	$m = 1.30784$	$m = 1.34774$

(\*) Gomez-Nieto and Thodos equation

$$\ln P_r = \beta \left( \frac{1}{T_r^m} - 1 \right) + r (T_r^7 - 1) \quad (4-7)$$

where  $P_r = P/P_c$  and  $T_r = T/T_c$

(\*\*) Antoine equation

$$\ln P = A - \frac{B}{C+T} \quad (4-8)$$

Table 4-5. Densities at the reference temperature used in Gunn and Yamada equation (118),  $\rho$  in  $\text{g/cm}^3$ ,  $T$  in K.

	Propene	Isobutene
$T^R$	233.	293.
$\rho^R$	0.612	0.594

Gunn-Yamada equation:

$$\rho = \frac{M}{V^R} \cdot \frac{V_F^{(0)}(T_F^R) \cdot \{1 - \omega \Gamma(T_F^R)\}}{V_F^{(0)}(T_F) \cdot \{1 - \omega \Gamma(T_F)\}} \quad (4-9)$$

(i)  $V_F^{(0)}$ :

$$0.2 < T_F < 0.8: V_F^{(0)} = 0.33593 - 0.33953 T_F + 1.51941 T_F^2 - 2.02512 T_F^3 + 1.11422 T_F^4 \quad (4-10)$$

$$0.8 < T_F < 1.0: V_F^{(0)} = 1.0 + 1.3 (1 - T_F)^{0.5} \log_{10} (1 - T_F) - 0.50879 (1 - T_F) - 0.91534 (1 - T_F)^2 \quad (4-11)$$

(ii)  $\Gamma$ :

$$0.2 < T_F < 1.0: \Gamma = 0.29607 - 0.09045 T_F - 0.04842 T_F^2 \quad (4-12)$$

$$T_F = T/T_C$$

$$T_F^R = T^R/T_C$$

M: molecular weight

$V^R$ : liquid specific volume ( $= \frac{M}{\rho^R}$ )

$\omega$ : Piter's acentric factor

CHAPTER V

EXPERIMENTAL EQUIPMENT AND PROCEDURES

Several different experimental devices were used in this investigation. For the density measurement of pure solvents at atmospheric pressure, an Anton Paar density meter for atmospheric pressure was utilized. An apparatus for the measurement of gas solubility at atmospheric pressure was similar in type to that initially proposed by Hayduk and Cheng (20). Some modifications were made to the original apparatus in the interest of improving the reliability or accuracy. The densities of gas-saturated solutions at elevated pressures, which were necessary for the precise determination of gas solubilities also at elevated pressures, were measured utilizing an Anton Paar high pressure density meter. For the measurement of gas solubilities at moderate pressures, a dynamic or solvent-flow type volumetric apparatus was developed. Also developed was an apparatus to analyze gas-saturated solutions. The last-mentioned apparatus, which involved a gas chromatographic technique, was utilized in order to check independently the validity of the high pressure solubility measurements using the high pressure volumetric apparatus.

5.1 APPARATUS AND OPERATING PROCEDURE FOR DENSITY MEASUREMENTS OF PURE SOLVENTS AT ATMOSPHERIC PRESSURE

Preceding the measurement of gas solubilities at atmospheric pressure, the densities of solvents were measured at three temperatures, 298.15 K, 323.15 K and 343.15 K. For the precise measurements of solvent densities, an Anton Paar density meter was utilized. This density meter consisted of two components. One was the sensing unit, DMA 601, which contained a U-shaped sample tube within which was mounted a glass reed oscillator. The other component, DMA 60, which was essentially a frequency counter, displayed in numbers the period of oscillation of the reed characteristic of the liquid or gas in the sampling tube. In this investigation, the electrical output of the DMA 60 was combined with a Fisher analog recorder so that changes in the period of oscillation could be observed. The sample tube was equipped with a circulating chamber within which the temperature could be controlled to within 0.01 C. For density measurements using the Anton Paar density meter, the density of a liquid,  $\rho$  is related to the period of oscillation,  $Q$  of the liquid by the equation:

$$\rho = g (Q^2 - h) \quad (5-1)$$

In the above equation,  $g$  and  $h$  are apparatus constants, which are determined by the operator as a result of two

measurements of frequency for two samples of known density. Let the densities of two reference substances be  $\rho_1$  and  $\rho_2$ , and the corresponding periods of oscillation read from DMA 60 be  $Q_1$  and  $Q_2$ . The substitution of these variables into equation (5-1) results in:

$$g = \frac{\rho_2 - \rho_1}{Q_1^2 - Q_2^2} \quad (5-2)$$

$$h = \frac{\rho_2 Q_1^2 - \rho_1 Q_2^2}{\rho_2 - \rho_1} \quad (5-3)$$

With the apparatus constants thus obtained, Equation (5-1) was utilized to determine experimental densities of solvents. In this investigation, nitrogen and distilled water were used as reference substances for which densities were accurately known and which could be used for the determination of the apparatus constants.

Briefly, the operating procedure for the measurement of liquid densities involved setting the temperature of the sample tube at the measurement temperature, and then cleaning the inside of the sample tube with distilled water and acetone. After the cleaning procedure was repeated several times, nitrogen was passed through the sample tube to dry the residual acetone. Then a degassed sample of liquid was injected into the sample tube by means of a syringe, such that the sample tube was completely filled homogeneously without any entrapped gas. The sample tube, made of glass,

is visible through the window installed on DMA 601 and therefore the liquid being injected into the sample tube can be observed. In order to avoid entraining any gas in the sample tube during the filling procedure the liquids were charged slowly so that the shape of the meniscus at the gas-liquid interface did not deform significantly. Approximately 0.7 cm<sup>3</sup> of liquid sample was required for each measurement. After the charging operation was completed, the DMA 60 was switched on and the period of oscillation appearing on the display was recorded by means of a Fisher analog recorder. Usually in about 8 to 10 minutes, the sample liquid was observed to reach thermal equilibrium inside the thermostatted sample tube. Finally, the stabilized period of oscillation was recorded and subsequently used to calculate the density. The operation for the measurement of the nitrogen (gas) density involved a procedure similar to that mentioned for liquids. In this case, nitrogen was trapped in the sample tube utilizing two teflon stoppers at both ends of the sample tube. The calibration was conducted at each measurement temperature to determine the apparatus constants.

## 5.2 APPARATUS AND OPERATING PROCEDURE FOR MEASUREMENT OF GAS SOLUBILITY AT ATMOSPHERIC PRESSURE

Gas solubilities of propene, isobutene, n-butane and isobutane were measured at atmospheric pressure in the solvents n-octane, chlorobenzene and n-butanol. Experiments

were conducted at three temperatures, 298.15 K, 323.15 K and 343.15 K. The apparatus used for these measurements was similar to that initially proposed by Cheng and Hayduk. The schematic diagrams of the apparatus used in the measurement are shown in Figures 5-1 and 5-2.

The diagram shown in Figure 5-1 is the degassing apparatus. The degassing technique chosen for this apparatus is the most frequently used method, and consisted in boiling away a portion of the solvent under vacuum. Since the gas solubility measurement at atmospheric pressure required a very small amount of solvent, this conventional and effective technique for degassing the solvent was utilized.

The procedure for degassing the solvent involved first providing a suitable amount of solvent (about 30 cm<sup>3</sup>) in a flask equipped with a tape heater, and then applying a vacuum. After a boiling time of about 20 to 30 minutes had elapsed, the solvent was allowed to flow into an evacuated column packed with glass beads, where further degassing was performed. When the lower portion of the column was filled with degassed solvent, the vacuum was released, and a portion of the solvent stored in the void space between the beads was withdrawn by means of a syringe, the needle of which was inserted through a septum rubber stopper installed at the lower end of the packed column. The reasons for using the bead packing in the column are first, to provide an extensive surface area to the liquid for further boiling and second, to avoid the exposure or dissolution of air into

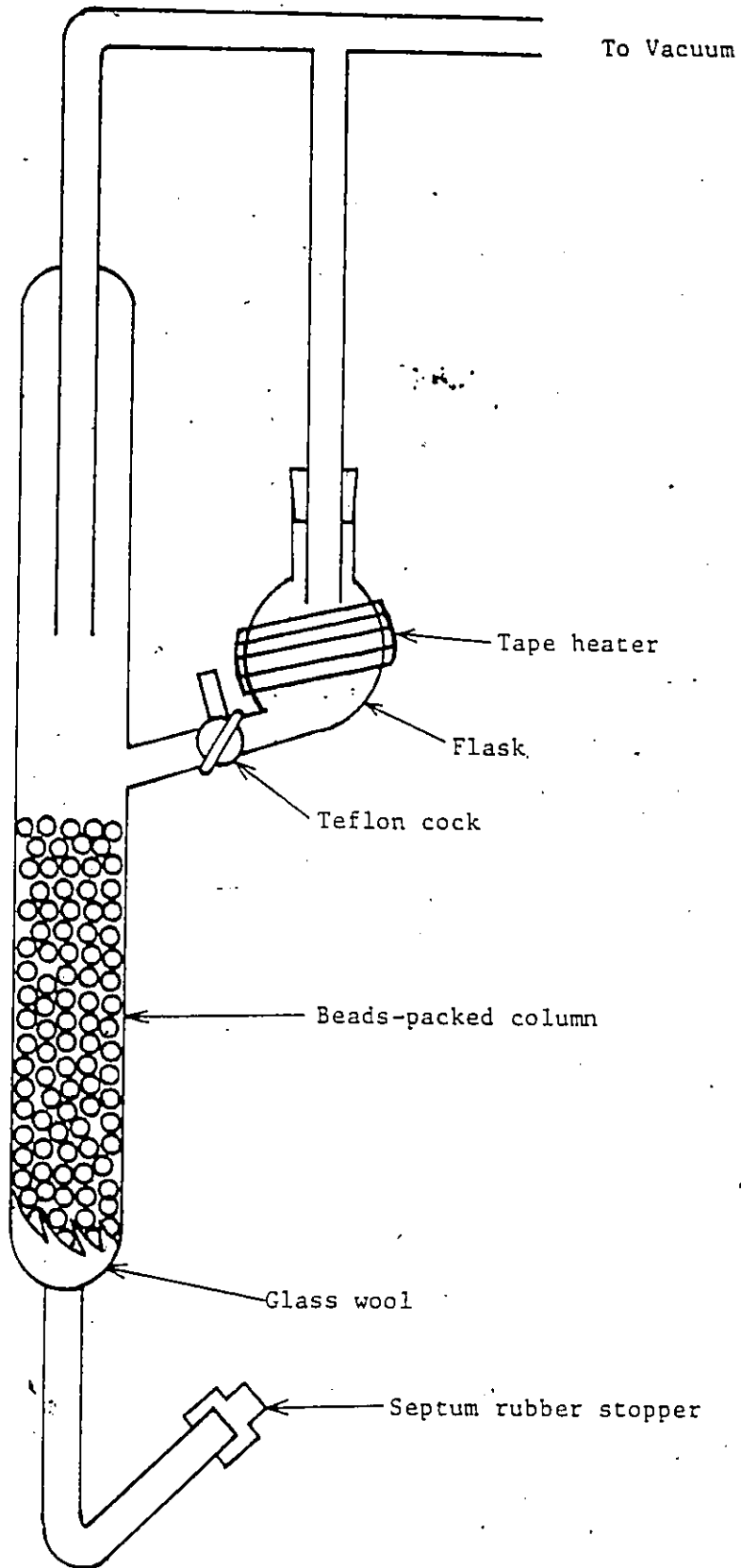


Figure 5-1 Degassing apparatus used for the solubility measurements at atmospheric pressure.

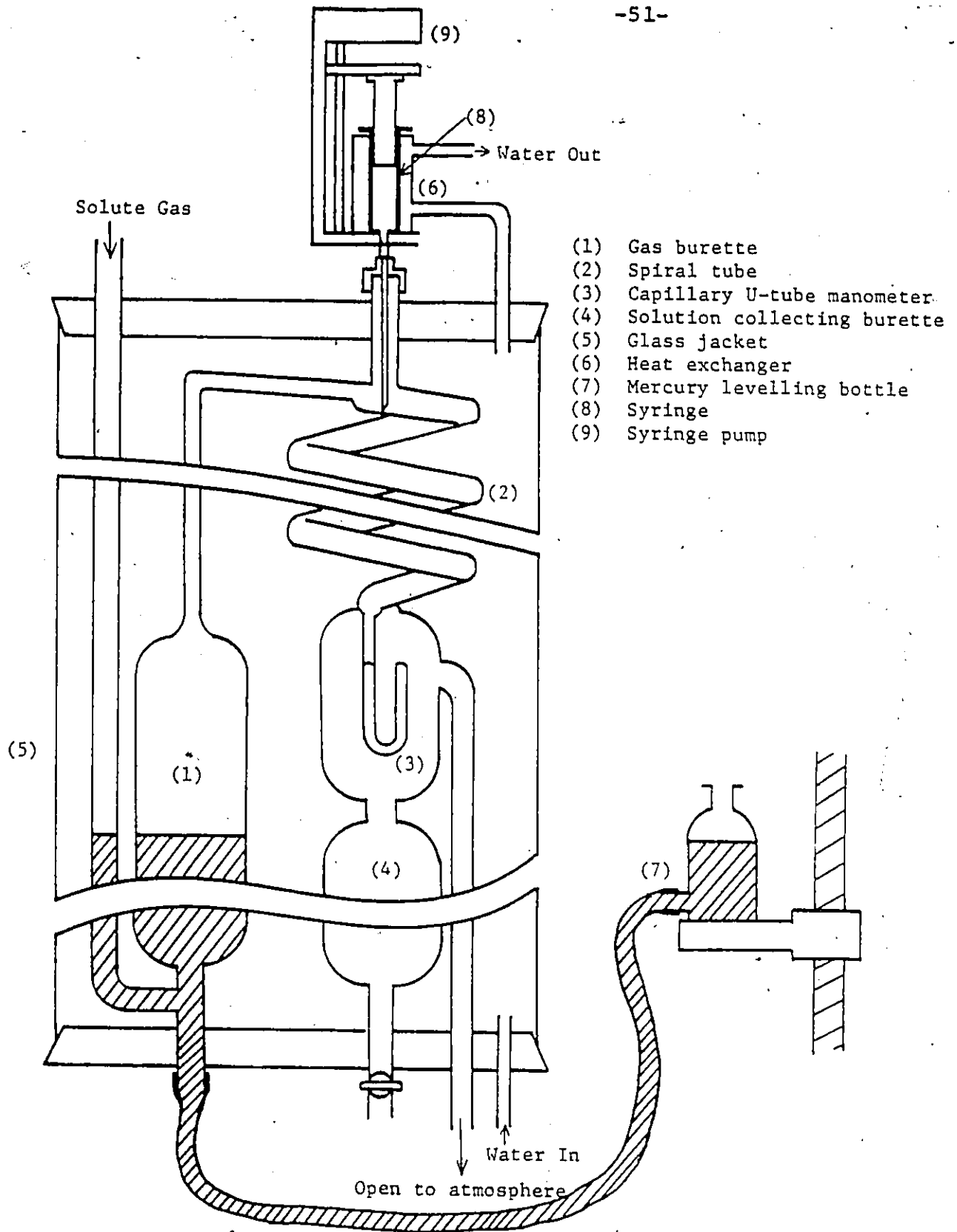


Figure 5-2 Solubility apparatus for the measurements of gas solubilities at atmospheric pressure.

the degassed solvent when the vacuum was released. The glass wool installed at the bottom of the bead-packing was to avoid the passage of glass beads into the bottom tubing. The septum rubber stopper was replaced by a new one after each degassing operation. The syringe containing the degassed solvent was then attached to a syringe-pump, and the degassed solvent was injected into the spiral tube of the solubility apparatus.

The syringe used was a 5 cm<sup>3</sup> gas-tight Hamilton syringe, and the syringe-pump device was a Harvard Apparatus syringe pump which operated with a interchangeable constant speed motor. Motor speeds of 1/10 rpm and 1/20 rpm were used for the solubility measurement and the corresponding solvent infusion rates were 0.01723 cm<sup>3</sup>/min and 0.00873 cm<sup>3</sup>/min, respectively. The volumetric infusion rates were determined accurately by weighing the quantity of distilled water delivered in a given period of time. The very low infusion rate for degassed solvent was consistent with the high solubilities anticipated.

In figure 5-2 is shown a schematic diagram of the solubility apparatus for the measurement of gas solubility at atmospheric pressure. The apparatus consisted of a gas burette(1), a spiral tube(2), a miniature capillary U-tube manometer(3) and a solution collecting burette(4). All these were enclosed inside a cylindrical glass jacket(5) through which water at constant temperature was circulated. The heat exchanger (6) to which the syringe was attached,

was also installed for the solvent to be heated to the temperature of the experiment. The mercury shown in the gas burette was connected through a tube to the mercury leveling bottle (7). By raising the mercury leveling bottle, the dissolved volume of the solute gas stored in the gas burette was replaced by mercury. The gas solubility in the mercury was assumed to be negligibly small.

For the high solubilities of gases involved in this investigation, some modifications were made to the original apparatus used by Hayduk and Cheng, the latter having been designed for low solubility measurements.

The residence time for the solvent liquid as it passed through the spiral tube, was usually 15 to 30 minutes for the low solubility systems. This residence time was determined by measuring the duration of time from the initial starting time of the syringe pump to the time when the liquid was first observed in the U-tube manometer. When the apparatus designed for the low solubility systems was used for the high solubility systems, the solvent residence time was found to be three to five times greater than when low solubilities were measured, because of the very low liquid flow rate. The reason for utilizing the very low flow rate for the high solubility systems was to ensure that the solvent was saturated with the solute gas, but the resulting time required for a single measurement was excessively long.

There were two possible ways to reduce the residence

time for the high solubility measurements. One way was to modify the spiral tube so that the residence time became shorter, and the other way was to adopt appropriately higher liquid flow rates. In selecting an appropriate method, consideration was given to the fact that for the same residence time, the lower liquid flow rates always resulted in more consistent, and slightly higher, experimental solubilities. Therefore, modifications were made to the spiral tube in order to shorten the time required for the measurement while still utilizing the lower solvent flow rates. The necessary modifications involved changes to the number of coils in the spiral tube, the radius of the spiral coil, and the radius of the spiral itself. These were all reduced in size when compared with those previously used in the measurement involving gases of low solubility, but, at the same time, the slope of the spiral tube was increased.

The experimental procedure for solubility measurements will be briefly described. While the solvent was being degassed, the solubility apparatus was purged with solute gas. Then the syringe(8), filled with degassed solvent, was first attached to the heat exchanger (6) and then to the syringe pump(9). The needle of the syringe was inserted into the spiral tube(2) passing through the heat exchanger (6). It was confirmed at the beginning of each run that the tip of the needle actually touched the wall of the spiral tube in order to ensure a continuous supply of solvent; otherwise a dropwise supply of the solvent caused an

intolerable fluctuation in gas pressure. Next, the stopcock of the solvent collecting burette(4) was closed and the syringe pump device was switched on. The solubility apparatus was left with the solute gas slowly flowing through the apparatus until a gas-saturated solvent solution appeared in the U-tube manometer (3) one end of which was open to the atmosphere. Then the flow of solute gas was shut off and the mercury level in the gas burette(1) was raised by mechanically adjusting the position of the mercury levelling bottle so that the liquid in the U-tube manometer remained at a constant level indicating a constant gas pressure in the solubility apparatus. The volume replaced by the mercury in the gas burette, which was identical to the volume of solute gas dissolved in the solvent, was recorded at 5-minute time intervals. With the knowledge of volumes of dissolved solute gas and those of degassed solvent supplied to the apparatus the gas solubility was determined.

### 5.3 TREATMENT OF DATA FOR GAS SOLUBILITY AT ATMOSPHERIC PRESSURE

The volumes of dissolved gas as measured at fixed time intervals were always found to be directly proportional to the volumes of solvent supplied. Gas solubilities were determined utilizing the slopes of the lines as obtained by a linear regression for all the systems.

Let the slope (gas to liquid) of the linear line resulting from the least squares fitting be (SP). Also, let the

molar densities of solute gas and solvent, and the liquid phase mole fractions of solute gas and solvent be  $(MD)_2$ ,  $(MD)_1$ ,  $x_2$  and  $x_1$ , respectively. Then these variables can be related to the following equation:

$$\frac{x_2}{x_1} = (SP) \cdot \frac{(MD)_2}{(MD)_1} \quad (5-4)$$

In the above equation, the molar density of solvent,  $(MD)_1$  was calculated from the mass density measured at atmospheric pressure in this investigation, and the molar density of solute gas was calculated by the method described in chapter 4.

The gas solubility,  $x_2$  at atmospheric pressure,  $P$  and temperature,  $T$  was then obtained by Equation (5-5).

$$x_2(P, T) = \frac{\frac{x_2}{x_1}}{\frac{x_2}{x_1} + 1} \quad (5-5)$$

It is conventional to convert the gas solubility measured at temperature,  $T$  and atmospheric pressure,  $P$  into the gas solubility in which the partial pressure of solute gas is one atmosphere (101.325 kP). Let the latter be  $x_2(P_2 = 101.325, T)$ . Also, let the vapor pressure of the solvent at the temperature be  $P_1^S$ . Then, assuming Henry's law and the ideality for the liquid phase,  $x_2(P_2 = 101.325,$

T) can be expressed as:

$$x_2(P_2 = 101.325, T) = x_2(P, T) \frac{101.325}{P - P_1^S \{1 - x_2(P, T)\}} \quad (5-6)$$

A further discussion concerning the conversion of gas solubility and the presentation of the gas solubility results is made in Chapter 6.

#### 5.4 APPARATUS AND OPERATING PROCEDURE FOR THE DETERMINATION OF GAS-SATURATED SOLUTION DENSITY

For the precise determination of gas solubilities, at high pressures, the densities of the gas-saturated solutions were required. For this purpose, the Anton Paar density meter intended for the density measurement at high pressures was purchased and utilized in this investigation. This density meter, as described in the section 5-1 for the density meter for atmospheric pressure, also consisted of two components. One was DMA 512 for pressures up to 40 MPa and temperatures to 423 K which contained a stainless-steel sample tube, functioning as a sensing component for the density. The capacity of the sample tube is approximately 1.0 cm<sup>3</sup>, and the sample tube is enclosed by a jacket for circulating constant temperature fluid controlled to within 0.01 °C. Both ends of the stainless-steel sample tube are equipped with 3 mm Swagelok fittings. This component of the densitometer is suitable for dynamic measurements in which

the liquid to be analyzed under pressure can be circulated through the sample tube. The other component was DMA 60, the electronic and digital display component, the same equipment as described for the density measurements at atmospheric pressure. The period of oscillation of the compressed liquid sample in the sample tube of DMA 512 was determined by means of this component. In the actual measurement the sample tube was connected to the equilibration cell by means of a stainless steel tube such that the gas-saturated solution was circulated through the sample tube. For circulation of gas-saturated solution, a Milton Roy high pressure metering pump was installed in the tubing between the equilibration cell and the sample tube. For confirmation that the solvent was saturated with gas, the period of oscillation which was read from the DMA 60 was also recorded by means of a Fisher analog recorder. When there was no more change in the period of oscillation, it was considered that equilibrium had been established.

For the purpose of enhancing the rate of equilibration for density measurements at elevated pressures, a new equilibration technique was devised in this work. A schematic diagram of the equilibration cell is shown in Figure 5-3. The cell body (1) is a Whitey high pressure vessel of 300 cm<sup>3</sup> capacity, made of stainless steel. The cell was enclosed in a cylindrical jacket (3) through which water at constant temperature was circulated. The gas-liquid contactor was a spiral coil made from a 1/8-in stainless steel

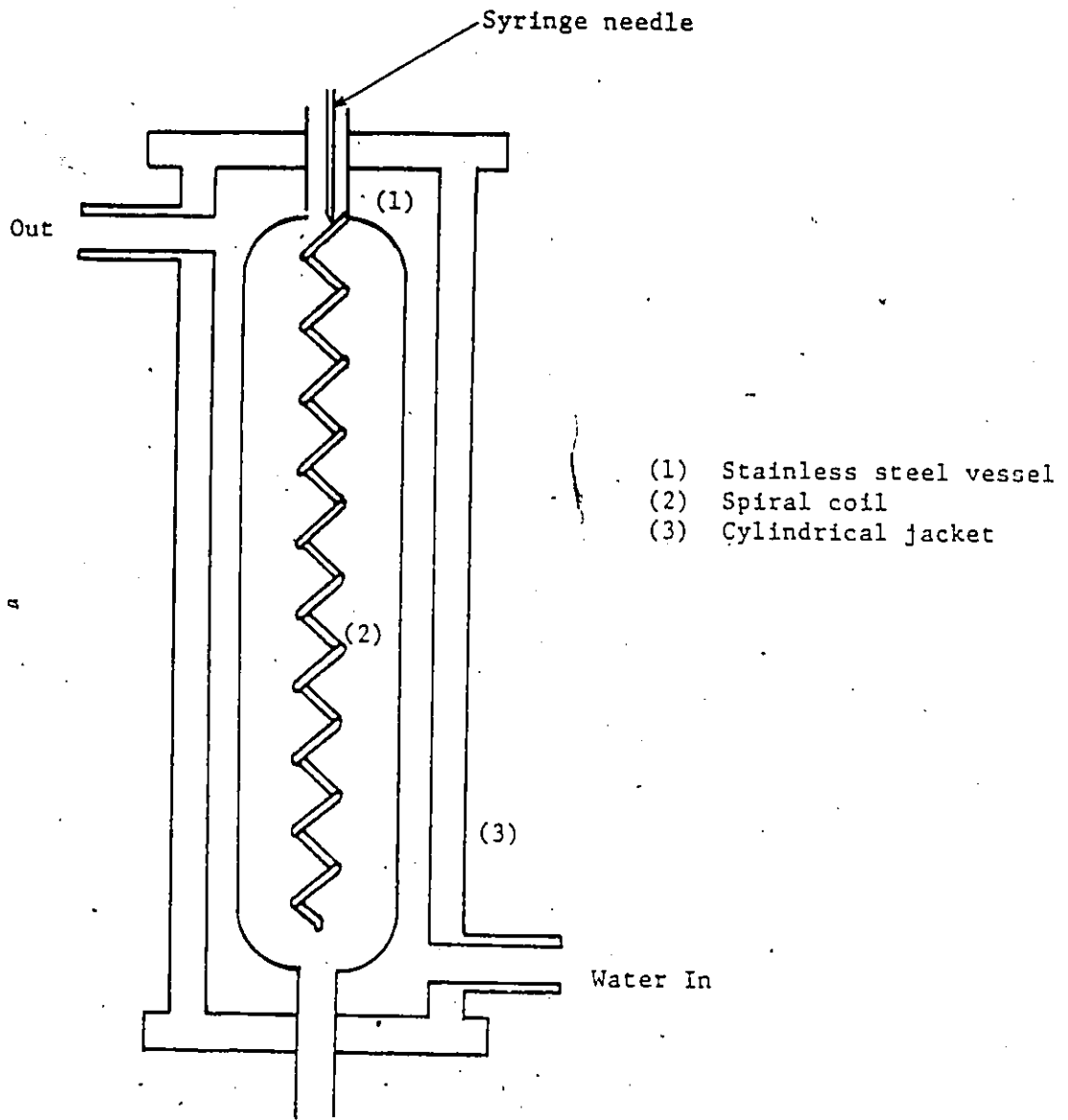
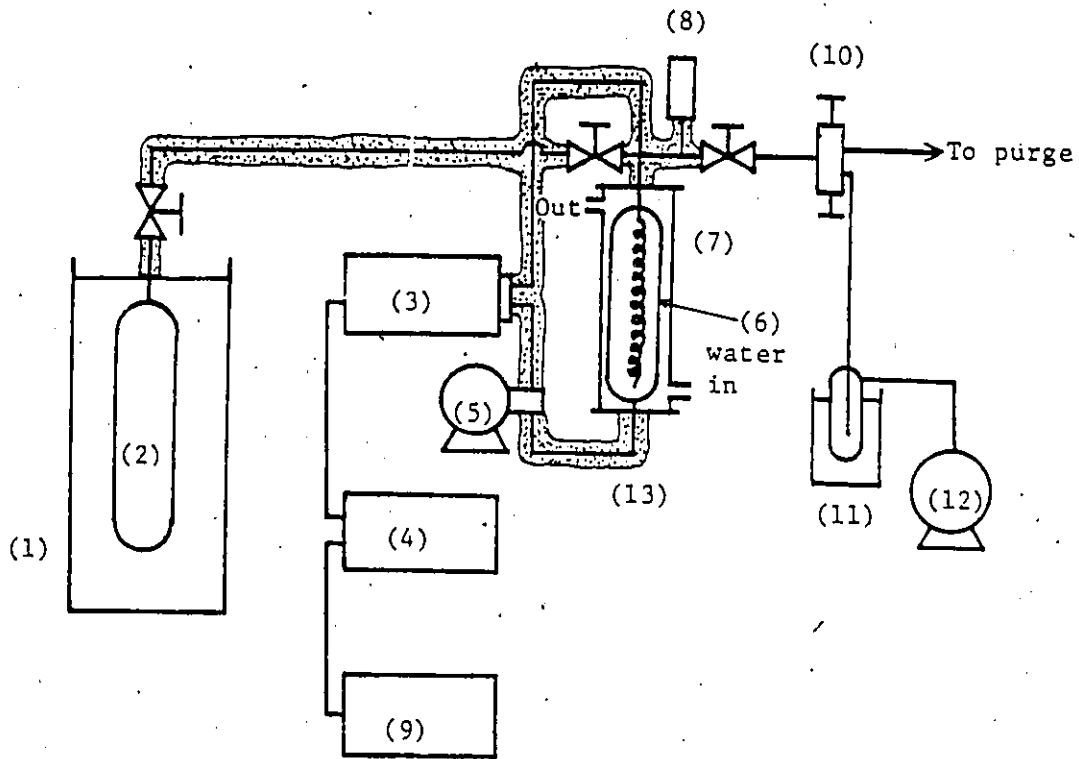


Figure 5-3 Equilibration cell used for the measurements of gas-saturated solution densities.

rod. The solvent which was to be fully saturated, was provided through a syringe needle onto the surface of the coil at the top end of the spiral coil. Saturation was enhanced while the liquid flowed downward creeping on the outside surface of the spiral coil, exposing a thin film and providing good contact with the solute gas present in the vessel. The gas-saturated solvent which passed down the spiral coil was then circulated from the equilibration cell to the sample tube of the density meter by means of the metering pump, and returned back to the equilibration cell via the syringe needle. Thus the solvent liquid was circulated and saturation was promoted. By utilizing such an equilibration technique, complete saturation was rapidly achieved.

A schematic diagram of the apparatus used for the density measurements of gas-saturated solutions is shown in Figure 5-4. With reference to this figure, the operating procedure was as follows. First, approximately 10 cm<sup>3</sup> of solvent was provided into the equilibration cell (6) and then vacuum was applied while hot water was circulating through the jacket (7) in order to degass the solvent. After the degassing operation was completed, the temperatures of the circulating water and the thermostat of the sample tube in DMA 512 were adjusted to the measurement temperature. Then the solute gas was introduced into the cell and brought to the experimental pressure. Then the solvent which was in contact with the solute gas in the cell, was circulated through the sample tube in DMA 512 (3)



- (1) Water bath
- (2) Gas storage cylinder
- (3) DMA 512
- (4) DMA 60
- (5) High pressure precision metering pump
- (6) Equilibration cell
- (7) Jacket for water circulation
- (8) Pressure transducer
- (9) Analog recorder
- (10) Two way valve
- (11) Liquid nitrogen trap
- (12) Vacuum pump
- (13) Insulation

Figure 5-4 Schematic diagram of the apparatus used for the density measurements of gas-saturated solutions.

by means of the high pressure precision metering pump (5). The pressure measurement in the equilibration cell was made by means of a pressure transducer(8) obtained from Data Instruments. In order to maintain the constant temperature condition, the system tubing through which the solvent was circulated was well insulated. As time elapsed, the pressure tended to decrease since the gas dissolved in the solvent. The operation was carried out in such a manner that the pressure was kept essentially constant by constantly providing solute gas from the storage cylinder(2) into the equilibration cell(6). Equilibrium was considered to have been established when the gas pressure and the output of the digital display (4) of DMA 60 remained constant. Finally, the period of oscillation appearing on the display of DMA 60 was recorded. Density measurements were carried out for each solvent-solute gas system at constant temperature and at several pressures ranging from a pressure slightly higher than atmospheric to that close to the saturation pressure of the solute gas.

#### 5.5 CALIBRATION OF THE HIGH PRESSURE DENSITY METER

Prior to the density measurements of gas-saturated solutions, calibration of the density meter was necessary. The calibration was conducted for the same temperatures as those used for the density measurements. Two reference substances whose densities under pressure were known were required for the calibration. For these substances distilled water and

nitrogen were used. The densities of distilled water at the calibration temperatures and elevated pressures were taken from those available in the tables by Haar Kell et al. (117). The density data of distilled water at three different calibration temperatures, 298.15 K, 323.15 K, and 343.15 K at different pressures are shown in Table 5-1.

Since the densities of nitrogen required for the calibration were very accurately reproduced by utilizing the Pitzer-Curl method to predict the second virial coefficient (described in Chapter 4) when compared to those available in the tables prepared by Din (119), the Pitzer-Curl method was used. For comparison, molar volumes of nitrogen by prediction, and those of Din, are both shown in Table 5-2.

At constant temperature and varied pressures, the calibration constant for the density measurement at high pressures as obtained by means of the Anton Paar density meter is expressed by the following equation:

$$A = \frac{Q_1^2 - Q_2^2}{\rho_1 - \rho_2} \quad (5-7)$$

In the above equation,  $\rho_2$  and  $\rho_1$  are the densities of the reference substances, nitrogen and distilled water, and  $Q_2$  and  $Q_1$  are the periods of oscillation read from the DMA 60 for nitrogen and distilled water, respectively. The "A" in the above equation is the calibration constant. At constant temperature, the calibration constant (A) values resulting from the calibration at varied pressures changed very little

as expected, and therefore these values were regarded as pressure-independent constants. Thus the density,  $\rho$  of any solution whose period of oscillation was read as  $Q$  from the DMA 60, was expressed by the following equation:

$$\rho = \frac{1}{A} (Q^2 - Q_2^2) + \rho_2 \quad (5-8)$$

In the above equation, the period of oscillation for nitrogen,  $Q_2$  was linearly correlated with pressure accurately at all the calibration temperatures:

$$Q_2 = k_1 + k_2 P \quad (5-9)$$

In the above equation,  $k_1$  and  $k_2$  are temperature-dependent constants.

On the other hand, the density of nitrogen,  $\rho_2$  was also expressed as a function only of pressure at constant temperature based on the Pitzer-Curl method to predict the second virial coefficient:

$$\rho_2 = M_2 (MD)_2 \quad (5-10)$$

In the above equation,  $M_2$  is the molecular weight of nitrogen, and  $(MD)_2$  is the molar density of nitrogen given by Equation (4-3).

Thus by substituting Equations (5-9) and (5-10) into Equation (5-8), the density of any solution was expressed as a function only of pressure, P, and the period of oscillation, Q, the resulting form of the equation is:

$$\rho = \frac{1}{A} \{Q^2 - (k_1 + k_2P)^2\} + M_2(MD)_2 \quad (5-11)$$

The values for the calibration constants, A,  $k_1$ ,  $k_2$  and the second virial coefficient for nitrogen, B, are listed in Table 5-3 for the measurement temperatures, 298.15 K, 323.15 K and 343.15 K.

Table 5-1. Densities of water at temperatures of 298.15 K, 323.15 K and 343.15 K at elevated pressures (117).

Pressure (Bar)	Density		
	298.15 K	323.15 K	343.15 K
1	0.99706	0.98803	0.97778
2	0.99711	0.98807	0.97782
3	0.99715	0.98812	0.97787
4	0.99720	0.98816	0.97791
5	0.99724	0.98820	0.97796
6	0.99729	0.98825	0.97800
7	0.99733	0.98829	0.97805
8	0.99738	0.98834	0.97809
9	0.99742	0.98838	0.97813
10	0.99747	0.98842	0.97818
11	0.99751	0.98847	0.97822
12	0.99756	0.98851	0.97827
13	0.99760	0.98855	0.97831
14	0.99765	0.98860	0.97835
15	0.99769	0.98864	0.97840
16	0.99774	0.98868	0.97844
17	0.99778	0.98873	0.97849
18	0.99783	0.98877	0.97853
19	0.99787	0.98881	0.97857
20	0.99792	0.98886	0.97862
21	0.99796	0.98890	0.97866
22	0.99801	0.98894	0.97871
23	0.99805	0.98899	0.97875
24	0.99810	0.98903	0.97879
25	0.99814	0.98908	0.97884

Table 5-2. Comparison of molar volumes of nitrogen available in Din's table with those calculated by Pitzer-Curl method.

Pressure (atm)	Molar volumes of nitrogen				
	290°K	300°K	320°K	340°K	360°K
1	23791	24613	26258	27902	29546
	23791	24614	26259	27903	29547
5	4753.3	4919.4	5251.2	5582.5	5913.4
	4753.4	4919.6	5251.5	5582.9	5913.9
10	2373.9	2457.9	2625.5	2792.6	2959.4
	2373.7	2457.8	2625.6	2792.9	2959.7
15	1580.9	1637.6	1750.5	1862.9	1974.9
	1580.4	1637.2	1750.3	1862.8	1975.0
20	1184.6	1227.6	1313.0	1398.0	1482.7
	1183.8	1226.9	1312.6	1397.8	1482.6
25	946.9	981.7	1050.7	1119.3	1187.5
	945.8	980.7	1050.0	1118.8	1187.2

Upper column: from tables by H. Din (119).  
 Lower column: calculated by Pitzer-Curl method.

Table 5-3. Calibration constants for high pressure density meter and the second virial coefficients for nitrogen.

Temperature (K)	$k_1$ (*)	$k_2$ (*)	A	B (cm <sup>3</sup> /mol)
298.15	376514.3	29.503	$1.90129 \times 10^{10}$	-4.353
323.15	378329.4	27.476	$1.92524 \times 10^{10}$	0.1877
343.15	379918.2	26.000	$1.93505 \times 10^{10}$	3.294

(\*) In Equation (5-9), the units of pressure, P is atm.

5.6 APPARATUS AND OPERATING PROCEDURE FOR MEASUREMENT OF GAS SOLUBILITY AT ELEVATED PRESSURES

A gas solubility apparatus for use up to 20 MPa was developed based on the dynamic or solvent-flow method. In this method, the solubilities were determined by measuring the volumes of solute gas required to steadily form a gas-saturated solution when using a small constant flow of degassed solvent. Degassed solvent, prepared by the boiling method, was provided into the equilibration cell by means of a high pressure precision metering pump. The gas-liquid equilibration technique adopted was similar to that utilized for the density measurement of the gas-saturated solution. That is, while the liquid was flowing downward at a very low flow rate on the surface of the stainless steel coil installed inside the gas-filled equilibration cell, it became saturated with the compressed solute gas.

The new apparatus developed in this investigation has several advantages. First it requires only a small amount of gas and liquid for a measurement; it also requires only a short time for a measurement. The design of the apparatus is simple, and therefore, the operation for a solubility measurement is also simple. This apparatus is suitable for solubility measurements of highly soluble gases, at elevated pressures.

As well as advantages, there are several disadvantages of the new apparatus. First, the pressure needs to be kept very constant since the pressure effect on gas solubility is

significant and hand control of pressure is tedious. Next, the apparatus is not entirely suitable for solubility measurements of slightly soluble gases.

With regard to the second disadvantage, although actual solubility measurements have not been made for slightly soluble gases, it is considered that much more solvent would be required for such systems than for gases of high solubility. However, in order to ensure the saturation of solvent with solute gas, the flow rate could not be increased significantly. Therefore, the time required for a measurement would become much longer than for gases of high solubility. Also, the correction for the change in gas volume would be affected by the significant increase in the volume of gas-saturated solution which results.

The problem of the volume occupied by the gas-saturated solution was also considered for the highly soluble gases as measured in this investigation. Only a small amount of liquid solvent was required for the highly soluble gases. However, in light of this problem, an appropriate data reduction method was established in order to precisely determine the gas solubilities. This aspect is further discussed in the following section concerning the treatment of data for gas solubility at elevated pressures.

The major components utilized in the high pressure solubility apparatus include a volume-regulating cylinder equipped with a piston, for the quantitative supply of solute gas into the equilibration cell, a stainless steel

vessel for the storage of liquified gas, and the equilibration cell. Also used were a high precision metering pump to provide a constant flow of degassed solvent to the equilibration cell, and a pressure transducer for the precise measurement of the system pressure. More detailed descriptions of these major items of the apparatus are given below.

The gas volume-regulating cylinder was a Ruska positive displacement pump of 100 cm<sup>3</sup> capacity suitable for pressures up to 13 MPa. This pump consisted of a piston and a cylinder. The position of the piston in the cylinder was adjusted by rotating the head. Connected to the head was a vernier scale readable to 0.1 cm<sup>3</sup>. The piston was sealed by means of teflon packing. For the solubility measurements, the volumetric displacement and position readings were calibrated utilizing distilled water.

A stainless steel vessel of 400 cm<sup>3</sup> capacity was purchased from Whitey and used as the gas supply cylinder. The gas storage cylinder was included as part of the apparatus to avoid any chance for condensation within the measurement system since the whole cylinder was immersed in the constant temperature bath. Such an arrangement was also considered to ensure that the gas remained at the measurement temperature.

A high pressure precision metering pump, which was used to provide the degassed solvent to the equilibration cell, was supplied by Milton Roy. This pump with an extremely

small pump capacity was capable of delivering solvents at pressures up to 41 MPa over flow ranges of 1.9 ml/hr to 19 ml/hr. The flow rate was adjustable, and the pump components that contacted the solvents were made of stainless steel, sapphire and teflon. Very low, but constant and highly reproducible flow rates of solvents, as required in the solubility measurement were made possible by utilizing this metering pump.

For the purpose of measuring the system pressure during solubility experiments, a pressure transducer purchased from Data Instruments and suitable for pressures up to 2.7 MPa was utilized. Calibration of the transducer was accomplished with a dead-weight gauge.

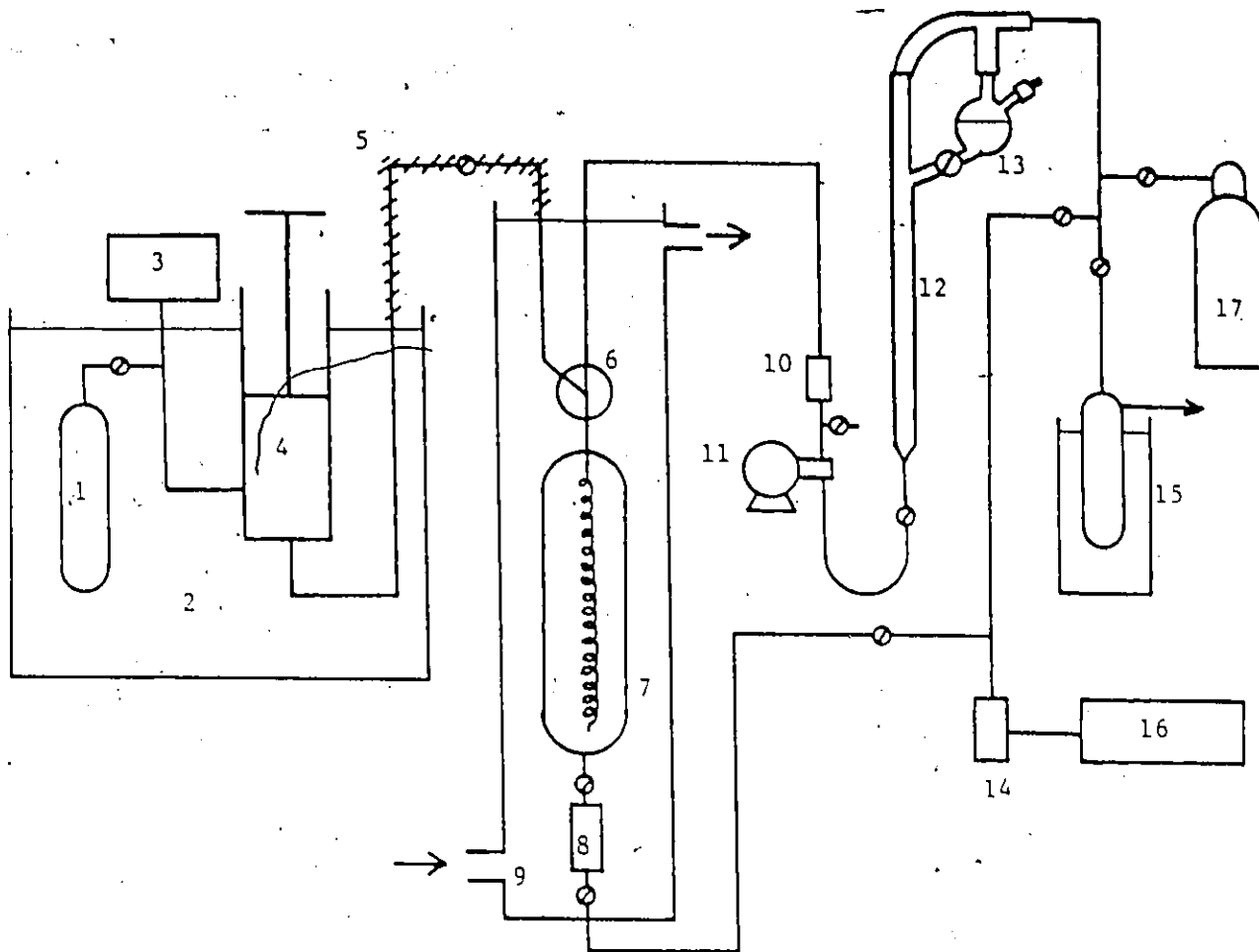
A stainless-steel vessel, 300 cm<sup>3</sup> in capacity, was used as the equilibration cell. The gas-liquid equilibration technique used was similar to that utilized in the measurement of gas-saturated solution densities. In this measurement, instead of circulating the solvent, solvent was provided to the equilibration cell at a very low flow rate such that the liquid attained equilibrium by the time it passed down the spiral coil inside the equilibration cell.

Preliminary experiments were made to ensure that equilibrium was actually established in the equilibration cell. These attempts involved first providing small portions of degassed solvent intermittently into the cell filled with solute gas at a predetermined pressure and then observing the pressure drop. In all cases, the pressure drop was

rapid and corresponded to the solvent supply because of the dissolution of the gas in solvent. It was confirmed from these attempts that the saturation process of the solvent with solute gas was fairly prompt. Furthermore, the partially-filled cell containing gas was left for an extended period of time (one day) without any further change in pressure. As a result, it was considered that on reaching the end of the coil in the equilibration cell, the solvent was completely saturated.

The schematic diagram of the solubility apparatus used in this study and details of the equilibration cell are presented in Figure 5-5 and 5-6 respectively.

The operating procedure for the gas solubility measurement will be described with reference to Figure 5-5. First approximately 30 cm<sup>3</sup> of solvent was charged into the degassing flask(13). Vacuum and heat were applied to this flask to cause boiling of the solvent so that the solvent was completely degassed. The degree of vacuum in the flask was checked by means of a pressure transducer(14) and a recorder(16). The degassed solvent was then transferred to a burette(12) from which it was pumped into the equilibration cell(7) by means of a high pressure precision metering pump(11). Helium gas was introduced from a cylinder(17) to make the pump intake pressure at least atmospheric pressure, thereby allowing the pump to function well. Helium was used as a pressuring medium because of its extremely low solubility in all solvents.



- 1 Solute storage cylinder
- 2 Constant temperature water bath
- 3 Pressure measurement system
- 4 Solute gas volume-regulating cylinder
- 5 Tape heater
- 6 Gas-liquid connector
- 7. Equilibrium cell
- 8 Solution sampler
- 9 Constant water circulation jacket
- 10 One way valve
- 11 Precision metering pump for high pressure
- 12 Solvent burette
- 13 Degassing flask
- 14 Pressure transducer
- 15 Liquid nitrogen trap
- 16 Chart recorder
- 17 Helium gas cylinder

Figure 5-5 Schematic diagram of the volumetric apparatus used for the measurements of gas solubilities at elevated pressures.

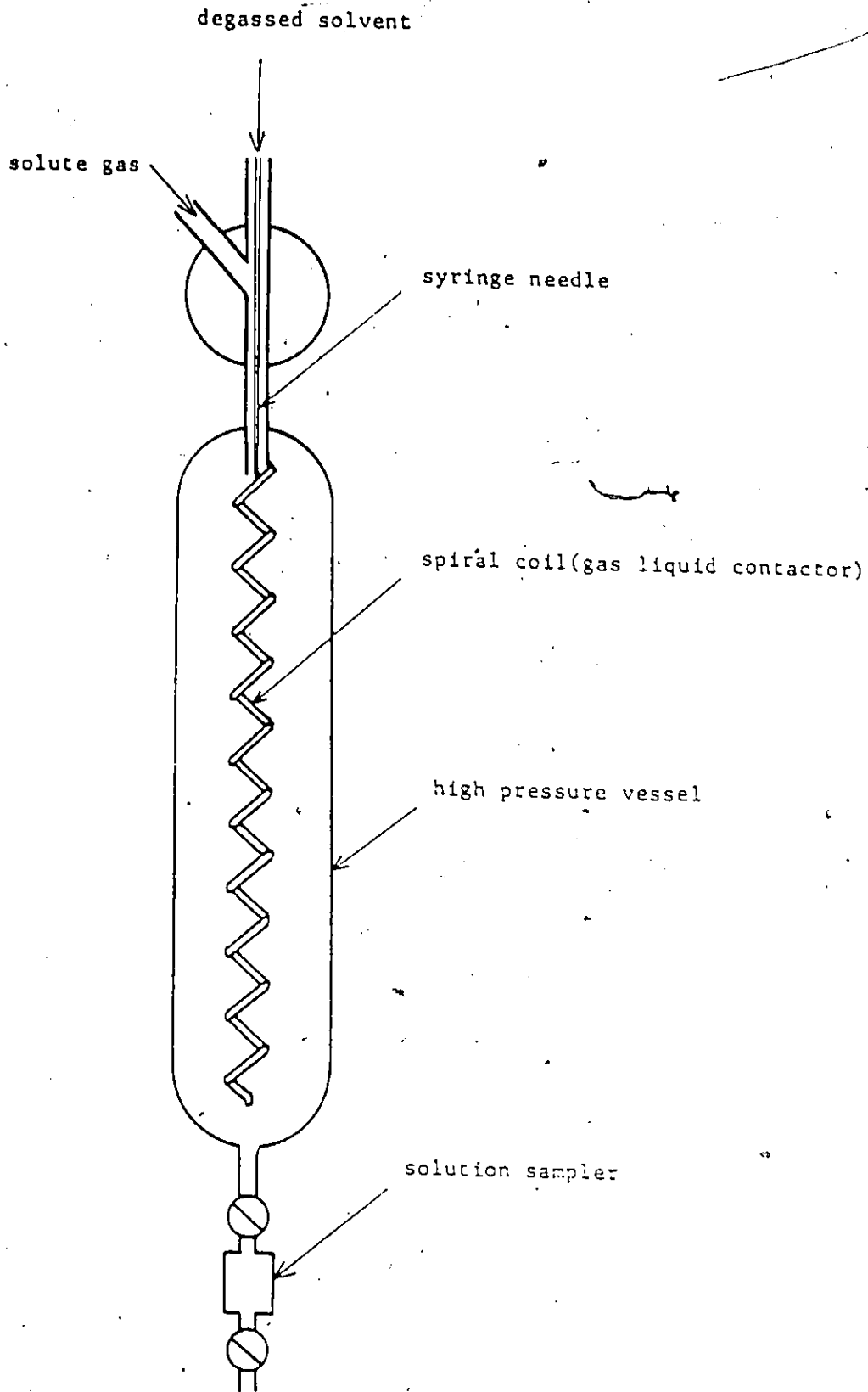


Figure 5-6 Equilibration cell used for the measurements of gas solubilities at elevated pressures.

In preparation for a solubility experiment, solute gas was charged into an evacuated and refrigerated storage cylinder(1) causing liquefaction of the gas. The solute gas storage cylinder was then attached to the system as shown in Figure 5-5. The system involving the gas volume-regulating cylinder(4), the equilibrium cell(7) and the solution sampler(8) was then evacuated until a high degree of vacuum was established ( $2.5 \times 10^{-2}$  Torr). The degree of vacuum was checked with a pressure transducer(14) and a recorder(16). Gas was then introduced into the evacuated equipment until the pressure reached the experimental pressure. A constant temperature condition for the complete solubility apparatus was achieved by means of the water baths(2,9), which were controlled to 0.02 K.

As the solvent was pumped into the equilibration cell by means of the precision metering pump, the pressure of the gas tended to drop slightly, as the gas dissolved in the solvent. Immediately, additional gas was added to compensate for the gas dissolved. Measurement of changes in gas volume was made by means of the movable indicator and vernier scale of the volume-regulating cylinder while keeping the total pressure essentially the same. During operation, the volumes of both solute gas and solvent were read at regular time intervals. The volume of solvent was read from the solvent supply burette. For all the solubilities measured, the volume change of solute gas and that of solvent were linearly related.

5.7 TREATMENT OF DATA FOR GAS SOLUBILITY AT ELEVATED PRESSURES

If it was assumed that the volume of the gas-saturated solution in the equilibration cell was negligible, it would be very simple to calculate the solubility for data obtained with the solubility apparatus for use at elevated pressures. The calculation would be the same as for solubility measurements at atmospheric pressure: Equations (5-4) and (5-5) would be equally useful for solubility measurements at elevated and atmospheric pressure. Although the amount of degassed solvent required for an actual measurement was relatively small (usually less than 3 cm<sup>3</sup>) when compared with the cell capacity (300 cm<sup>3</sup>), for all the systems investigated, a procedure was developed for the precise determination of gas solubility.

It was considered that in the actual measurement, the volume of solute gas dissolved was underestimated by a volume equivalent to that of the gas-saturated solution accumulated in the equilibration cell. Hence the volume of gas dissolved is equivalent to the volume of pure gas supplied to the cell, added to the net gas volume displaced by the accumulated solution. Therefore, it was first considered necessary to know the volume of gas-saturated solution formed in each experiment for the precise determination of gas solubility.

For the calculation of solubility, let the volumes of gas dissolved and solvent used, as measured over a certain

time period, be  $v_2$  and  $v_1$ . Also, let the volume of the gas-saturated solution formed in the cell be  $v_s$ , assuming this volume to be directly measurable. Further, the volume of gas displaced by the saturated liquid solution is itself saturated by the solvent vapor. A pressure correction is therefore necessary to determine the equivalent volume of pure gas. Let the total pressure and the partial pressure of solute gas be  $P$  and  $P_2$ , respectively. Then the mole ratio of the solute to solvent in the gas-saturated solution may be expressed as:

$$\frac{x_2}{x_1} = \frac{v_2(\text{MD})_2 + v_s \frac{P_2}{P} (\text{MD})_2}{v_1(\text{MD})_1 + v_s \frac{P - P_2}{P} (\text{MD})_2} \quad (5-12)$$

In the above equation,  $(\text{MD})_2$  is the molar density of solute at the measurement pressure,  $P$  and temperature,  $T$ , and  $(\text{MD})_1$  is the molar density of solvent at the temperature at which the volume measurement of solvent was made.

In Equation (5-12), it was considered that the term,  $P_2/P$  was approximately unity, especially at high pressures and for non-volatile solvents as investigated in this work. Then Equation (5-12) was rewritten as:

$$\frac{x_2}{x_1} = \frac{v_2 + v_s}{v_1} \cdot \frac{(\text{MD})_2}{(\text{MD})_1} \quad (5-13)$$

The volume of the gas-saturated solution,  $v_s$ , may be expressed by the following equation utilizing the value for the mass density of the gas-saturated solution:

$$v_s = v_1(\text{MD})_1 \cdot \frac{x_1 M_1 + x_2 M_2}{x_1 \rho_s} \quad (5-14)$$

In the above equation,  $x_1$ ,  $x_2$ ,  $M_1$ ,  $M_2$  and  $\rho_s$  are, respectively, the mole fractions of solvent and solute in the solution, the molecular weights of solvent and solute, and the mass density of gas-saturated solution. The last property was measured in this investigation.

The combination of Equations (5-5), (5-13), and (5-14) results in the following equation:

$$x_2 (P, T) = \frac{v_2/v_1 + (\text{MD})_1 M_1/\rho_s}{v_2/v_1 + (\text{MD})_1/(\text{MD})_2 + (\text{MD})_1(M_1 - M_2)/\rho_s} \quad (5-15)$$

In actual measurements, for all the systems investigated, a linear relationship was found between the volumes of gas dissolved and the volumes of solvent used. Therefore, the best value of the volume ratio,  $v_2/v_1$ , was obtained by means of the least squares method. Using the slope of the linear relation to be (SP), Equation (5-15) becomes:

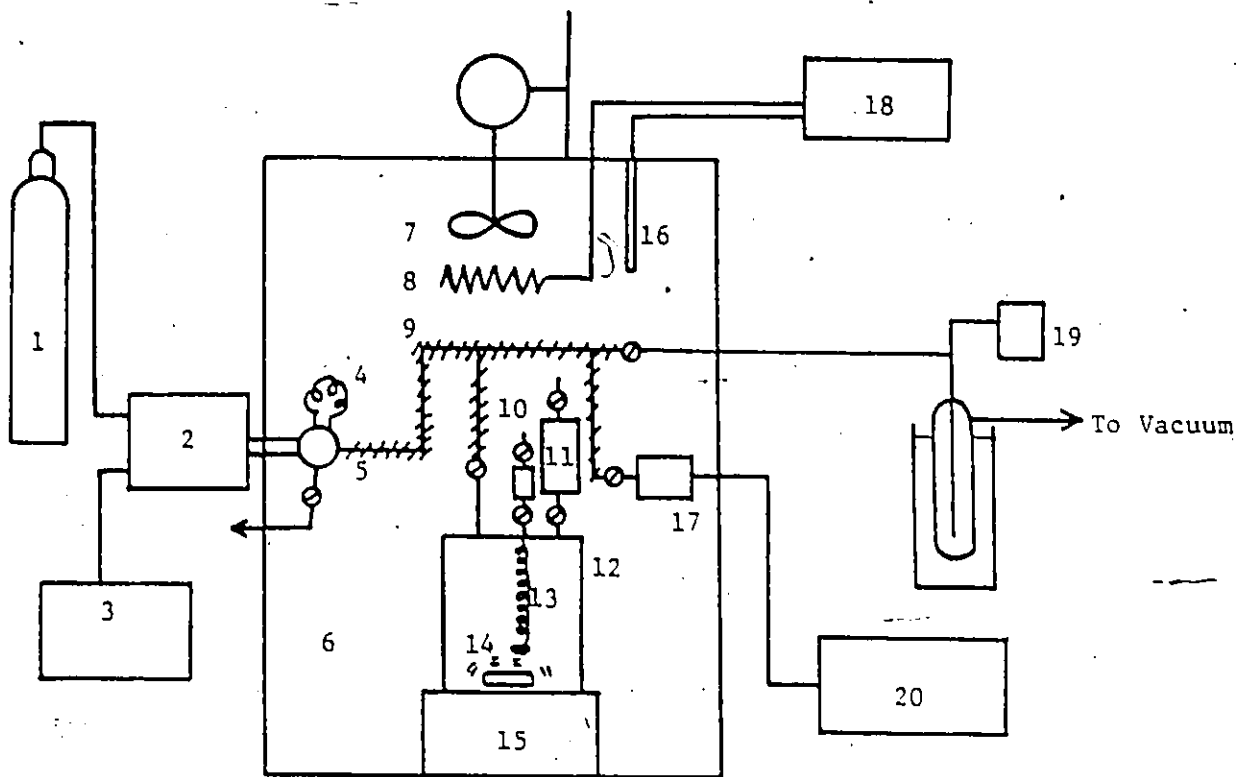
$$x_2 (P, T) = \frac{(\text{SP}) + (\text{MD})_1 M_1/\rho_s}{(\text{SP}) + (\text{MD})_1/(\text{MD})_2 + (\text{MD})_1(M_1 - M_2)/\rho_s} \quad (5-16)$$

Equation (5-16) was utilized for the calculation of the gas solubilities measured at elevated pressures.

#### 5.8 APPARATUS AND OPERATING PROCEDURE FOR GAS CHROMATOGRAPHIC ANALYSIS OF GAS-SATURATED SOLUTIONS

A system for gas chromatographic analysis of gas-saturated solutions was designed and constructed in order to check the validity of the volumetric determination of gas solubility as described in the previous section. The apparatus was constructed according to the design described by Ohgaki et al. (121) for such analyses, but with some modifications. Gas chromatographic analyses were made for solutions of n-octane saturated with propene or isobutene at temperatures of 298.15 K and 323.15 K and pressures ranging from 152 to 1600 kPa.

The gas chromatograph utilized in this investigation was a Varian Aerograph Series 1400 model, which utilized a Hewlett Packard model 3390 A integrator. The gas chromatographic column was made of stainless steel tubing 1/8 inch in diameter and 1.5 meters in length, and was packed with Porasil C supplied by Chromatographic Specialities. Descriptive diagrams of the equipment involved in the gas chromatographic analysis are shown in Figures 5-8 and 5-9 along with the calibration lines required for the gas-chromatographic analysis. The procedure for calibrating the gas chromatograph for analyzing gas-saturated liquid solutions under pressure will be described using Figure 5-7.



- 1 Helium gas cylinder
- 2 Gas chromatograph
- 3 Recorder/integrator
- 4 Sample loop
- 5 Six-way valve
- 6 Air bath
- 7 Fan
- 8 Heater
- 9 Tape heater
- 10 Solvent sampler
- 11 Solute gas sampler
- 12 Solution expansion cell
- 13 liquid leading coil
- 14 Magnet rod
- 15 Magnet stirrer
- 16 Temperature sensor
- 17 Pressure transducer
- 18 Temperature controller
- 19 McLeod gauge
- 20 Chart recorder

Figure 5-7 Schematic diagram of the apparatus used for the gas chromatographic analysis of gas-saturated solutions.

Prior to the actual analysis of the gas-saturated solutions, calibration lines were obtained to relate the area ratio of solute gas to solvent as obtained by gas chromatography to the actual mole ratio as determined by weight. To accomplish this, gas mixtures of known composition were prepared and analyzed by a gas chromatograph (2) equipped with an integrator (3) to obtain the corresponding area ratio. A gas mixture of known mole ratio was prepared by accurately weighing the liquefied solute gas and solvent in miniature samplers (10 and 11) before and after discharging small quantities of each into the solution expansion cell (12) for analysis. Dry ice was used to cause liquefaction of the solute gas in the gas sampler.

After the air bath (6) reached the predetermined temperature of 323 K, the gas and solvent sample tubes of known weights were attached (but not discharged) to the solution expansion cell. Then, the expansion cell was evacuated to the maximum degree of vacuum possible by the vacuum pump. The degree of vacuum was always checked by means of a McLeod gauge. When the pressure became as low as  $2.5 \times 10^{-2}$  Torr, the valve above the solution expansion cell was closed and the solvent and solute gas were partially released from the samplers into the expansion cell by momentarily opening the valves. Then a magnet (14), driven by a magnetic stirrer (15) to enhance the mixing of the solute gas and solvent, was started. Subsequently, a portion of the gas mixture was introduced into the gas chromatograph by

way of a sample loop (4), for analysis. After the analysis was complete, the samplers were detached and weighed. The difference in weights before and after removal of the solute gas and solvent allowed the calculation of the actual mole ratio. Let the weights of samplers which contain solute, and solvent before removal be  $W_2$ , and  $W_1$ , respectively. Also, let these weights after removal be  $W_2'$ , and  $W_1'$ , respectively. Then the actual mole ratio may be simply expressed by the following equation:

$$\frac{x_2}{x_1} = \frac{(W_2 - W_2')/M_2}{(W_1 - W_1')/M_1} \quad (5-17)$$

In the above equation,  $M_2$  and  $M_1$  are the molecular weights of solute and solvent.

The area ratio of solute to solvent, was directly calculated by utilizing the integrated areas resulting from the gas chromatographic analysis of the mixture of known mole ratio.

Such a procedure was repeated for many gas mixtures and hence a calibration line for a solute-solvent system was obtained. Figures 5-8 and 5-9 are the calibration lines for n-octane-propene and n-octane-isobutene systems, respectively. In these diagrams, the abscissa represents the area ratio of solute to solvent, and the ordinate represents the actual mole ratio.

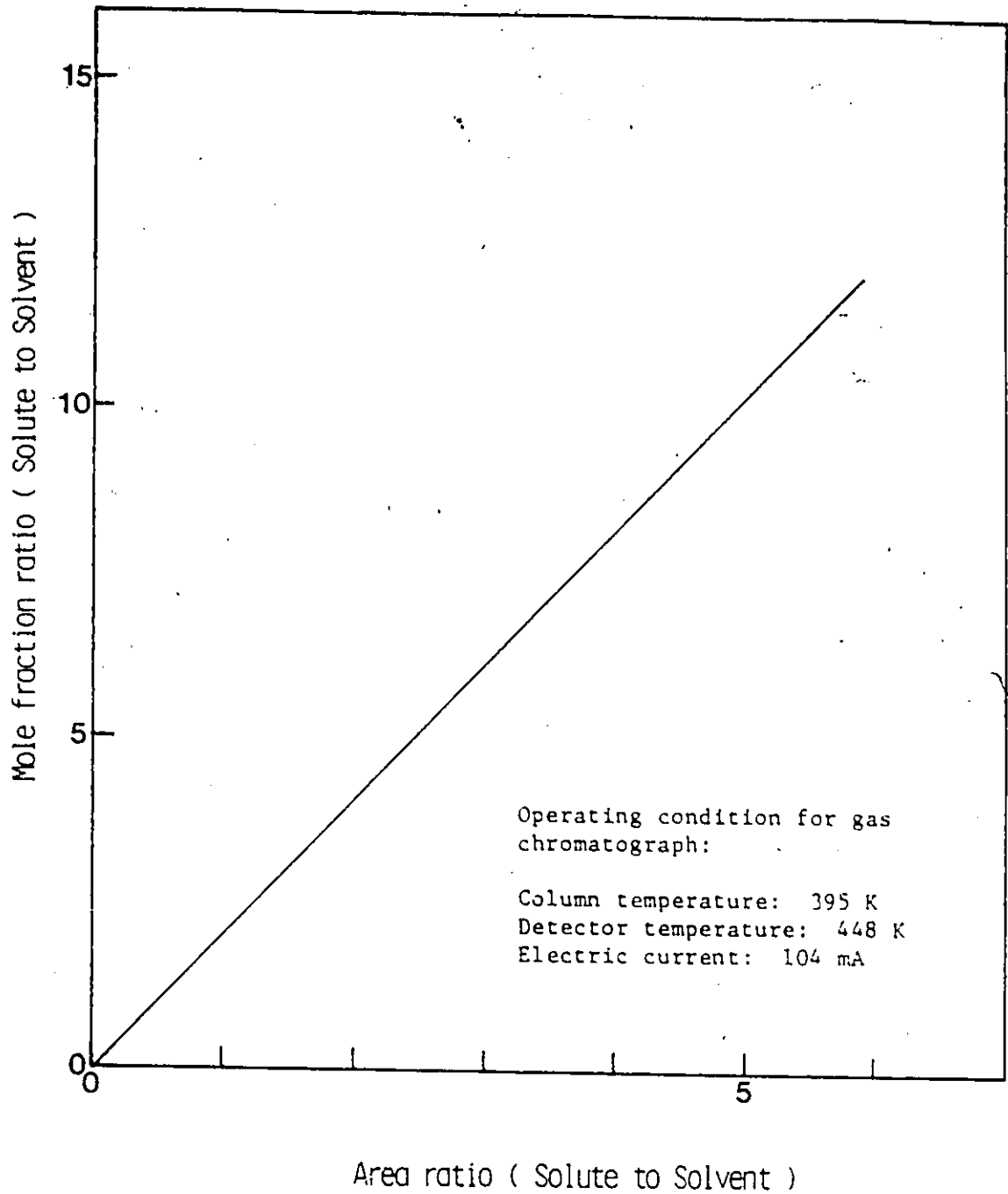


Figure 5-8 Calibration line used for the gas chromatographic analysis for Propene-saturated n-Octane solutions.

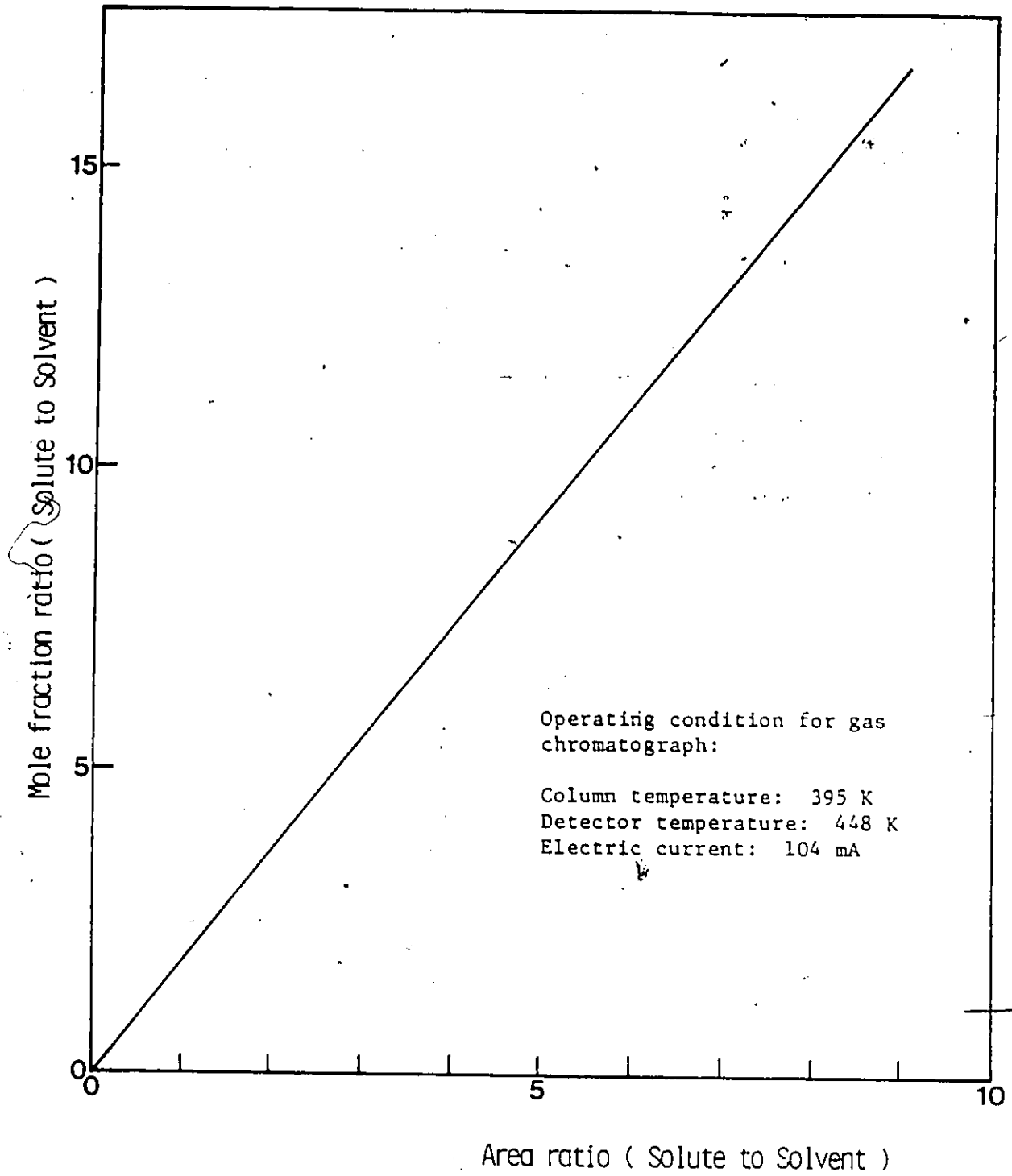


Figure 5-9 Calibration line used for the gas chromatographic analysis for isobutene-saturated n-Octane solutions.

The procedure for analyses of the gas-saturated liquid solutions under pressure was similar to that used for calibration of the gas chromatograph. After the solubility experiment was complete, a small portion (approximately 0.5 cm<sup>3</sup>) of gas-saturated solution was sampled from the volumetric apparatus. Then the sampler was attached to the expansion cell and was completely vaporized into the evacuated cell (12). The resulting area ratio as obtained by the integrator could then be immediately converted to the corresponding mole ratio by use of the calibration curves previously prepared.

CHAPTER VI

RESULTS AND DISCUSSION

The presentation and discussion of the experimental results have been separated into various sections. Section one deals with the density measurement of solvents and gas solubilities at atmospheric pressure. Section two discusses the measurement of gas-saturated solution densities at elevated pressures and their prediction by the SRK equation of state. Section three deals with the gas solubilities as measured at elevated pressures and compared with two prediction methods for gas solubility. One prediction method involves the use of the SRK equation of state and the other utilizes the UNIFAC method. The former method utilizes solvent-solute binary interaction parameters which have to be determined using known vapor-liquid equilibrium data. The latter method utilizes activity coefficients for the liquid phase, which can be directly estimated. In section four, the gas-chromatographic analysis of gas-saturated solutions is discussed. The results from the volumetric gas solubility measurements are compared with those obtained by gas-chromatographic analyses. Finally, in the last section, the gas solubility correlation developed in this investigation is discussed. Summary of the estimated precision for each measurement is available in Appendix F.

6.1 SOLVENT DENSITY AND GAS SOLUBILITY MEASUREMENTS AT ATMOSPHERIC PRESSURE

Prior to the measurement of gas solubilities at atmospheric pressure, the densities of the solvents, n-octane, chlorobenzene and n-butanol were measured utilizing the Anton Paar density meter designed for use at atmospheric pressure. These data were required for the precise determination of gas solubilities. The measurements were conducted at three different temperatures, 298.15 K, 323.15 K, and 343.15 K. The results obtained are tabulated in Table 6-1 along with those available in the literature.

The densities of n-octane as measured by Chappelow, Winnick et al. (126) were available for comparison. These are tabulated in Table 6-2 and are shown in Figure 6-1. These workers made precise density measurements for n-octane at atmospheric pressure by means of a displacement technique. In their method, a sinker made of borosilicate glass, of known mass and volume at a specified temperature, was immersed and suspended in the liquid to be examined. The top end of the suspension chain that suspended the sinker was connected to a balance so that the weight of the sinker immersed in the liquid could be precisely measured. The liquid densities were calculated based on the difference in the weights before and after immersion of the sinker. The accuracy claimed in their density measurements is  $\pm 0.00001 \text{ g/cm}^3$ .

Table 6-1. Densities of n-octane, chlorobenzene and n-butanol solvents at atmospheric pressure.

Solvent	Temperature (K)	Density (g/cm <sup>3</sup> )	
		This work	Literature value
n-octane	298.15	0.6987	0.69879 (*)
	323.15	0.6781	0.67825 (*)
	343.15	0.6613	0.66137 (*)
chlorobenzene	298.15	1.1008	1.10085 (124)
	323.15	1.0733	
	347.15	1.0517	
n-butanol	298.15	0.8060	0.8060 (125)
	323.15	0.7866	0.7867 (125)
	343.15	0.7703	0.7703 (125)

(\*) Interpolated utilizing densities shown in Table 6-2.

Table 6-2. Densities of n-octane at atmospheric pressure by Chappelow, Winnick et al. (126).

Temperature (K)	Density (g/cm <sup>3</sup> )
278.67	0.71439
283.14	0.71082
288.87	0.70624
299.25	0.69788
303.60	0.69435
308.72	0.69016
313.99	0.68614
318.06	0.68249
323.31	0.67815
328.06	0.67417
333.12	0.66994
337.93	0.66550
342.78	0.66172
347.66	0.65755
352.85	0.65306

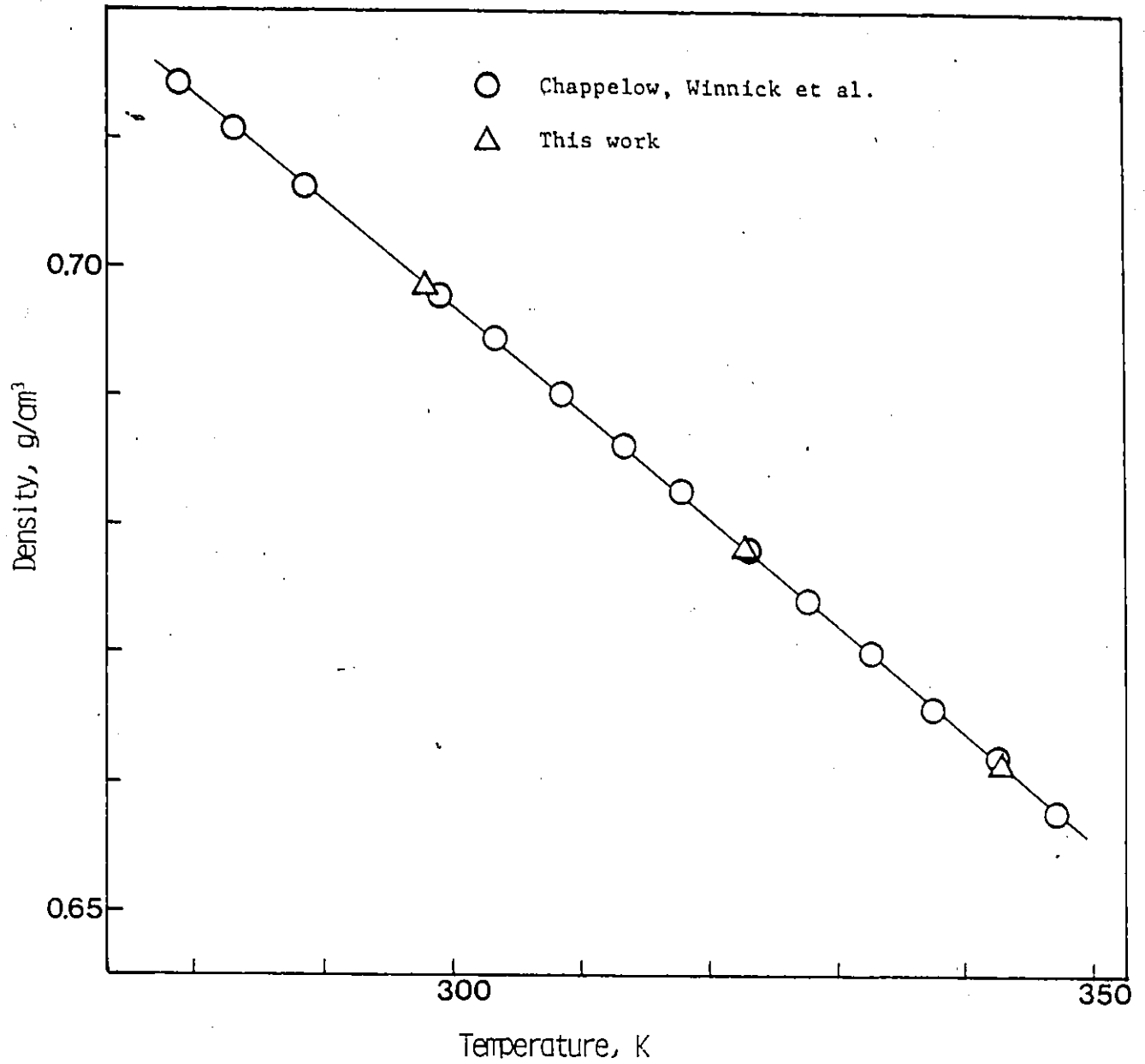


Figure 6-1 Densities of n-Octane at atmospheric pressure as a function of the absolute temperature.

As indicated in Table 6-1, the densities of n-octane by Chappelow, Winnick et al. and those of this investigation agree with good accuracy, to at least  $\pm 0.0002$  g/cm<sup>3</sup>. Therefore it was concluded that the method utilized for the density measurements at atmospheric pressure in this investigation was able to produce satisfactory density data.

The solubilities of propane, isobutene, n-butane and isobutane were measured at atmospheric pressure in the solvents n-octane, chlorobenzene and n-butanol. The experiments were conducted at three different temperatures, 298.15 K, 323.15 K and 343.15 K. The solubilities of propene and isobutene in these solvents were subsequently compared with those obtained at elevated pressures. The density measurements of these solvents were utilized in the calculation of gas solubilities. A sample calculation for the determination of gas solubility is shown for the n-octane-propene system measured at 298.15 K and 100.89 kPa in Appendix B.

The gas solubilities measured at atmospheric pressure are tabulated in Tables 6-3 to 6-6. The experiment was repeated two times for each system at the same temperature. In these tables, the numbers in brackets indicate the experimental pressures in kPa at which the measurements were made. The deviations of the two solubilities measured for the same system and at the same temperature were always less than 1% from the average.

It is conventional to convert gas solubilities measured at atmospheric pressure to ones calculated for a partial

Table 6-3. Solubilities of propene measured at atmospheric pressure in the solvents, n-octane, chlorobenzene and n-butanol.

Solvent	Temp. (K)	1		2	
n-octane	298.15	0.104	(100.89)*	0.104	(100.87)
	323.15	0.0584	(99.765)	0.0588	(99.992)
	343.15	0.0350	(100.79)	0.0351	(100.79)
chlorobenzene	298.15	0.0680	(100.63)	0.0684	(100.63)
	323.15	0.0380	(101.86)	0.0379	(101.25)
	343.15	0.0242	(101.06)	0.0247	(100.66)
n-butanol	298.15	0.0381	(100.02)	0.0379	(99.765)
	323.15	0.0212	(101.86)	0.0214	(101.86)
	343.15	0.0151	(100.79)	0.0153	(100.85)

Table 6-4. Solubilities of isobutene measured at atmospheric pressure in the solvents, n-octane, chlorobenzene and n-butanol.

Solvent	Temp. (K)	1		2	
n-octane	298.15	0.323	(99.125)*	0.320	(99.125)
	323.15	0.170	(99.765)	0.172	(100.01)
	343.15	0.102	(100.79)	0.102	(100.81)
chlorobenzene	298.15	0.229	(100.79)	0.231	(100.79)
	323.15	0.127	(102.03)	0.125	(101.46)
	343.15	0.691	(100.79)	0.0695	(100.66)
n-butanol	298.15	0.127	(99.992)*	0.127	(99.792)
	323.15	0.0667	(101.54)	0.0661	(100.50)
	343.15	0.0398	(101.33)	0.0398	(100.79)

\* Numbers in brackets indicate the measurement pressures in kPa; solubility in mole fraction

Table 6-5. Solubilities of n-butane measured at atmospheric pressure in the solvents, n-octane, chlorobenzene and n-butanol.

Solvent	Temp. (K)	1		2	
n-octane	298.15	0.430	(101.75)	0.427	(101.74)
	323.15	0.223	(101.86)	0.220	(101.18)
	343.15	0.132	(100.37)	0.129	(100.97)
chlorobenzene	298.15	0.270	(101.72)	0.274	(101.78)
	323.15	0.123	(100.98)	0.120	(100.97)
	343.15	0.0693	(99.992)	0.0689	(100.10)
n-butanol	298.15	0.137	(100.07)	0.137	(100.10)
	323.15	0.0685	(100.75)	0.0686	(100.75)
	343.15	0.0395	(100.77)	0.0398	(100.65)

Table 6-6. Solubilities of isobutane measured at atmospheric pressure in the solvents, n-octane, chlorobenzene and n-butanol.

Solvent	Temp. (K)	1		2	
n-octane	298.15	0.295	(100.07)	0.294	(100.89)
	323.15	0.152	(101.33)	0.151	(101.43)
	343.15	0.0860	(100.79)	0.0858	(100.79)
chlorobenzene	298.15	0.152	(100.58)	0.155	(100.49)
	323.15	0.0805	(101.51)	0.0804	(101.47)
	343.15	0.0472	(100.75)	0.0470	(100.79)
n-butanol	298.15	0.0887	(101.25)	0.0888	(100.62)
	323.15	0.0456	(100.59)	0.0461	(100.71)
	343.15	0.0273	(100.65)	0.0271	(100.66)

pressure of solute equal to one standard atmosphere. It is considered that such a conversion allows a comparison of solubilities for a common gas partial pressure. In order to make the conversion of gas solubilities measured at atmospheric pressure to those for a gas partial pressure of one atmosphere, Equation (5-6), as described in section three in Chapter 5, was utilized. The gas solubilities based on Equation (5-6) are tabulated in Table 6-7.

Equation (5-6) is developed using the assumption that Henry's law is applicable and that the liquid phase is ideal. Although these assumptions are usually valid, especially for non-volatile solvents such as those used in this investigation, another method of converting the gas solubility was tried for the purpose of comparison. This method involved the use of the Soave-Redlich-Kwong (SRK) equation of state. As discussed in Chapter 2, when applying equations of state to mixtures, binary interaction parameters are required at the temperature of interest. The best values of the parameters are usually determined by utilizing the data for phase equilibria. However, it is possible to determine the binary interaction parameters based on a single equilibrium datum. In this investigation, therefore, the binary interaction parameters were determined utilizing gas solubility data measured at atmospheric pressures. Once the interaction parameters were available for each solvent-solute system at the temperatures of gas solubility measurements, the SRK equation of state was used for the vapor-

Table 6-7. Gas solubilities for a gas partial pressure of 101.325 kPa.

Temperature = 298.15 K

Solute Gas	Solvent		
	n-Octane	Chlorobenzene	n-Butanol
Propene	0.106 (0.106)*	0.0697 (0.0698)	0.0389 (0.0389)
Isobutene	0.333 (0.333)	0.234 (0.237)	0.131 (0.131)
n-Butane	0.432	0.274	0.140
Isobutane	0.301	0.157	0.0904

Temperature = 323.15 K

Solute Gas	Solvent		
	n-Octane	Chlorobenzene	n-Butanol
Propene	0.635 (0.0636)	0.0400 (0.0402)	0.0221 (0.0222)
Isobutene	0.184 (0.184)	0.132 (0.133)	0.0695 (0.0700)
n-Butane	0.233	0.129	0.718
Isobutane	0.161	0.0847	0.0482

Temperature = 343.15 K

Solute Gas	Solvent		
	n-Octane	Chlorobenzene	n-Butanol
Propene	0.0416 (0.0419)	0.0283 (0.0284)	0.0176 (0.0177)
Isobutene	0.119 (0.120)	0.0796 (0.0804)	0.0458 (0.0469)
n-Butane	0.152	0.0800	0.0397
Isobutane	0.101	0.0542	0.0314

\* Calculated using the SRK equation of state.

liquid equilibrium calculation considering that the partial pressure of solute gas was equal to one atmosphere.

In this investigation, the SRK equation of state was also to be utilized for the systems involving propene and isobutene to predict the gas-saturated solution densities and solubilities of these gases at elevated pressures. Therefore, the calculations for the solubilities for a gas partial pressure of one atmosphere using the SRK equation of state were made for the same systems. The calculation results are shown in brackets in Table 6-7. It is found by comparison that the solubility data based on Equation (5-6) are nearly identical to the calculation results regardless of temperature. It may be noted that the agreement extends to the systems involving the polar substances, chlorobenzene and n-butanol. Based on the agreement thus obtained, it was concluded that Equation (5-6) was applicable for converting gas solubilities measured at atmospheric pressure to those for solute partial pressures equal to one atmosphere.

Gas solubilities that were previously reported by other workers are compared with those obtained in this investigation in Table 6-8. It may be seen in this table that generally good agreement was obtained between the solubilities reported by other workers and those obtained in this work, except for the solubility of n-butane in n-butanol at 323.15 K and the solubility of isobutane in chlorobenzene at 298.15 K. The deviation for the former system is small (less than 1 percent) only if the value of Blais et al.

Table 6-8. A comparison of gas solubilities reported for a gas partial pressure of 101.325 kPa.

Solute	Solvent	Temp. (K)	Solubility	This work
n-Butane	n-Octane	298.15	0.432 (2)	0.432
	Chlorobenzene	298.15	0.269 (127)	0.274
		325.15	0.131 (127)	0.129
n-Butanol		298.15	0.139 (128), 0.141 (127) 0.1401 (129)	0.140
		323.15	0.0686 (2), 0.0725 (127)	0.0718
Isobutane	Chlorobenzene	298.15	0.162 (127)	0.157
		323.15	0.0853 (127)	0.0847
	n-Butanol	298.15	0.0889 (127)	0.0904
		323.15	0.0486 (127)	0.0482

(127), as obtained in this laboratory some years ago, is considered. In the latter system (for the solubility of isobutane in chlorobenzene at 298.15 K), the solubility in this work is less than that reported by Blais et al. by 3 percent.

Three independent sources for the experimental data are available for the solubility of n-butane in n-butanol at 298.15 K. As shown in Table 6-8, the three reported solubilities agree within 1.4 percent. The solubility of 0.1401 as recently reported by Miyano et al. (129) was based on a solubility measurement that did not involve volumetric measurement. Instead, the method of Miyano was based on the mass of dissolved gas. Miyano utilized a mechanically agitated absorption cell of 70-cm<sup>3</sup> capacity in which degassed solvent contacted the solute gas to attain equilibrium. The solubility was determined from the weights of the cell before and after absorption. The estimated error was reported to be less than 0.1 percent. The good agreement between the solubility of Miyano et al. and that obtained in this work is considered to indicate that the apparatus used in this investigation for the measurement of solubilities of highly soluble gases at atmospheric pressure is accurate.

The logarithm of the mole fraction solubility, as obtained in this investigation, is shown as a function of the logarithm of the absolute temperature in Figure 6-2 to 6-4. When these are within the temperature scale shown, the normal boiling point of the solute and the freezing point

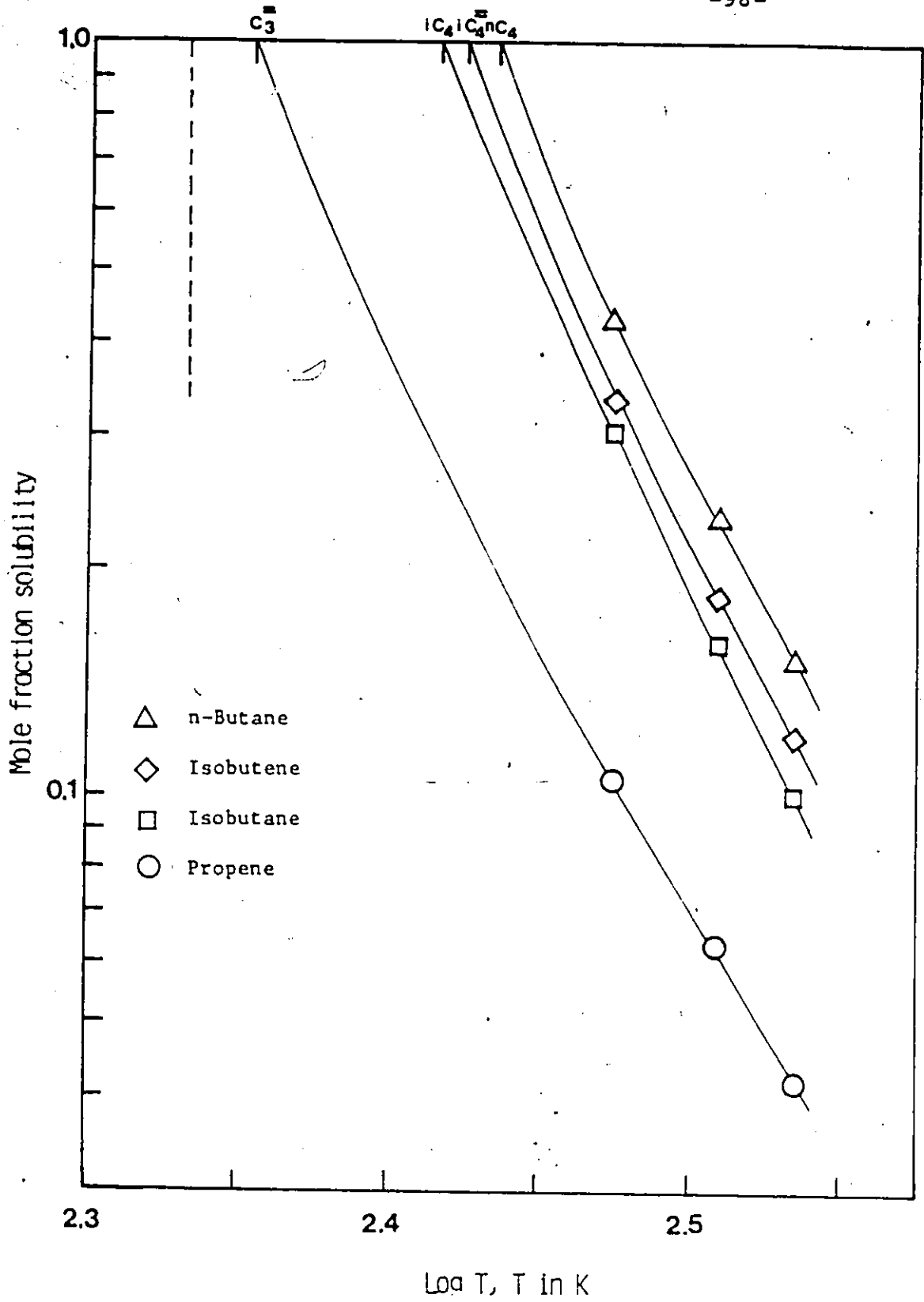


Figure 6-2 Gas solubilities in n-Octane measured at atmospheric pressure.

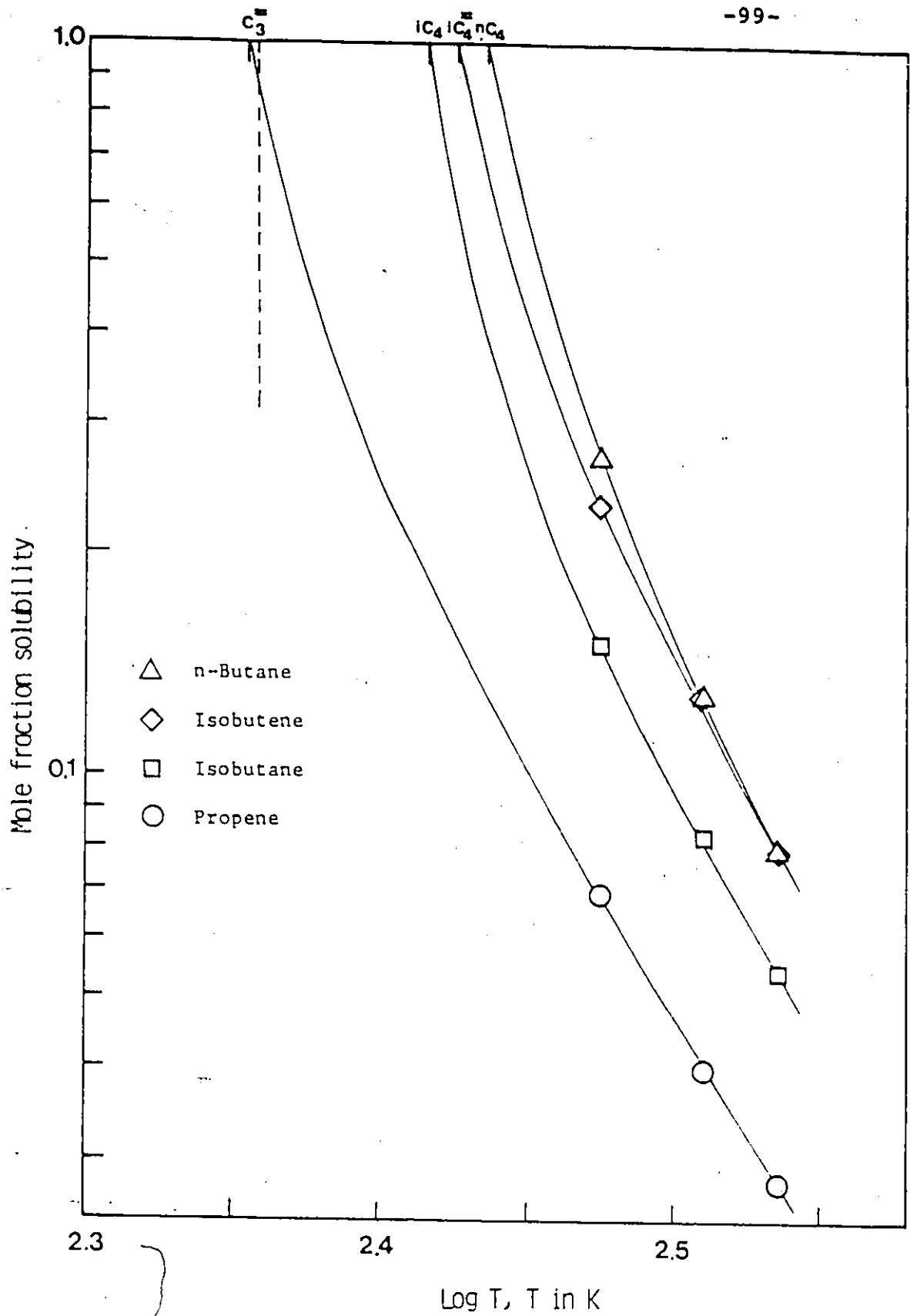


Figure 6-3 Gas solubilities in Chlorobenzene measured at atmospheric pressure.

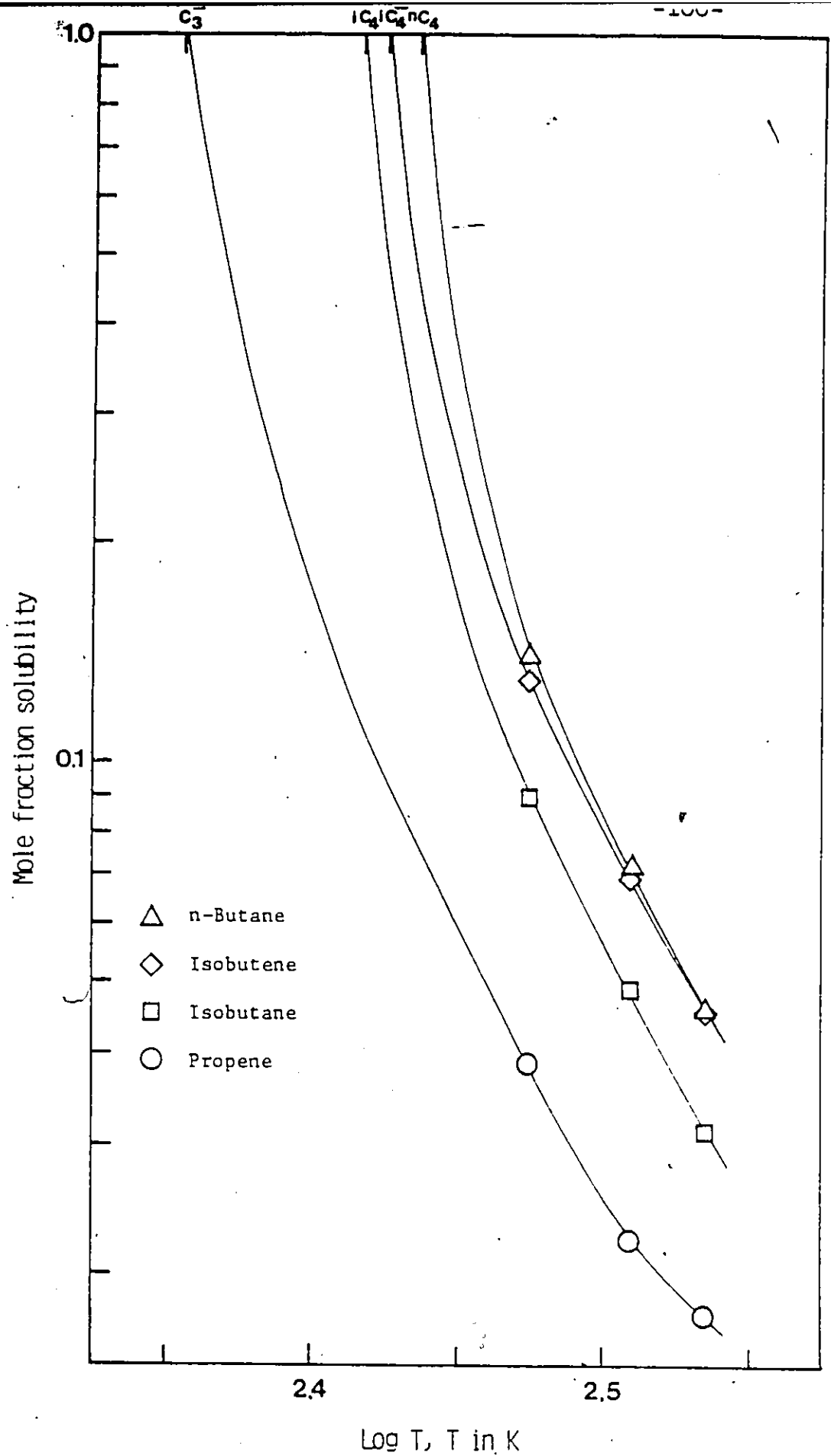


Figure 6-4 Gas solubilities in n-Butanol measured at atmospheric pressure,

of the solvent are also shown. The normal freezing point of n-butanol is very low (183.9 K); therefore it is not indicated in Figure 6-4. Solubility measurements at atmospheric pressure are possible only within the temperature range from the solvent freezing point to the normal boiling point, provided that the solute gas is not liquefied. Such considerations are required when dealing with gases of high solubility such as those investigated in this work.

The solubilities at higher temperatures are extrapolated using smooth curves to the normal boiling points of the solute gases. At the normal boiling point of the gas, the saturated liquid composition corresponds to that of the pure gas. In one case (the solubility of propene in chlorobenzene), the freezing point of the solvent only slightly exceeds the boiling point of the gas. Based on these figures, the order of the solubilities of gases in the same solvent corresponds to the order of normal boiling points for the gases. Such a tendency is most clearly observed for the systems which involve the non-polar solvent, n-octane. This tendency is characteristic for gases of high solubility and indicates that the experimental results agree with the concept of ideal gas solubility as described by Equation (1-1):

$$x_2^{\text{ideal}} = \frac{101.325}{P_2^S} \quad (1-1)$$

The equation above indicates that the ideal gas solubility

becomes unity at the boiling point of the solute gas.

In Figures 6-5 to 6-8, the solubilities of propene, isobutene, n-butane, and isobutane are separately shown for the three different solvents in each case, as a function of the absolute temperature. In these figures, the ideal gas solubilities as calculated by Equation (1-1), are indicated by a dashed line. It may be observed that the solubilities of all four gases are highest in n-octane, lower in chlorobenzene and lowest in n-butanol. Furthermore, the solubilities in n-octane always exceed the ideal gas solubilities, while the solubilities in chlorobenzene and n-butanol are always below the ideal gas solubilities.

It appears possible that the polarity of the solvent, or its tendency for self-association, influences its ability to dissolve gases. While n-octane is non-polar, chlorobenzene is polar, but non-associating, and n-butanol is highly polar and associating. Thus, it would appear that the solubilities of gases are reduced in polar solvents which tend to self-associate.

Gas solubilities are most difficult to correlate for polar solvents in which molecular association occurs. The effect of the association in the solvent on solubility varies widely depending on the nature of the gas. Hayduk and Laudie (85) proposed an empirical correlation for the solubilities of gases in polar solvents based on the "hydrogen-bonding factor (HBF)", which was defined by them as the ratio of actual gas solubility to ideal gas solubili-

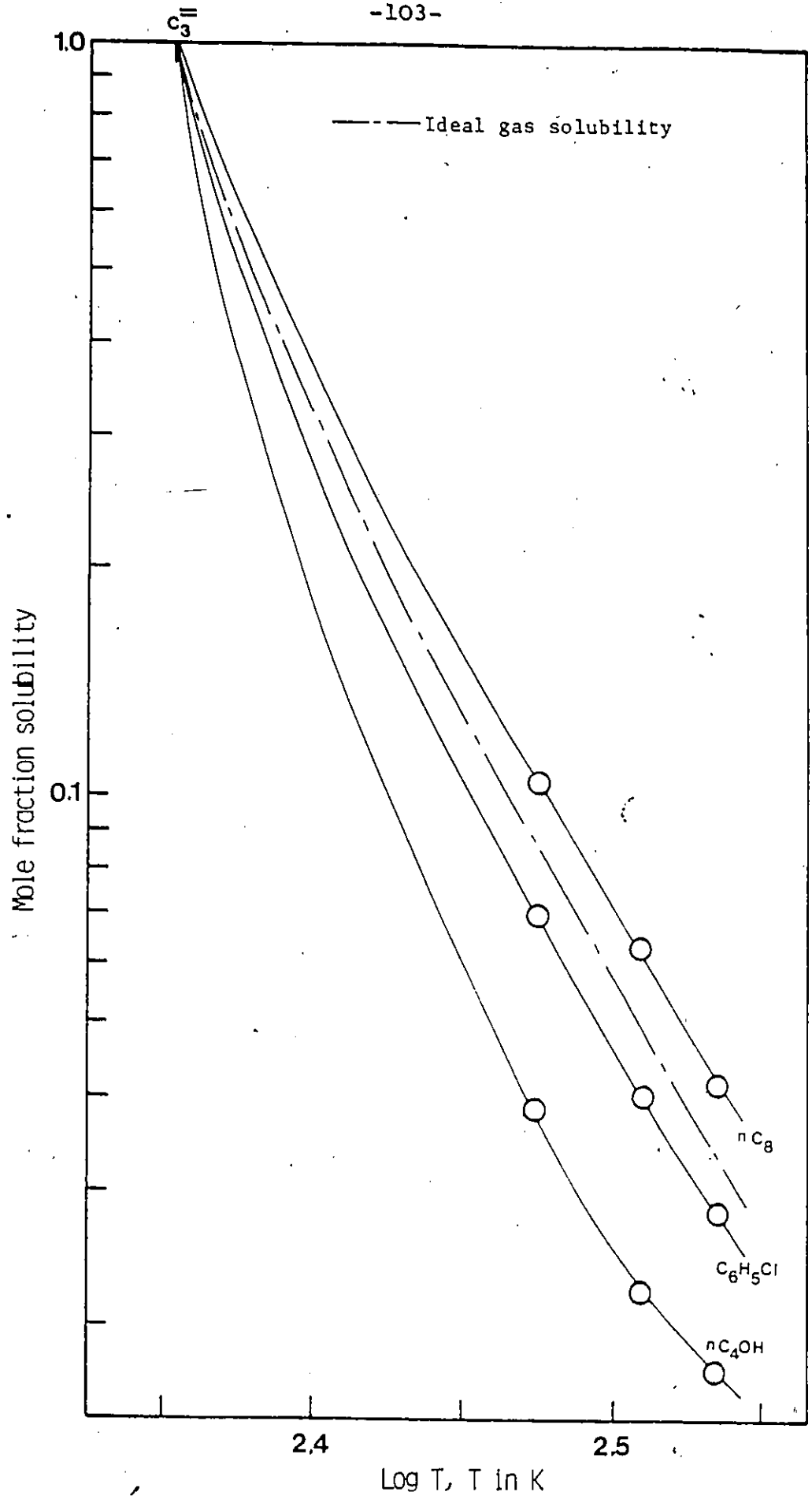


Figure 6-5. Solubilities of propene in the solvents, n-octane, chlorobenzene and n-butanol.

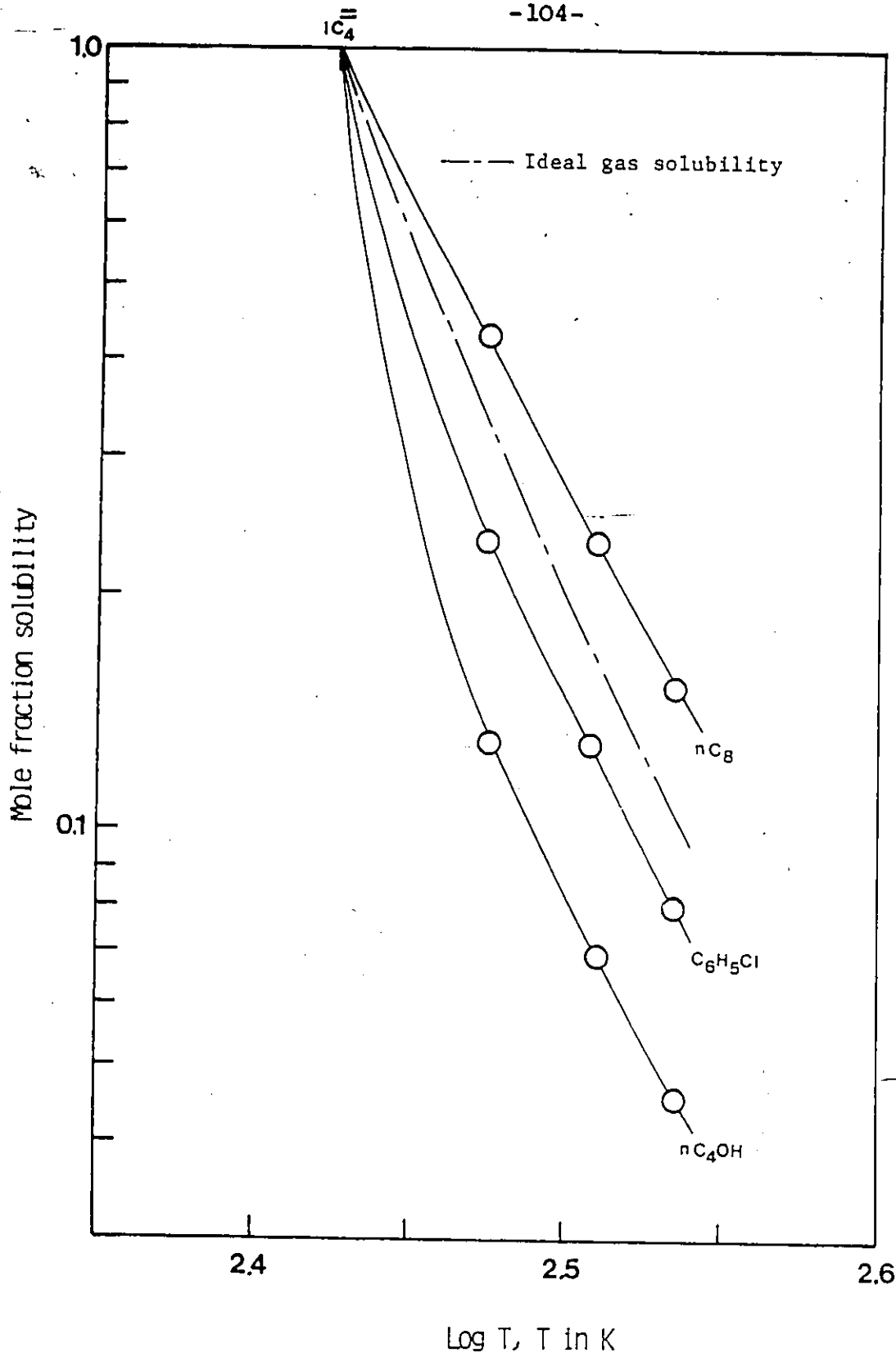


Figure 6-6 Solubilities of isobutene in the solvents, n-octane chlorobenzene and n-butanol.

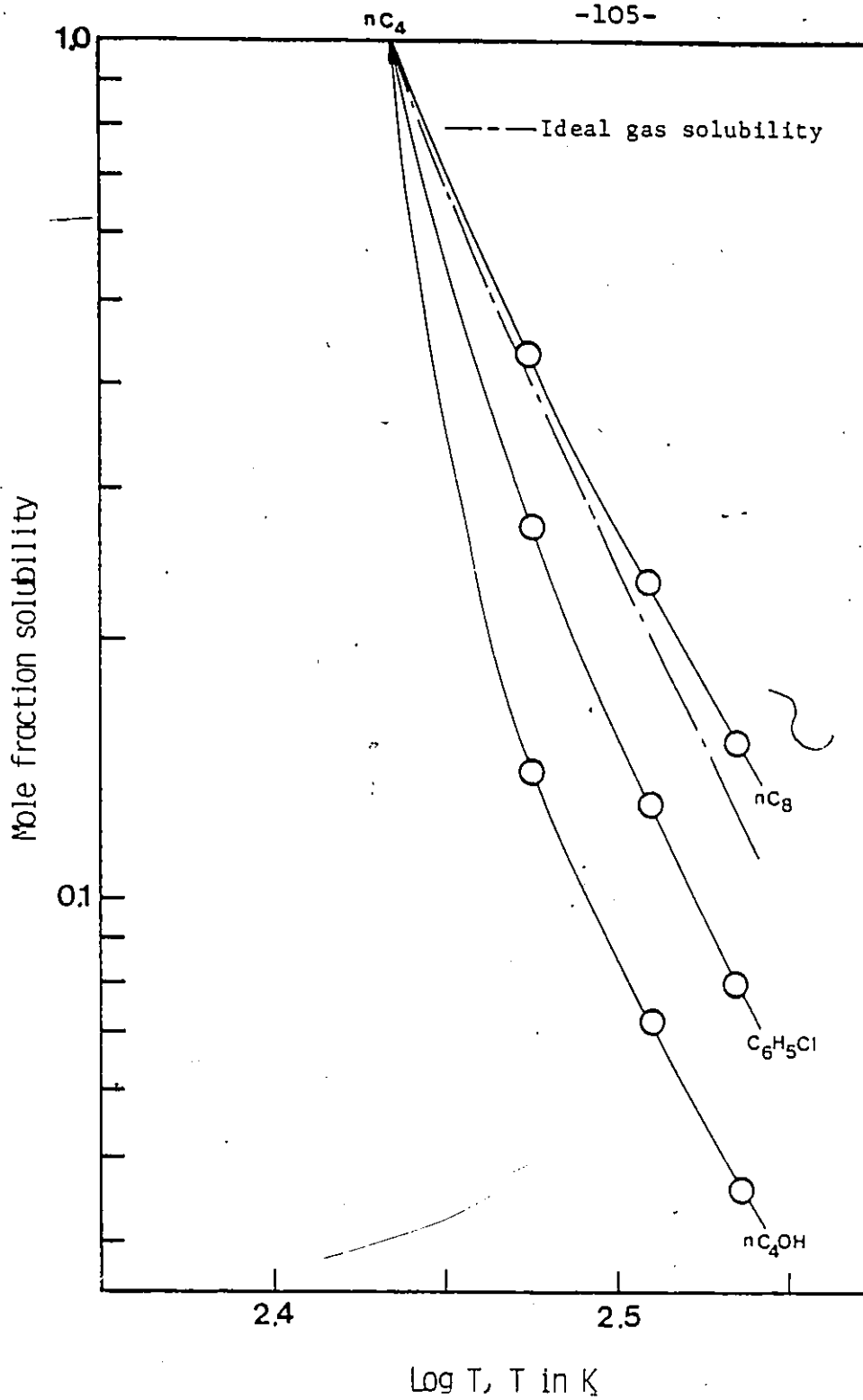


Figure 6-7 Solubilities of n-butane in the solvents, n-octane, chlorobenzene and n-butanol.

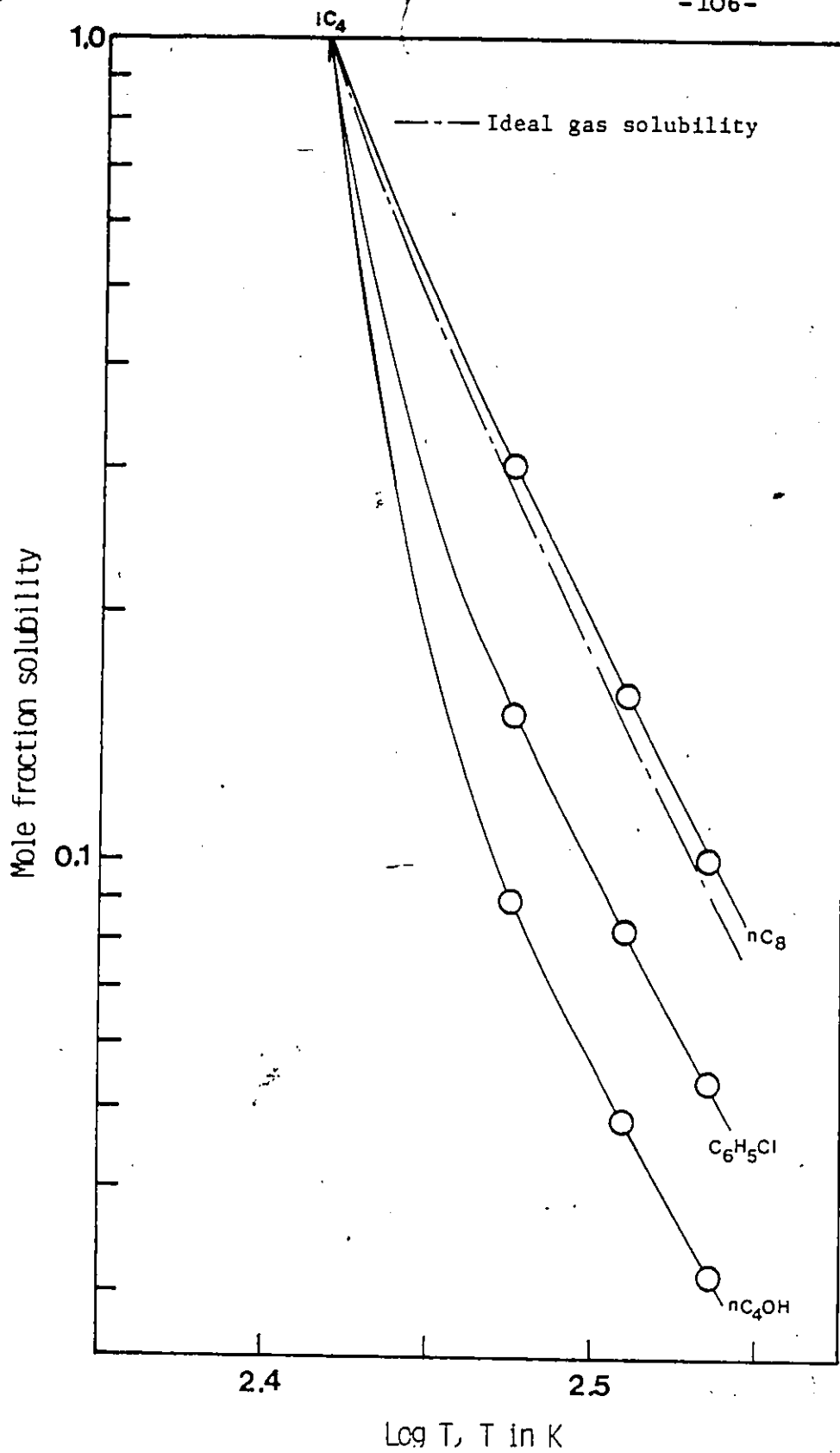


Figure 6-8 Solubilities of isobutane in the solvents n-octane, chlorobenzene and n-butanol.

ty:  $(\text{HBF}) = x_2/x_2$  ideal. They considered that a large reduction in solubility from the ideal gas solubility was attributed to the formation of strong hydrogen-bonds in the solvent, and successfully correlated hydrogen-bonding factors of gases in a polar solvent to those of the same gases in other polar solvents.

In this investigation, attempts were made to relate hydrogen bonding factors for several gases, including a number that may be considered highly soluble in polar and associating solvents, to those for the same gases in n-butanol. For the purpose of indicating the relation between gas solubilities in polar and associating solvents, solubilities reported by other workers, in addition to relevant solubilities measured in this investigation, were used. The associated solvents utilized in the correlation included methanol, ethanol, ethylene glycol, methyl acetate, ethyl acetate and acetonitrile. The gases whose solubilities were available in at least some of the above-mentioned solvents utilized in the correlation included methane, ethane, ethene, ethyne, propane, isobutene, n-butane, isobutane and hydrogen sulfide. The correlation was made utilizing solubilities of these gases for a temperature of 298.15 K. The hydrogen-bonding factors for specific solvent-solute systems are tabulated in Table 6-9.

In Figure 6-9, the hydrogen-bonding factors of the gases in n-butanol are plotted on a log scale as a function of those in the solvents, methanol and ethylene glycol. It may

Table 6-9. Hydrogen-bonding factors in polar and associating solvents. (298.15 K).

Solvent	Solute gas				
	Methane	Ethane	Ethene	Ethyne	Propane
n-Butanol	0.514(136)	0.435(136)	0.491 (136)	0.710(128)	0.343 (2)
Methanol	0.249(136)	0.155(136)	0.256 (136)	0.850(128)	0.107(135)
Ethanol	0.365(136)	0.302(136)	0.360 (136)		0.211(134)
Ethylene glycol		0.0196(44)	0.0421(137)	0.340(128)	
Methyl acetate	0.560 (92)	0.424 (92)	0.691 (92)	3.40 (92)	
Ethyl acetate					
Acenitrile					

Solvent				
	Isobutene	n-Butane	Isobutane	Hydrogen sulfide
n-Butanol	0.392 (*)	0.337 (*)	0.311 (*)	0.653(133)
Methanol	0.0879(135)	0.0906(135)		0.568(132)
Ethanol		0.196 (134)		
Ethylene glycol				0.236(133)
Methyl acetate				
Ethyl acetate	0.704 (122)		0.460 (122)	1.69 (132)
Acenitrile	0.192 (122)		0.0787(122)	0.928(132)

The numbers in brackets indicate the literature source.  
 (\*): This work.

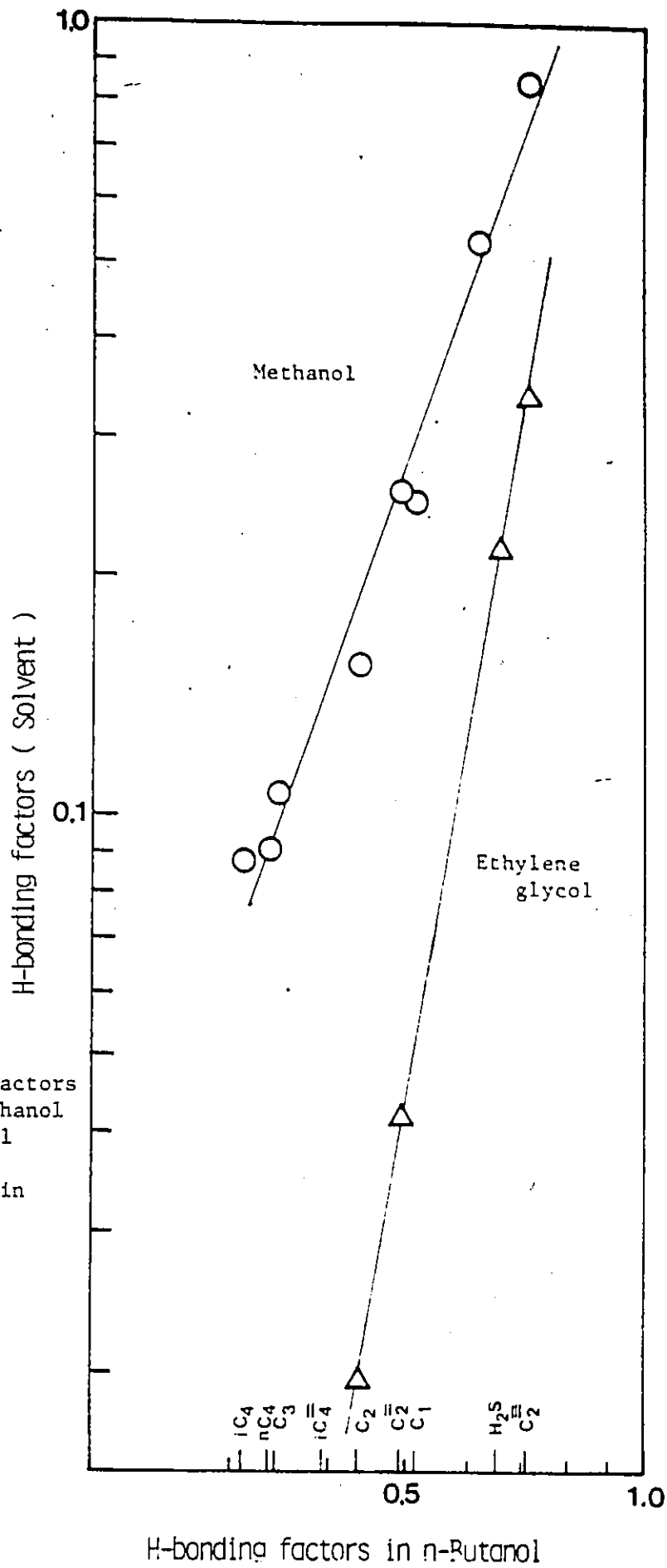


Figure 6-9 Hydrogen-bonding factors at 298.15 K in methanol and ethylene glycol as a function of H-bonding factors in n-butanol

7

be observed in this figure that the hydrogen-bonding factors in n-butanol are approximately linearly related to those in methanol and ethylene glycol. Such linear relationships indicate that the prediction of gas solubility is possible using the diagram as shown in Figure 6-9. That is, if the solubility of a gas in n-butanol is known, then the solubility of the same gas in methanol or ethylene glycol can be predicted. Also, when the solubility of a gas in n-butanol is required, it may be estimated, provided that the solubility of that same gas is available in either methanol or ethylene glycol.

As an illustration of the relation between solubility and hydrogen-bonding factors, a diagram for methanol-n-butanol is shown in Figure 6-10. With reference to this figure, the solubilities of n-butanol are plotted as a function of those in methanol on a log scale. Then the hydrogen-bonding factors, which correspond to the solubility data in both solvents, are also shown. It may be observed in this figure that the lines joining the respective solubilities and hydrogen-bonding factors have a slope of one. Furthermore, it is noted that the length of the lines between the respective solubilities and hydrogen-bonding factors is a function of the ideal gas solubility and is analytically expressed as  $\sqrt{2} \ln (1/x_1^{\text{ideal}})$ . The operation of transferring solubility data to hydrogen-bonding factors in such a manner thus results in a successful correlation between hydrogen-bonding factors as indicated in this figure.

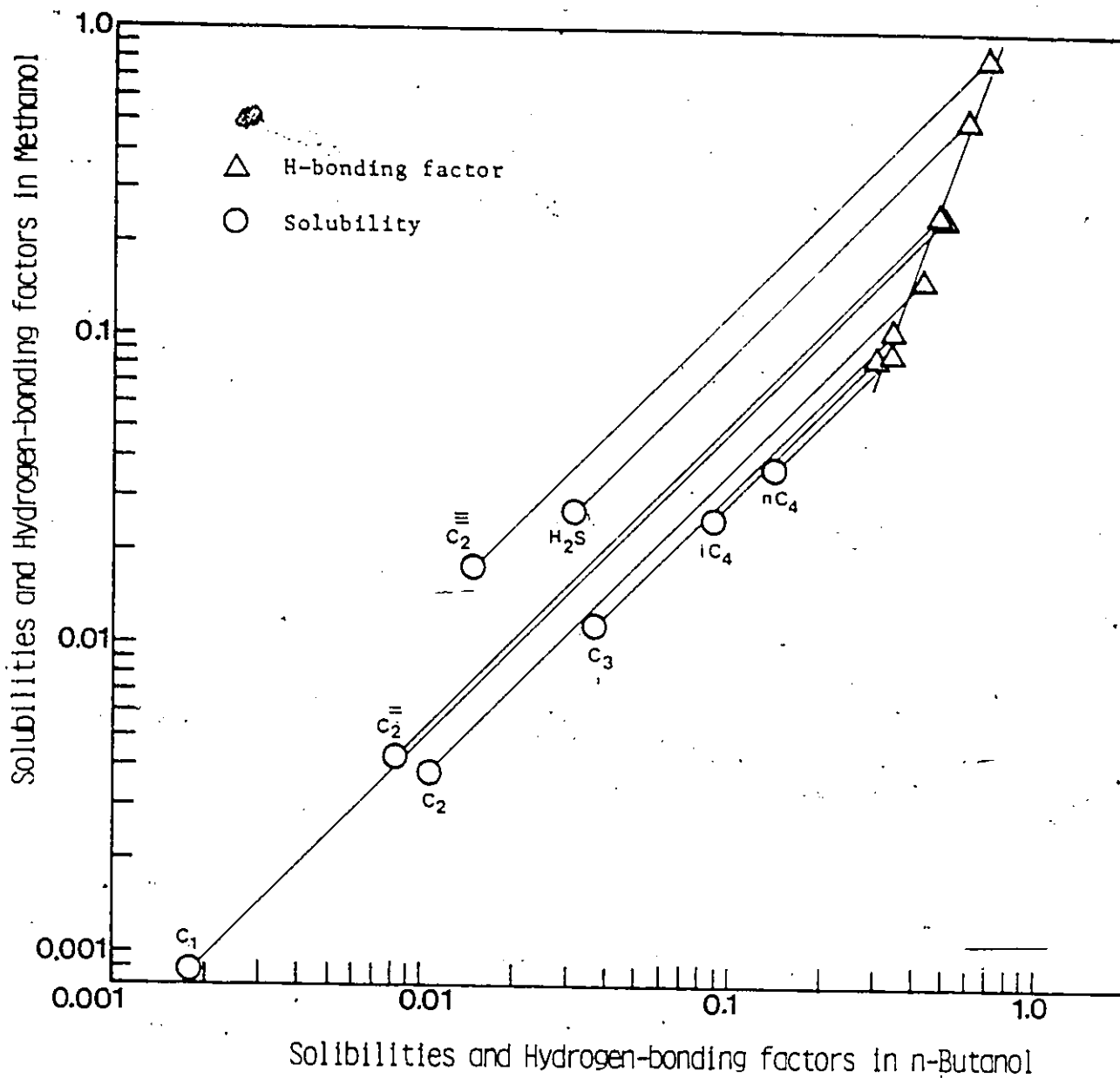


Figure 6-10 Gas solubilities and hydrogen-bonding factors at 298.15 K in methanol and n-butanol.

Hayduk et al. (Hayduk and Pahlevanzadeh, to be published) pointed out that the correlation for hydrogen-bonding factors was likely to be successful when two solvents used in this correlation had similar solvent properties. For example, if both solvents are alcohols, nitriles or ketones, they will probably have similar solubility characteristics. Although ethylene glycol is somewhat different in molecular structure from n-butanol and methanol, having two hydroxyl groups instead of one, the resulting correlation for hydrogen-bonding factors for ethylene glycol and n-butanol appears successful as shown in Figure 6-9.

In Figure 6-11, the hydrogen-bonding factors of gases in n-butanol are plotted as a function of those of the same gases in ethanol. As expected the relation between the two appears to be linear. Solubility data are lacking for a more complete comparison of the relation between hydrogen-bonding factors in these two solvents.

In Figures 6-12 and 6-13, similar diagrams are shown for the hydrogen-bonding factors in methyl acetate, ethyl acetate and acetonitrile as a function of these factors in n-butanol. In these diagrams, the solvents considered do not have molecular structures similar to those of n-butanol, but the solvent properties for gases seem to be similar. Prediction of gas solubility based on such diagrams appears to be possible, although the accuracy would be low. Further investigation for these systems involving associated solvents is required if a general application of hydrogen-bond-

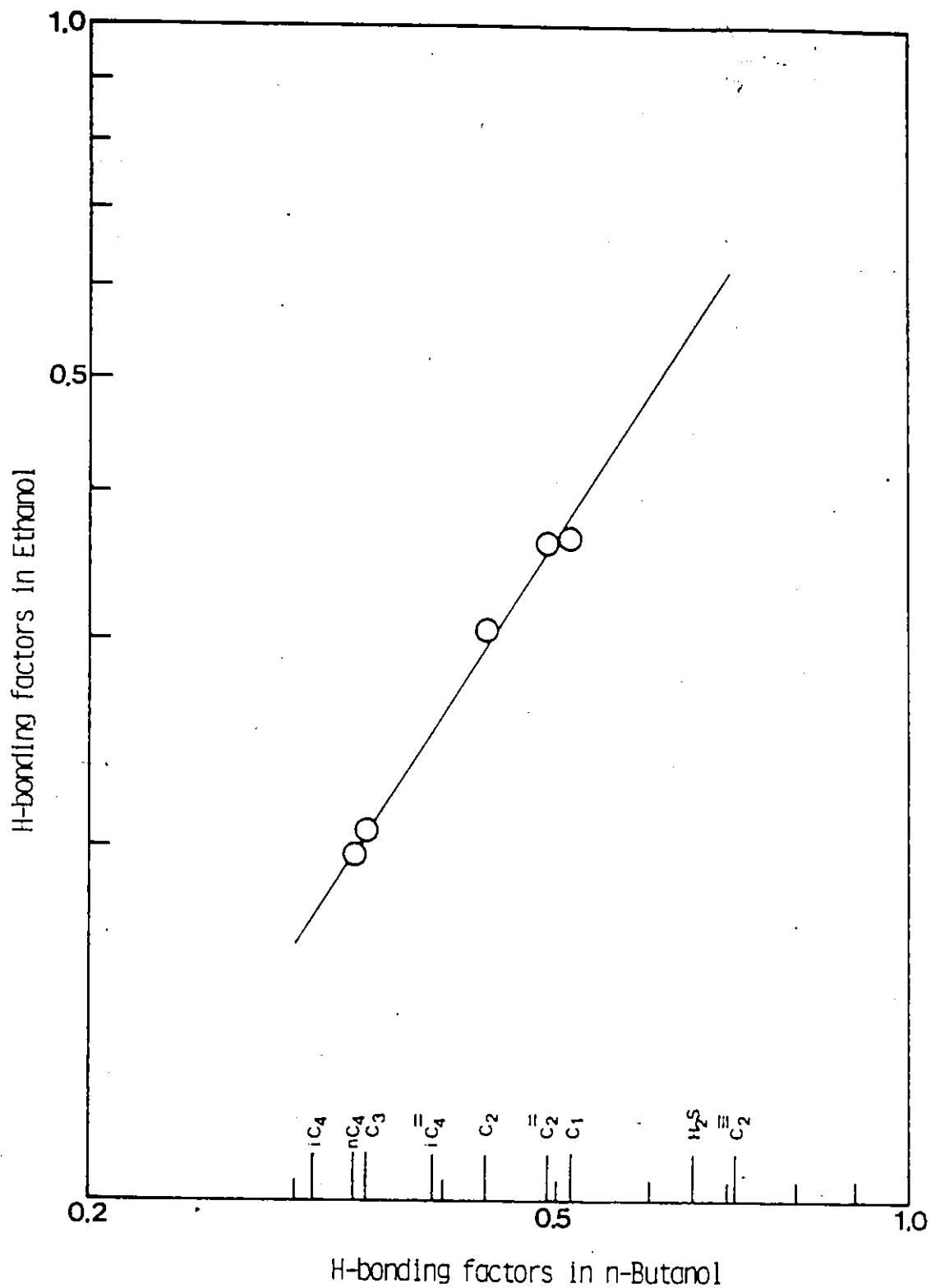


Figure 6-11 Hydrogen-bonding factors at 298.15 K in ethanol as a function of H-bonding factors in n-butanol.

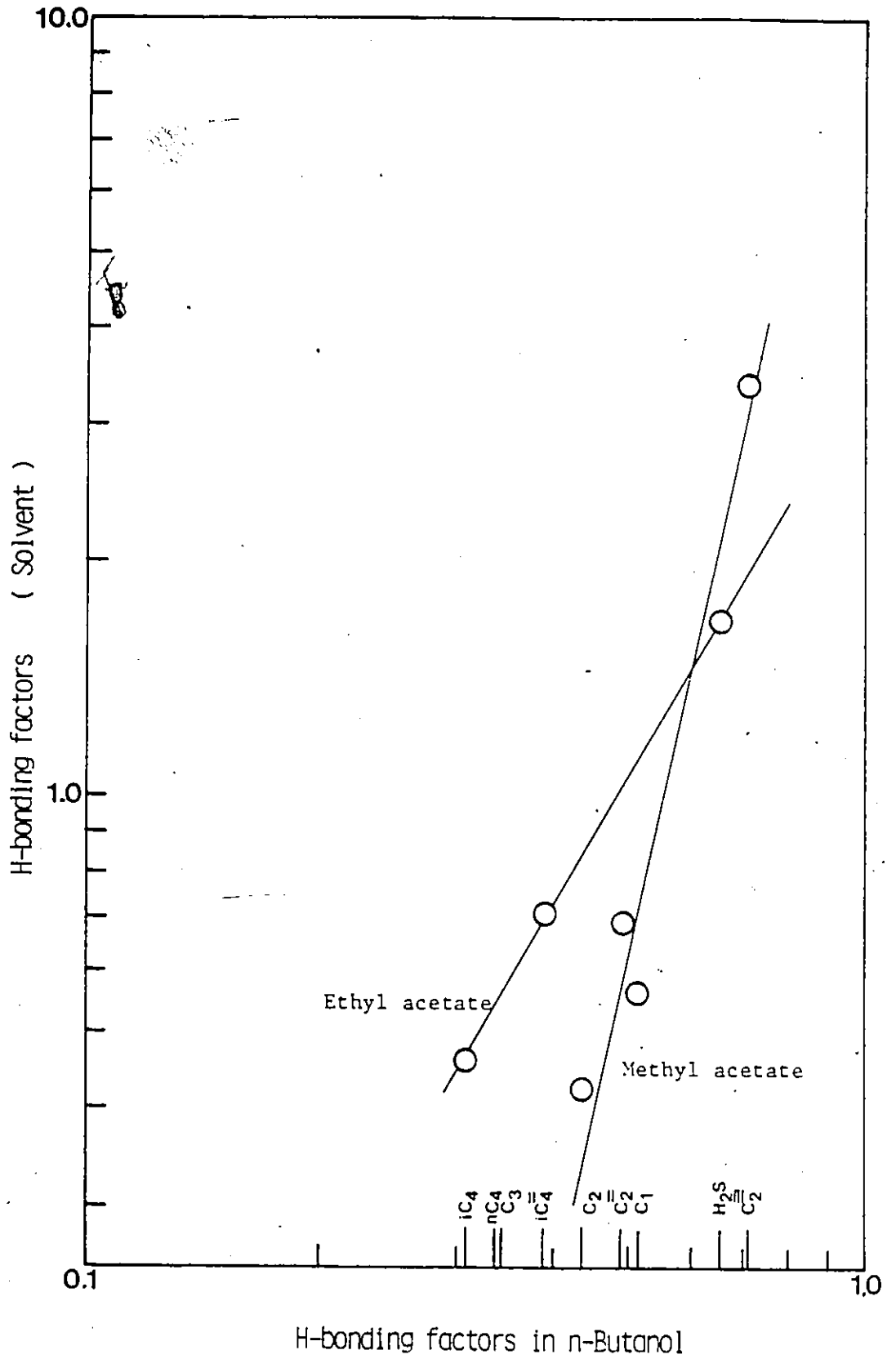


Figure 6-12 Hydrogen-bonding factors at 298.15 K in methyl acetate and ethyl acetate as a function of H-bonding factors in n-butanol.

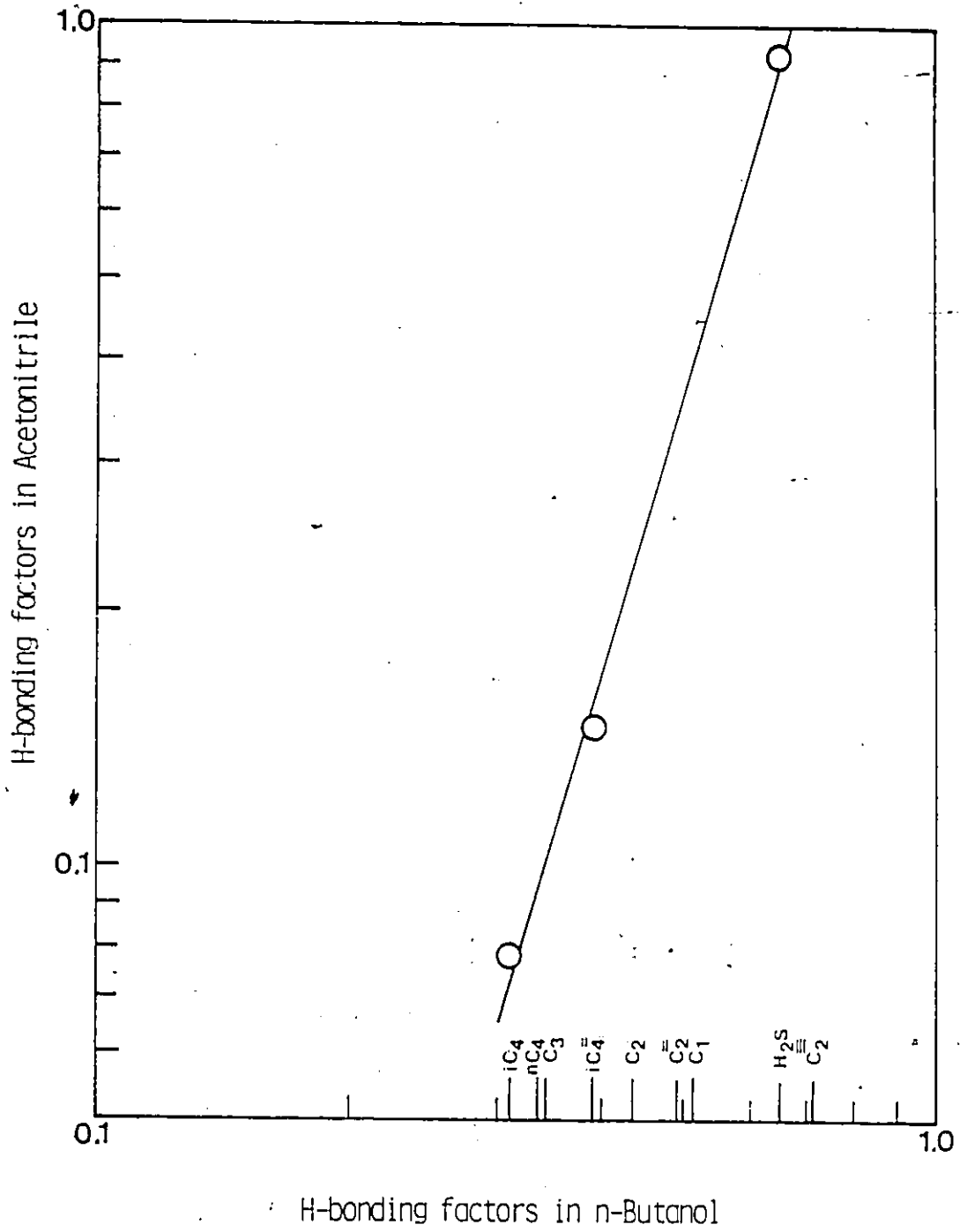


Figure 6-13 Hydrogen-bonding factors at 298.15 K in acetonitrile as a function of H-bonding factors in n-butanol.

ing factors for the prediction of gas solubility is to become possible.

## 6.2 DENSITY OF GAS-SATURATED SOLUTIONS AT ELEVATED PRESSURES

In order to precisely determine gas solubilities at elevated pressures utilizing the solubility apparatus developed in this investigation, a knowledge of the volumes of gas-saturated solution formed in the equilibration cell was necessary. For this purpose, the densities of gas-saturated solutions were measured at elevated pressures utilizing an Anton Paar density meter. The experimental density results obtained are presented in this section. Also presented are the predicted densities of gas-saturated solutions utilizing the Soave-Redlich-Kwong (SRK) equation of state. The binary interaction parameters required for the calculation using the SRK equation were based on the solubility data measured at atmospheric pressure. First, the detailed procedure to predict densities of gas-saturated solutions at elevated pressures by means of the SRK equation of state will be described. Then the experimental results together with the predicted results will be presented and discussed.

### 6.2.1 PREDICTION OF DENSITY OF GAS-SATURATED SOLUTIONS AT ELEVATED PRESSURES

The SRK equation of state (63), which is capable of describing the phase behavior of multi-component systems, is

expressed by the following equation:

$$P = \frac{RT}{V-b} - \frac{a}{V(V+b)} \quad (6-1)$$

In the above equation, P, T, R and V are the pressure, the temperature, the gas constant and the molar volume of mixture in the phase of interest (vapor or liquid). The a and b in the equation above are constants that are functions of temperature and composition and are applicable to a specified phase. They are further expressed by the following equations:

$$a = \sum_i \sum_j a_{ij} x_i x_j \quad (6-2)$$

$$a_{ij} = a_{ji} = (a_{ii} \cdot a_{jj})^{0.5} \cdot (1 - k_{ij}) \quad (6-3)$$

$$a_{ii} = \Omega_{ai} R^2 T_{ci}^2 / P_{ci} \cdot [1 + m_i \{1 - (T/T_{ci})^{0.5}\}]^2 \quad (6-4)$$

$$m_i = 0.48 + 1.574 \omega_i - 0.176 \omega_i^2 \quad (6-5)$$

$$b = \sum b_i x_i \quad (6-6)$$

$$b_i = \Omega_{bi} RT_{ci} / P_{ci} \quad (6-7)$$

In the equations above,  $x_i$  is the mole fraction of the i-th component in the specified phase;  $T_{ci}$ ,  $P_{ci}$  and  $\omega_i$  are the

critical temperature, critical pressure and the acentric factor of the  $i$ -th component, respectively;  $\Omega_{ai}$  and  $\Omega_{bi}$  are the temperature-dependent constants characteristic of the  $i$ -th component and  $k_{ij}$  is the binary interaction parameter to be determined for a specific molecule pair and at the specified temperature.

Once the constants involved in the SRK equation of state are known, calculation of vapor-liquid equilibria is possible, and the equilibrium properties such as molar volumes of both phases can be determined.

For vapor-liquid equilibrium to be established, the fugacity of the  $i$ -th component in the vapor phase,  $f_i^v$  and that in the liquid phase,  $f_i^l$  have to be equal:

$$f_i^v = f_i^l \quad (6-8)$$

From thermodynamic considerations, the fugacity of the  $i$ -th component in the liquid phase,  $f_i^l$ , is expressed by the following equation:

$$RT \ln \frac{f_i^l}{P x_i} = RT \ln \phi_i^l = \int_{V^l}^{\infty} \left\{ \left( \frac{\partial P}{\partial n_i} \right)_{T, V^l, n_{j \neq i}} - \frac{RT}{V^l} \right\} dV^l - RT \ln Z^l \quad (6-9)$$

In the expression above,  $x_i$  and  $\phi_i^l$  are the mole fraction of the  $i$ -th component in the liquid phase, and the fugacity

coefficient of the  $i$ -th component in the liquid phase, respectively;  $V^l$  and  $Z^l$  are the molar volume and compressibility, both of which are for the liquid phase, and  $n_i$  represents the number of moles of the  $i$ -th component.

By substituting Equation (6-1) into Equation (6-9), the fugacity coefficient of the  $i$ -th component in the liquid phase for the SRK equation of state is obtained:

$$\ln \phi_i^l = -\ln \left\{ \frac{P(V^l - b^l)}{RT} \right\} + \frac{b_i}{b^l} \left( \frac{PV^l}{RT} - 1 \right) - \frac{a^l}{b^l RT} \left( \frac{2 \sum_j a_{ij} x_j}{a^l} - \frac{b_i}{b^l} \right) \times \ln \frac{V^l + b^l}{V^l} \quad (6-10)$$

The fugacity coefficient of the  $i$ -th component in the vapor phase,  $\phi_i^v$ , is also expressed by an equation similar to Equation (6-10), but, in this case  $V^l$ ,  $b^l$ ,  $a^l$ ,  $x_j$  are all replaced by those in the vapor phase:

$$\ln \phi_i^v = -\ln \left\{ \frac{P(V^v - b^v)}{RT} \right\} + \frac{b_i}{b^v} \left( \frac{PV^v}{RT} - 1 \right) - \frac{a^v}{b^v RT} \left( \frac{2 \sum_j a_{ij} y_j}{a^v} - \frac{b_i}{b^v} \right) \times \ln \frac{V^v + b^v}{V^v} \quad (6-11)$$

The vapor-liquid equilibrium calculation is then possible utilizing Equations (6-10) and (6-11) in such a manner that Equation (6-8) is satisfied. The molar volumes in the

liquid and vapor phases are then uniquely determined. By utilizing the liquid phase molar volume, and the equilibrium composition in the liquid phase, both of which are also uniquely determined by the calculation, the liquid phase density of the gas-saturated solution,  $\rho_s$  is expressed by:

$$\rho_s = \frac{\sum_i M_i x_i}{V^l} \quad (6-12)$$

In the above equation,  $M_i$  is the molecular weight of the  $i$ -th component.

Thus, the density of a gas-saturated solution can be predicted by the procedure above. It is, however, necessary to determine the values for the constants involved in the calculation, which are  $\Omega_{ai}$ ,  $\Omega_{bi}$  and  $k_{ij}$ , before the procedure described above is employed. First, the detailed procedure to determine the values of  $\Omega_{ai}$  and  $\Omega_{bi}$  will be described, followed by the method for determining the binary interaction parameters,  $k_{ij}$ .

In order to determine the values of  $\Omega_{ai}$  and  $\Omega_{bi}$ , which are characteristic of a substance and are determined at the specified temperature, Equations (6-1) to (6-11) were applied to pure substances by setting  $x_i = y_i = 1$  and  $k_{ij} = 0$ . The properties of the pure substances used for the calculation were the vapor pressures and saturated liquid densities, which were obtained by the methods described in Chapter 4. The actual calculation first involved assuming

the value of  $\Omega_{bi}$ , then calculating the values of  $b$ ,  $a$ ,  $\Omega_{ai}$  and the molar volume in the vapor phase,  $v_i^v$ . Utilizing the values thus determined, the fugacities in the liquid phase and the vapor phase were then calculated. If the condition of fugacity equality as described by Equation (6-8) (for the pure substance) was not satisfied, the value of  $\Omega_{bi}$  was reassumed and the same calculation procedure was repeated until the condition was satisfied. The final values of  $\Omega_{ai}$  and  $\Omega_{bi}$  were then those for which the fugacity equality was satisfied. The flow chart for the calculation is shown in Figure 6-14 and the calculated values for  $\Omega_{ai}$  and  $\Omega_{bi}$  for each substance, at the temperatures of 298.15 K, 323.15 K and 343.15 K are tabulated in Table 6-10.

In order to determine the values for the binary interaction parameters,  $k_{ij}$ 's, gas solubilities which were measured at atmospheric pressure in this investigation were used. In the calculation involved, the values of  $\Omega_{ai}$  and  $\Omega_{bi}$  determined previously were used. Equations (6-1) to (6-11) were applied to the two-component system for this calculation. The calculation procedure involved first assuming the value of  $k_{12}$  and the vapor phase composition,  $y_2$ . Then the equilibrium constants,  $k_1^0 = y_1/x_1$  and  $k_2^0 = y_2/x_2$ , were calculated using the particular solubility values obtained by experiment. Then the fugacity coefficients for the liquid phase and vapor phase were calculated using Equations (6-2) to (6-7) and Equations (6-10) and (6-11). Thus a new

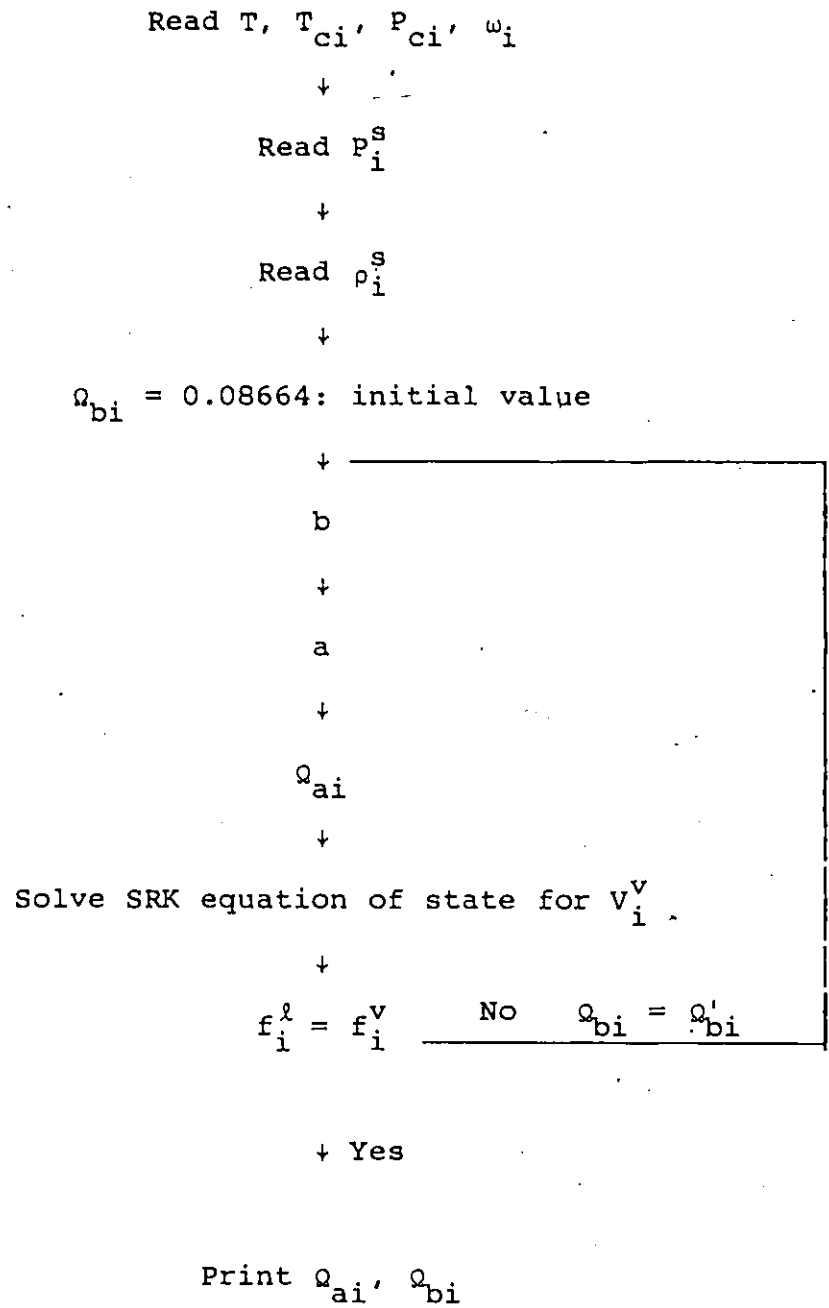


Figure 6-14 Flow chart for the determination of  $\Omega_{ai}$  and  $\Omega_{bi}$  for solutes and solvents when the SRK equation of state is used.

Table 6-10. Values for  $\Omega_{ai}$  and  $\Omega_{bi}$  of the SRK equation of state for solutes and solvents.

Substance	Temperature (K)	$\Omega_{ai}$	$\Omega_{bi}$
n-Octane	298.15	0.37202	0.074292
	323.15	0.37492	0.074769
	343.15	0.37702	0.075069
Chlorobenzene	298.15	0.38282	0.076851
	323.15	0.38478	0.077230
	343.15	0.38631	0.077471
n-Butanol	298.15	0.39652	0.076658
	323.15	0.39270	0.076706
	343.15	0.39017	0.076669
Propylene	298.15	0.40575	0.080696
	323.15	0.40368	0.079647
	343.15	0.39962	0.078284
Isobutylene	298.15	0.40422	0.080578
	323.15	0.40339	0.079977
	343.15	0.40318	0.079496

equilibrium constant,  $K_1 = \phi_1^l / \phi_1^v$ , was calculated and compared with that calculated earlier,  $K_1^0$ .

If the difference between the values of  $K_1^0$  and  $K_1$  was not within an acceptable limit, a new value of  $y_2$  was assumed and the complete calculation procedure was repeated with the same value of  $k_{12}$ . When good agreement between  $K_1^0$  and  $K_1$  was obtained, another equilibrium constant,  $K_2 = \phi_2^l / \phi_2^v$  was calculated and compared with  $K_2^0$ . If the agreement between these two was not good enough, then a new value of  $k_{12}$  was assumed and the calculation procedure up to this stage was repeated until the values of  $K_2^0$  and  $K_2$  became essentially identical. Finally, as a result of the iterative calculation procedure, the value of  $k_{12}$  was uniquely determined for the specific gas-liquid system and at the specified temperature,  $T$ . The flow chart for this calculation to determine the values of  $k_{12}$  is shown in Figure 6-15, and the calculated constants are tabulated in Table 6-11.

Based on the values of  $\Omega_{ai}$ 's,  $\Omega_{bi}$ 's and  $k_{12}$ 's thus determined, the molar volume in the liquid phase and the composition in the liquid phase were calculated for the elevated pressures. Then the density in the liquid phase was calculated by means of Equation (6-12).

The flow chart for the calculation of the liquid solution density is shown in Figure 6-16 and the calculated values are tabulated in Tables 6-12 to 6-17 for the systems investigated in this study. These calculated values will be compared with the experimental results for the gas-saturated solution densities in the following section.

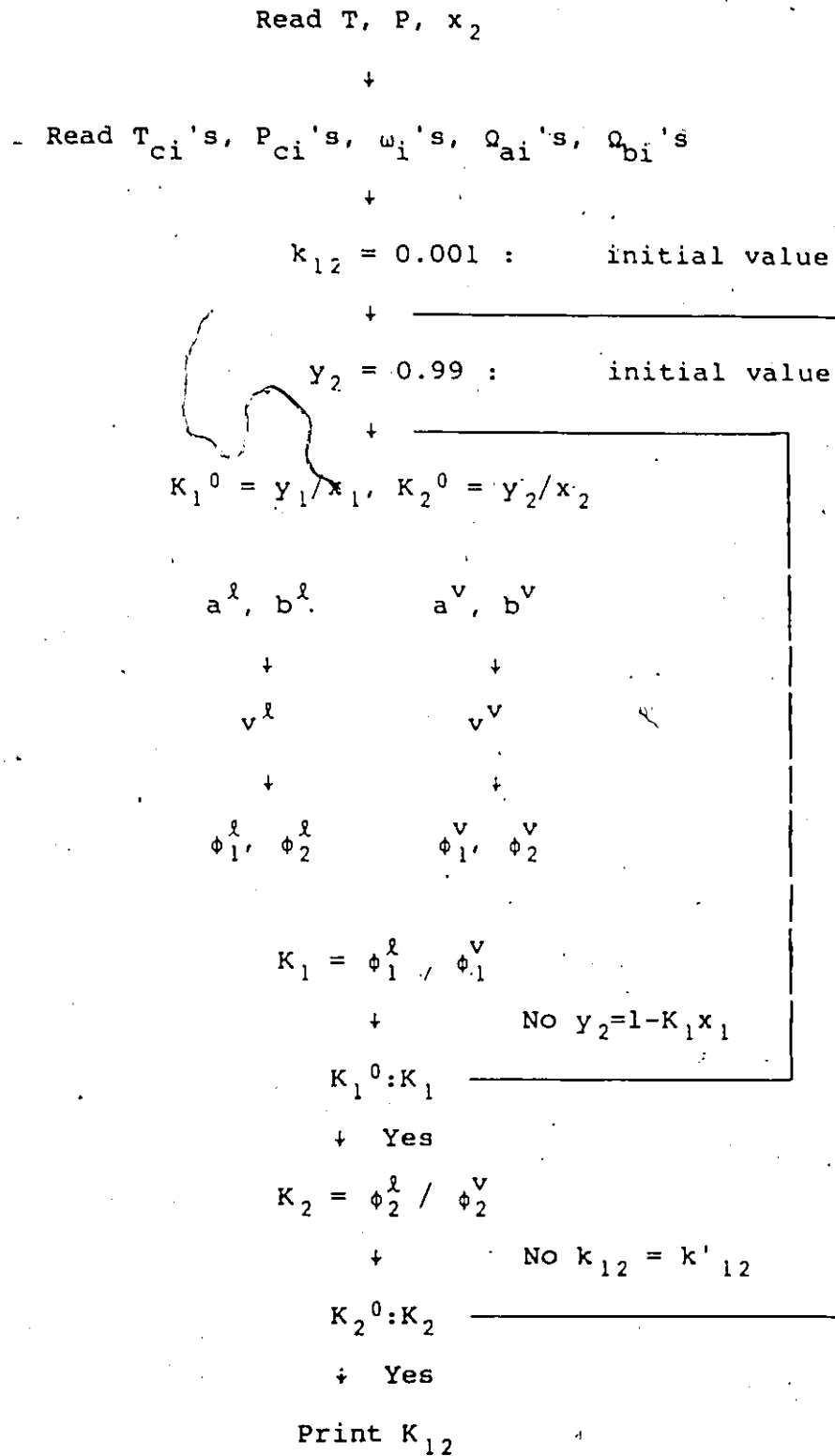


Figure 6-15 Flow chart for the determination of  $k_{12}$  for the specific solute-solvent systems when the SRK equation of state is utilized.

Table 6-11. Values for  $k_{12}$  for solvent-solute systems when the SRK equation of state is utilized.

Solute	Solvent	Temperature	$k_{12}$
Propene	n-Octane	298.15	-0.0078650
		323.15	-0.0054701
		343.15	0.0092435
	Chlorobenzene	298.15	-0.0040296
		323.15	-0.0036573
		343.15	0.0086200
	n-Butanol	298.15	0.021009
		323.15	0.042440
		343.15	0.045029
Isobutene	n-Octane	298.15	0.068269
		323.15	-0.00081510
		343.15	-0.00032529
	Chlorobenzene	298.15	0.0074719
		323.15	-0.0041250
		343.15	0.0029622
	n-Butanol	298.15	0.024477
		323.15	0.029445
		343.15	0.037026

Read T, P, T<sub>ci</sub>'s, P<sub>ci</sub>'s, ω<sub>i</sub>'s,

Ω<sub>ai</sub>'s, Ω<sub>bi</sub>'s, k<sub>12</sub>

+

$$x_2^0 = 10^{-10}$$

+

$$y_2^0 = 1 - 10^{-10}$$

+

$$K_1^0 = y_1^0/x_1^0, \quad K_2^0 = y_2^0/x_1^0$$

a<sup>l</sup>, b<sup>l</sup>

a<sup>v</sup>, b<sup>v</sup>

+

+

v<sup>l</sup>

v<sup>v</sup>

+

+

φ<sub>1</sub><sup>l</sup>, φ<sub>2</sub><sup>l</sup>

φ<sub>1</sub><sup>l</sup>, φ<sub>2</sub><sup>v</sup>

$$K_1 = \phi_1^l / \phi_1^v$$

+

No

$$K_1^0 : K_1$$

+ Yes

$$x_1^0 = \frac{K_2 - 1}{K_2 - K_1}$$

$$K_2 = \phi_2^l / \phi_2^v$$

+ Yes

No

$$y_2^0 = K_1 x_1^0$$

$$K_2^0 : K_2$$

+ Yes

$$\rho_s = (M_1 x_1 + M_2 x_2) / v^l$$

+

Print x<sub>2</sub>, ρ<sub>s</sub>

Figure 6-16 Flow chart for the calculation of solution density and solution composition when the SRK equation of state is utilized.

Table 6-12. Solution densities predicted by the SRK equation of state for the (1) n-Octane - (2) Propene system at elevated pressures.

Temperature								
298.15 K			323.15 K			343.15 K		
P(MPa)	x <sub>2</sub>	ρ(g/cm <sup>3</sup> )	P(MPa)	x <sub>2</sub>	ρ(g/cm <sup>3</sup> )	P(MPa)	x <sub>2</sub>	ρ(g/cm <sup>3</sup> )
0.2027	0.207	0.682	0.2027	0.122	0.668	0.2027	0.0766	0.655
0.4053	0.400	0.662	0.4053	0.241	0.657	0.4053	0.157	0.647
0.6080	0.578	0.636	0.6080	0.354	0.644	0.6080	0.236	0.639
0.8106	0.744	0.603	0.8106	0.461	0.630	0.8106	0.312	0.630
0.8613	0.783	0.593	1.013	0.563	0.613	1.013	0.386	0.620
0.9119	0.822	0.582	1.216	0.659	0.594	1.216	0.458	0.609
1.013	0.898	0.556	1.419	0.750	0.571	1.419	0.528	0.597
1.064	0.936	0.541	1.520	0.794	0.558	1.621	0.596	0.584
			1.621	0.837	0.543	1.824	0.662	0.569
			1.723	0.878	0.527	2.027	0.726	0.552
			1.824	0.918	0.509	2.229	0.787	0.532
			1.925	0.957	0.488	2.432	0.846	0.509
						2.634	0.901	0.482
						2.837	0.951	0.451

Table 6-13. Solution densities predicted by the SRK equation of state for the (1) Chlorobenzene - (2) Propene system at elevated pressures.

Temperature								
298.15 K			323.15 K			343.15 K		
P(MPa)	x <sub>2</sub>	ρ(g/cm <sup>3</sup> )	P(MPa)	x <sub>2</sub>	ρ(g/cm <sup>3</sup> )	P(MPa)	x <sub>2</sub>	ρ(g/cm <sup>3</sup> )
0.2027	0.141	1.05	0.2027	0.0787	1.05	0.2027	0.0530	1.03
0.4053	0.294	0.986	0.4053	0.162	1.01	0.4053	0.111	1.01
0.6080	0.466	0.903	0.6080	0.250	0.978	0.6080	0.169	0.990
0.8106	0.664	0.787	0.8106	0.342	0.937	0.8106	0.230	0.965
0.9119	0.992	0.911	1.013	0.441	0.888	1.013	0.292	0.938
1.013	0.879	0.625	1.216	0.548	0.829	1.216	0.356	0.909
			1.419	0.664	0.956	1.419	0.422	0.876
			1.621	0.788	0.666	1.621	0.492	0.839
			1.824	0.904	0.563	1.824	0.565	0.796
						2.027	0.643	0.747
						2.229	0.923	0.699
						2.432	0.805	0.624
						2.634	0.881	0.553
						2.837	0.945	0.483

Table 6-14. Solution densities predicted by the SRK equation of state for the (1) n-Butanol - (2) Propene system at elevated pressures.

Temperature								
298.15 K			323.15 K			343.15 K		
P(MPa)	x <sub>2</sub>	ρ(g/cm <sup>3</sup> )	P(MPa)	x <sub>2</sub>	ρ(g/cm <sup>3</sup> )	P(MPa)	x <sub>2</sub>	ρ(g/cm <sup>3</sup> )
0.2027	0.0804	0.794	0.2027	0.0441	0.780	0.2027	0.0332	0.765
0.4053	0.176	0.778	0.4053	0.0930	0.772	0.4053	0.0704	0.759
0.6080	0.301	0.755	0.6080	0.147	0.763	0.6080	0.110	0.753
0.8106	0.493	0.712	0.8106	0.207	0.752	0.8106	0.151	0.745
0.8613	0.567	0.693	1.013	0.278	0.738	1.013	0.196	0.737
0.9119	0.659	0.665	1.216	0.367	0.719	1.216	0.244	0.728
0.9626	0.762	0.629	1.419	0.489	0.689	1.419	0.298	0.717
1.013	0.853	0.591	1.621	0.689	0.625	1.621	0.358	0.703
			1.723	0.806	0.577	1.824	0.428	0.686
			1.824	0.891	0.533	2.027	0.514	0.662
			1.925	0.950	0.496	2.229	0.623	0.627
						2.432	0.754	0.575
						2.634	0.867	0.515
						2.837	0.943	0.462

Table 6-15. Solution densities predicted by the SRK equation of state for the (1) n-Octane - (2) Isobutene system at elevated pressures.

Temperature								
298.15 K			323.15 K			343.15 K		
P(MPa)	x <sub>2</sub>	ρ(g/cm <sup>3</sup> )	P(MPa)	x <sub>2</sub>	ρ(g/cm <sup>3</sup> )	P(MPa)	x <sub>2</sub>	ρ(g/cm <sup>3</sup> )
0.1520	0.498	0.662	0.1520	0.264	0.660	0.2027	0.221	0.645
0.2027	0.669	0.643	0.2027	0.353	0.653	0.2280	0.279	0.640
0.2280	0.754	0.631	0.2533	0.440	0.645	0.3040	0.336	0.635
0.2533	0.839	0.618	0.3040	0.525	0.636	0.3546	0.391	0.630
0.2786	0.921	0.604	0.3546	0.609	0.626	0.4053	0.447	0.624
			0.4053	0.692	0.615	0.4560	0.501	0.618
			0.4560	0.772	0.603	0.5066	0.554	0.612
			0.5066	0.851	0.589	0.5573	0.606	0.605
			0.5573	0.928	0.573	0.6080	0.658	0.598
						0.6586	0.709	0.590
						0.7093	0.758	0.582
						0.7599	0.807	0.573
						0.8106	0.855	0.563
						0.8613	0.902	0.552
						0.9119	0.947	0.541

Table 6-16. Solution densities predicted by the SRK equation of state for the (1) Chlorobenzene - (2) Isobutene system at elevated pressures.

Temperature								
298.15 K			323.15 K			343.15 K		
P(MPa)	$x_2$	$\rho$ (g/cm <sup>3</sup> )	P(MPa)	$x_2$	$\rho$ (g/cm <sup>3</sup> )	P(MPa)	$x_2$	$\rho$ (g/cm <sup>3</sup> )
0.1520	0.393	0.928	0.1520	0.198	0.992	0.2027	0.156	0.988
0.2027	0.594	0.826	0.2027	0.275	0.958	0.2533	0.202	0.968
0.2280	0.706	0.765	0.2533	0.357	0.920	0.3040	0.250	0.947
0.2533	0.816	0.702	0.3040	0.444	0.878	0.3546	0.300	0.924
0.2786	0.916	0.642	0.3546	0.538	0.831	0.4053	0.352	0.900
			0.4053	0.635	0.779	0.4560	0.407	0.874
			0.4560	0.735	0.723	0.5066	0.464	0.846
			0.5066	0.833	0.665	0.5573	0.524	0.815
			0.5573	0.923	0.608	0.6080	0.585	0.783
						0.6586	0.648	0.748
						0.7093	0.712	0.712
						0.7599	0.774	0.675
						0.8106	0.835	0.637
						0.8613	0.892	0.600
						0.9119	0.944	0.565

Table 6-17. Solution densities predicted by the SRK equation of state for the (1) n-Butanol - (2) Isobutene system at elevated pressures.

Temperature								
298.15 K			323.15 K			343.15 K		
P (MPa)	x <sub>2</sub>	ρ (g/cm <sup>3</sup> )	P (MPa)	x <sub>2</sub>	ρ (g/cm <sup>3</sup> )	P (MPa)	x <sub>2</sub>	ρ (g/cm <sup>3</sup> )
0.1520	0.234	0.768	0.1520	0.108	0.769	0.2027	0.0922	0.755
0.2027	0.422	0.733	0.2027	0.156	0.761	0.2533	0.122	0.750
0.2280	0.593	0.697	0.2533	0.213	0.751	0.3040	0.154	0.744
0.2533	0.779	0.652	0.3040	0.283	0.738	0.3546	0.190	0.738
0.2786	0.910	0.616	0.3546	0.375	0.720	0.4053	0.230	0.730
			0.4053	0.499	0.694	0.4560	0.275	0.721
			0.4560	0.655	0.658	0.5066	0.327	0.711
			0.5066	0.804	0.618	0.5573	0.389	0.698
			0.5573	0.917	0.583	0.6080	0.462	0.682
						0.6586	0.546	0.663
						0.7093	0.639	0.639
						0.7599	0.730	0.614
						0.8106	0.812	0.590
						0.8613	0.882	0.568
						0.9119	0.941	0.547

### 6.2.2 MEASURED DENSITIES OF GAS-SATURATED SOLUTIONS AT ELEVATED PRESSURES

The gas-saturated solutions whose densities were measured by means of the new measurement technique developed in this investigation included those of propene-saturated n-octane, chlorobenzene and n-butanol, and also of isobutene-saturated n-octane, chlorobenzene and n-butanol. Experiments were conducted at temperatures 298.15 K, 323.15 K and 343.15 K for each solute-solvent system. The measurement pressures ranged from a pressure slightly higher than atmospheric to that close to the saturated vapor pressure of solute at each measurement temperature. These measurements were, however, intended for the accurate determination of gas solubilities at pressures up to 2 MPa by means of the newly developed volumetric measurement method, but the highest measurement pressure did not exceed 2 MPa while the saturated vapor pressure of propene at 343.15 K was over 3 MPa. The obtained results were consistent with the saturated densities of the pure liquefied solutes and of the solvents used, as obtained from the literature.

The gas-saturated solution densities obtained in this investigation are tabulated for various elevated pressures for each solute-solvent system and measurement temperature in Tables 6-18 to 6-23. In Figure 6-17 the densities of propene-saturated solutions are shown as a function of total pressure, and similar plots for the isobutene-saturated solutions are shown in Figure 6-18.

Table 6-18. Solution densities measured at elevated pressures for the (1) n-Octane - (2) Propene system.

Temperature					
298.15 K		323.15 K		343.15 K	
P(MPa)	$\rho$ (g/cm <sup>3</sup> )	P(MPa)	$\rho$ (g/cm <sup>3</sup> )	P(MPa)	$\rho$ (g/cm <sup>3</sup> )
0.128	0.691	0.205	0.668	0.270	0.652
0.231	0.682	0.481	0.653	0.710	0.634
0.328	0.693	0.842	0.629	1.094	0.615
0.428	0.662	1.049	0.612	1.685	0.578
0.580	0.644	1.471	0.567	1.804	0.569
0.743	0.621	1.569	0.554		
1.003	0.595	1.630	0.545		

Table 6-19. Solution densities measured at elevated pressures for the (1) Chlorobenzene - (2) Propene system.

Temperature					
298.15 K		323.15 K		343.15 K	
P(MPa)	$\rho$ (g/cm <sup>3</sup> )	P(MPa)	$\rho$ (g/cm <sup>3</sup> )	P(MPa)	$\rho$ (g/cm <sup>3</sup> )
0.209	1.06	0.280	1.038	0.198	1.04
0.434	0.992	0.957	0.956	0.814	0.966
0.690	0.893	1.101	0.869	1.446	0.868
0.827	0.813	1.203	0.841	1.790	0.793
0.980	0.707	1.600	0.697		

Table 6-20. Solution densities measured at elevated pressures for the (1) n-Butanol - (2) Propene system.

Temperature					
298.15 K		323.15 K		343.15 K	
P(MPa)	$\rho$ (g/cm <sup>3</sup> )	P(MPa)	$\rho$ (g/cm <sup>3</sup> )	P(MPa)	$\rho$ (g/cm <sup>3</sup> )
0.228	0.791	0.280	0.773	0.194	0.765
0.413	0.976	0.588	0.757	0.716	0.746
0.703	0.746	1.161	0.717	1.358	0.714
0.827	0.729	1.551	0.674	1.780	0.687
0.989	0.688	1.690	0.648		
1.065	0.649				

Table 6-21. Solution densities measured at elevated pressures for the (1) n-Octane - (2) Isobutene.

Temperature					
298.15 K		323.15 K		343.15 K	
P(MPa)	$\rho$ (g/cm <sup>3</sup> )	P(MPa)	$\rho$ (g/cm <sup>3</sup> )	P(MPa)	$\rho$ (g/cm <sup>3</sup> )
0.104	0.682	0.118	0.668	0.142	0.652
0.153	0.669	0.189	0.658	0.240	0.644
0.198	0.655	0.295	0.642	0.398	0.628
0.254	0.634	0.383	0.624	0.586	0.606
		0.430	0.614	0.655	0.597
		0.492	0.598	0.711	0.589

Table 6-22. Solution densities measured at elevated pressures for the (1) Chlorobenzene - (2) Isobutene system.

Temperature					
298.15 K		323.15 K		343.15 K	
P(MPa)	$\rho$ (g/cm <sup>3</sup> )	P(MPa)	$\rho$ (g/cm <sup>3</sup> )	P(MPa)	$\rho$ (g/cm <sup>3</sup> )
0.112	1.01	0.162	0.994	0.305	0.953
0.171	0.930	0.233	0.946	0.448	0.884
0.213	0.861	0.283	0.907	0.592	0.809
0.269	0.745	0.371	0.824	0.671	0.764
		0.469	0.724	0.725	0.729

Table 6-23. Solution densities measured at elevated pressures for the (1) n-Butanol - (2) Isobutene system.

Temperature					
298.15 K		323.15 K		343.15 K	
P(MPa)	$\rho$ (g/cm <sup>3</sup> )	P(MPa)	$\rho$ (g/cm <sup>3</sup> )	P(MPa)	$\rho$ (g/cm <sup>3</sup> )
0.101	0.788	0.138	0.769	0.303	0.744
0.169	0.766	0.271	0.947	0.508	0.718
0.221	0.741	0.401	0.915	0.629	0.696
0.262	0.711	0.489	0.698	0.747	0.671
				0.804	0.65

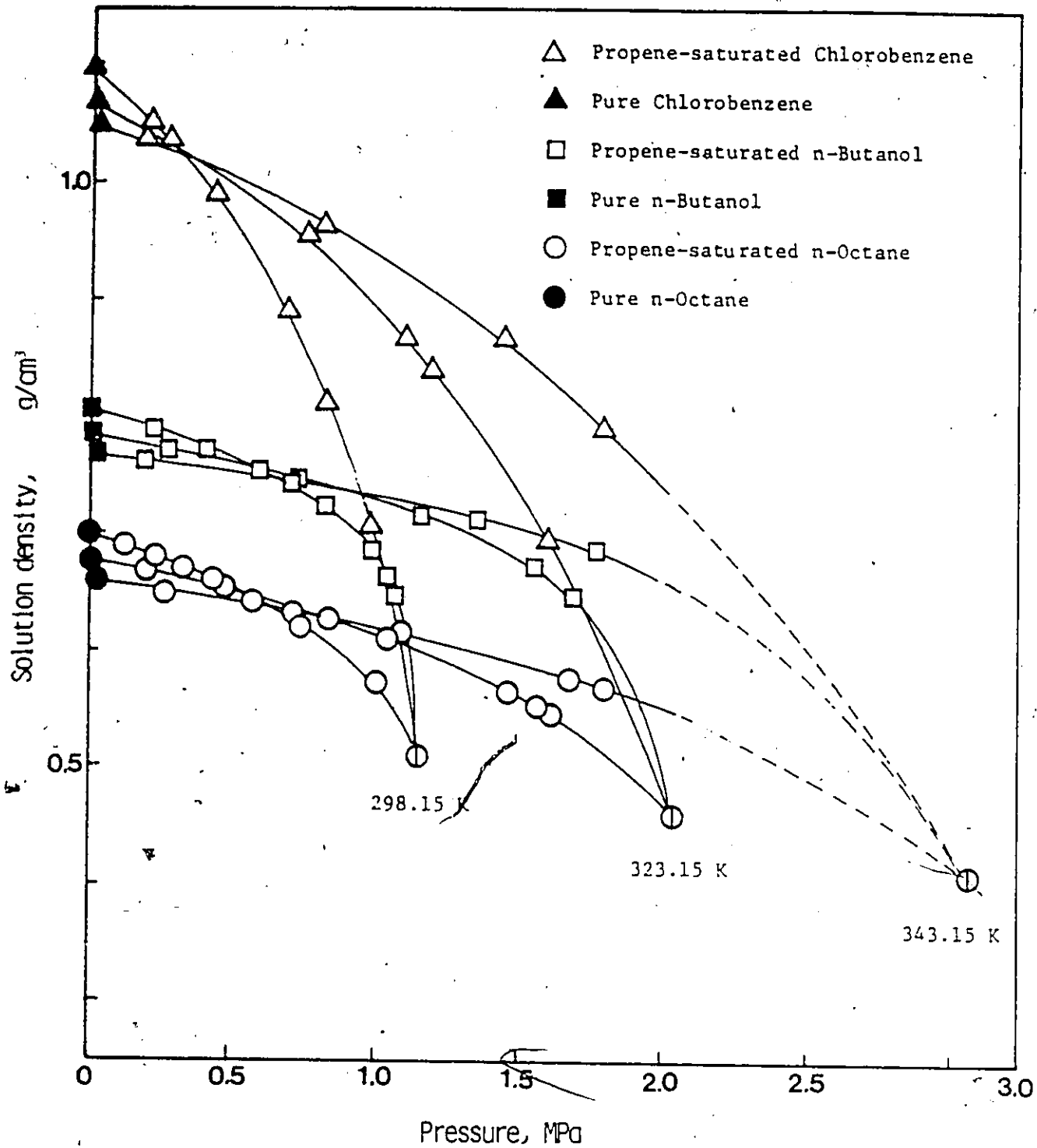


Figure 6-17 Densities of propene-saturated solutions under pressure.

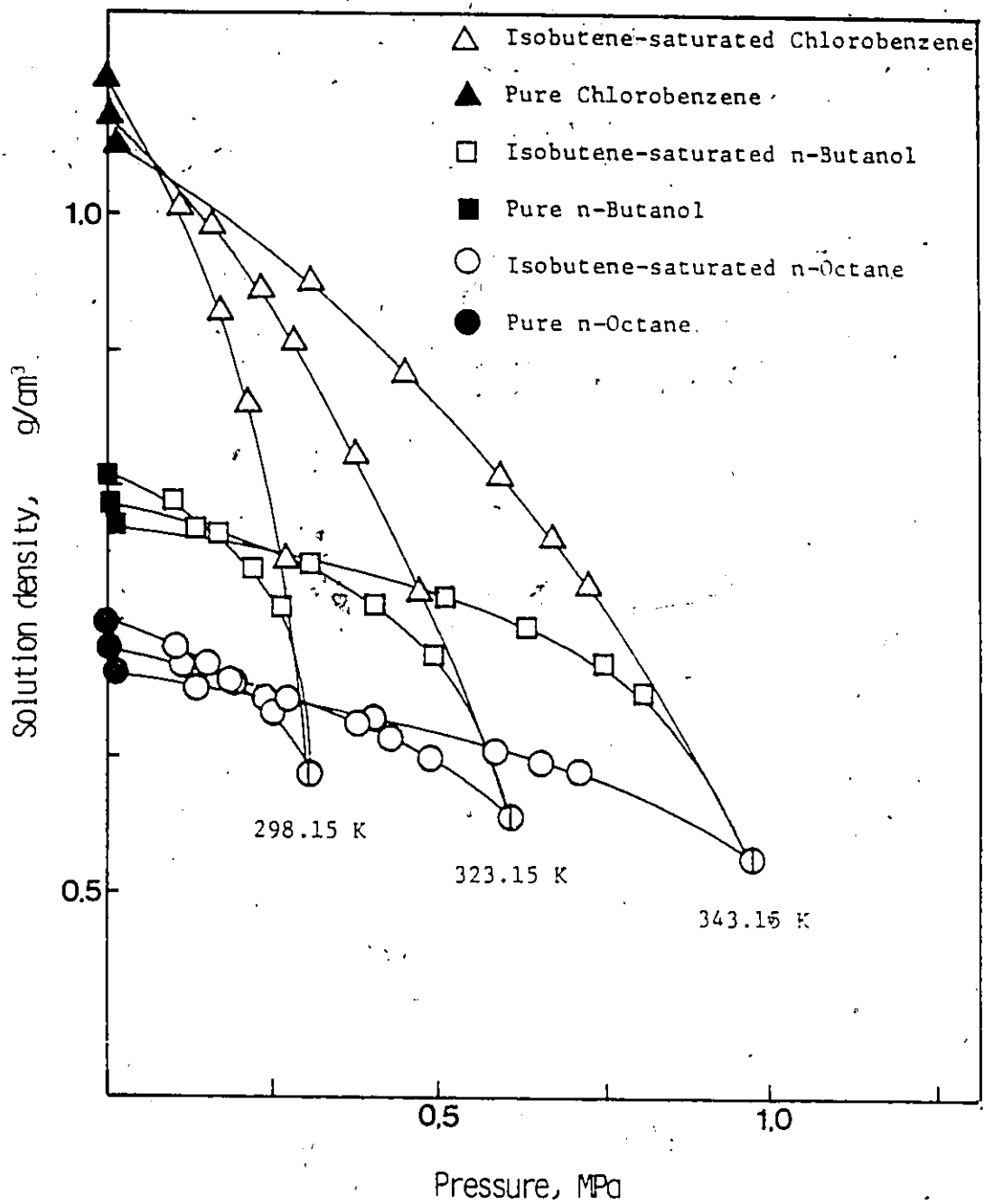



Figure 6-18 Densities of isobutene-saturated solutions under pressure.

With reference to Figures 6-17 and 6-18, it was considered that the differences between the vapor-saturated liquid solvent densities at low pressures and densities of liquid solvents at atmospheric pressure were negligibly small. Therefore, the densities of pure solvents measured at atmospheric pressure in this investigation were considered to be equivalent to the densities of vapor-saturated solvents. The saturated densities of liquefied solutes, were estimated by the method proposed by Gunn and Yamada (118) as described in Chapter 4.

In order to use the gas-saturated solution densities for the calculation of gas solubilities at elevated pressures, it was necessary to determine the gas-saturated solution densities which correspond to the actual pressures of the solubility experiments. For this purpose, all the gas-saturated solution densities were fitted to polynomial equations in pressure. The constants obtained by means of a least-squares fitting utilizing the computer are shown, along with the average percent deviations between the experimental and fitted densities in Appendix C. For most cases, the percent deviations were much less than 1.0%, but for the n-butanol-propene system at 298.15 K, the percent deviation exceeds 1.0% as seen in the table of Appendix C. This accuracy is considered quite sufficient for estimating the volume of gas displaced by the saturated liquid solution in the high pressure solubility cell.

In Figures 6-19 to 6-21, the densities of propene-saturated solutions of n-octane for temperatures, 298.15 K, 323.15 K and 343.15 K are plotted as a function of pressure. Also shown in the same figures as dotted lines, are the densities predicted by the SRK equation of state. As shown in those figures, the predicted densities agree well with those determined experimentally for this system, especially for the temperatures 323.15 K and 343.15 K. It was found that despite the slightly polar nature of propene, the SRK equation of state was useful for predicting the densities of propene-saturated n-octane, a nonpolar solvent. But it may be noticed in these figures that the predicted solution densities were slightly lower than the experimental densities, especially at 298.15 K. It has been generally recognized that the prediction of molar volumes in the liquid phase by means of cubic equations of state such as the SRK equation often results in large deviations from the experimental data. However, for the n-octane-propene system investigated for temperatures ranging from 298.15 K to 323.15 K, the prediction of the solution densities was satisfactory.

In Figure 6-22, the densities of propene-saturated chlorobenzene at 323.15 K are shown as a function of pressure. As shown in this figure, a good agreement between predicted and experimental solution densities was obtained for this system. Good agreement was also observed for the same system at the temperatures 298.15 K and 343.15 K. Similar



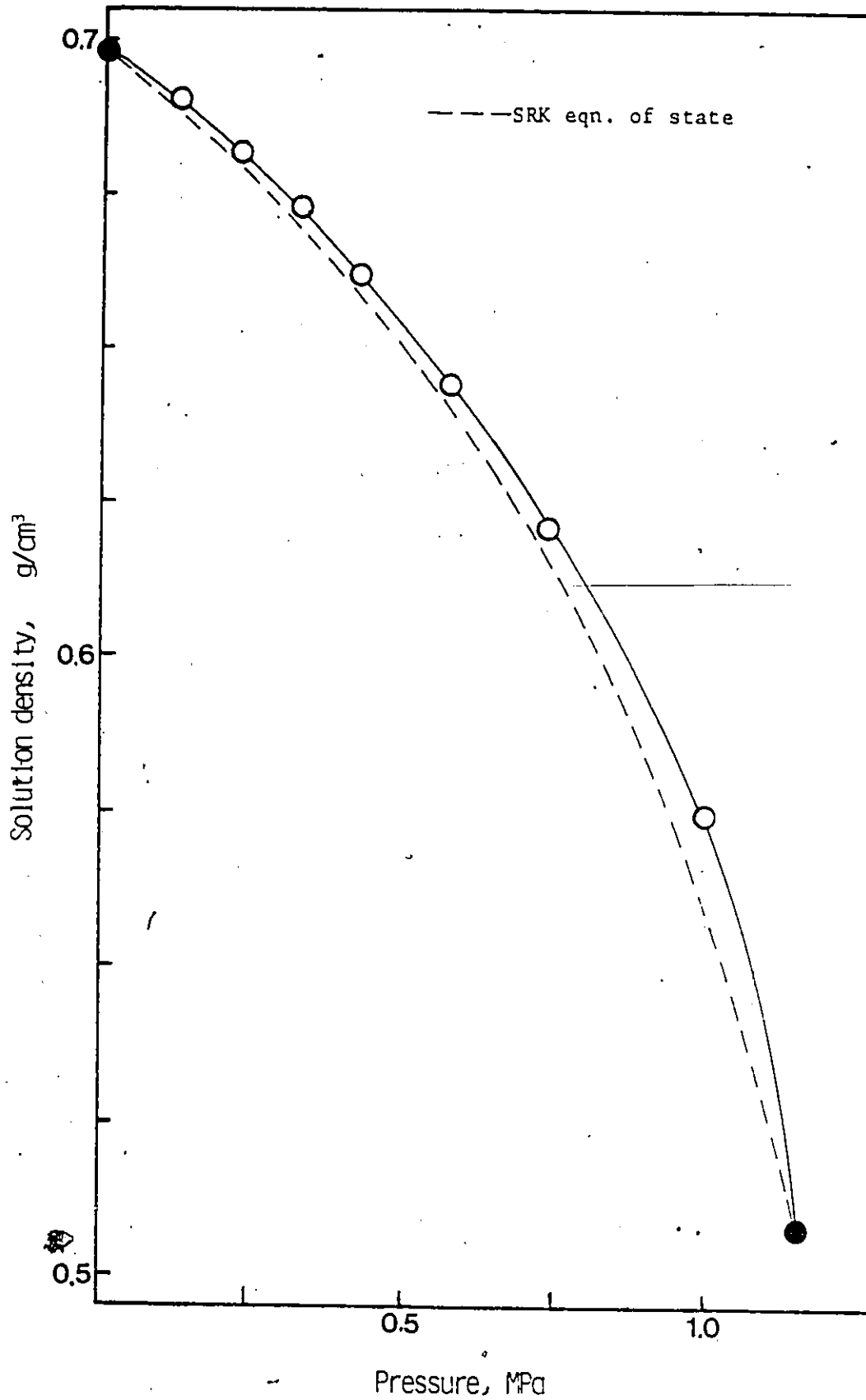


Figure 6-19 Experimental and predicted densities of propene-saturated n-octane solutions at 298.15 K as a function of pressure.

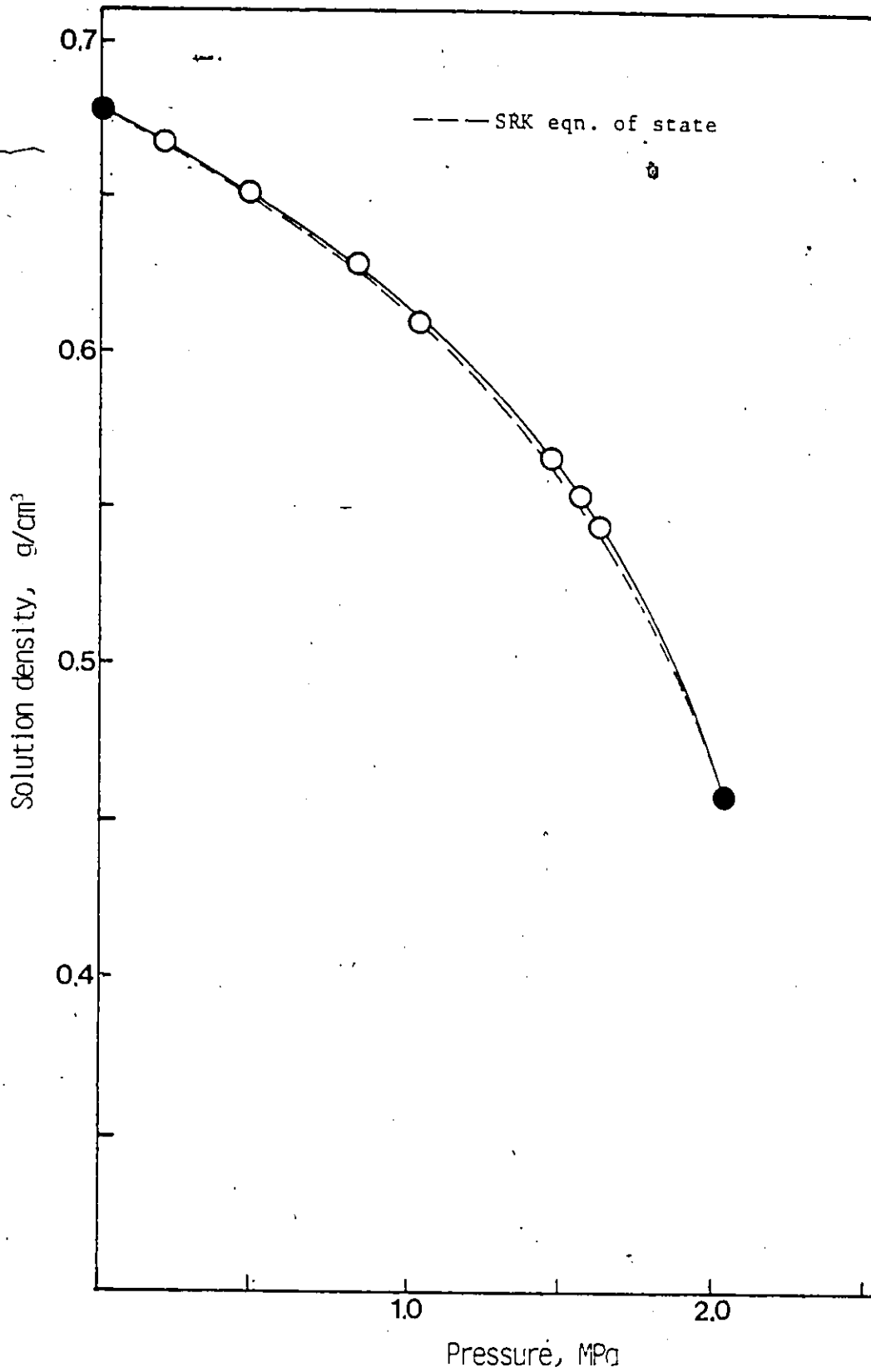


Figure 6-20 Experimental and predicted densities of propene-saturated n-octane solutions at 323.15 K as a function of pressure.

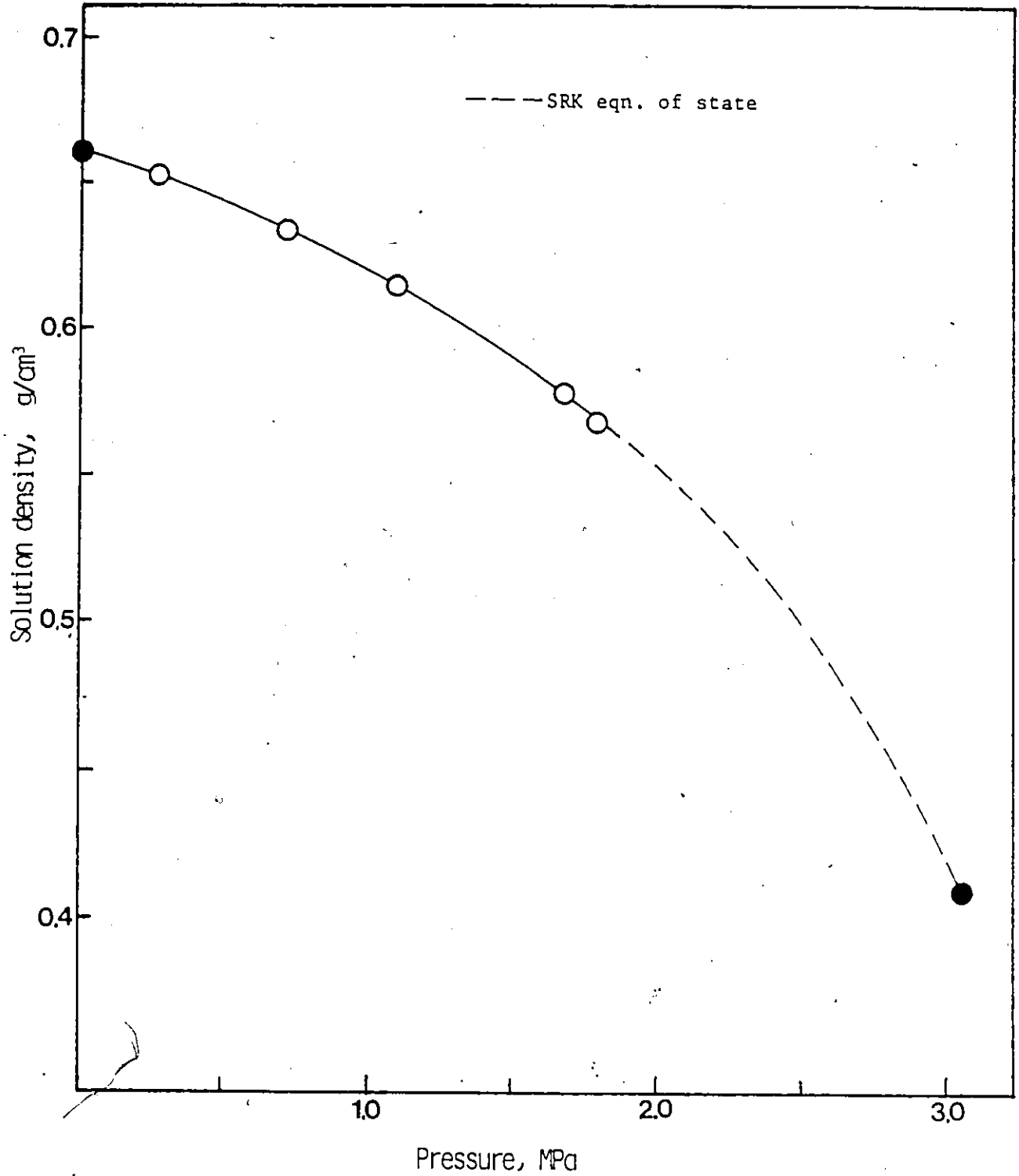


Figure 6-21 Experimental and predicted densities of propene-saturated n-octane solutions at 343.15 K as a function of pressure.

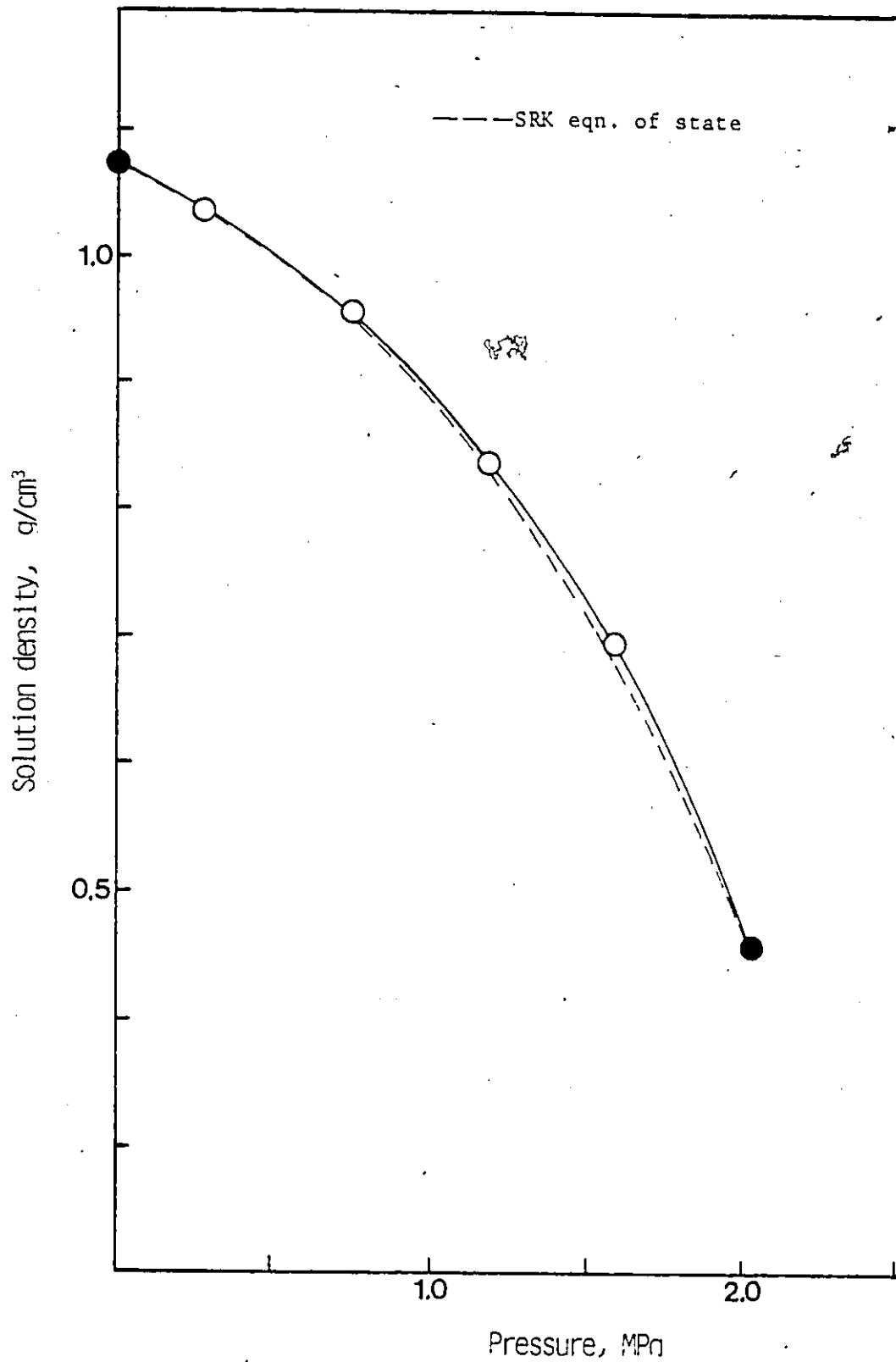


Figure 6-22 Experimental and predicted densities of propene-saturated chlorobenzene solutions at 323.15 K as a function of pressure.

plots for these latter systems are shown in Appendix C.

The densities of propene-saturated n-butanol measured at 298.15 K, 323.15 K and 343.15 K are plotted as a function of pressure in Figures 6-23, 6-24 and 6-25, respectively. What is common in those figures is that only approximate agreement is obtained for pressures up to about half the saturation pressure of the solute, propene. For pressures higher than this, the deviation between the predicted and experimental solution densities are significant. It is, therefore, considered that the prediction of solution densities using the SRK equation for highly polar and associating systems such as the n-butanol-propene system are likely to be erroneous. A maximum deviation of about 14 percent was observed for this system. This fact was considered to indicate that for the precise measurements of gas solubilities for the systems involving polar and associating substances utilizing the high pressure solubility apparatus developed in this investigation, actual density measurements of gas-saturated solutions were most useful.

The prediction of isobutene-saturated solution densities, using the SRK equation of state, resulted in similar behavior for solution densities to those obtained with the propane-saturated solutions. Generally the solution densities estimated by means of the SRK equation are lower than the experimentally determined densities as measured in this investigation, but these densities agree with relatively small deviations for the n-octane-isobutene systems and

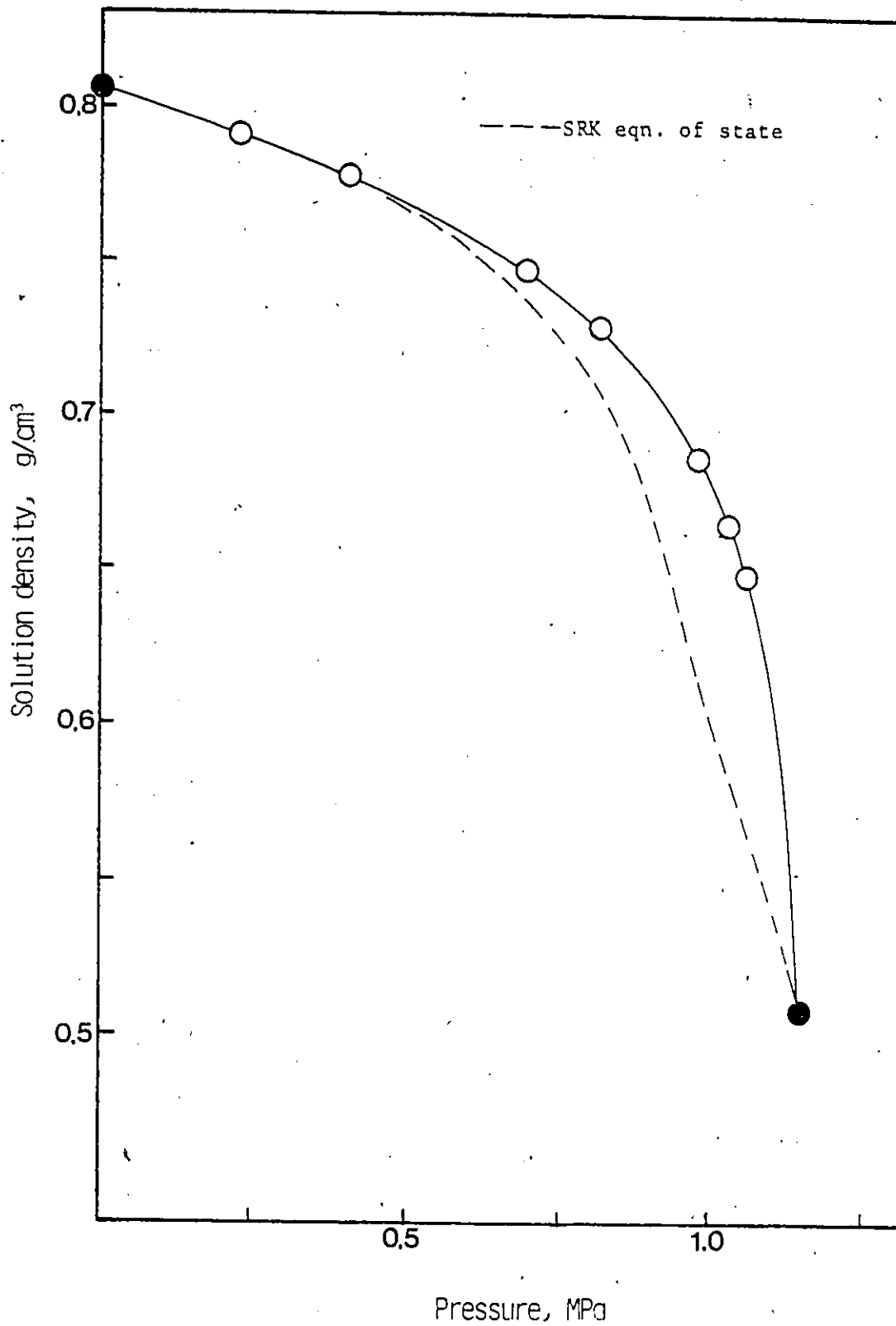


Figure 6-23 Experimental and predicted densities of propene-saturated n-butanol solutions at 298.15 K as a function of pressure.

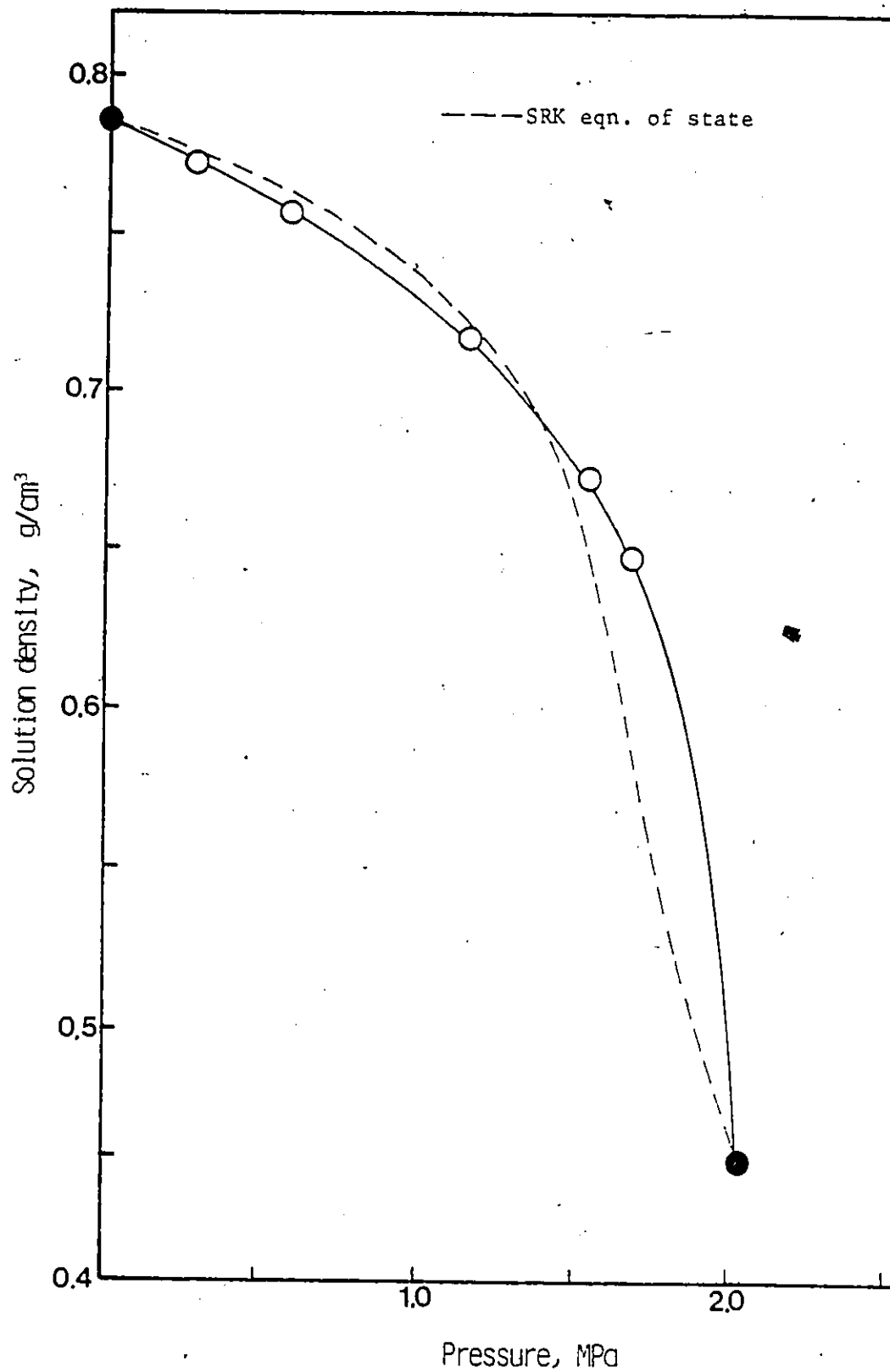


Figure 6-24 Experimental and predicted densities of propene-saturated n-butanol solutions at 323.15 K as a function of pressure.

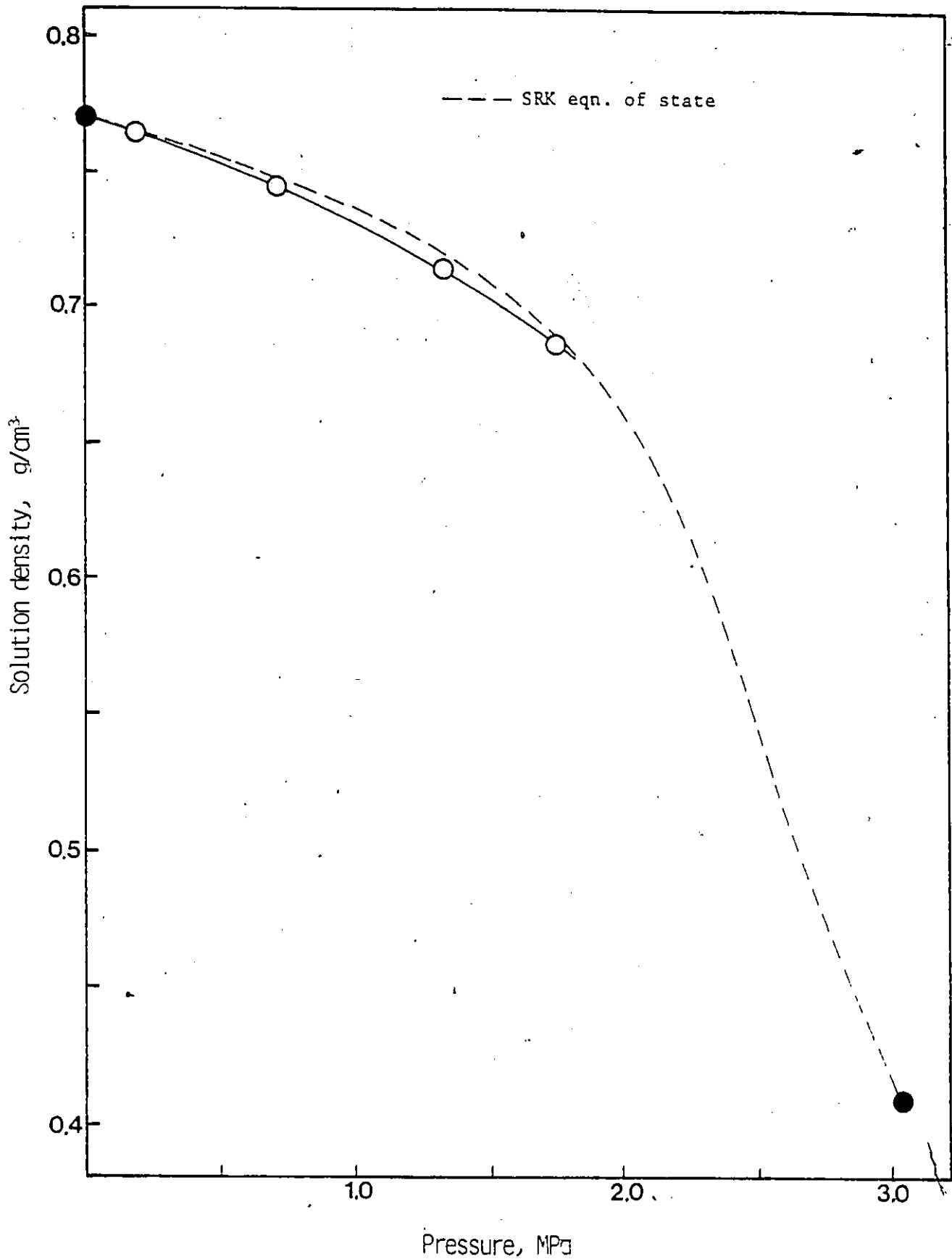


Figure 6-25 Experimental and predicted densities of propene-saturated n-butanol solutions at 343.15 K as a function of pressure.

chlorobenzene-isobutene systems. As for n-butanol-isobutene systems, predictions of the solution densities were only approximate. The figures in which the densities of isobutene-saturated solutions are shown as a function of pressure are presented in Appendix C.

### 6.3 GAS SOLUBILITY AT ELEVATED PRESSURES

A new solubility apparatus was designed and constructed for use at elevated pressures. The equilibration technique utilized in this apparatus was a dynamic equilibration method. While the solvent was passing downward at a very low flow rate on the outside surface of a stainless-steel coil, exposing a very thin film to the solute gas in the equilibration cell, it became saturated with the gas. An experiment was performed by supplying solute gas at the rate required to saturate the solvent, thus keeping the system pressure essentially constant. During the experiment, the volume of degassed solvent supplied to the cell and that of solute gas used, were recorded at regular time intervals. Throughout all the experiments, these two volumes were linearly related. In the calculation of solubility, the volume of gas displaced by the gas-saturated solution formed in the cell, was considered. For the purpose of determination of gas solubility at elevated pressures, the results of the density measurements of gas-saturated solutions were used.

The solubilities measured at elevated pressures were those of propene in n-octane, chlorobenzene and n-butanol, and also those of isobutene in the same solvents. Experiments were conducted at temperatures of 298.15 K, 323.15 K and 343.15 K and pressures ranging from 0.152 MPa to 1.93 MPa.

Two methods of predicting gas solubilities at elevated pressures were tried in this investigation. One was to use the SRK equation of state, the details of which were already mentioned in the previous section concerning the density of gas-saturated solutions. The solubilities predicted by means of the SRK equation of state are presented together with the gas-saturated solution densities in Tables 6-12 to 6-17. The other method was to utilize the UNIFAC method (81, 115, 123) by which the activity coefficients in the liquid phase were fully predictable based on the properties of the gas and solvent. The solubilities of the highly soluble gases were then predicted using the estimated activity coefficients.

The UNIFAC method is presented in the first section, and in the following section, the experimentally determined results are presented and compared with those obtained by prediction as mentioned above.

#### 6.3.1 GAS SOLUBILITY PREDICTION BY UNIFAC METHOD

The UNIFAC method for predicting activity coefficients in the liquid phase provides the process design engineer

with a useful tool for calculating vapor-liquid equilibrium compositions in the frequently encountered situation where no binary (or higher) experimental information is available. In this method, a molecule is regarded as an aggregate of functional groups, and the phase equilibria are described by the summation of group contributions in the mixture. The advantage of the UNIFAC method is that whereas there are thousands of chemical compounds of interest in chemical technology, the number of functional groups which constitute these compounds is much smaller. Therefore, by introducing interaction parameters specific to each pair of functional groups, it is possible to describe the phase behavior of multicomponent systems.

Fredenslund et al. (123) proposed the UNIFAC equation for the liquid phase activity coefficient of component  $i$  as:

$$\ln \gamma_i = \ln \gamma_i^C + \ln \gamma_i^R \quad (6-13)$$

In the above equation, the first term is the combinatorial activity coefficient and the second term is the residual activity coefficient. They are further expressed as follows:

$$\ln \gamma_i^C = \ln \frac{\phi_i}{x_i} + \frac{z}{2} q_i \ln \frac{\phi_i}{\phi_i^*} + \lambda_i - \frac{\phi_i}{x_i} \sum_j x_j l_j \quad (6-14)$$

$$\lambda_i = \frac{z}{z} (r_i - q_i) - (r_i - 1) ; z = 10 \quad (6-15)$$

$$\theta_i = q_i x_i / \sum_j q_j x_j \quad (6-16)$$

$$\phi_i = r_i x_i / \sum_j r_j x_j \quad (6-17)$$

$$r_i = \sum_k v_k^{(i)} R_k \quad (6-18)$$

$$q_i = \sum_k v_k^{(i)} Q_k \quad (6-19)$$

$$\ln \gamma_i^R = \sum_k v_k^{(i)} (\ln \Gamma_k - \ln \Gamma_k^{(i)}) \quad (6-20)$$

$$\ln \Gamma_k = Q_k \left\{ 1 - \ln(\sum_m \theta_m \psi_{mk}) - \frac{\sum_m (\theta_m \psi_{km})}{\sum_n \theta_n \psi_{nm}} \right\} \quad (6-21)$$

$$\theta_m = Q_m X_m / \sum_n Q_n X_n \quad (6-22)$$

$$\psi_{mn} = \exp(-a_{mn}/T) \quad (6-23)$$

In these equations,  $x_i$  is the mole fraction of component  $i$ ,  $\theta_i$  is the area fraction and  $\phi_i$  is the segment fraction. The pure component parameters,  $r_i$  and  $q_i$  are, respectively, measures of molecular van der Waals volumes and molecular surface areas, and are calculated by Equations (6-18) and (6-19). The parameters  $R_k$  and  $Q_k$  are characteristic of each

functional group;  $v_i^{(k)}$  is the number of groups of type  $k$  in molecule  $i$ ;  $\Gamma_k$  is the group residual activity coefficient and  $\Gamma_k^{(i)}$  is the residual activity coefficient of group  $k$  in a solution containing only molecules of type  $i$ . These group activity coefficients are both calculated by Equations (6-21) to (6-23) in which  $\theta_m$  is the area fraction of group  $m$ , and  $X_m$  is the mole fraction of group  $m$  in the mixture. Finally,  $a_{mn}$  is the group interaction parameter characteristic of each group pair, and  $T$  is the absolute temperature.

For the actual calculation to predict the liquid phase activity coefficients based on Equations (6-13) to (6-23), the values of the parameters required were taken from those available in the tables prepared by Fredenslund et al. (123). However, for the systems involving chlorobenzene, the parameters required for the calculation of activity coefficients were not fully available, therefore the prediction of gas solubilities were not carried out for those systems.

The liquid phase activity coefficients obtained by the UNIFAC method were then utilized for the vapor-liquid equilibrium calculation. The total pressure of the system is expressed by the following equation utilizing the activity coefficients:

$$P = \frac{\gamma_1 x_1 P_1^s}{\Phi_1} + \frac{\gamma_2 x_2 P_2^s}{\Phi_2} \quad (6-24)$$

In the above equation,  $\gamma_1$  and  $\gamma_2$  are the activity coefficients of solvent and solute, obtained by the UNIFAC method;  $x_1$ ,  $x_2$ ,  $P_1^s$  and  $P_2^s$  are the mole fractions of solvent and solute in the liquid phase, and the saturated vapor pressures of solvent and solute. The symbol  $\phi_1$  represents the ratio of the fugacity coefficient of solvent component in the vapor phase at temperature,  $T$  and pressure,  $P$  to the fugacity coefficient of pure solvent at temperature,  $T$  and its saturated vapor pressure,  $P_1^s$ ;  $\phi_2$  is for the solute defined in a similar way. These ratios,  $\phi_1$  and  $\phi_2$ , are further expressed by the following equations using second virial coefficients:

$$\phi_1 = \exp\left\{\frac{B_1(P - P_1^s) + PY_2^2\sigma_{12}}{RT}\right\} \quad (6-25)$$

$$\phi_2 = \exp\left\{\frac{B_2(P - P_2^s) + PY_1^2\sigma_{12}}{RT}\right\} \quad (6-26)$$

where

$$\sigma_{12} = 2B_{12} - B_{11} - B_{22} \quad (6-27)$$

In the above equations,  $B_1$  and  $B_2$  are the second virial coefficients of solvent and solute, and  $y_1$  and  $y_2$  are the mole fractions in the vapor phase for solvent and solute components, respectively;  $R$  is the gas constant, and  $B_{12}$  is the cross second virial coefficient characteristic of the

binary pair. In this investigation,  $B_{12}$  was estimated by the method proposed by Prausnitz (115):

$$B_{12} = RT_{c12}/P_{c12} \cdot (B^0 + \omega_{12} B^1) \quad (6-28)$$

$$B^0 = 0.083 - 0.422 / T_r^{1.6} \quad (6-29)$$

$$B^1 = 0.139 - 0.172 / T_r^{4.2} \quad (6-30)$$

$$\omega_{12} = (\omega_1 + \omega_2) / 2 \quad (6-31)$$

$$T_{c12} = (T_{c1} + T_{c2})^{0.5} \quad (6-32)$$

$$P_{c12} = Z_{c12} R T_{c12} / V_{c12} \quad (6-33)$$

$$Z_{c12} = (Z_{c1} + Z_{c2}) / 2 \quad (6-34)$$

$$V_{c12} = \left( \frac{V_{c1}^{1/3} + V_{c2}^{1/3}}{2} \right)^3 \quad (6-35)$$

In the above equations,  $T_r$  is the reduced temperature;  $\omega_1$  and  $\omega_2$  are the acentric factors of solvent and solute;  $T_{c1}$  and  $T_{c2}$  are the critical temperatures of solvent and solute;  $Z_{c1}$  and  $Z_{c2}$  are the critical compressibilities of solvent and solute, and  $V_{c1}$  and  $V_{c2}$  are the critical molar volumes of solvent and solute.

The flow chart for the vapor-liquid equilibrium calculation utilizing Equations (6-13) to (6-35) is shown in Figure 6-26. In the actual calculation, the equilibrium pressure was calculated for the given value of solubility,  $x_2$ . The results obtained are shown in Tables 6-24 to 6-27. These solubility vs pressure relations, as well as those by the SRK equation of state, will be presented together with the experimental results in the same figures for comparison in the next section.

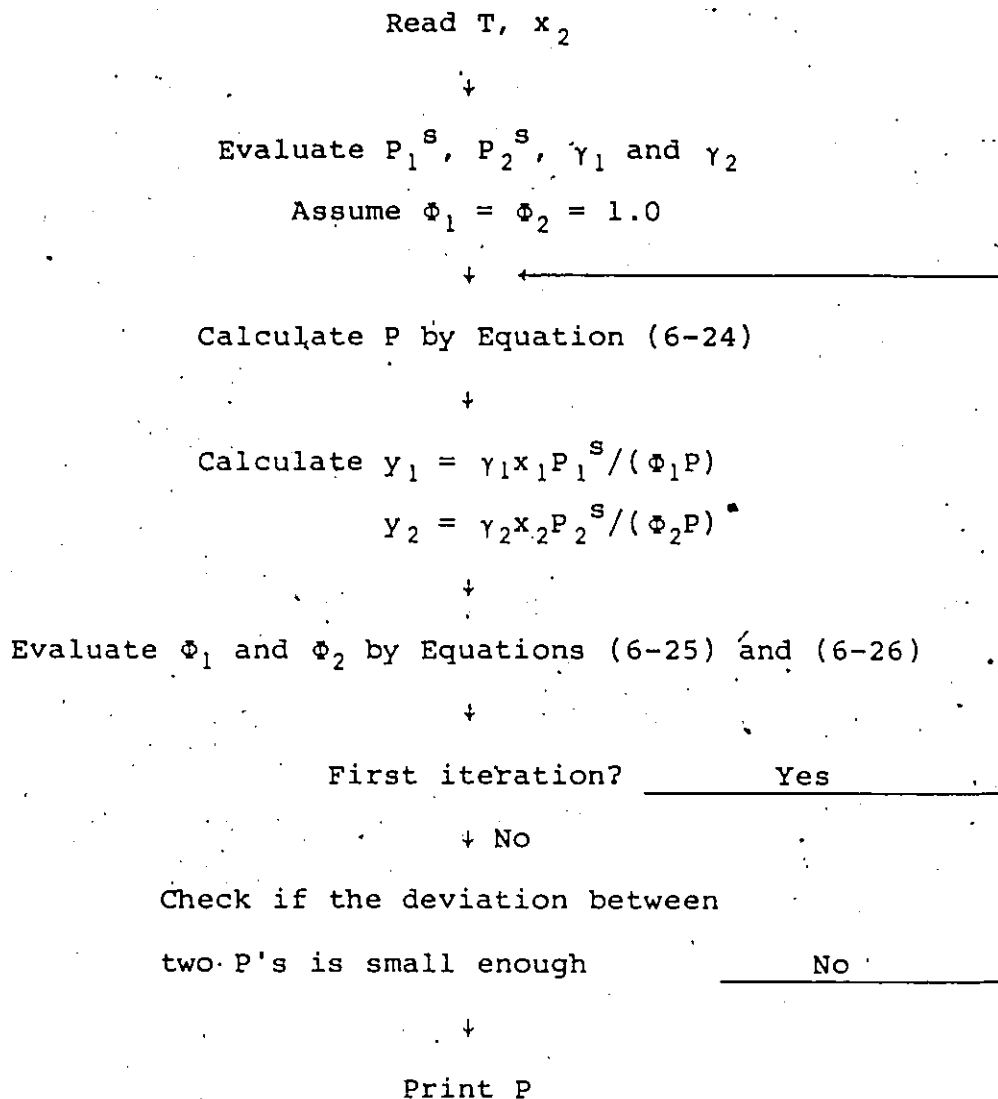


Figure 6-26 Flow chart for the vapor-liquid equilibrium calculation utilizing the UNIFAC method.

Table 6-24. Results of vapor-liquid equilibrium calculation utilizing the UNIFAC method for the (1) n-Octane - (2) Propene system.

x <sub>2</sub>	Pressure (MPa)		
	298.15 K	323.15 K	343.15 K
0.1	0.07976	0.1403	0.2098
0.2	0.1653	0.2893	0.4237
0.3	0.2592	0.4493	0.6602
0.4	0.3623	0.6279	0.9219
0.5	0.4751	0.8244	1.211
0.6	0.5979	1.040	1.531
0.7	0.7302	1.274	1.880
0.8	0.8700	1.524	2.259
0.9	1.014	1.785	2.660
0.95	1.085	1.917	2.866

Table 6-25. Results of vapor-liquid equilibrium calculation utilizing the UNIFAC method for the (1) n-Butanol - (2) Propene system.

x <sub>2</sub>	Pressure (MPa)		
	298.15 K	323.15 K	343.15 K
0.1	0.2487	0.4114	0.5844
0.2	0.4574	0.7615	1.084
0.3	0.6296	1.057	1.513
0.4	0.7687	1.301	1.874
0.5	0.8780	1.496	2.169
0.6	0.9610	1.649	2.404
0.7	1.021	1.763	2.586
0.8	1.063	1.848	2.727
0.9	1.095	1.919	2.854
0.95	1.114	1.965	2.937

Table 6-26. Results of vapor-liquid equilibrium calculation utilizing the UNIFAC method for the (1) n-Octane - (2) Isobutene system.

$x_2$	Pressure (MPa)		
	298.15 K	323.15 K	343.15 K
0.1	0.02780	0.05710	0.09455
0.2	0.05487	0.1098	0.1770
0.3	0.08305	0.1648	0.2634
0.4	0.1123	0.2221	0.3536
0.5	0.1425	0.2817	0.4478
0.6	0.1737	0.3433	0.5459
0.7	0.2056	0.4069	0.6477
0.8	0.2381	0.4922	0.7531
0.9	0.2709	0.5388	0.8617
0.95	0.2873	0.5726	0.9171

Table 6-27. Results of vapor-liquid equilibrium calculation utilizing the UNIFAC method for the (1) n-Butanol - (2) Isobutene system.

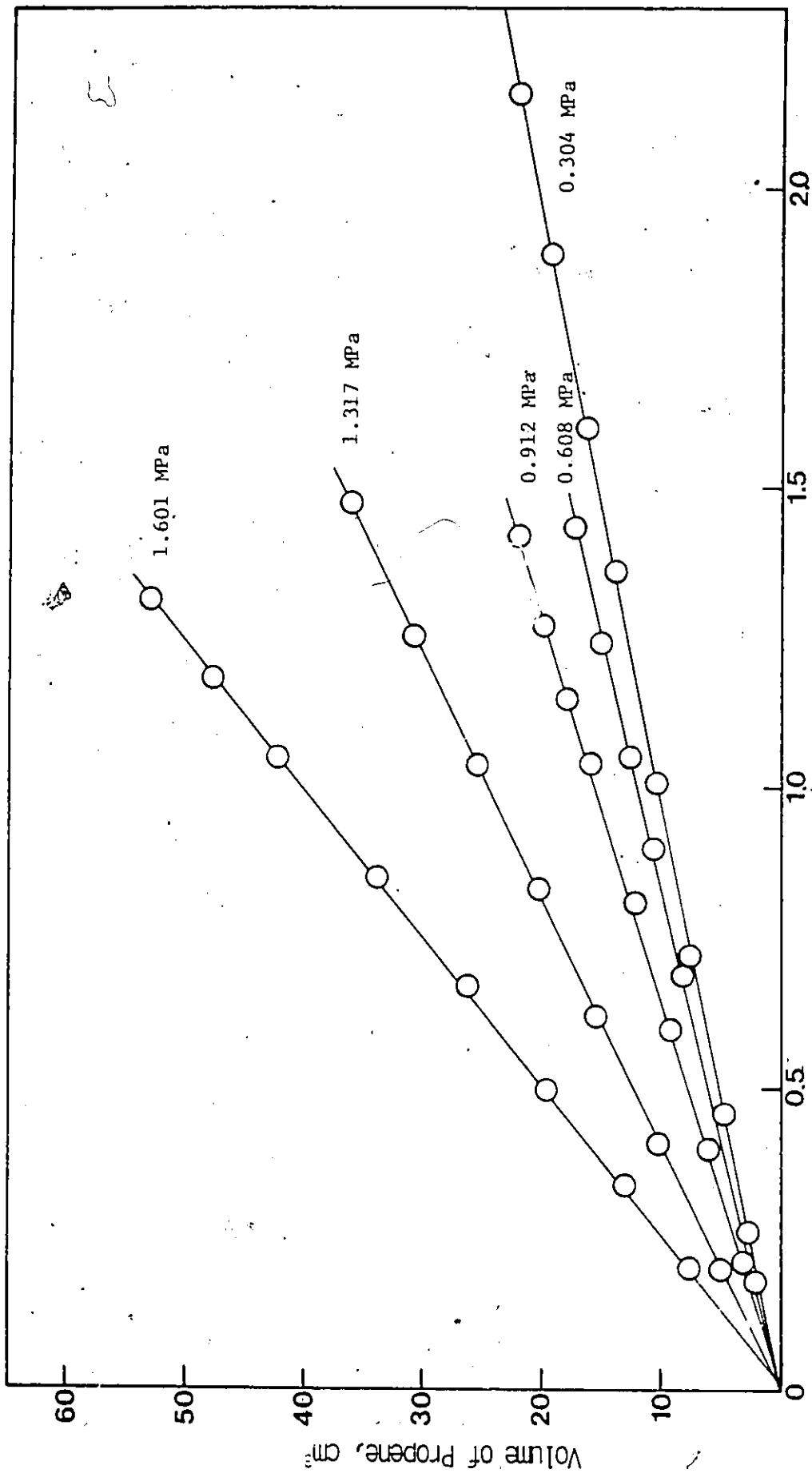
$x_2$	Pressure (MPa)		
	298.15 K	323.15 K	343.15 K
0.1	0.1076	0.2020	0.3105
0.2	0.1753	0.3316	0.5109
0.3	0.2183	0.4162	0.6447
0.4	0.2453	0.4709	0.7332
0.5	0.2620	0.5059	0.7915
0.6	0.2721	0.5282	0.8302
0.7	0.2782	0.5431	0.8574
0.8	0.2825	0.5550	0.8809
0.9	0.2879	0.5703	0.9111
0.95	0.2931	0.5835	0.9353

### 6.3.2 SOLUBILITY RESULTS AT ELEVATED PRESSURES

When using the apparatus developed in this investigation, the volume of solvent supplied and the volume of solute gas used were recorded at regular time intervals. For all the experiments conducted, the volumes of solvent and those of solute gas were linearly related. For the determination of gas solubilities, the total volume of solute gas required to saturate the solvent was determined in the manner discussed in Chapter 5. Thus solubilities were calculated by means of Equation (5-16), utilizing the constant factor relating the volumes of gas and solvent used and the density of the gas-saturated solution for the system involved.

As an example in Figure 6-27 for the n-octane-propene system at 323.15 K, the volumes of n-octane supplied to the equilibration cell are plotted as a function of the volume of propene used, for various pressures from 0.304 MPa, to 1.601 MPa. It may be observed in this figure that the higher the experimental pressure, the higher the propene volume required for a unit volume of n-octane solvent. It is also evident that at higher pressures the increase in volume of propene was greater than at lower pressures. This resulted from the fact that at higher pressures the solvent was a minor component in the saturated solution while the dissolved gas was the major component.

In Figure 6-28, the volume of propene-saturated n-octane is shown as a function of the volume of pure n-octane



Volume of n-Octane supplied to the cell, cm<sup>3</sup>

Figure 6-27. Volumes of propene used for the solubility measurements at 323.15 K and elevated pressures as a function of the volumes of n-octane supplied to the equilibration cell.

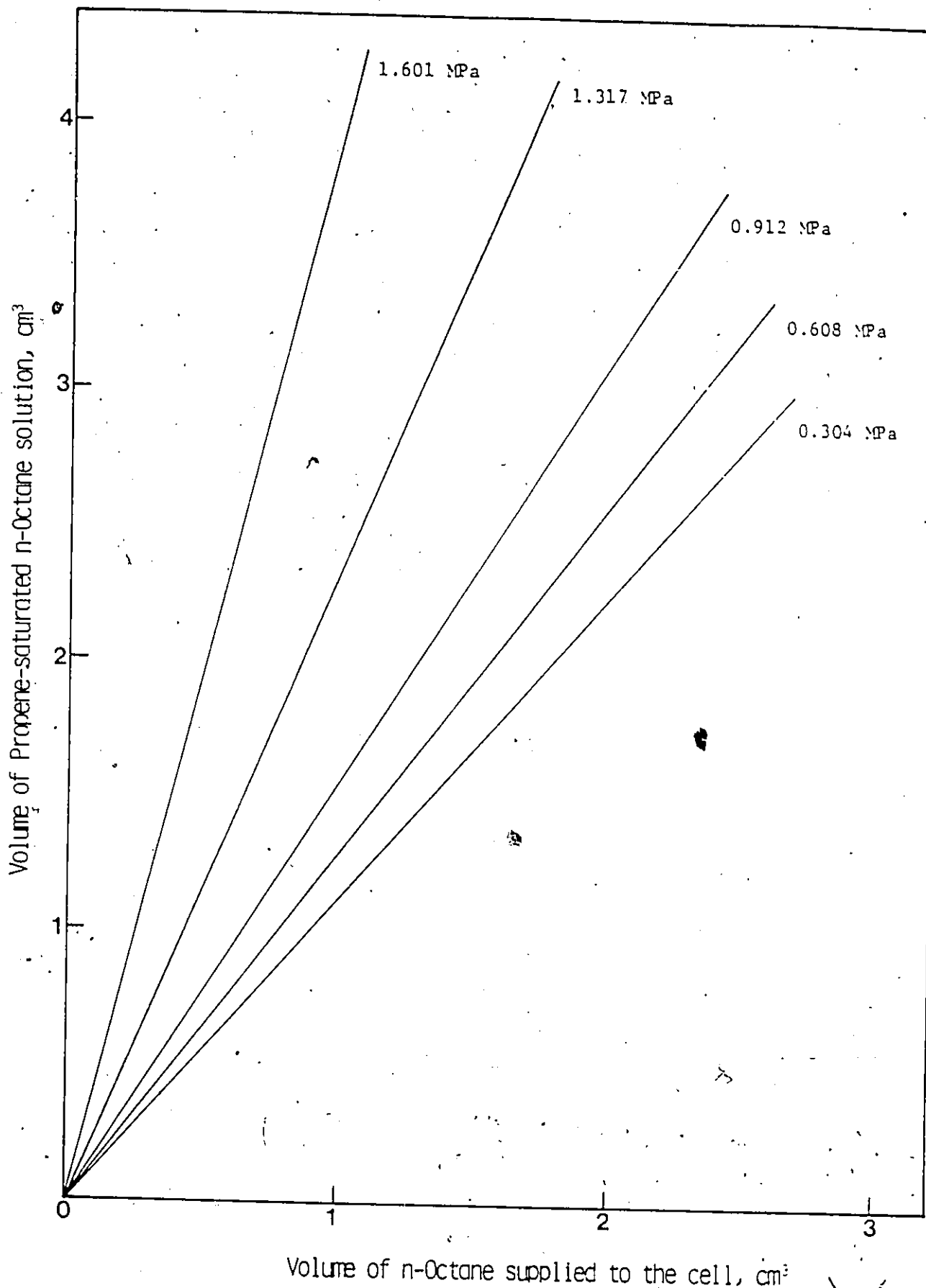


Figure 6-28 Volumes propene-saturated n-octane solutions at 323.15 K formed in the equilibration cell as a function of the volumes of n-octane supplied to the cell.

required to form the solution. This relationship indicates the extent of the expansion of the solvent as it becomes gas-saturated in the equilibration cell. With reference to this figure, it is clear that as the pressure increases, the volume of propene-saturated solution becomes much greater than the volume of n-octane originally supplied to the cell. At 1.601 MPa, it may be observed that 1 cm<sup>3</sup> of n-octane produces approximately 4 cm<sup>3</sup> of propene-saturated solution. This fact indicates that the volume correction for the volume of solute gas displaced in the cell should not be made on the basis of the volume of pure solvent supplied but of the volume of gas-saturated solution formed in the cell.

The results of the solubility measurements at elevated pressures as obtained in this investigation are tabulated in Tables 6-28 to 6-33 for each system and measurement temperature. These results are also shown as a function of pressures in Figure 6-29 to 6-34. Also plotted in these figures are the predicted solubilities using the SRK equation of state and the UNIFAC method. In each case the solubility predicted by the SRK equation is indicated by a dotted line and the solubility predicted by the UNIFAC method is indicated by a continuous line. The solubilities shown by triangles are those measured at atmospheric pressure.

As indicated in Figure 6-29, for the propene-n-octane system, the agreement between the experimental and predicted solubilities as obtained utilizing the SRK equation of state is considered excellent. Regardless of the change in

Table 6-28. Solubilities of Propene in n-Octane at elevated pressures.

Temperature					
298.15 K		323.15 K		343.15 K	
P (MPa)	$x_2$ (-)	P (MPa)	$x_2$ (-)	P (MPa)	$x_2$ (-)
0.203	0.206	0.304	0.179	0.608	0.238
0.405	0.396	0.608	0.348	1.006	0.363
0.608	0.576	0.912	0.521	1.419	0.535
0.811	0.758	1.317	0.724	1.723	0.638
1.013	0.905	1.601	0.850		

Table 6-29. Solubilities of Propene in Chlorobenzene at elevated pressures.

Temperature					
298.15 K		323.15 K		343.15 K	
P (MPa)	$x_2$ (-)	P (MPa)	$x_2$ (-)	P (MPa)	$x_2$ (-)
0.203	0.131	0.304	0.110	0.517	0.128
0.405	0.273	0.608	0.159	0.983	0.229
0.608	0.424	0.912	0.338	1.439	0.367
0.811	0.645	1.317	0.538	1.925	0.530
1.013	0.868	1.601	0.713		

Table 6-30. Solubilities of Propene in n-Butanol at elevated pressures.

Temperature					
298.15 K		323.15 K		343.15 K	
P(MPa)	$x_2$ (-)	P(MPa)	$x_2$ (-)	P(MPa)	$x_2$ (-)
0.203	0.0789	0.405	0.0897	0.520	0.0867
0.405	0.173	0.608	0.138	1.027	0.182
0.608	0.298	0.709	0.177	1.637	0.322
0.811	0.492	0.912	0.226		
1.013	0.715	1.317	0.381		
		1.621	0.557		

Table 6-31. Solubilities of Isobutene in n-Octane at elevated pressures.

Temperature					
298.15 K		323.15 K		343.15 K	
P(MPa)	$x_2$ (-)	P(MPa)	$x_2$ (-)	P(MPa)	$x_2$ (-)
0.152	0.508	0.152	0.256	0.203	0.221
0.203	0.682	0.253	0.434	0.362	0.403
0.210	0.691	0.304	0.524	0.569	0.611
0.244	0.802	0.380	0.642	0.853	0.888
		0.456	0.774		
		0.565	0.936		

Table 6-32. Solubilities of Isobutene in Chlorobenzene at elevated pressures.

Temperature					
298.15 K		323.15 K		343.15 K	
P(MPa)	$x_2$ (-)	P(MPa)	$x_2$ (-)	P(MPa)	$x_2$ (-)
0.152	0.419	0.152	0.180	0.215	0.133
0.203	0.555	0.253	0.325	0.352	0.268
0.228	0.652	0.355	0.513	0.521	0.440
		0.476	0.765	0.659	0.608
				0.875	0.862

Table 6-33. Solubilities of Isobutene in n-Butanol at elevated pressures.

Temperature					
298.15 K		323.15 K		343.15 K	
P(MPa)	$x_2$ (-)	P(MPa)	$x_2$ (-)	P(MPa)	$x_2$ (-)
0.152	0.179	0.152	0.0977	0.385	0.179
0.203	0.296	0.253	0.181	0.634	0.351
0.253	0.445	0.355	0.273	0.881	0.759
		0.405	0.338		

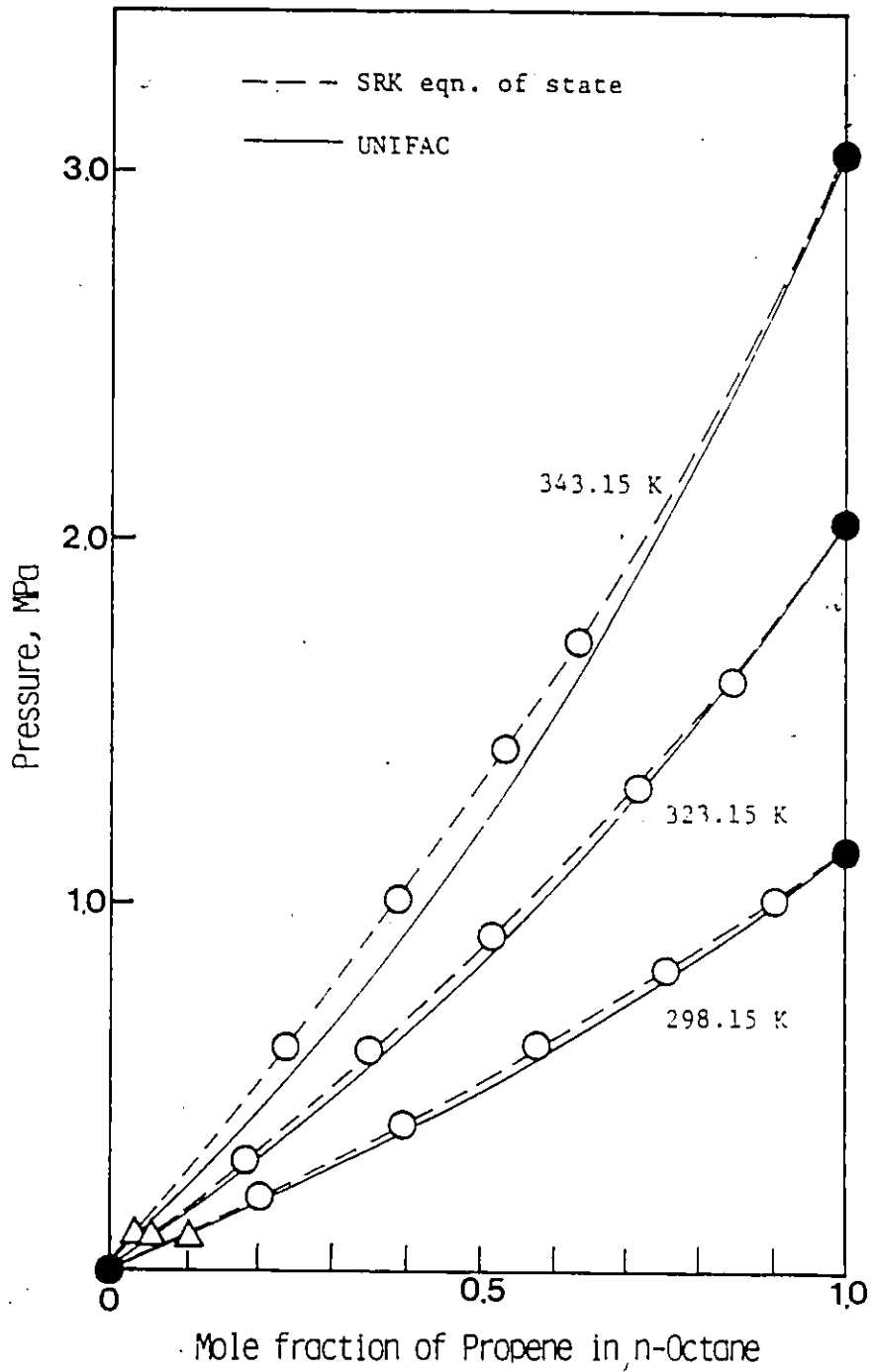


Figure 6-29 Experimental and predicted solubilities of propene in n-octane at elevated pressures.

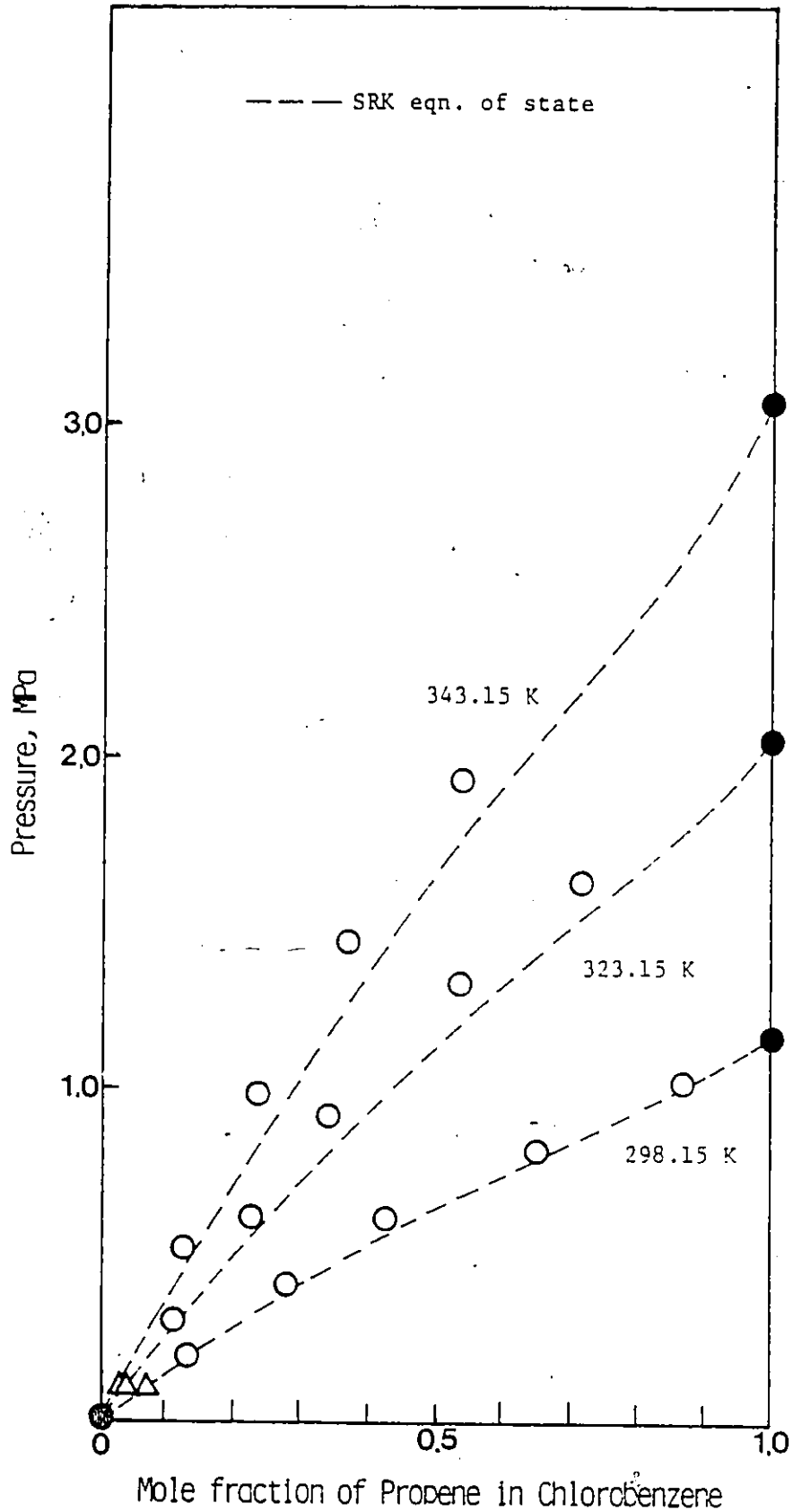


Figure 6-30. Experimental and predicted solubilities of propene in chlorobenzene at elevated pressures.

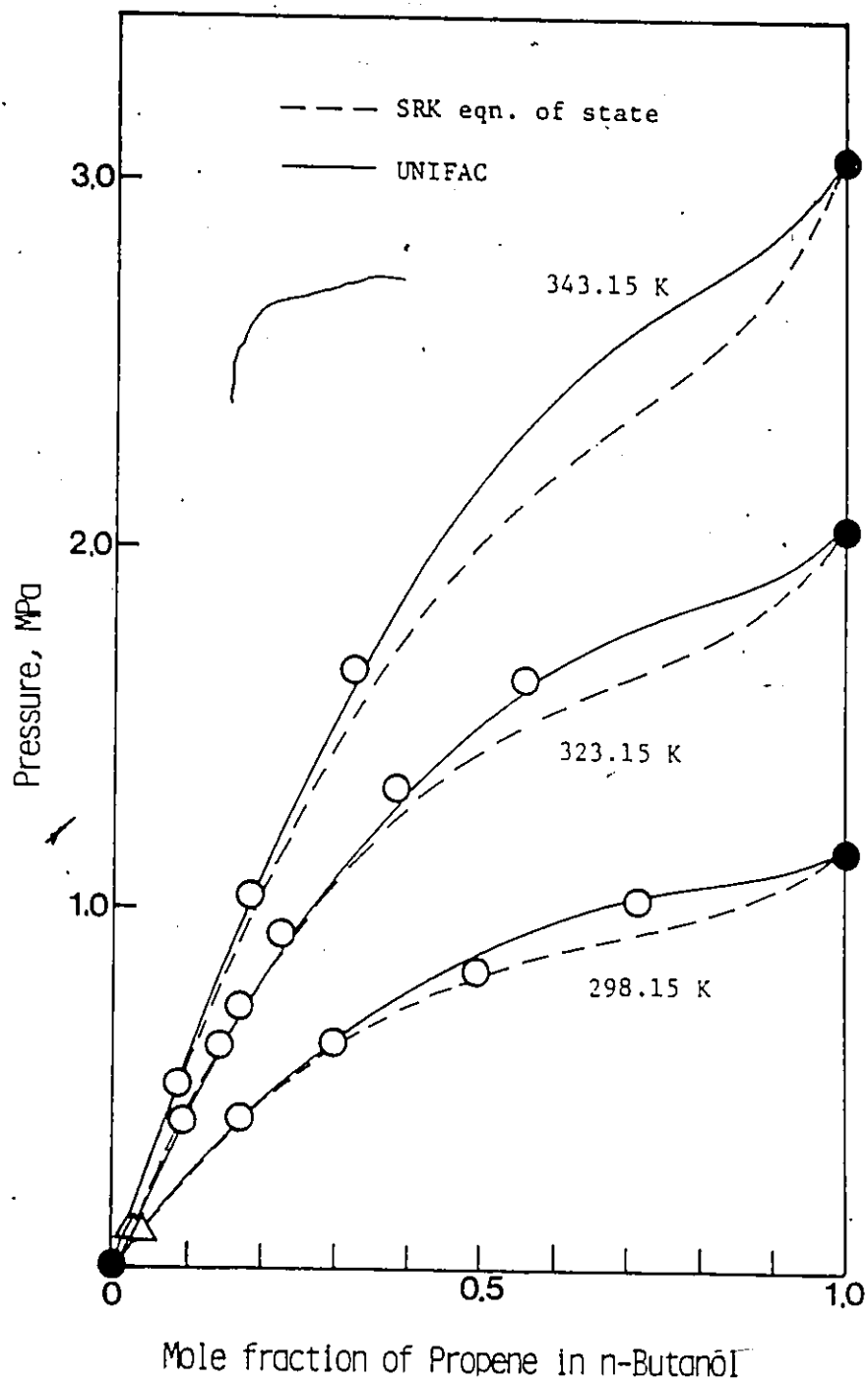


Figure 6-31 Experimental and predicted solubilities of propene in n-butanol at elevated pressures.

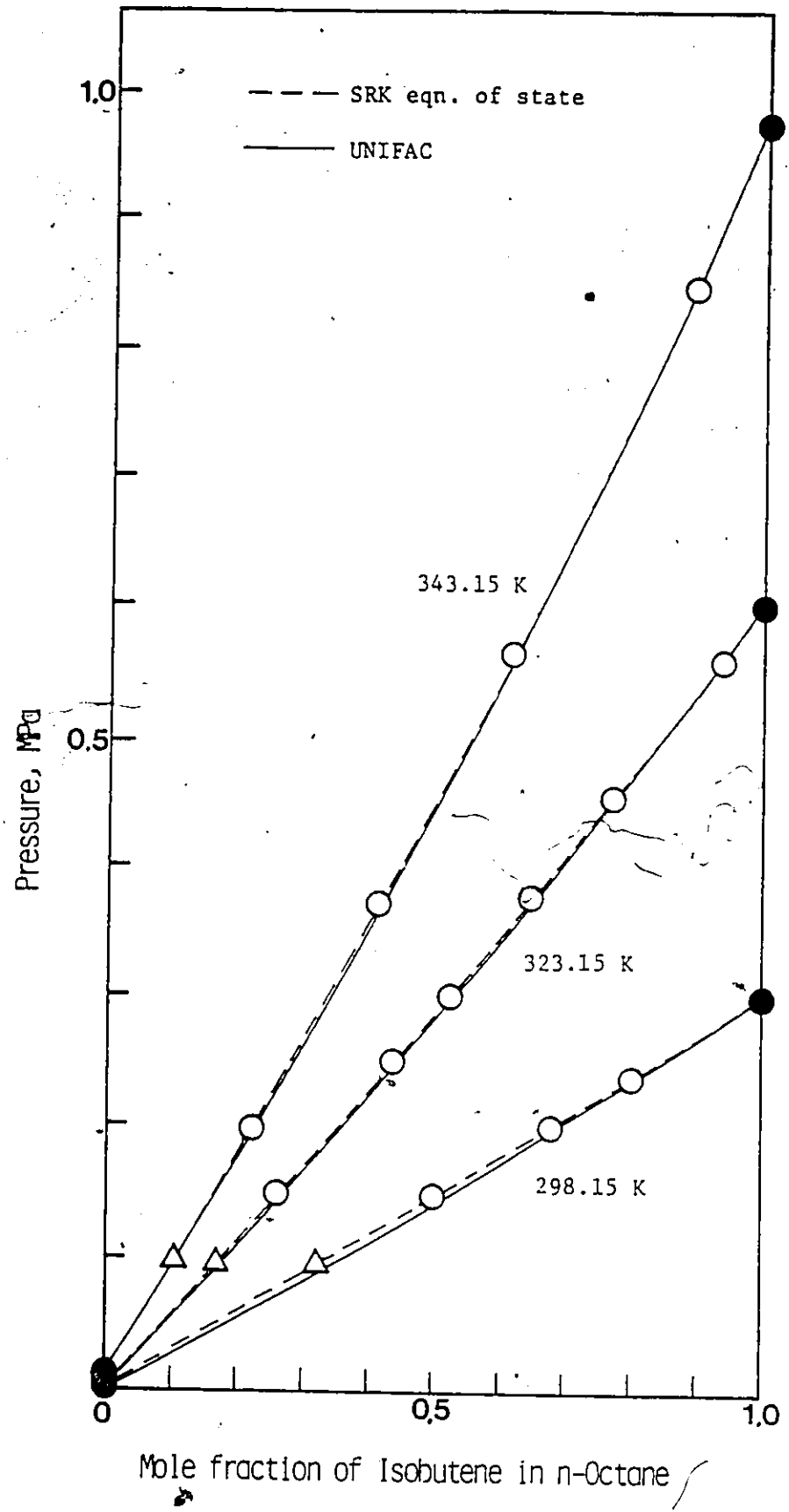


Figure 6-32 Experimental and predicted solubilities of isobutene in n-octane at elevated pressures.

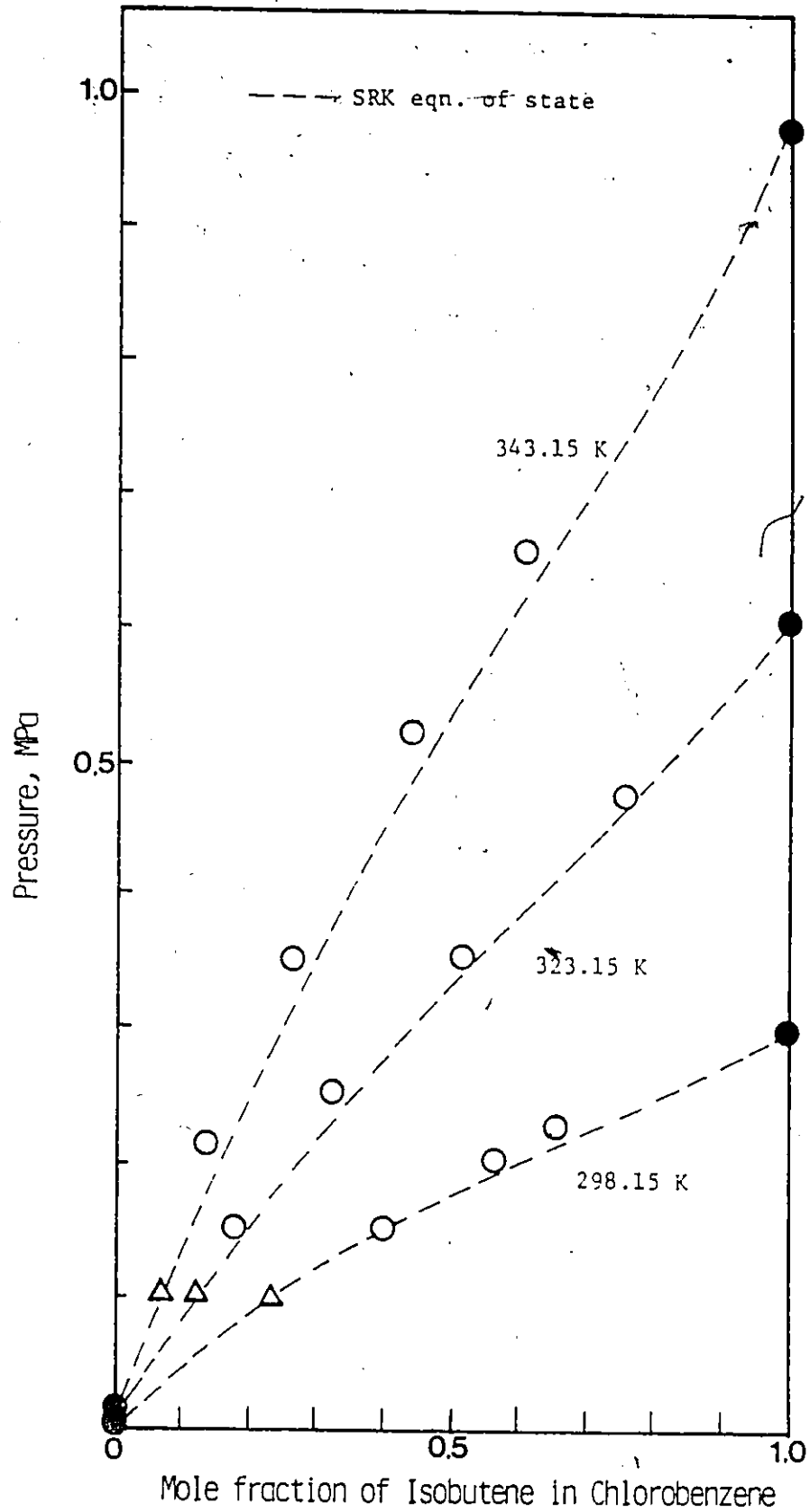


Figure 6-33 Experimental and predicted solubilities of isobutene in chlorobenzene at elevated pressures.

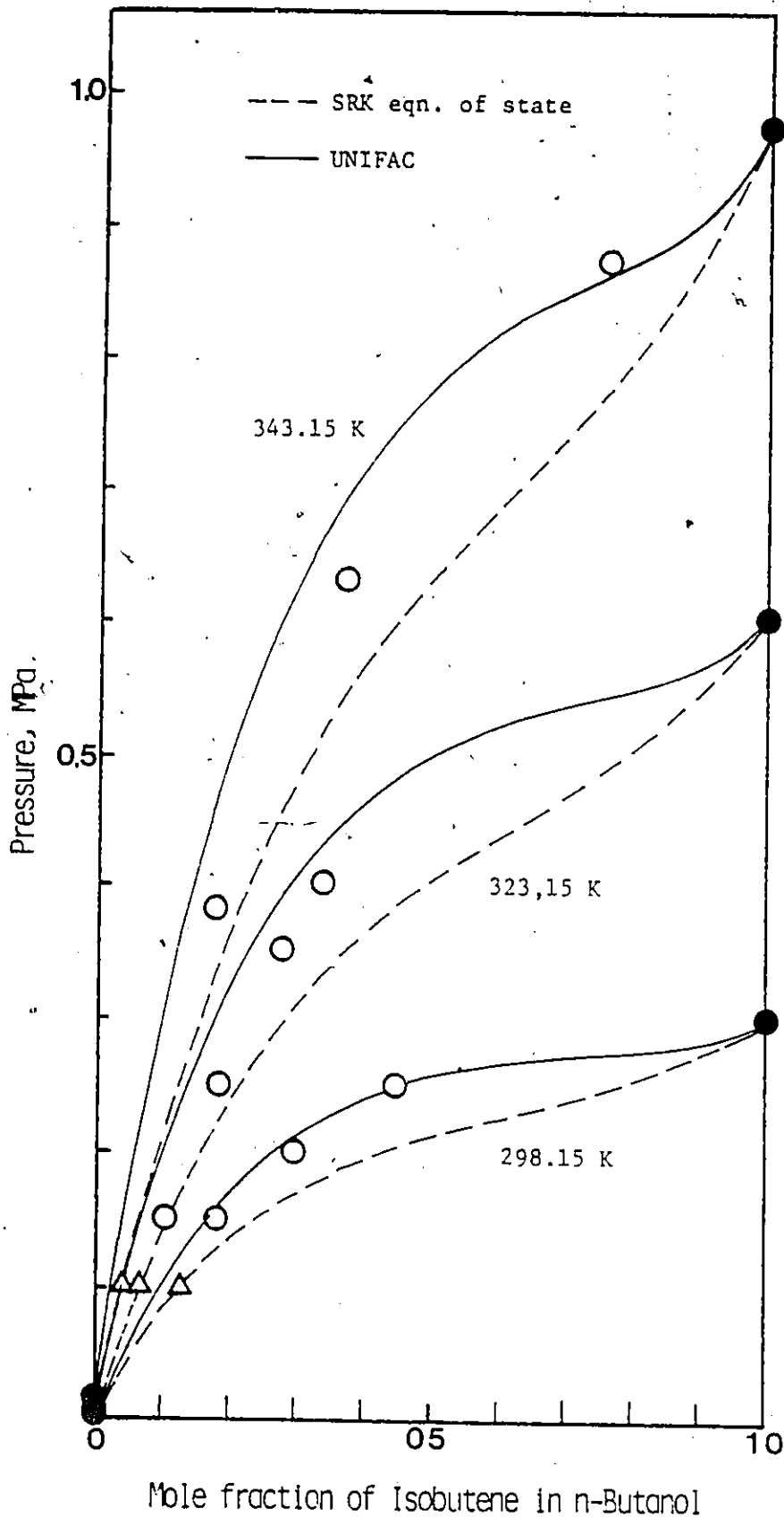


Figure 6-34 Experimental and predicted solubilities of isobutene in n-butanol at elevated pressures.

temperature and pressure, the prediction by this method was consistently very good. As mentioned in Chapter 2, binary interaction parameters are usually determined by using as many vapor-liquid equilibrium data as available to produce the best possible fit of the data and to use them for the multi-component vapor-liquid equilibrium calculations. In this investigation, however, the binary interaction parameter for each system and each temperature was based on a single solubility measured at atmospheric pressure. Using this binary interaction parameter, the solubilities can be predicted at the same temperature and at elevated pressures. Therefore, the solubilities predicted by the SRK equation of state at atmospheric pressures must necessarily agree with those measured at atmospheric pressure. But, particularly for the solubilities in n-octane, good agreement was obtained for pressures higher than atmospheric.

The prediction of the solubility of propene in n-octane by the UNIFAC method was most successful at the lowest temperature, 298.15 K, for this system, but deviations from the experimental data were considerably greater than those obtained using the SRK equation of state.

In Figure 6-30 are shown the solubility results for the chlorobenzene-propene system. Since the group parameters required for the prediction by the UNIFAC method were not available for chlorobenzene, the prediction of solubility in chlorobenzene using this method was not possible. Hence, only the solubilities predicted by means of the SRK equation

of state are shown in this figure for comparison with the experimental results. It may be observed that the predicted solubility differs significantly from that experimentally determined. For a polar and non-associating solvent such as chlorobenzene, the solubilities predicted by the SRK equation of state seem to be just approximate at the elevated pressures.

The solubilities for the n-butanol-propene system are shown in Figure 6-31. The solubilities in butanol are lower than in the other two solvents at otherwise comparable conditions. It is considered that this may result from the strong association in n-butanol preventing the penetration of propene into the molecular complex in the polar solvent. Solubilities predicted by the UNIFAC method were closer to the experimentally determined results than were those predicted by the SRK equation of state. It may be noticed that the solubilities predicted by the SRK equation of state become erroneous at higher pressures. Despite the larger values of binary interaction parameters for this system when compared to those of other systems (Table 6-1), the solubilities predicted using the SRK equation of state are significantly different from those experimentally measured. This suggests that the application of the SRK equation of state to polar and associated solvents such as n-butanol is not appropriate.

In Figures 6-32 to 6-34, are shown the experimental and predicted solubilities of isobutene in n-octane, chloroben-

zene and n-butanol. Nearly the same discussion as made in the case of the propene solubilities applies to these systems, with the exception of the discussion concerning the n-butanol-isobutene system. For the latter system, both prediction methods yielded solubilities which had large deviations from the experimental solubilities, especially at temperatures 323.15 K and 343.15 K. It was apparent that neither prediction method was successful in predicting solubilities in polar and associated solvents at high pressure.

In Figure 6-35, the densities of propene-saturated n-octane solutions at 323.15 K are shown as a function of the propene concentration. While the data were obtained at a constant temperature, the increasing propene concentration corresponded to an increase in pressure. The dotted line in this figure denotes the solution densities predicted by the SRK equation of state with its binary interaction parameter based on the solubility measured at atmospheric pressure. The SRK equation of state gives predicted densities which are nearly identical to the experimentally determined solution densities.

In Figure 6-36, the densities of propene saturated n-octane at 323.15 K are presented as a function of the volume fraction of propene in the solution. In this case the volume fraction is based on the liquid volumes that the components of the solution had before mixing. With reference to this figure, it may be observed that the experimental densities of propene-saturated n-octane have

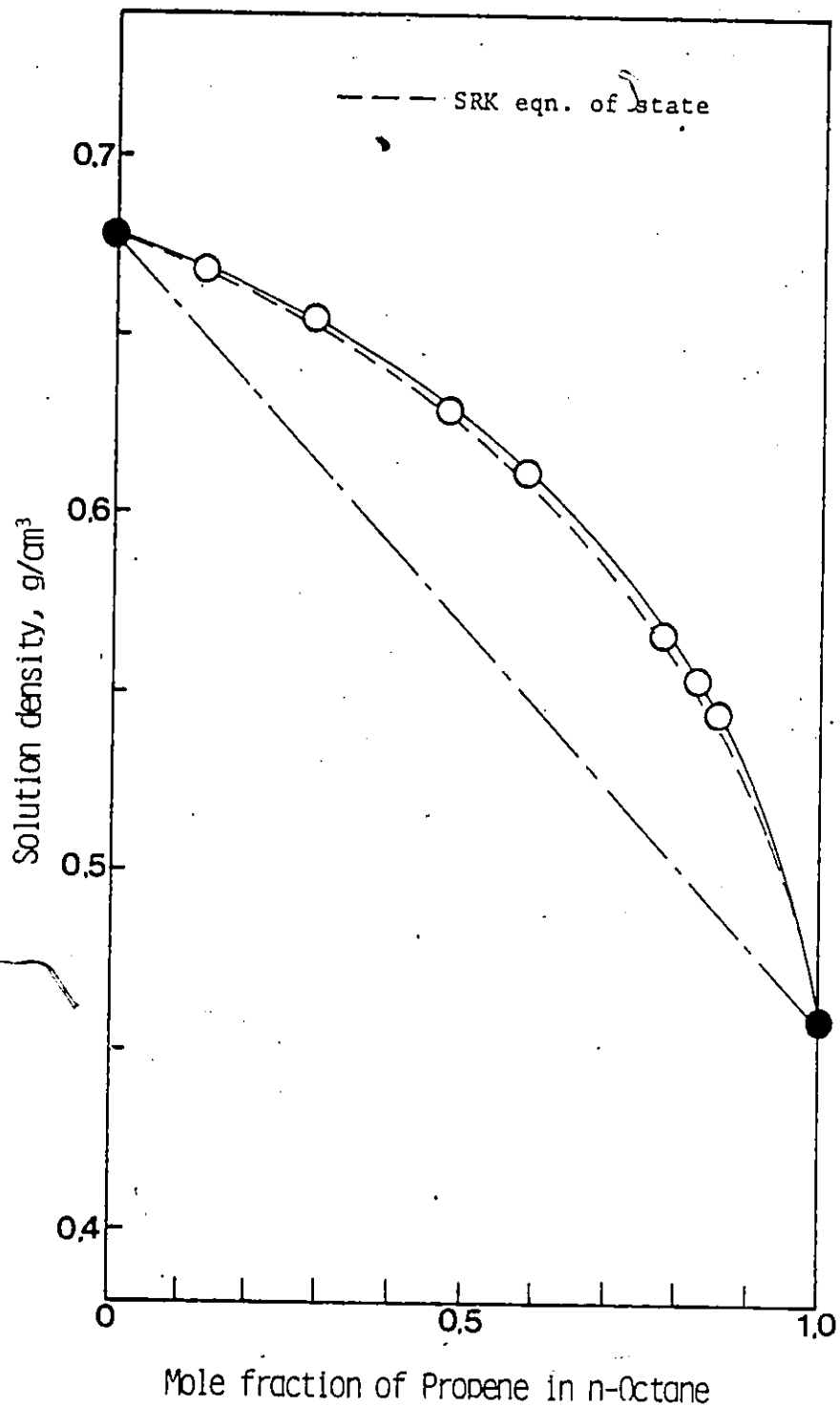


Figure 6-35 Experimental and predicted densities of propene-saturated n-octane solutions at 323.15 K as a function of mole fraction of propene in the solution.

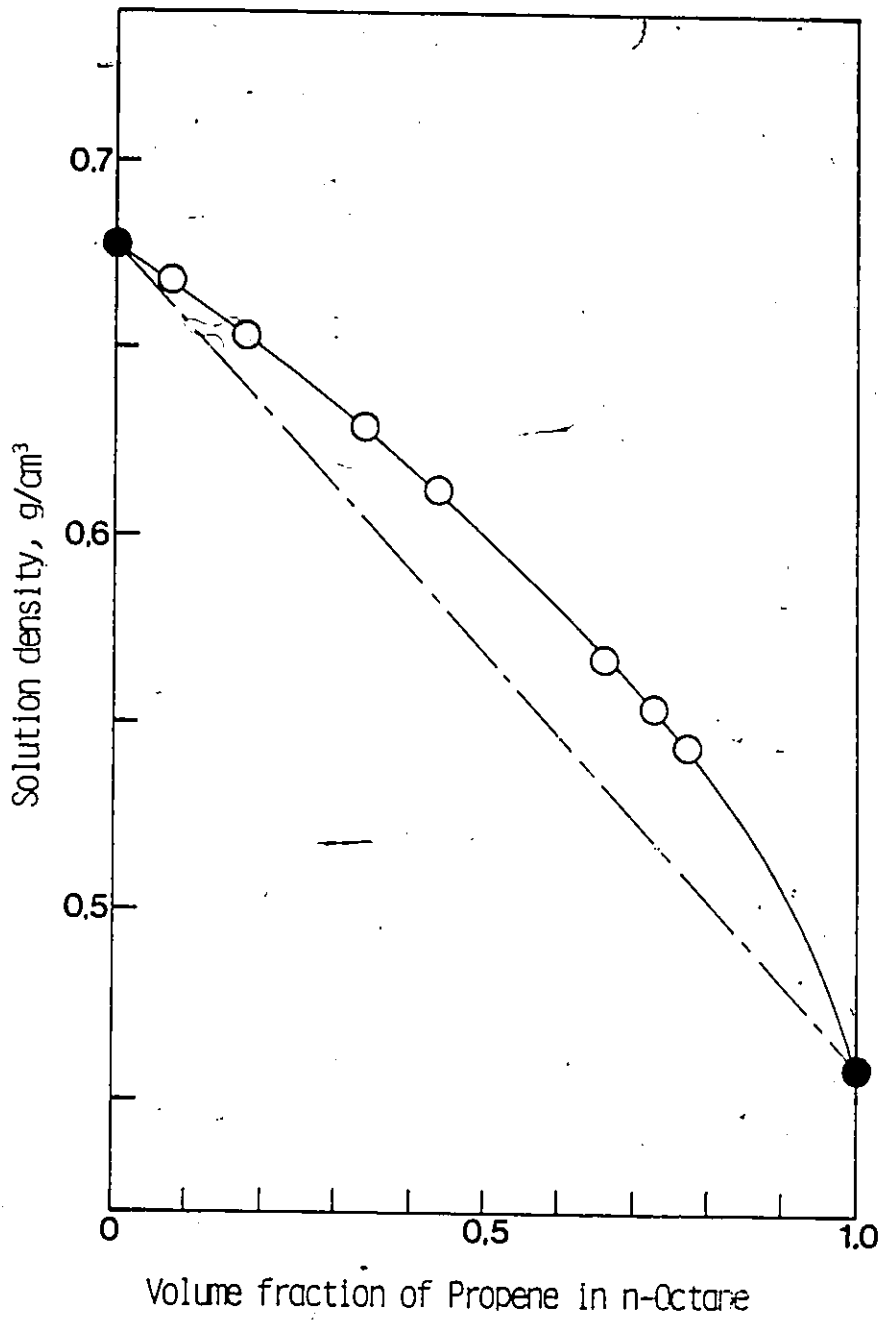


Figure 6-36 Densities of propene-saturated n-octane solutions at 323.15 K as a function of volume fraction of propene in the solution.

positive deviations from a simple linear approximation of solution densities with respect to volume fraction, over the whole range of compositions. It can be shown that a linear relation would result if there was no volume change on mixing of the liquid components, and the liquids were incompressible. Based on the observed data it was considered that there was a certain volume change on formation of the solutions since it appears most unlikely that the liquids were compressed at the relatively low pressures used. The positive deviations were then considered to indicate the volume contraction on mixing of the liquid components.

In Figures 6-37 and 6-38, the densities of propene-saturated chlorobenzene solution at 323.15 K and those of propene-saturated n-butanol solution at 323.15 K are shown, respectively, as a function of the volume fraction of propene in each solution. The solution densities in both figures have also positive deviations from the linear approximations, indicating that the volume contractions occurred in both systems. It may be noted that the densities of propene-saturated n-butanol solution have as large positive deviations from the linear approximation as those of propene-saturated n-octane at 323.15 K, while the densities of propene-saturated chlorobenzene have only slightly positive deviations from the linear approximation. It was therefore considered that the volume contraction on mixing of the liquid components for the chlorobenzene and propene system was not as significant as that for the n-octane and

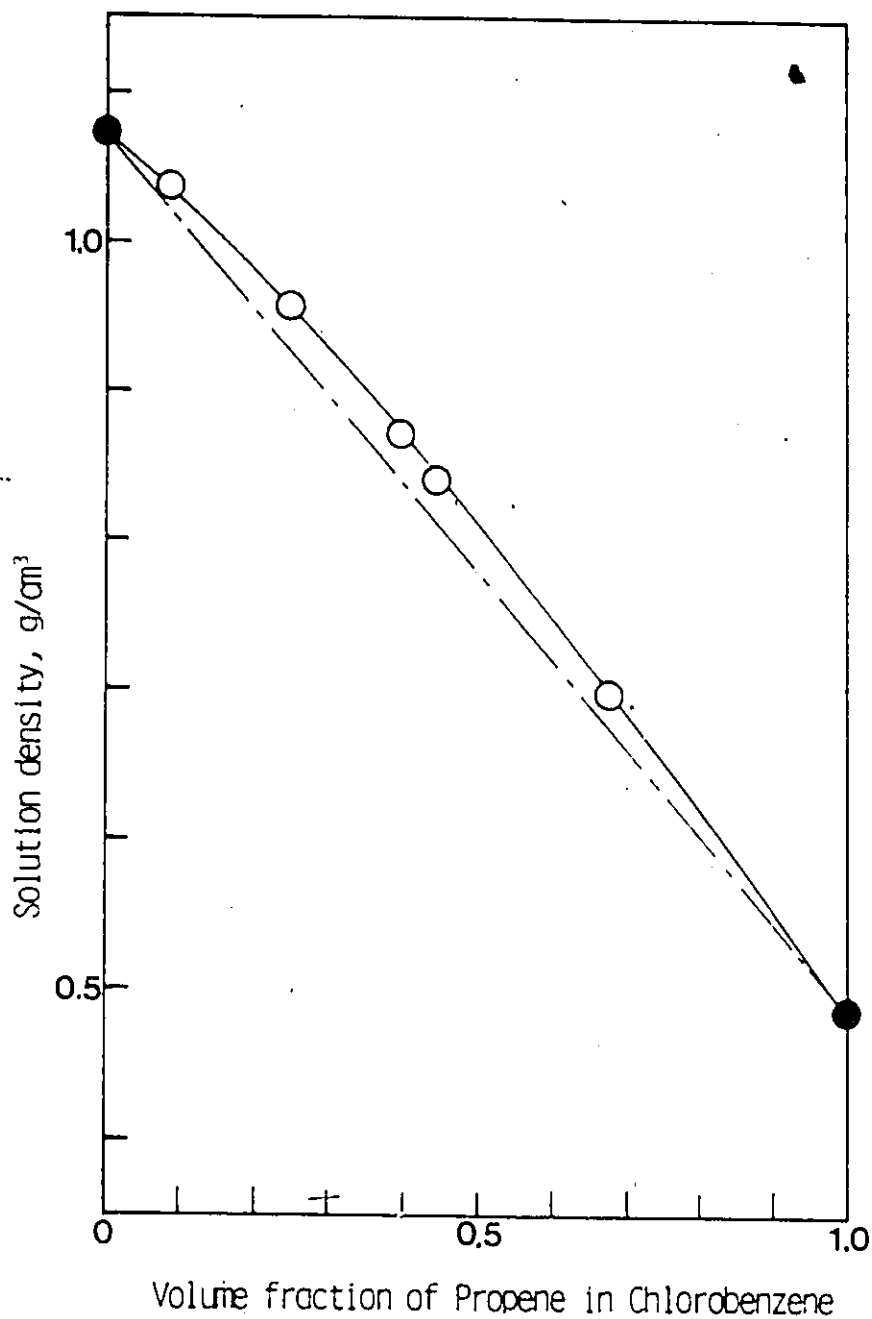


Figure 6-37 Densities of propene-saturated chlorobenzene solutions at 323.15 K as a function of volume fraction of propene in the solution.

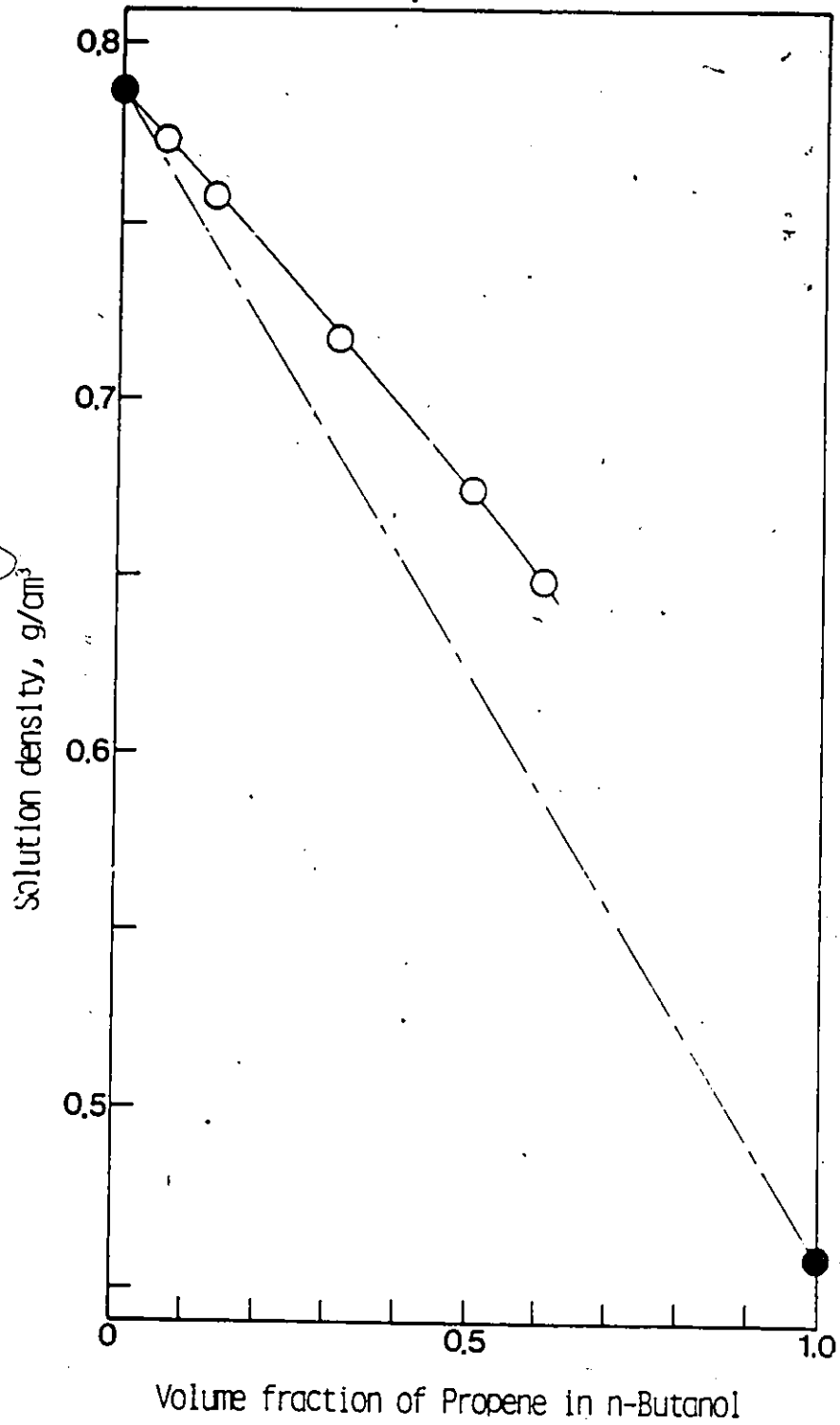


Figure 6-38 Densities of propene-saturated n-butanol solutions at 323.15 K as a function of volume fraction of propene in the solution.

propene system, and that for the n-butanol and propene system. The experimental solution densities for other systems also investigated in this study are shown as a function of the solute gas concentration in the solutions, along with the solution densities predicted by means of the SRK equation of state.

#### 6.4 RESULTS OF SOLUBILITY MEASUREMENTS BASED ON GAS CHROMATOGRAPHIC ANALYSIS OF GAS-SATURATED SOLUTIONS

In order to check the measurements of gas solubility at elevated pressures as developed in this investigation, the gas-saturated solutions were analyzed by gas chromatography. It was initially considered that this procedure of analysis for the gas-saturated solutions would provide a simple means of determining the gas solubilities. The analysis consisted of obtaining the area ratio for solute to solvent as determined for each gas-saturated solution by means of the gas chromatographic analysis. The area ratio was converted to the actual mole ratio utilizing the calibration line which had been previously prepared. Then the mole ratio was reduced to the solute mole fraction by calculation.

Gas chromatographic analyses were made for the propene-saturated solutions of n-octane at 298.15 K and 323.15 K and for the isobutene-saturated solutions at 298.15 K and 323.15 K. A sample calculation for converting the results of a gas chromatographic analysis to the mole fraction solubility is provided in Appendix E.

The results of the gas chromatographic analysis for the n-octane-propene system at 298.15 K and 323.15 K are shown in Table 6-34 along with the gas solubilities determined by the volumetric measurements. It is observed from this table, that there is good agreement between the results obtained by the gas chromatographic analyses and those by the method using volumetric measurements of gas and solvent. In the results shown in Table 6-34, the largest percent deviation is observed for the temperature of 298.15 K and pressure of 0.405 Mpa, the actual difference being 4.3 percent. However, the overall absolute average percent deviation for the propene-n-octane system was 1.6 percent.

In Table 6-35 are shown the gas chromatographic analysis results for the n-octane-isobutene system at 298.15 K and 343.15 K, together with the solubilities determined by the volumetric measurements at elevated pressures. In this system as well, good agreement was obtained between the two results. The absolute average percent deviation for this latter system is 1.2 percent.

Based on the good agreement between the two methods for determining gas solubilities at elevated pressures, it was considered that either method would be satisfactory for the determination of solubility. However, the volumetric method for determining the solubilities at elevated pressures had fewer sources of error, and was the faster and more consistent of the two. Hence, it was utilized for most of the solubility determination.

Table 6-34 Comparison of gas solubilities obtained by the volumetric measurements with those obtained by the gas chromatographic analysis for the (1) n-Octane-(2) Propene system.

P (MPa)	298.15 K		323.15 K	
	$X_2^{VOL}$	$X_2^{GC}$	$X_2^{VOL}$	$X_2^{GC}$
0.203	0.206	0.199		
0.304			0.179	0.180
0.405	0.396	0.378		
0.608	0.576	0.597	0.348	0.355
0.811	0.758	0.745		
0.912			0.521	0.528
1.013	0.905	0.898		
1.317			0.724	0.714
1.601			0.850	0.846

Table 6-35 Comparison of gas solubilities obtained by the volumetric measurements with those obtained by the gas chromatographic analysis for the (1) n-Octane-(2) Isobutene system.

P (MPa)	298.15 K		323.15 K	
	$X_2^{VOL}$	$X_2^{GC}$	$X_2^{VOL}$	$X_2^{GC}$
0.152	0.508	0.504	0.256	0.267
0.210	0.691	0.682		
0.244	0.802	0.814		
0.304			0.524	0.531
0.380			0.642	0.653
0.456			0.774	0.767
0.565			0.936	0.932

6.5 DEVELOPMENT OF A CORRELATION FOR INTERPOLATION OR  
EXTRAPOLATION OF GAS SOLUBILITIES AT ATMOSPHERIC  
PRESSURE

Many methods of predicting or correlating gas solubilities in liquids at atmospheric pressure are available in the literature. However, the application of these methods are usually limited to specific systems and conditions. In some cases, methods are available only for non-polar systems or for specific temperatures. Also, it is observed that prediction methods which do not utilize any solubility data are subject to large errors. Part of the reason for such large deviations between the experimental and predicted solubilities may be related to the range of solubilities which are observed for the many gases and solvents commonly utilized. These solubilities may vary in mole fraction from the order of  $10^{-1}$  to  $10^{-5}$  depending upon the particular solute gas and solvent.

The solubility correlation which was developed in this investigation is intended for practical engineering applications and requires a minimum of a single solubility value at atmospheric pressure. The solute gases utilized in developing the correlation included all types of gases from slightly soluble to highly soluble ones and included hydrogen and helium. The solvents utilized were limited to non-polar or slightly polar non-associating solvents. The solubility range considered, in mole fraction, was from approximately  $1 \times 10^{-5}$  to 0.15. The correlation results for various gases

are tabulated in Table 3-2. For the purpose of correlating solubility behavior equation (3-4) was used. An example of the application of the correlation is shown in Figure 3-3 for the solubilities in n-heptane. Similar diagram for the solubilities in other solvents also investigated in the study are shown in Figure A-1 to A-9 in Appendix A.

With reference to Table 3-2, the average percent deviations indicated in column (5) are those between experimental and correlated solubilities when Equation (3-4) was utilized along with the correlated reference solubilities calculated by Equation (3-11). The constants  $A_1$  and  $A_2$  used in Equation (3-4) are based on experimental and reference solubilities utilizing a computer optimization technique. The resulting deviations as indicated in column (5) were less than 1.0 percent except for the system involving n-hexadecane as a solvent. Thus, it is apparent that Equation (3-4), when used with the reference solubilities calculated by Equation (3-11), is capable of describing experimental solubilities with good accuracy. Graphical comparisons between experimental and predicted solubilities are shown in Figure 3-3 and Figures A-1 to A-9 in Appendix A.

As a next step in the development of a correlation, attempts were made to determine the constants  $A_1$  and  $A_2$  which are characteristic of each specific solute and solvent pair. When two values of gas solubility at different temperatures are available, the two constants  $A_1$  and  $A_2$  can be determined analytically utilizing the reference solubility

given by Equation (3-11), and expressed by Equations (3-12) and (3-13). Shown in column (6) of Table 3-2, are average percent deviations between the experimental solubilities and those obtained using Equation (3-4) along with the constants,  $A_1$  and  $A_2$  determined using Equations (3-12) and (3-13). The two solubilities used for each system for the determination of the constants  $A_1$  and  $A_2$  were the experimental solubilities corresponding to the lowest and highest temperatures. Therefore, the percent deviations indicated in column (6) are the results of interpolation when Equation (3-4) is used. As indicated in column (6), the resulting average deviations are less than 2.0 percent for all the solvent-solute systems except for the systems involving n-hexadecane.

Further attempts were made to determine the constants  $A_1$  and  $A_2$  to be used in Equation (3-4) for the case when only a single value of solubility is available. Such a situation is often encountered by process engineers and the extrapolation of a single gas solubility to the temperature of interest is expected to be difficult without having any further information concerning the temperature coefficient of solubility. The reference solubility which is characteristic of an individual solvent can be determined by the method developed in this investigation and may be useful for an approximate estimate of gas solubilities at other temperatures. At least the direction of the change in solubility with respect to temperature can be obtained, that is,

whether the temperature coefficient of solubility is positive or negative. A simple linear interpolation or extrapolation based on the single solubility value and the reference solubility is not always satisfactory. As observed in Figure 3-3 and Figures A-1 to A-9, gas solubilities are not linearly related (on a log-log plot) to the reference solubilities. Therefore, the resulting deviations between the actual solubilities and those obtained by simple linear interpolation or extrapolation are expected to be appreciable.

The temperature coefficient of the general solubility equation is expressed by Equation (3-15). Any method available to estimate the temperature coefficient of solubility at the temperature at which a gas solubility value is known, would permit the evaluation of the constants  $A_1$  and  $A_2$  utilizing Equations (3-4) and (3-15). For this purpose, the method recently proposed by Jonah and King (109) to predict the temperature coefficient of solubility was used. The resulting expressions for the constants  $A_1$  and  $A_2$  when the Jonah-King method was utilized are given by Equations (3-17) and (3-18).

In column (7) of Table 3-2, average percent deviations between the experimental solubilities and those calculated by Equations (3-4), (3-17) and (3-18) are shown. In this calculation, the single solubility value was always the experimental one measured at the lowest temperature. As indicated in column (7) the average deviations were always

less than 6.0 percent except for the system involving n-hexadecane.

The gas solubilities in n-hexadecane used in this investigation were those reported by Prausnitz and co-workers (130, 131). The measurement temperatures in their work ranged from 300 K to 475 K; the large temperature range was possible because of the high normal boiling point of n-hexadecane (560 K). The extrapolations as mentioned above for the systems involving n-hexadecane were carried out using solubilities measured at 300 K. It was considered, therefore, that the results of extrapolation were poorer than for the other solvents considered because of the large temperature range over which the extrapolation was made.

An example utilizing the extrapolation method developed will now be made for the case when a single value of gas solubility is known. We will consider that a single value of the solubility of ethane in benzene at 298.15 K as reported by Horiuti (92) is  $1.982 \times 10^{-2}$  mole fraction. This solubility will be extrapolated to a temperature of 323.15 K by the method developed in this investigation. The molar volume of benzene and its variation with temperature as required for application in Equation (3-14) were calculated by means of the method reported by Yamada and Gunn (110). The constants,  $A_1$  and  $A_2$  which were calculated by means of Equations (3-17) and (3-18) were found to be -2.5880 and 0.88964, respectively. Then the extrapolated solubility at 323.15 K as calculated by means of Equation (3-4) was

$1.137 \times 10^{-2}$  mole fraction. This last value may be compared with the experimental solubility of ethane in benzene at 323.15 K as also reported by Horiuti; which is  $1.131 \times 10^{-2}$  mole fraction. The deviation between the experimental and extrapolated solubility is 0.53 percent, a relatively small deviation.

CHAPTER VII

CONCLUSIONS

The solubilities of four highly soluble gases were measured at atmospheric pressure in the nonpolar solvent, n-octane, the polar but non-associating solvent, chlorobenzene, and the polar and highly associating solvent, n-butanol. For all the temperatures at which experiments were conducted, the resulting solubilities were highest in n-octane, lower in chlorobenzene and lowest in n-butanol. It was concluded, therefore, that the solubilities of gases are reduced in polar solvents and especially in associating solvents. Also, when the solubilities of the four gases, propene, isobutene, n-butane and isobutane in any one solvent were compared, the solubility of n-butane was highest, that of isobutene and isobutane was next in that order, and that of propene was always lowest. This order of solubilities corresponded to the order of the normal boiling points of these gases. Hence, the solubilities were successfully extrapolated using smooth curves to the gas normal boiling points. Such an extrapolation is expected to be useful for the estimation of gas solubility and agrees with the concept of an ideal gas solubility.

Based on the hydrogen-bonding factor, which is defined as the ratio of actual gas solubility to ideal gas solubility, the solubilities of highly soluble gases in n-butanol were successfully related to the solubilities in the other

polar and associating solvents, methanol, ethanol, ethylene glycol, methyl acetate, ethyl acetate and acetonitrile. It was concluded, based on the relationship observed, that the prediction of solubilities of highly soluble gases in polar and associating solvents is possible using a limited amount of solubility data for the solvents considered.

A new equilibration technique for saturating solvent with solute gas was developed in this investigation. This technique utilizes a spiral coil made from a stainless steel rod installed in the equilibration cell. While the solvent flows downward on the outside surface of the spiral coil, exposing a thin film, its saturation with the solute gas is enhanced. This technique was utilized in the measurement of gas-saturated solution densities and of gas solubilities, both at elevated pressures. In the former measurement, the new technique promoted the establishment of solubility equilibrium in the circulation system for measuring densities. In the latter experiment, while the solvent was supplied at a very low flow rate it became saturated with solute gas. In both cases it was found that such a technique for attaining gas-liquid equilibrium was very successful.

A system for measuring gas-saturated solution densities at elevated pressures was developed by utilizing the above mentioned equilibration technique with an Anton Paar density meter for high pressures. With this system, fast and precise measurements of gas-saturated solution densities were made possible. The experimental results obtained were then

compared with those obtained by prediction utilizing the SRK equation of state. It was found that for the systems involving a nonpolar solvent such as n-octane, the predicted densities were in relatively good agreement with the experimental ones. However, for the systems involving a nonpolar and associating solvent, n-butanol, the prediction method failed to give good agreement with the experimentally determined densities. It was therefore concluded that if accurate saturated solution densities were required, the system as developed in this investigation would be useful.

An apparatus for measuring gas solubilities at elevated pressures was constructed based also on the equilibration technique developed in this investigation. The precise measurement of gas solubility was possible with this apparatus when accurate gas-saturated solution densities were used for the data reduction. However, it may be noted that the solubility apparatus may not be very useful for systems of low solubility because of the relatively large quantity of solvent required for the measurement. It is also likely that the time required for the measurement of solubilities for such systems would be excessively long.

Also developed in this investigation was a system to analyze gas-saturated solutions by gas chromatography. The purpose of developing this system was to check the validity of the volumetric measurements of gas solubilities at elevated pressures. As a result of the comparison it is concluded that the solubilities obtained using volume readings of

gas and solvent agree with the results obtained using gas chromatographic analysis of the gas-saturated solutions. It was considered that the gas chromatographic analysis itself could be an alternative method to determine gas solubilities, but, from a practical viewpoint, it may be noted that the preparation of calibration lines for specific solute-solvent systems prior to the actual analysis by gas chromatograph is laborious and time-consuming. Therefore the volumetric measurement of gas solubilities as developed in this investigation is preferable.

The solubilities measured at elevated pressures were compared with those predicted by utilizing the SRK equation of state and also by utilizing the UNIFAC method. In the former method, the binary interaction parameters required for the calculation were based on solubilities measured at atmospheric pressure. As a result, good agreement between the experimental and predicted solubilities was observed for the systems involving n-octane as a solvent at all the measurement temperatures which included 298.15 K, 323.15 K and 343.15 K. However, the agreement was poorer for the systems involving chlorobenzene and poorest for the systems involving n-butanol. The solubilities predicted by utilizing the UNIFAC method also agreed with the experimental solubilities for the systems involving n-octane as a solvent, but with slightly larger deviations. For the systems involving n-butanol as a solvent the prediction of the solubilities utilizing the UNIFAC method was also unsuccessful.

It may be concluded, based on the results mentioned above, that the successful prediction of gas solubilities in polar and associating solvents such as n-butanol at elevated pressures cannot be achieved by utilizing the SRK equation of state or by utilizing the UNIFAC method.

For the purpose of interpolating or extrapolating gas solubilities measured at atmospheric pressure to temperatures at which the experimental solubilities are not available, an equation was developed:

$$\ln \frac{x}{x_{cl}} = A_1 \ln \frac{T}{T_{cl}} + A_2 \left( \ln \frac{T}{T_{cl}} \right)^2 \quad (3-4)$$

The equation above involves two parameters,  $A_1$  and  $A_2$ . The reference solubility,  $x_{cl}$  was correlated with solvent properties only. It is concluded that the equation above is capable of describing solubility behavior very well when the constants,  $A_1$  and  $A_2$ , which are characteristic of specific solute-solvent systems, are appropriately determined. It is noted that the equation is applicable only to nonpolar or slightly polar solvent systems.

REFERENCES

- (1) Fleury, D., Hayduk, W., Can. J. Chem. Eng., 53, 195 (1975).
- (2) Hayduk, W., Castaneda, R., Can. J. Chem. Eng., 51, 353 (1973).
- (3) Asatani, H., Master's Thesis, Univ. of Ottawa (1982).
- (4) Asatani, H., Hayduk, W., Can. J. Chem. Eng., 61, 227, (1983).
- (5) Markham, A.E., Kobe, K.A. Chem. Rev., 28, 519 (1941).
- (6) Clever, H.L., Battino, R., Chem. Rev., 66, 395 (1966).
- (7) Clever, H.L., Battino, R., "Solutions and Solubilities Part I", John Wiley & Sons, Toronto, Chapter 7, 379 (1975).
- (8) Katayama, T., "Saikin no Kagaku Kogaku", 83 (1966).
- (9) Wilhelm, E., Battino, R., Wilcock R.J., Chem. Rev., 77, 219 (1977).
- (10) Hildebrand, J.H., J. Am. Chem. Soc., 51, 66 (1929).
- (11) Hildebrand, J.H., Scott, R.L., "Solubility of nonelectrolytes", 3rd edition, Dover Publication Inc., New York (1964).
- (12) Pierotti, R.A., J. Phys. Chem., 67, 1840 (1963).
- (13) Cook, M.W., Hanson, D.N., Rev. Sci. Instr., 28, 370 (1957).
- (14) Carpenter, J.H., Limnol. Oceanogr., 11, 264 (1966).
- (15) Elmore, H.L., Hayes, T.W., J. Sanit. Eng. Div. Am. Soc. Civil Eng., 86, (SA), 41 (1960).

- (16) Montgomery, H.A.C., Thom, N.S., Cockburn, A., J. Appl. Chem., 14, 280 (1964).
- (17) Markham, A.E., Kobe, K.A., J. Am. Chem. Soc., 63, 449 (1941).
- (18) Scholander, P.F., J. Biol. Chem., 167, 2351 (1947).
- (19) Clever, H.L., Holland, C.J., J. Chem. Eng. Data, 13, 411 (1968).
- (20) Hayduk, W., Cheng, S.L., Can. J. Chem. Eng., 48, 93 (1970).
- (21) Cannon, W.A., Crane, W.E., Cryogenic Tech., 178 (1968).
- (22) Cheung, H., Zander, E.H., Chem. Eng. Progr. Symp. Ser., 64 34 (1968).
- (23) Benson, B.B., Parker, D.M., J. Phys. Chem., 65, 1489 (1961).
- (24) McAuliffe, A., Nature, 200, 1092(1963), J. Phys. Chem., 70, 1267 (1966).
- (25) Swinnerton, J.W., Linnenbom, V.J., J. Gas Chromatogr., 5, 570 (1967).
- (26) Ng, S., Harris, H.G., Prausnitz, J.M., J. Chem. Eng. Data, 14, 482 (1969).
- (27) Kresheck, G.C., Schneiner, H., Sheraga, H.A., J. Phys. Chem., 69, 1316, 3132 (1965).
- (28) Bell, T.N., Cussler, E.L., Harris, K.R., Pepela, L.N., Dunlop, P.J., J. Phys. Chem., 72, 4693 (1968).
- (29) Clever, H.L., Battino, R., Saylor, J.H., Gross, P.M., J. Phys. Chem., 61, 1078 (1957).

- (30) Baldwin, R.R., Daniel, S.G., J. Appl. Chem., 2, 161 (1952).
- (31) Battino, R., Banzhof, M., Bogan, M., Wilhelm, E., Anal. Chem., 43, 806 (1971).
- (32) Morrison, T.J., Billett, F., J. Chem. Soc., 2033 (1948).
- (33) Battino, R., Evans, F.D., Danforth, W.F., J. Am. Oil. Chem. Soc., 45, 830 (1968).
- (34) Dymond, J., Hildelwand, H., Ind. Eng. Chem. Fundam., 6, 130 (1967).
- (35) Gerrard, W., "Solubility of Gases and Liquids", Plenum Press, New York and London (1976).
- (36) Wiebe, R., Gaddy, V.L., Hein, C., Tremearne, T.H., Ind. Eng. Chem., 34, 823 (1932).
- (37) Wiebe, R., Gaddy, V.L., J. Am. Chem. Soc., 55, 947 (1933).
- (38) Wiebe, R., Gaddy, V.L., J. Am. Chem. Soc., 57, 847 (1935).
- (39) Gardiner, G.E., Smith, N.O., J. Phys. Chem., 76, 1195 (1972).
- (40) Pray, H.A., Schweickert, C.E., Minnich, B.H., Ind. Eng. Chem., 44, 1146 (1952).
- (41) Koonce, K.T., Kobayashi, R., J. Chem. Eng. Data, 9, 490 (1964).
- (42) Gjaldbaek, J.C., Andersen, E.K., Acta. Chem. Scand., 8, 1398 (1954).

- (43) Lachowicz, S.K., Weale, K.E., J. Chem. Eng. Data, 3, 162 (1958).
- (44) Gjaldbaek, J.C., Niemann, H., Acta. Chem. Scand., 12, 1015 (1958).
- (45) Prausnitz, J.M., Shair, F.H., A.I.Ch.E. J., 7, 682 (1961).
- (46) Yen, L.C., McKetta, J.J., A.I.Ch.E. J., 8, 501 (1962).
- (47) Prausnitz, J.M., Gunn, R.D., A.I.Ch.E. J., 4, 430 (1958).
- (48) Chueh, P.L., Prausnitz, J.M., A.I.Ch.E. J., 13, 1099 (1967).
- (49) Chueh, P.L., Prausnitz, J.M., A.I.Ch.E. J., 13, 1107 (1967).
- (50) Chueh, P.L., Prausnitz, J.M., Ind. Eng. Chem. Fundam., 6, 492 (1967).
- (51) Sazamoto, S., Mitsutomi, H., Yorizane, M., Kagaku Kogaku, 33, 867 (1969).
- (52) Redlich, O., Kwong, J.N.S., Chem. Rev., 44, 233 (1949).
- (53) Benedict, M., Webb, G., Rubin, L.C., Chem. Eng. Progr., 47, 449 (1951).
- (54) Benedict, M., Webb, G., Rubin, L.C., Chem. Eng. Progr., 47, 449 (1951).
- (55) Sagara, H., Arai, Y., Saito, S., J. Chem. Eng. Japan, 8, 93 (1975).
- (56) Chu, H., Lu, B.C.-Y., Can. J. Chem. Eng., 49, 140 (1971).

- (57) Preston, G.T., Prausnitz, J.M., Ind. Eng. Chem. Fundam., 10, 389 (1971).
- (58) Scott, R.L., J. Chem. Phys., 25, 193 (1956).
- (59) Gosman, A.L., McCarty, R.D., Hust, J.G., National Standard Reference Data Series, National Bureau of Standards, No. 27, Boulder, Colo., 1969.
- (60) Cysemski, G.R., Prausnitz, J.M., Ind. Eng. Chem. Fundam., 15, 304 (1976).
- (61) Carnahan, N.F., Starling, K.E., J. Chem. Phys., 51, 635 (1969).
- (62) Moysan, J.M., Huron, M.J., Paradowski, H., Vidal, J., Chem. Eng. Sci., 38, 1085 (1983).
- (63) Soave, G., Chem. Eng. Sci., 27, 1197 (1972).
- (64) Peng, D.Y., Robinson, D.B., Ind. Eng. Chem. Fundam., 15, 59 (1976).
- (65) Nakahara, T., Hirata, M., J. Chem. Eng., Japan, 2, 137 (1969).
- (66) Edward, W.F., Prausnitz, J.M., Ind. Eng. Chem. Process, Des. Dev., 10, 405 (1971).
- (67) Miyano, Y., Yorizane, M., A.I.Ch.E. J., 24, 181 (1978).
- (68) Bender, E., Klein, U., Schmitt, W., Prausnitz, J.M., Fluid Phase Equi., 15, 241 (1984).
- (69) Uhlig, H.H., J. Phys. Chem., 41, 1215 (1937).
- (70) Pieřotti, R.A., J. Phys. Chem., 69, 281 (1965).
- (71) Krichevsky, I.R., Kasarnovsky, J.S., J. Am. Chem. Soc., 57, 2168 (1935).

- (72) Dodge, B.F., Newton, R.H., Ind. Eng. Chem., 29, 718 (1937).
- (73) Krichevsky, I.R., Ilinskaya, A.A., Zh. Fiz. Khim. USSR, 19, 621, (1945).
- (74) Orentlicher, M., Prausnitz, J.M., Chem. Eng. Sci., 19, 775 (1964).
- (75) Snider, N.S., Herrington, T.M., J. Chem. Phys., 47, 2248 (1967).
- (76) Miller, R.C., Prausnitz, J.M., Ind. Eng. Chem. Fundam., 8, 449 (1969).
- (77) Barton, J.R., Hsu, C.C., Chem. Eng. Sci., 27, 1315 (1972).
- (78) Tiepel, E.W., Gubbins, K.E., Can. J. Chem. Eng., 50, 361 (1972).
- (79) Uno, K., Sarashina, E., Arai, Y., Saito, S., J. Chem. Eng. Japan, 8, 201 (1975).
- (80) Tochigi, K., Kojima, K., Fluid Phase Equi., 8, 221 (1982).
- (81) Antunes, C., Tasslos, D., Ind. Eng. Chem. Process Des. Dev., 22, 457 (1983).
- (82) Katayama, T., Mori, T., Nitta, T., Kagaku, Kogaku, 31, 559 (1967).
- (83) Katayama, T., Mori, T., Nitta, T., Tominaga, J., Kagaku, Kogaku, 31, 669 (1967).
- (84) Himmelblau, D.M., J. Chem. Eng. Data, 5, 10 (1960).
- (85) Hayduk, W., Laudie, H., A.I.Ch.E. J., 19, 1233 (1973).

- (86) Yen, L.C., McKetta, J.J., J. Chem. Eng. Data, 7, 288 (1962).
- (87) Kobatake, Y., Hildebrand, J.H., J. Phys. Chem., 65, 331 (1961).
- (88) Reeves, L.W., Hildebrand, J.H., 79, 1313 (1957).
- (89) Archer, G., Hildebrand, J.H., J. Phys. Chem., 67, 1830 (1963).
- (90) Hanson, D.N., Alder, B.J., J. Chem. Phys., 26, 748 (1957).
- (91) Cukor, P.M., Prausnitz, J.M., Ind. Eng. Chem. Fundam., 10, 638 (1971).
- (92) Horiuti, J., Sci. Papers Inst. Phys. Chem. Rev. (Tokyo), 17, 182 (1931).
- (93) Cook, M.W., Hanson, D.N., Alder, B.J., J. Chem. Phys., 26, 748 (1957).
- (94) Clever, H.L., Battino, R., Saylor, J.H., Gross, P.M., J. Phys. Chem., 61, 1078 (1957).
- (95) Clever, H.L., J. Phys. Chem., 62, 375 (1958).
- (96) Vitover, J., Fried, V., Coll. Czech. Chem. Commun., 25, 1552 (1960).
- (97) Saylor, J.H., Battino, R., J. Phys. Chem., 62, 1334 (1958).
- (98) Miller, K.W., J. Phys. Chem., 72, 2248 (1968).
- (99) Dymand, J.H., J. Phys. Chem., 71, 1829 (1967).
- (100) Hayduk, W., Buckley, W.D., 49, 667 (1971).
- (101) Hayduk, W., Walter, E.B., Simpson, P., J. Chem. Eng. Data, 17, 59 (1972).

- (102) Sahgal, A., La, H.M., Hayduk, W., Can. J. Chem. Eng., 56, 354 (1978).
- (103) Hiraoka, H., Hildebrand, J.H., 68, 213 (1964).
- (104) Kretschmer, C.B., Nowakowska, J., Wiebe, R., Ind. Eng. Chem., 38, 506 (1946).
- (105) Gjaldbaek, J.C., Hildebrand, J.H., J. Am. Chem. Soc., 71, 3147 (1949).
- (106) Beutier, D., Renon, H., A.I.Ch.E. J., 24, 1122 (1978).
- (107) Schotte, W., A.I.Ch.E. J., 31, 154 (1985).
- (108) Hala, E., Ind. Eng. Chem. Fundam., 14, 138 (1975).
- (109) Jonah, D.A., King, M.B., Proc. Roy. Lond. A., 323, 361 (1971).
- (110) Yamada, T., Gunn, R.D., J. Chem. Eng. Data, 18, 234 (1973).
- (111) Farrington, P.S., Sage, B.H., Ind. Engng. Chem., 41, 1734 (1949).
- (112) Dymond, J.H., Smith, E.B., "The virial coefficients of pure gases and Mixtures", Oxford University Press, New York (1980).
- (113) Das, T.R., Reed, C.O., Eubank, P.T., J. Chem. Eng. Data, 18, 253 (1973).
- (114) Pitzer, K.S., Curl, R.F., J. Am. Chem. Soc., 79, 2369 (1957).
- (115) Reid, R.C., Prausnitz, J.M., Sherwood, T.K., "The Properties of Gases and Liquids", McGraw-Hill, New York (1977).

- (116) Gometz-Nieto, M., Thodos, G., Ind. Eng. Chem. Fundam., 17, 45 (1978).
- (117) Haar, L., Gallagher, J.S., Kell, G.S., "Steam Tables", Hemisphere Pub. Co., New York (1984).
- (118) Gunn, R.D., Yamada, T., A.I.Ch.E. J., 17, 1341 (1971).
- (119) Din, F., "Thermodynamic Functions of Gases" Volume 3, Butterworths, London (1961).
- (120) Possati, S., Faulconer, A., Anesth. Analg. Curr. Res., 37, 338 (1958).
- (121) Ohgaki, K., Nakatani, T., Saito, T., Katayama, T., J. Chem. Eng. Japan, 15, 91 (1982).
- (122) Zhang, G., Hayduk, W., Can. J. Chem. Eng., 62, 713 (1984).
- (123) Fredenslund, A., Jones, R.L., Pransnitz, J.M., A.I.Ch.E. J., 21, 1086 (1975).
- (124) Le Fevre, C.J., Le Fevre, R.J.W., J. Chem. Soc. (London), 487 (1936).
- (125) Wilhoit, R.C., Zwolinski, B.J., "Physical and Thermodynamic Properties of Aliphatic Alcohols", ACS, AIP, NBS, New York (1973).
- (126) Chappelow, C.C., Synder, P.S., Winnick, J., J. Chem. Eng. Data, 16, 440 (1971).
- (127) Blais, C., Hayduk, W., J. Chem. Eng. Data, 28, 181 (1983).
- (128) Miyano, Y., Hayduk, W., Can. J. Chem. Eng., 59, 746 (1981).

- (129) Miyamo, Y., Hayduk, W., J. Chem. Eng. Data, 31, 77  
(1986).
- (130) Cukor, P.M., Prausnitz, J.M., J. Phys. Chem., 76, 598  
(1972).
- (131) Tremper, K.K., Prausnitz, J.M., J. Chem. Eng. Data,  
21, 295 (1976).
- (132) Hayduk, W., Pahlevanzadeh, H., to be published  
(1986).
- (133) Short, I., Sahgal, A., Hayduk, W., J. Chem. Eng. Data,  
28, 63 (1983).
- (134) Kretschmer, C.B., Wiebe, R., J. Am. Chem. Soc., 73,  
3778 (1951).
- (135) Kretschmer, C.B., Wiebe, R., J. Am. Chem. Soc., 74,  
1276 (1952).
- (136) Boyer, F.L., Bircher, L.J., J. Phys. Chem., 64, 1330  
(1960).
- (137) Sahgal, A., Hayduk, W., J. Chem. Eng. Data, 24, 222  
(1979).

Appendix A

Diagrams for the correlated solubilities  
measured at atmospheric pressure.

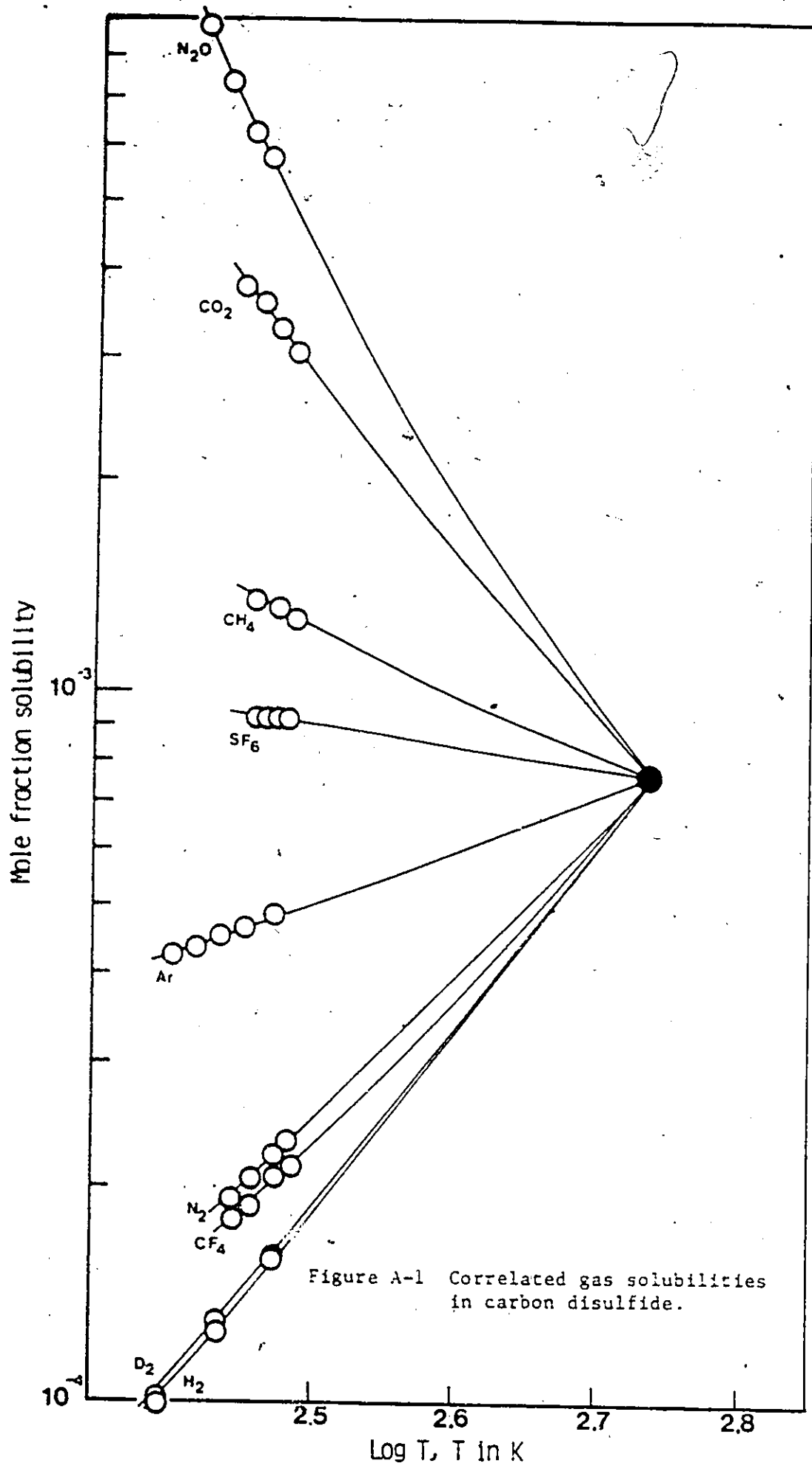


Figure A-1 Correlated gas solubilities in carbon disulfide.

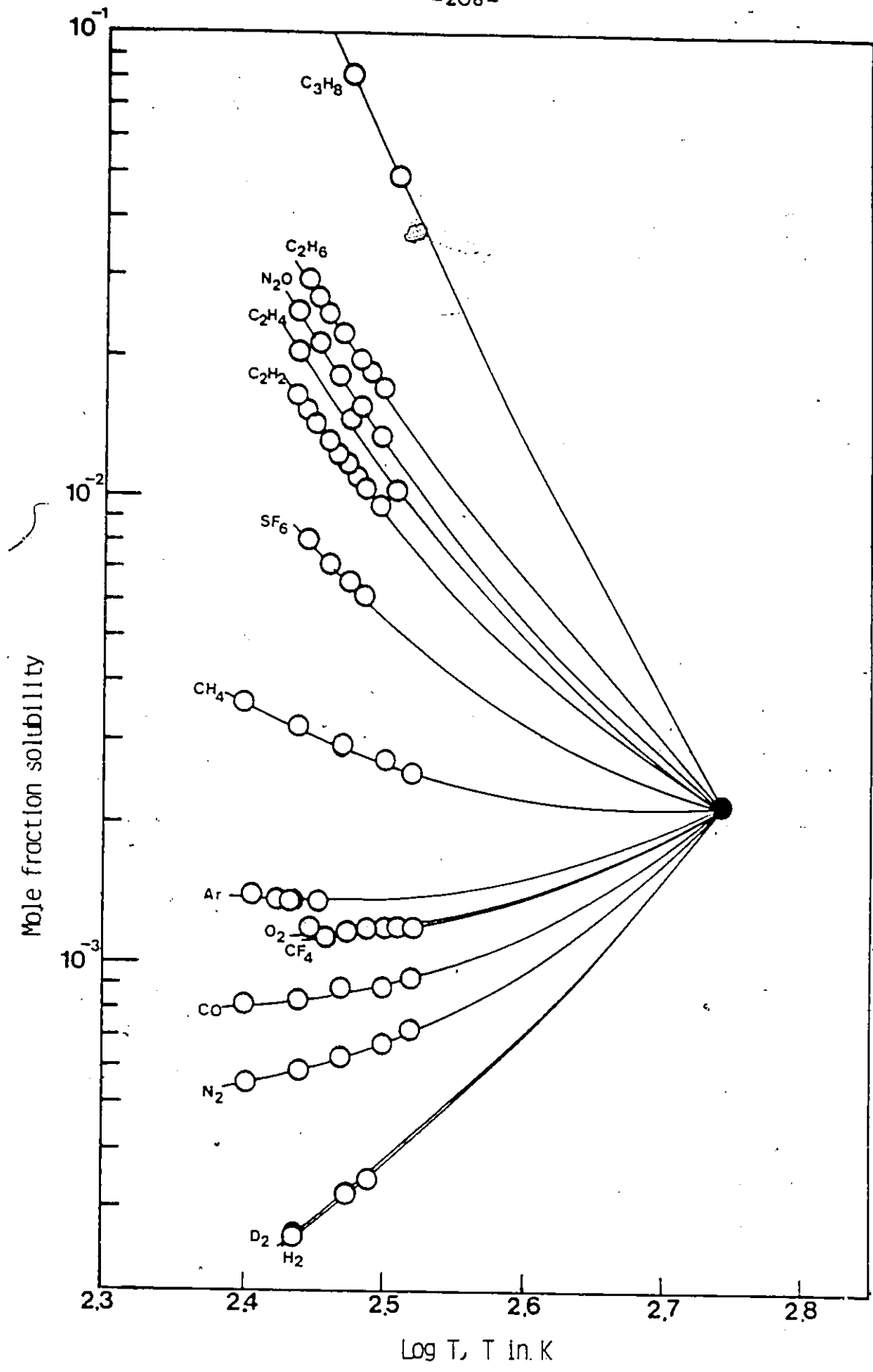


Figure A-2 Correlated gas solubilities in carbon tetrachloride.

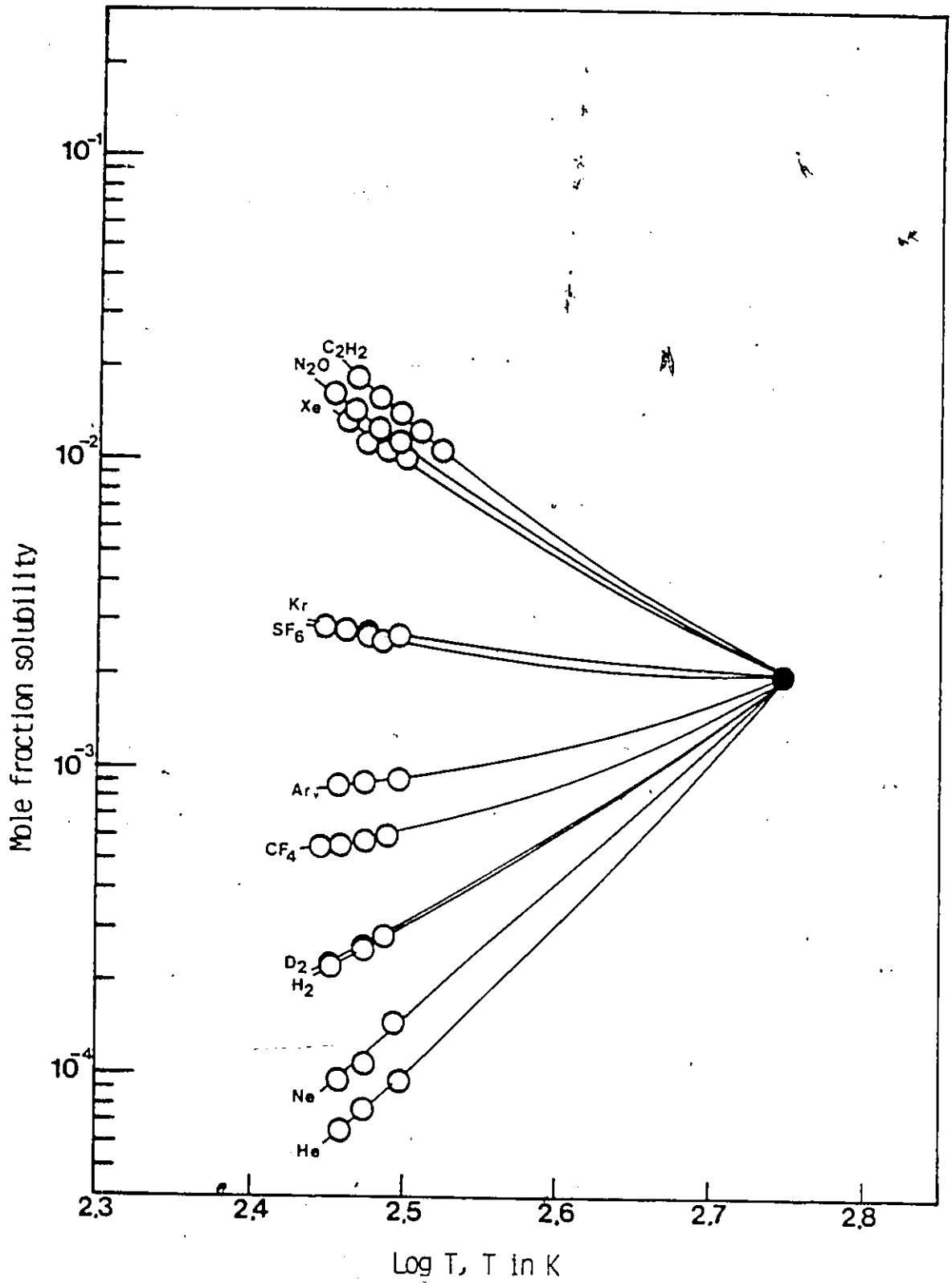


Figure A-3 Correlated gas solubilities in benzene.

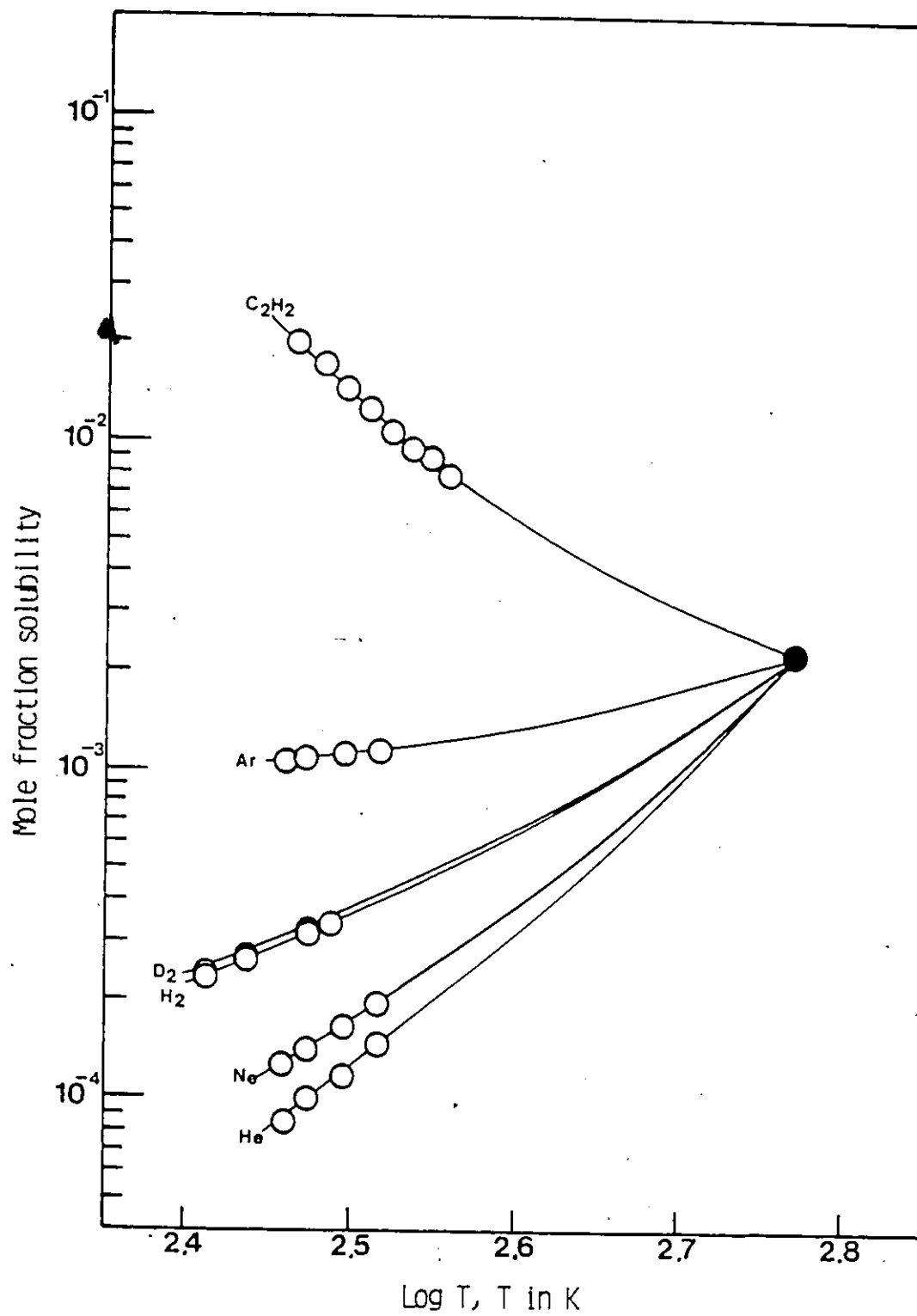


Figure A-4 Correlated gas solubilities in toluene.

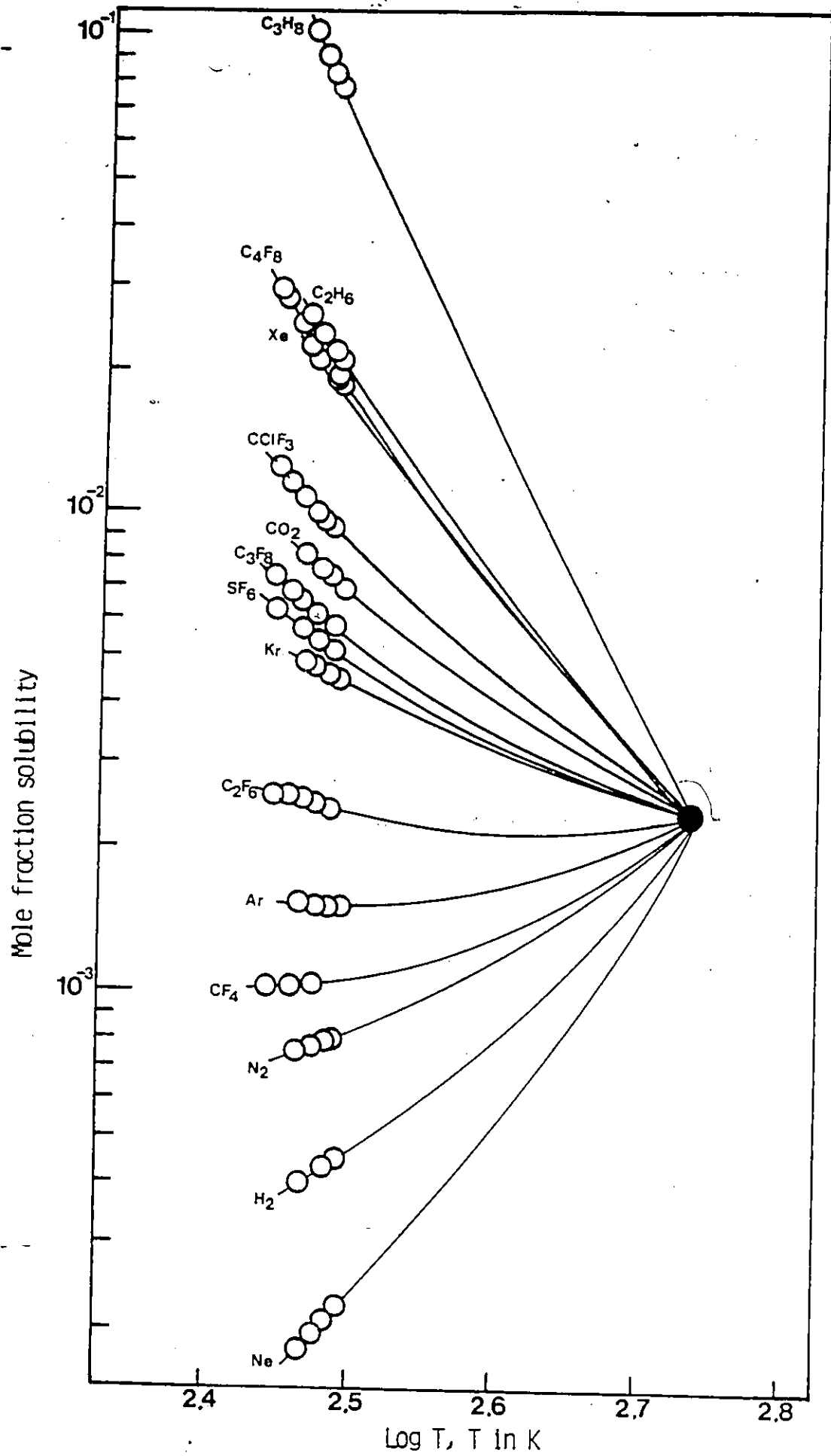


Figure A-5 Correlated gas solubilities in cyclohexane.

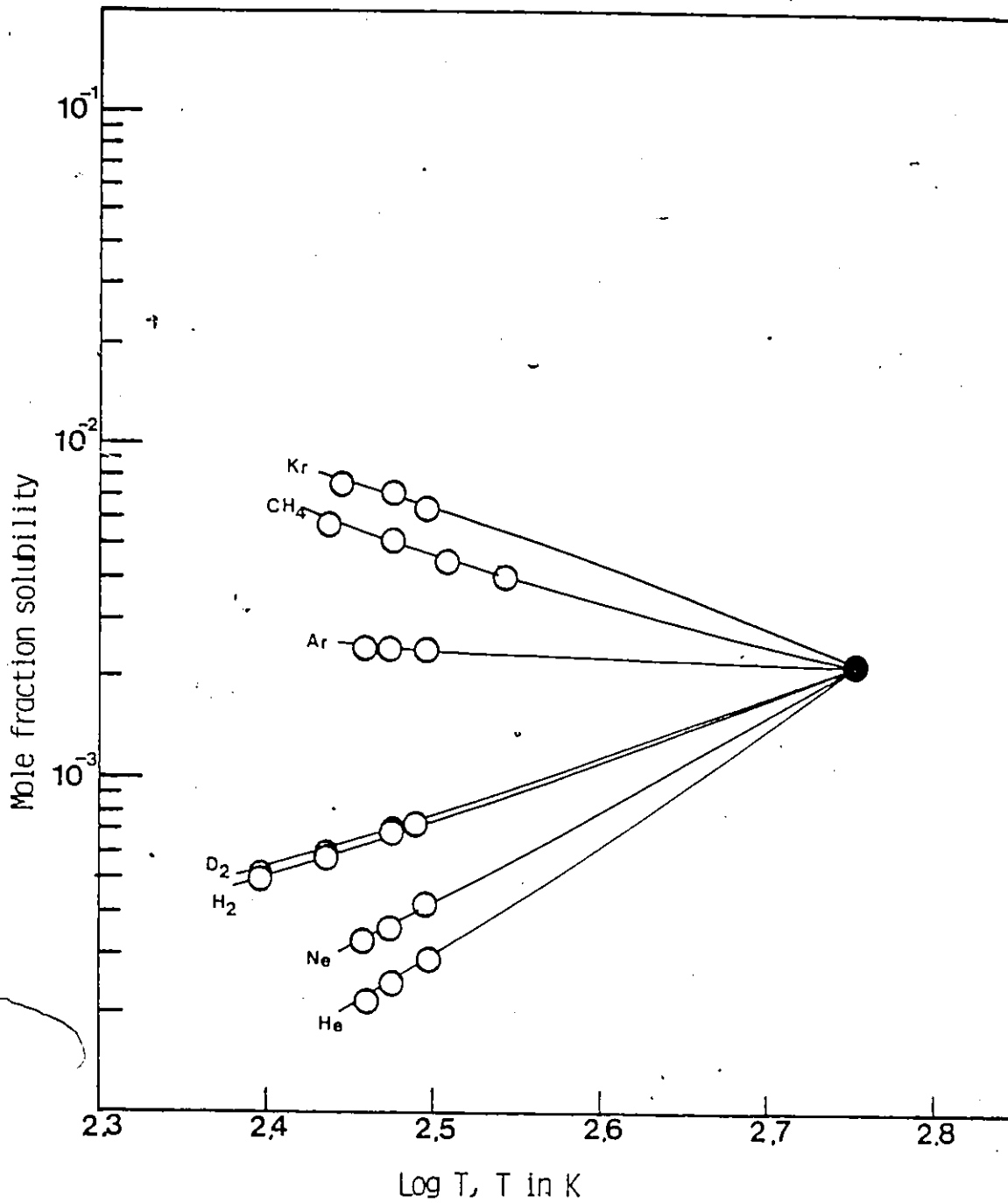


Figure A-6 Correlated gas solubilities in n-octane.

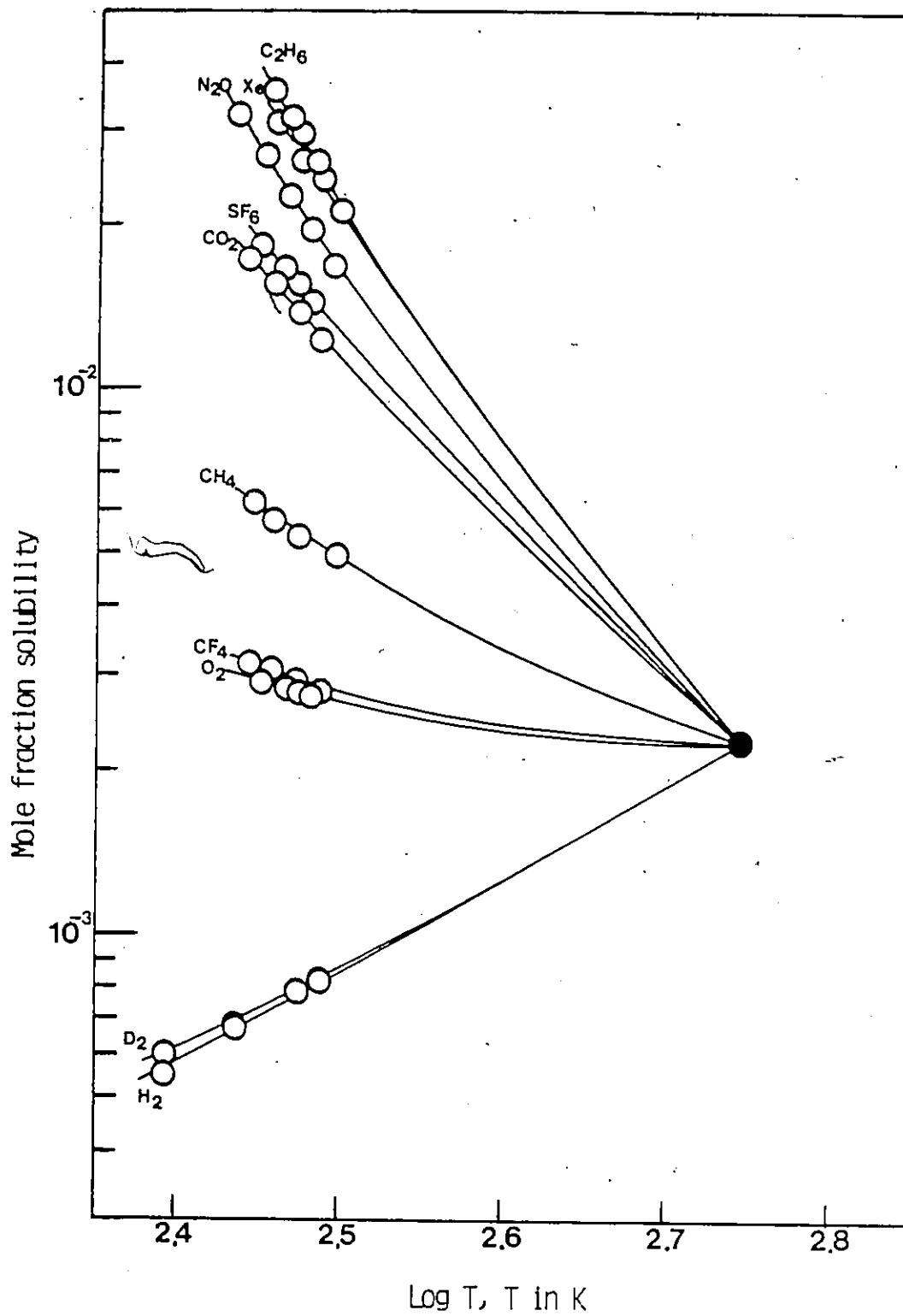


Figure A-7 Correlated gas solubilities in isooctane.

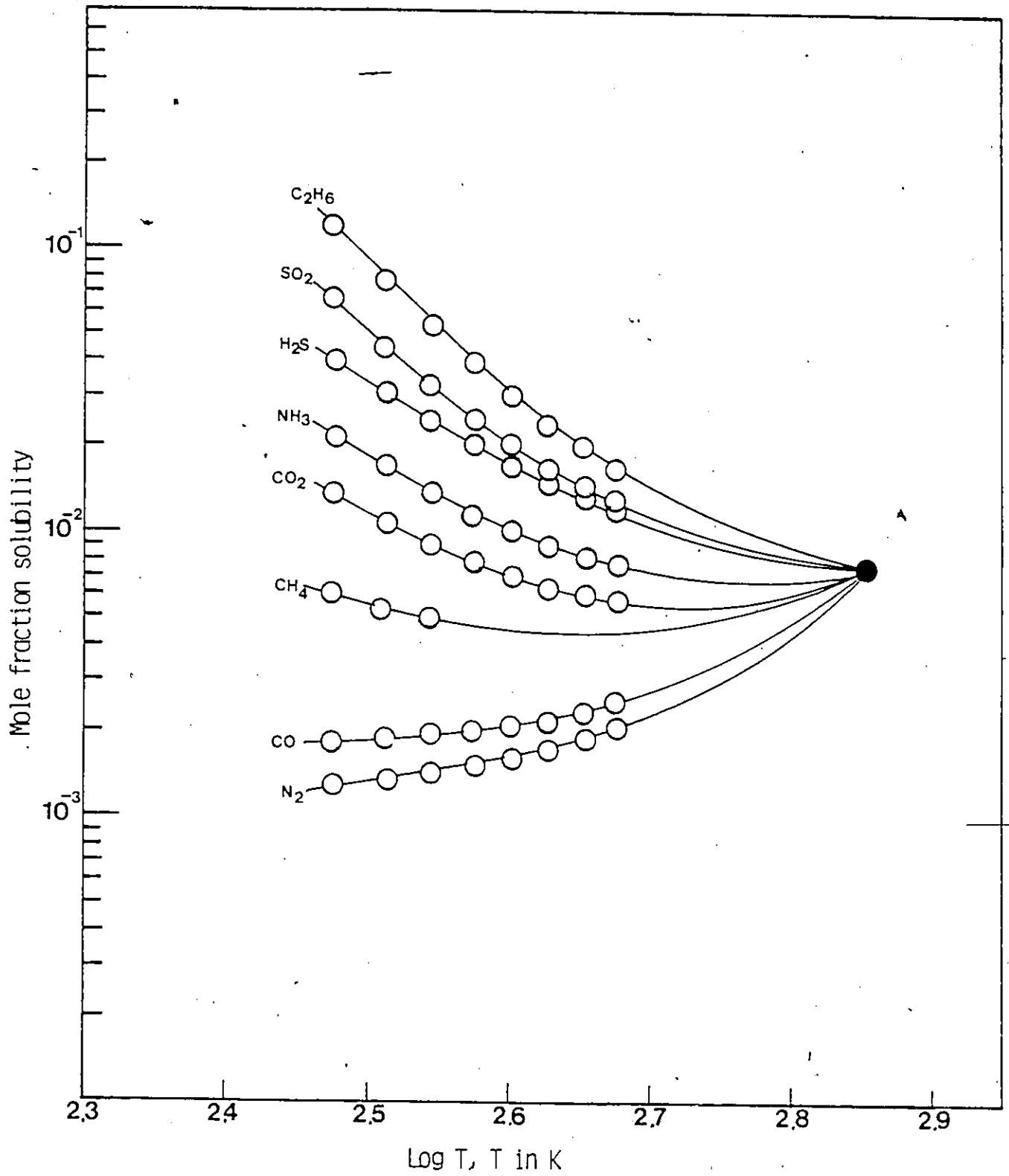


Figure A-8 Correlated gas solubilities in n-hexadecane.

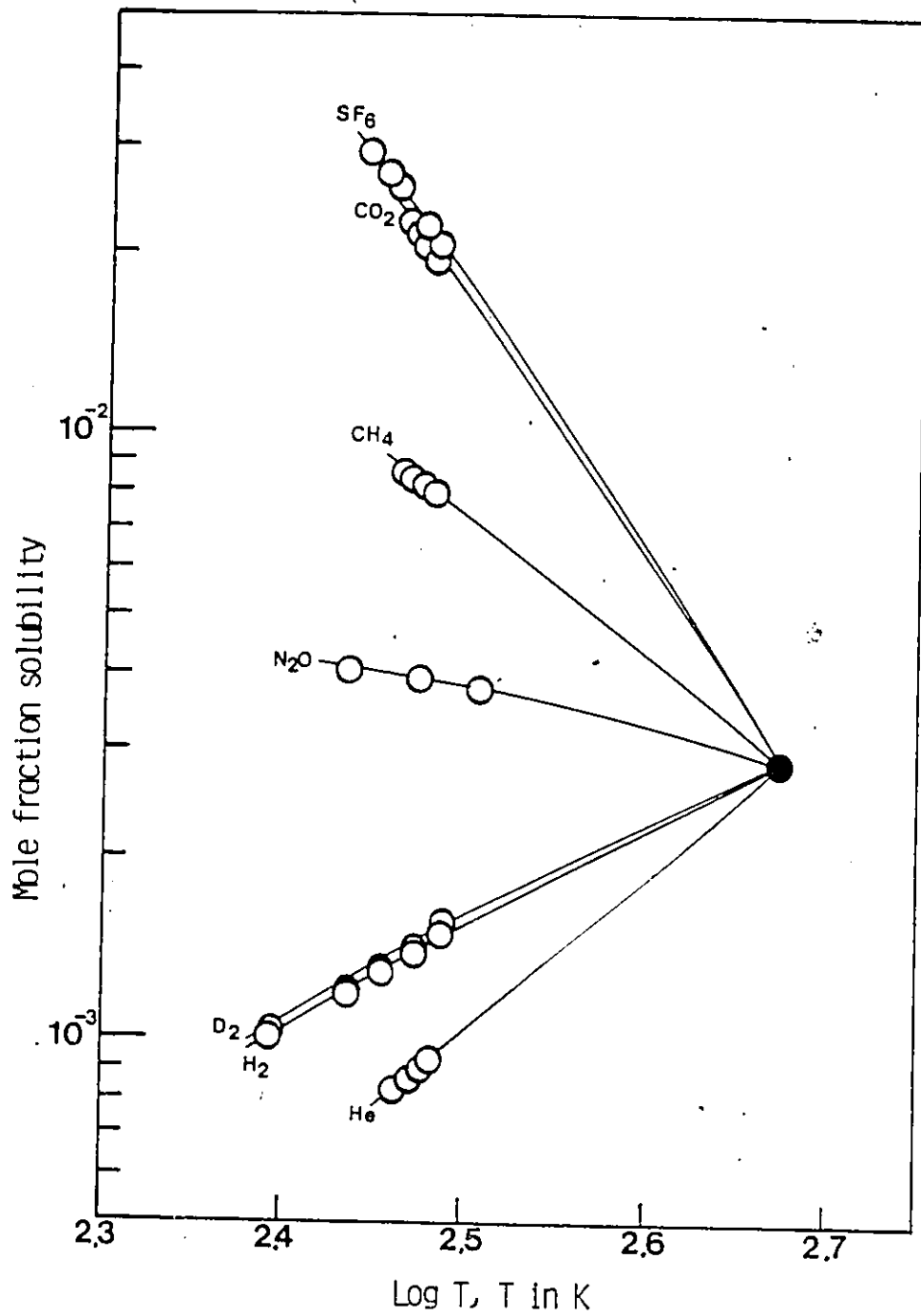


Figure A-9 Correlated gas solubilities in perfluoroheptane.

Appendix B

Sample calculation for the determination of gas  
solubility measured at atmospheric pressure.

The calculation procedure to determine the solubility of propene in n-octane at 298.15 K and 756.7 mmHg (100.89 kPa) will be illustrated.

System : (1) n-octane - (2) propene  
Measurement temperature : 298.15 K  
Measurement pressure : 756.7 mmHg  
Volumetric flow rate of degassed n-octane : 0.00873 cm<sup>3</sup>/min  
Molar density of n-octane : 6.115 x 10<sup>-3</sup> mole/cm<sup>3</sup>  
Molar density of propene : 4.130 x 10<sup>-5</sup> mole/cm<sup>3</sup>  
Vapor pressure of n-octane: 14.0 mmHg (1.87 kPa)

The volumes of propene dissolved in n-octane at 5 minutes time intervals were measured as:

<u>Time(min.)</u>	<u>Vol. of n-octane (cm<sup>3</sup>)</u>	<u>Vol. of propene (cm<sup>3</sup>)</u>
0	0.	0.
5	0.044	0.75
10	0.087	1.51
15	0.131	2.26
20	0.175	3.02
25	0.218	3.77
30	0.262	4.52
35	0.306	5.26
40	0.349	6.02
45	0.393	6.79
50	0.437	7.53
55	0.480	8.27
60	0.524,	9.04

The slope of the volumes of propene to those of n-octane, (SP) is calculated by means of the least squares method as:

$$(SP) = 0.1505$$

The mole ratio,  $x_2/x_1$  is calculated by Equation (5-4) as:

$$\frac{x_2}{x_1} = 0.1164$$

The solubility of propene in n-octane at 298.15 K and at 100.89 kPa is calculated by Equation (5-5) as:

$$x_2(100.89, 298.15) = 0.104 ,$$

The solubility of propene in n-octane for a propene partial pressure of 101.325 kPa is calculated by Equation (5-6) as:

$$x_2(P_2 = 101.325, 298.15) = 0.106$$

Appendix C

Densities of gas-saturated solutions  
as a function of pressure.

$$\rho_s = C_0P + C_1P + C_2P^2 + C_3P^3 \quad P \text{ in atm} \quad (C-1)$$

System (*)	C <sub>0</sub>	C <sub>1</sub> X10	C <sub>2</sub> X10 <sup>2</sup>	C <sub>3</sub> X10 <sup>3</sup>	Avg.abs.% (**)
O-P-298	0.701636	-0.119276	0.128269	-0.147879	0.59
O-P-323	0.67931	-0.064802	0.025069	-0.023189	0.16
O-P-343	0.662191	-0.039653	0.002920	-0.005718	0.06
O-I-298	0.699457	-0.298309	1.663208	-6.300926	0.34
O-I-323	0.679397	-0.113678	0.034999	-0.318527	0.19
O-I-343	0.663310	-0.094709	0.064659	-0.120163	0.15
C-P-298	1.103396	-0.279970	0.220394	-0.376641	0.56
C-P-323	1.074769	-0.131588	-0.011348	-0.365637	0.18
C-P-343	1.054611	-0.079507	-0.031036	-0.428404	0.21
C-I-298	1.102045	-0.729675	-0.358582	-7.583618	0.21
C-I-323	1.075254	-0.371398	-0.836467	-0.001907	0.09
C-I-343	1.056325	-0.317382	-0.067806	-0.185549	0.22
B-P-298	0.808782	-0.172882	0.370407	-0.338733	1.03
B-P-323	0.787880	-0.074387	0.058937	-0.039279	0.31
B-P-343	0.772452	-0.056629	0.037586	-0.019248	0.24
B-I-298	0.806540	-0.296173	1.786804	-8.239746	0.27
B-I-323	0.789553	-0.326232	1.318646	-2.383232	0.56
B-I-343	0.774795	-0.255432	0.639820	0.668227	0.75

(\*) : O=n-Octane  
 C=Chlorobenzene  
 B=n-Butanol  
 P=propene  
 I=Isobutene  
 298=298.15 K  
 323=323.15 K  
 343=343.15 K

(\*\*) : Average absolute percent deviation  
 between experimental and fitted  
 solution densities.

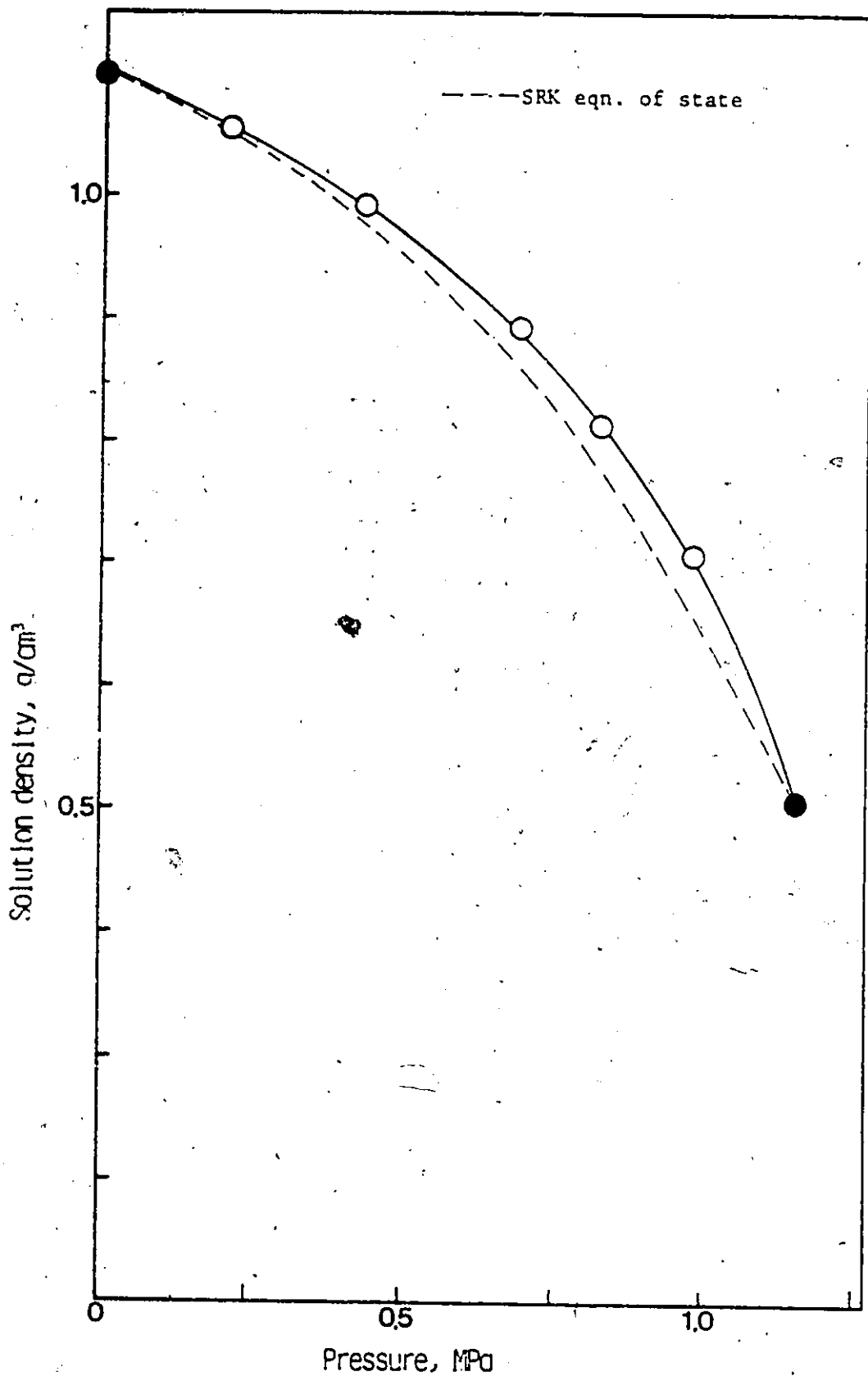


Figure C-1. Experimental and predicted densities of propene-saturated chlorobenzene solutions at 298.15 K as a function of pressure.

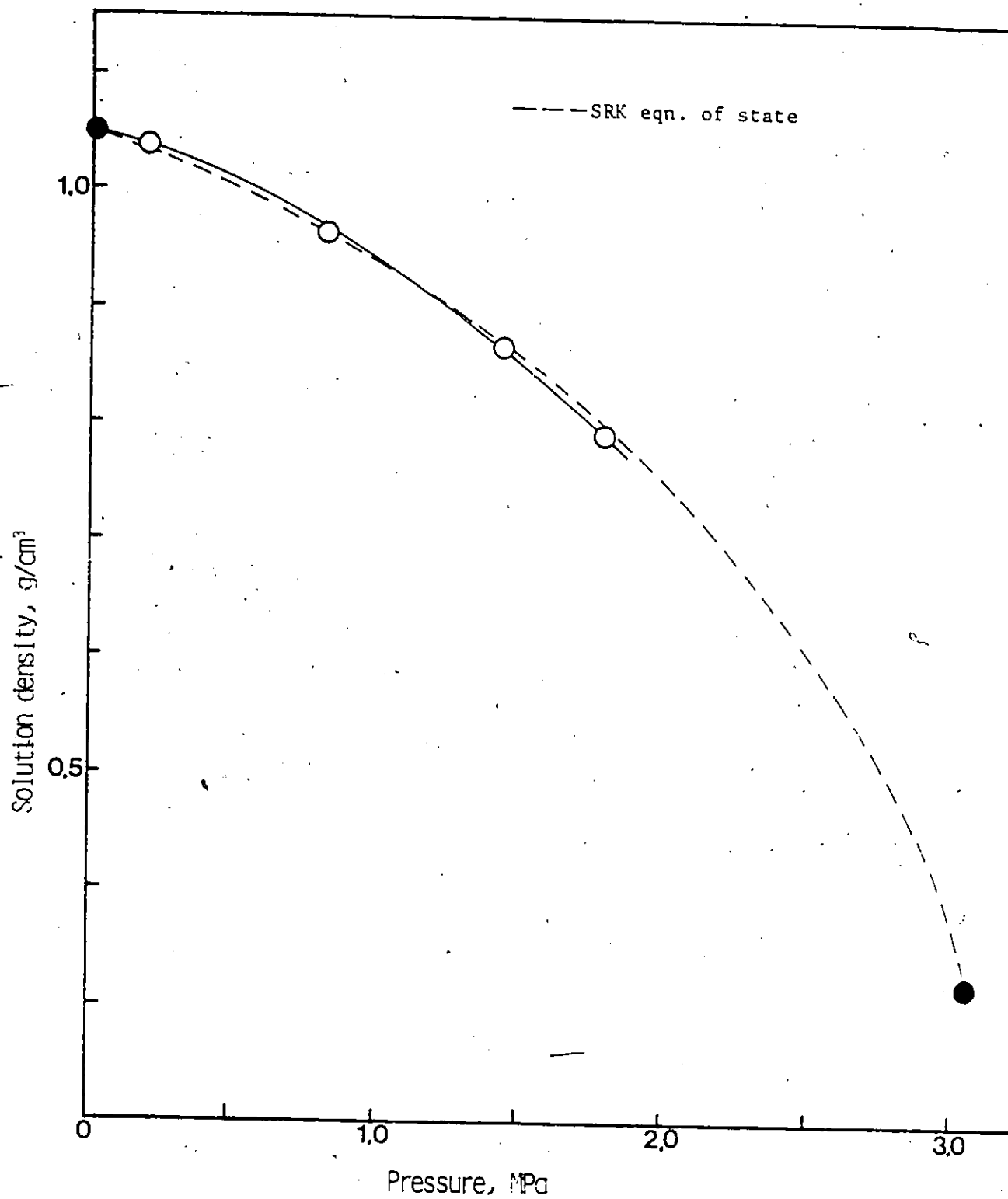


Figure C-2 Experimental and predicted densities of propene-saturated chlorobenzene solutions at 343.15 K as a function of pressure.

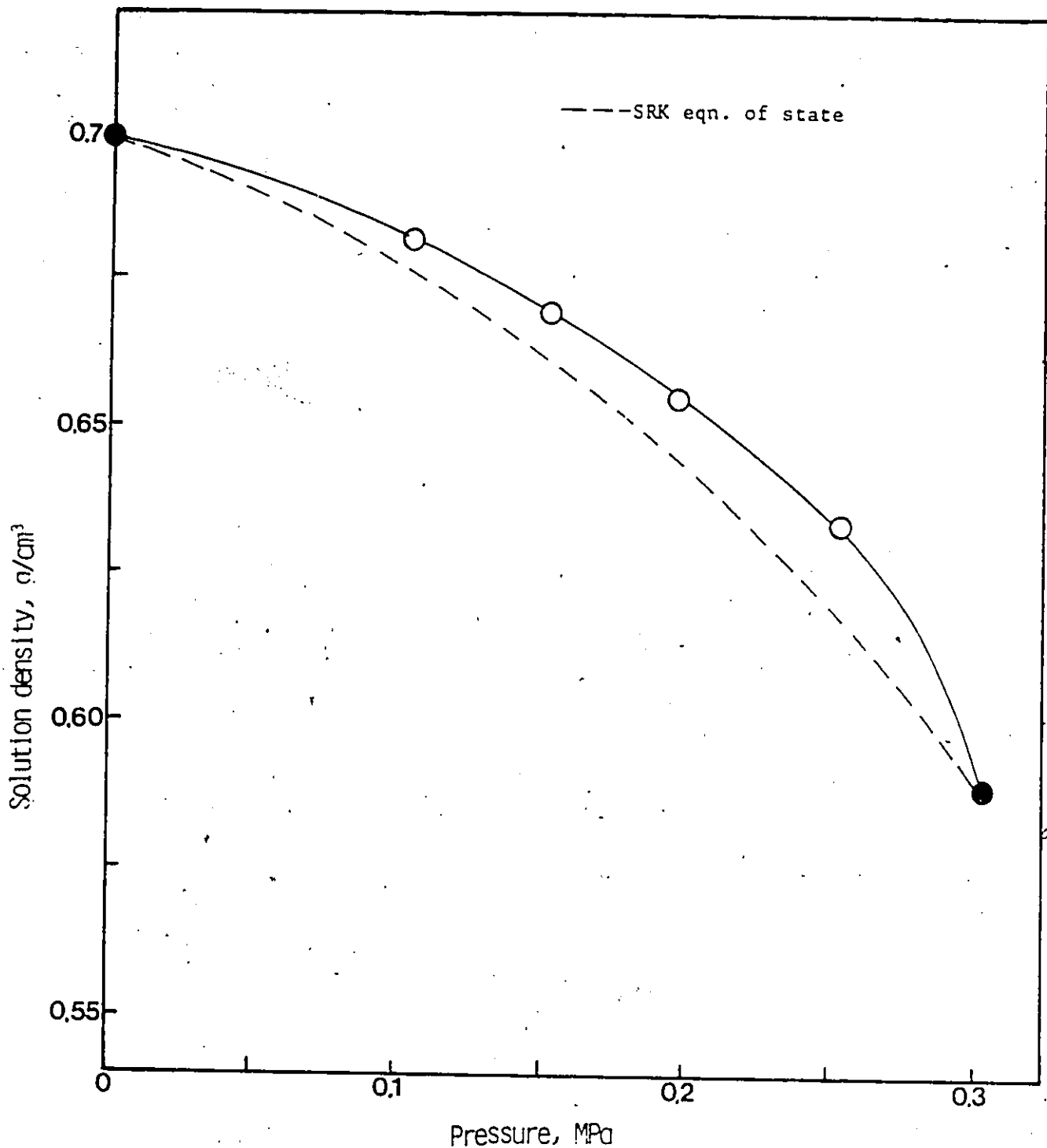


Figure C-3 Experimental and predicted densities of isobutene-saturated n-octane solutions at 298.15 K as a function of pressure.

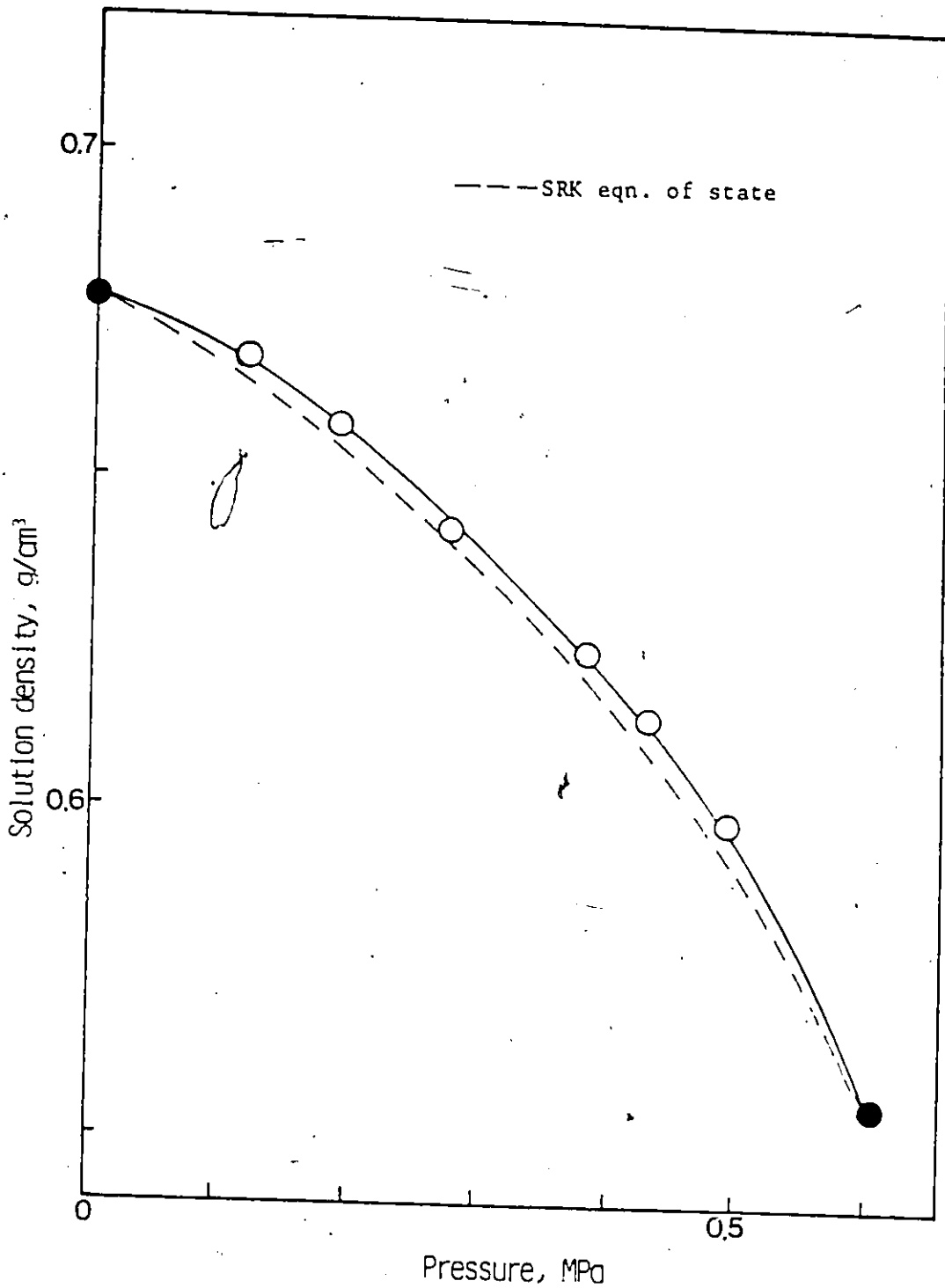


Figure C-4 Experimental and predicted densities of isobutene-saturated n-octane solutions at 323.15 K as a function of pressure.

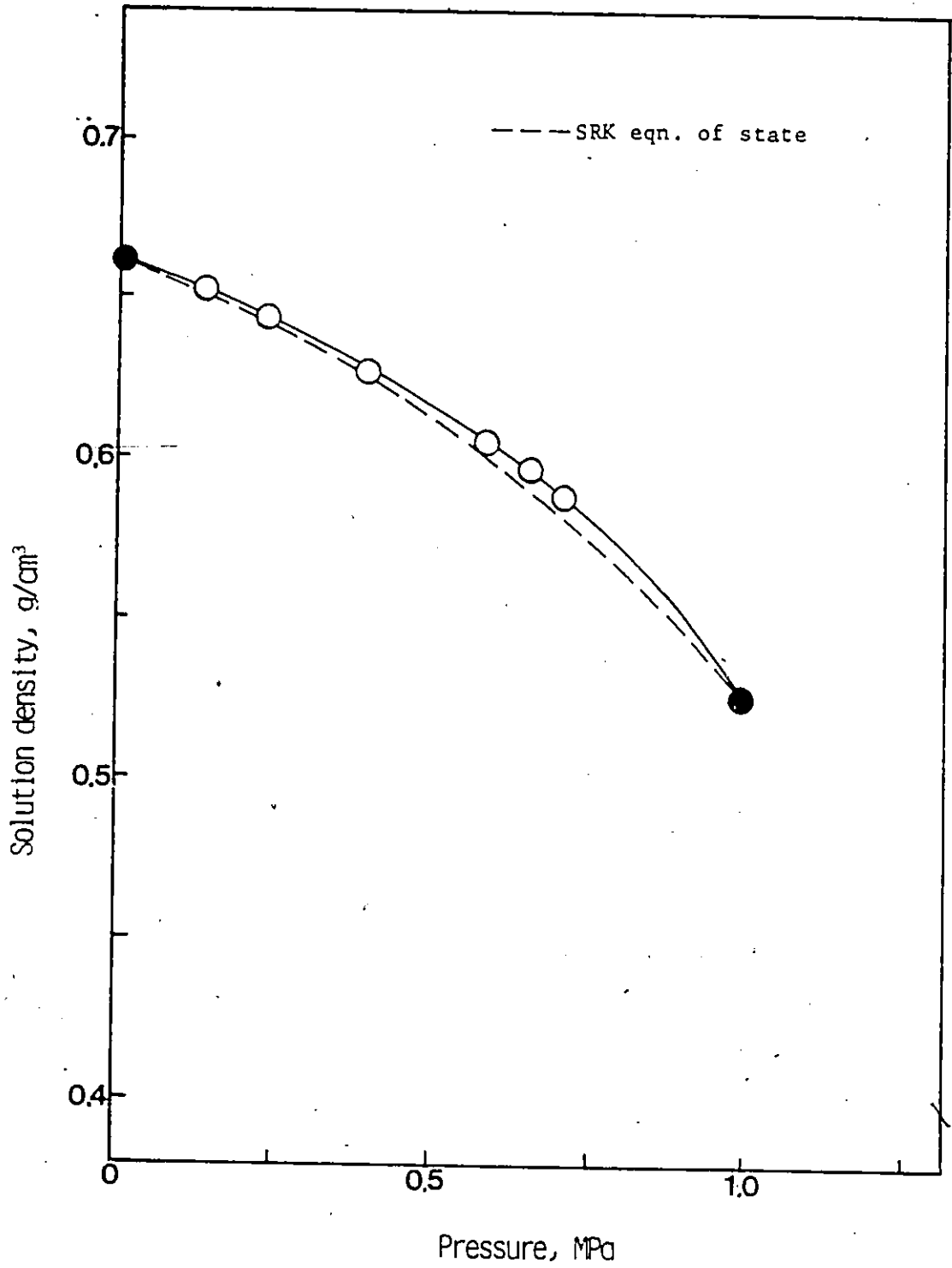


Figure C-5 Experimental and predicted densities of isobutene-saturated n-octane solutions at 343.15 K as a function of pressure.

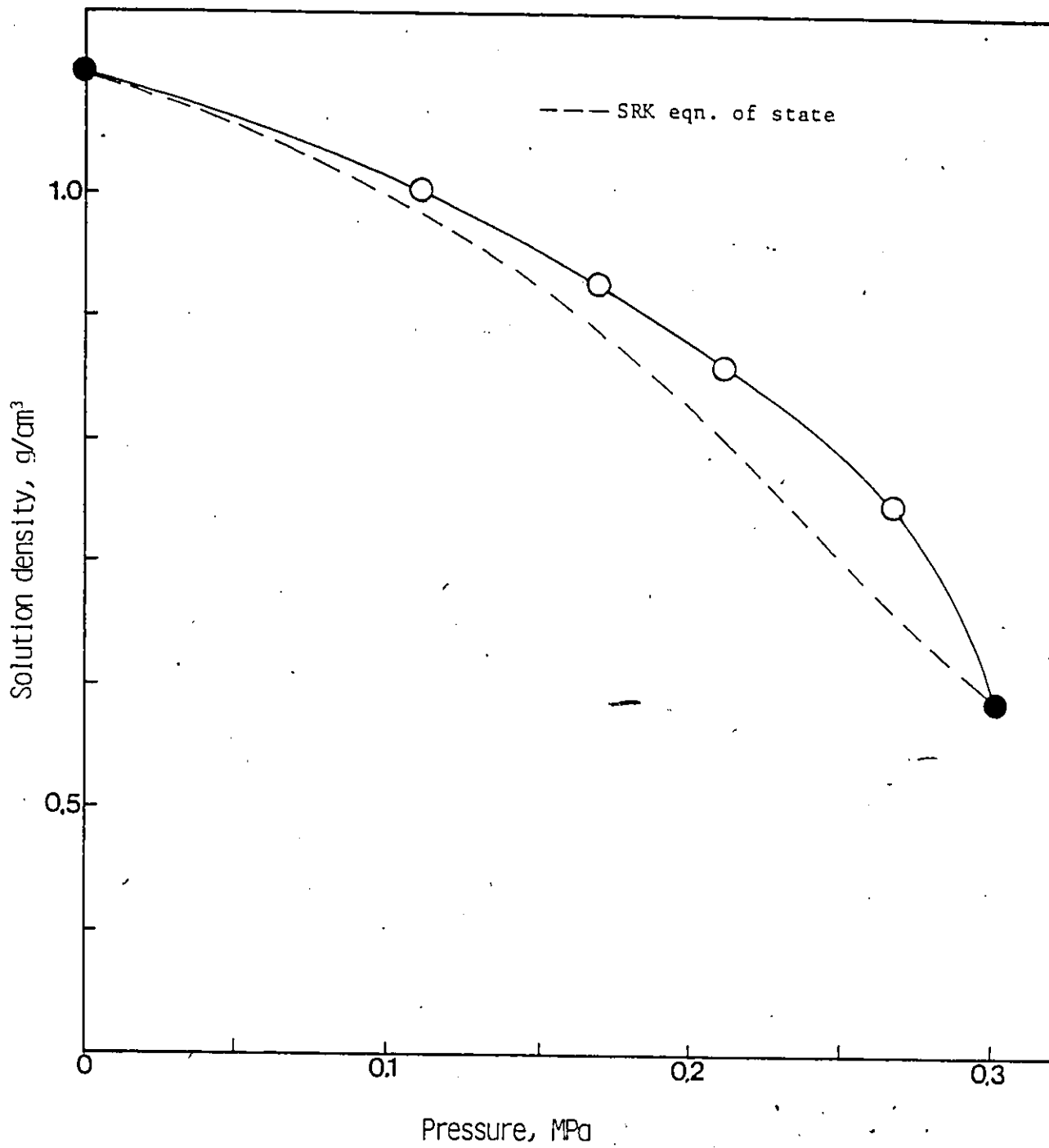


Figure C-6 Experimental and predicted densities of isobutene-saturated chlorobenzene solutions at 298.15 K as a function of pressure.

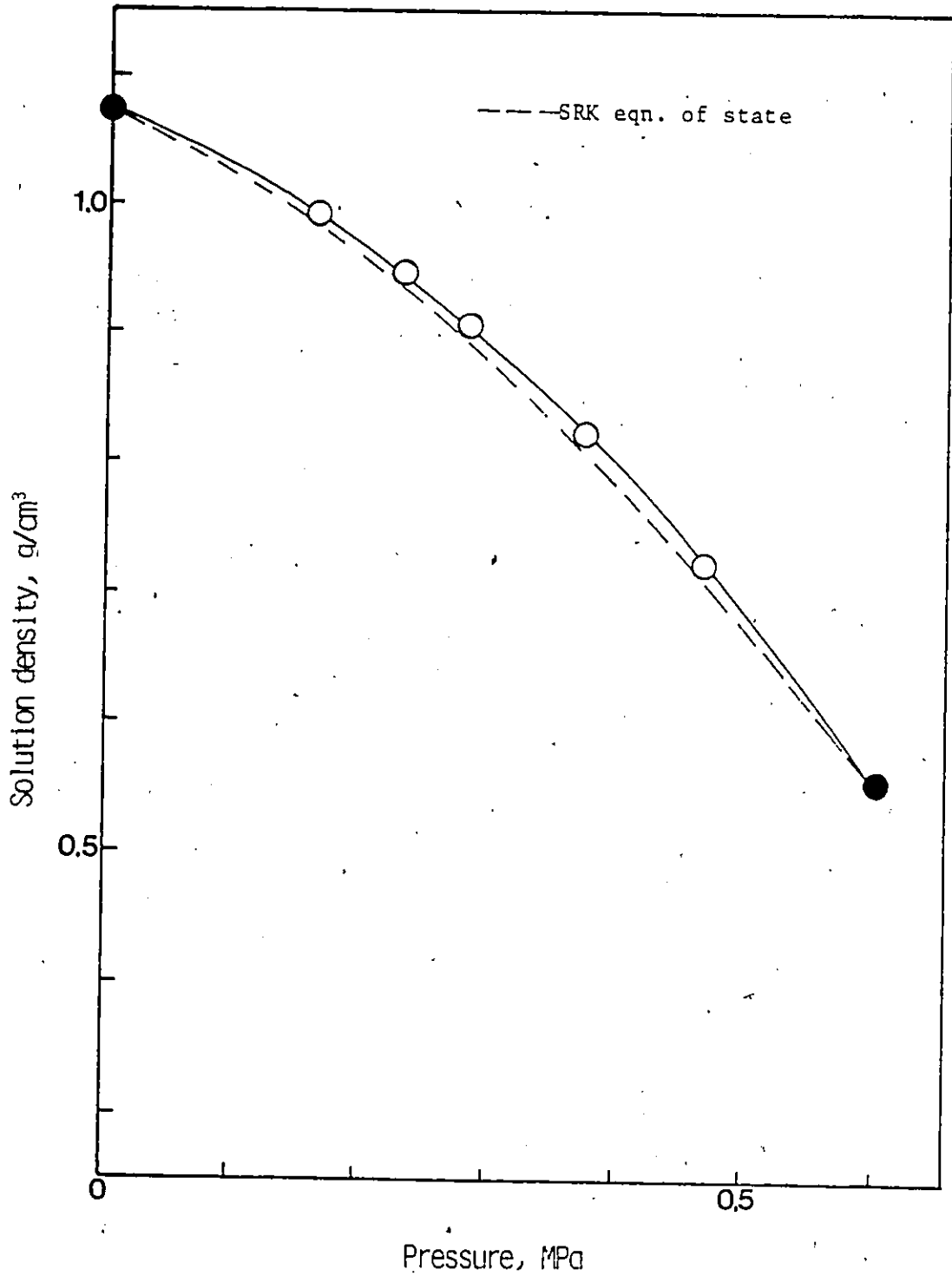


Figure C-7 Experimental and predicted densities of isobutene-saturated chlorobenzene solutions at 323.15 K as a function pressure.

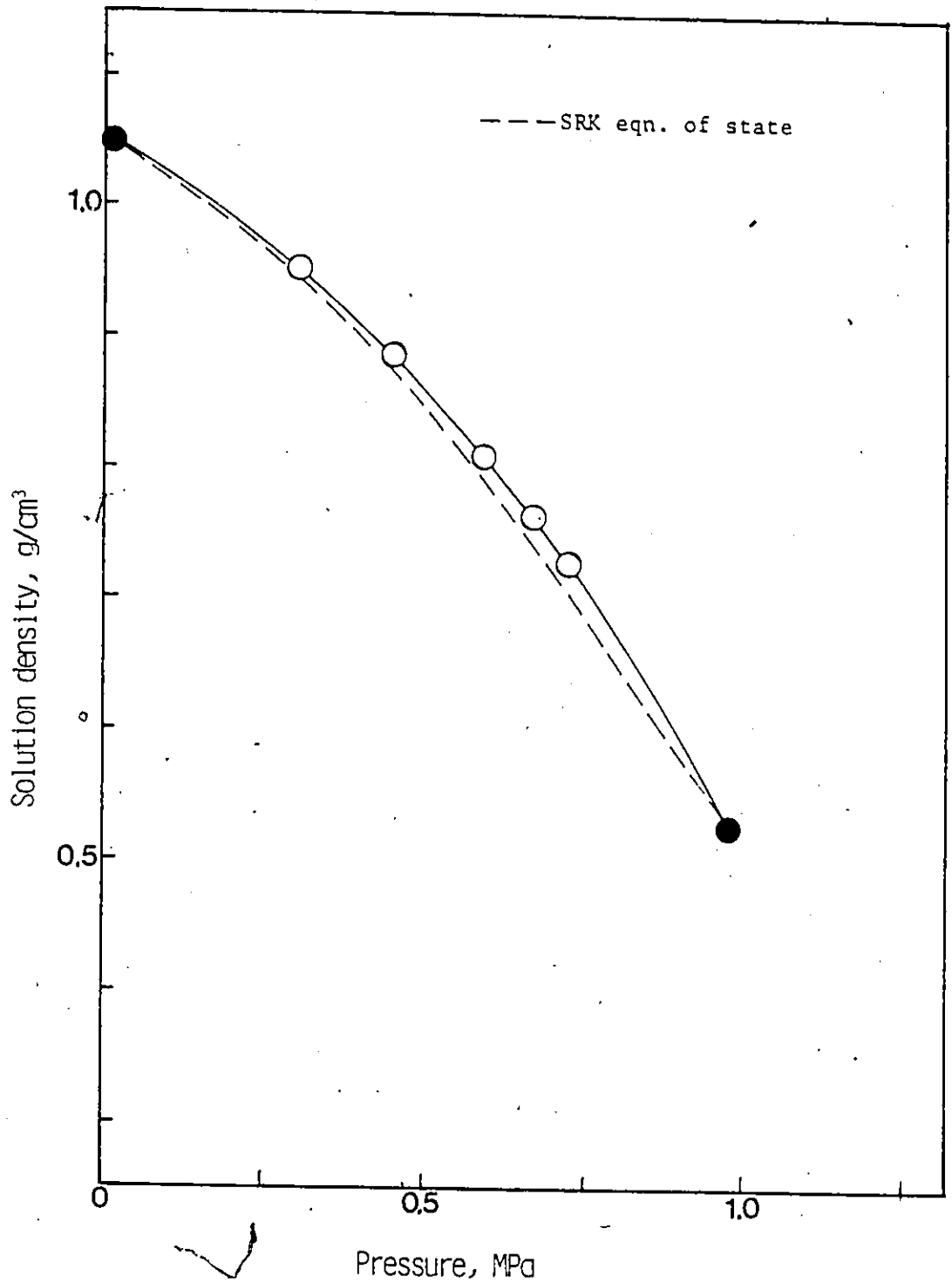


Figure C-8 Experimental and predicted densities of isobutene-saturated chlorobenzene solutions at 343.15 K as a function of pressure.

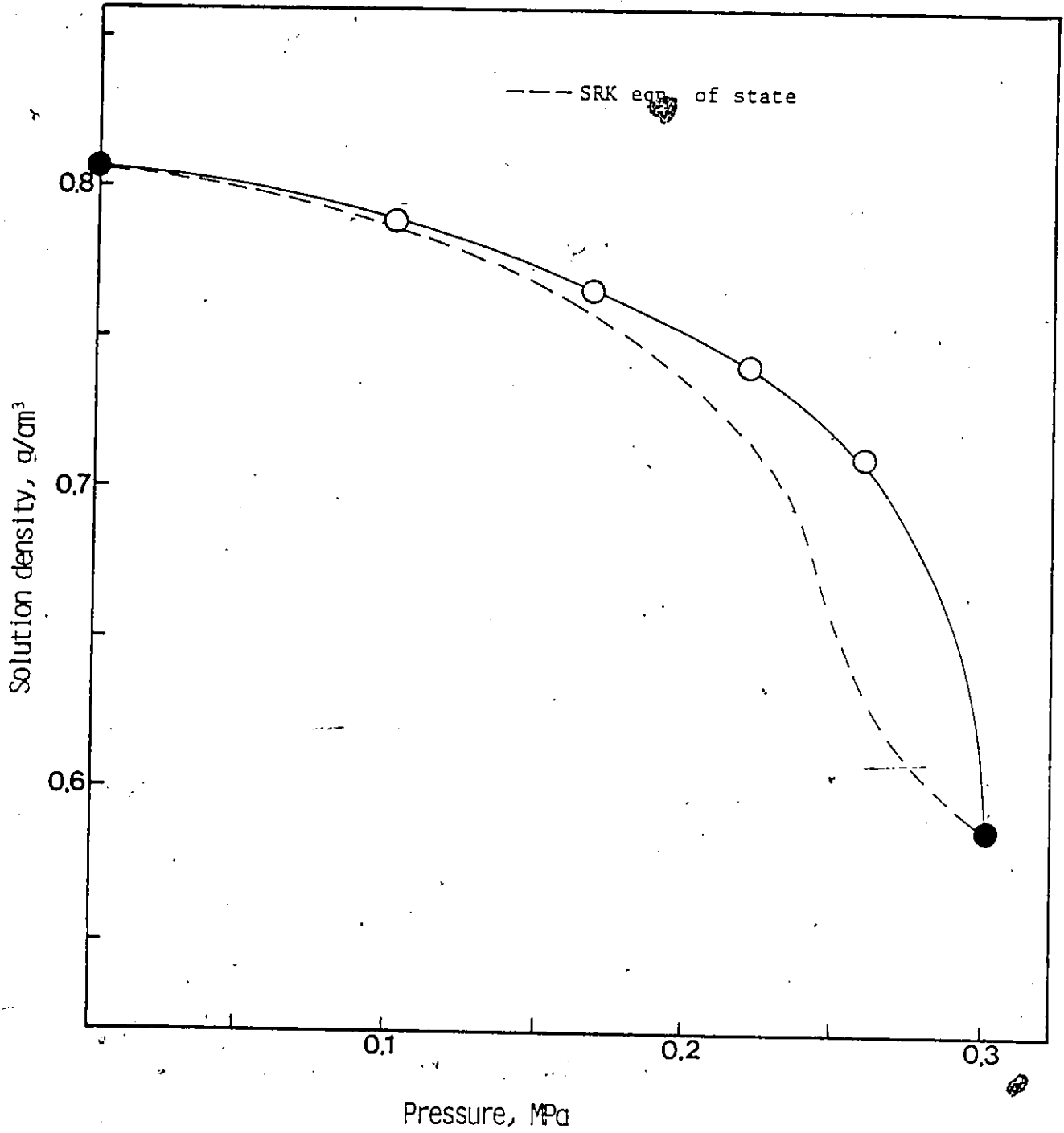


Figure C-9 Experimental and predicted densities of isobutene-saturated n-butanol solutions at 298.15 K as a function of pressure.

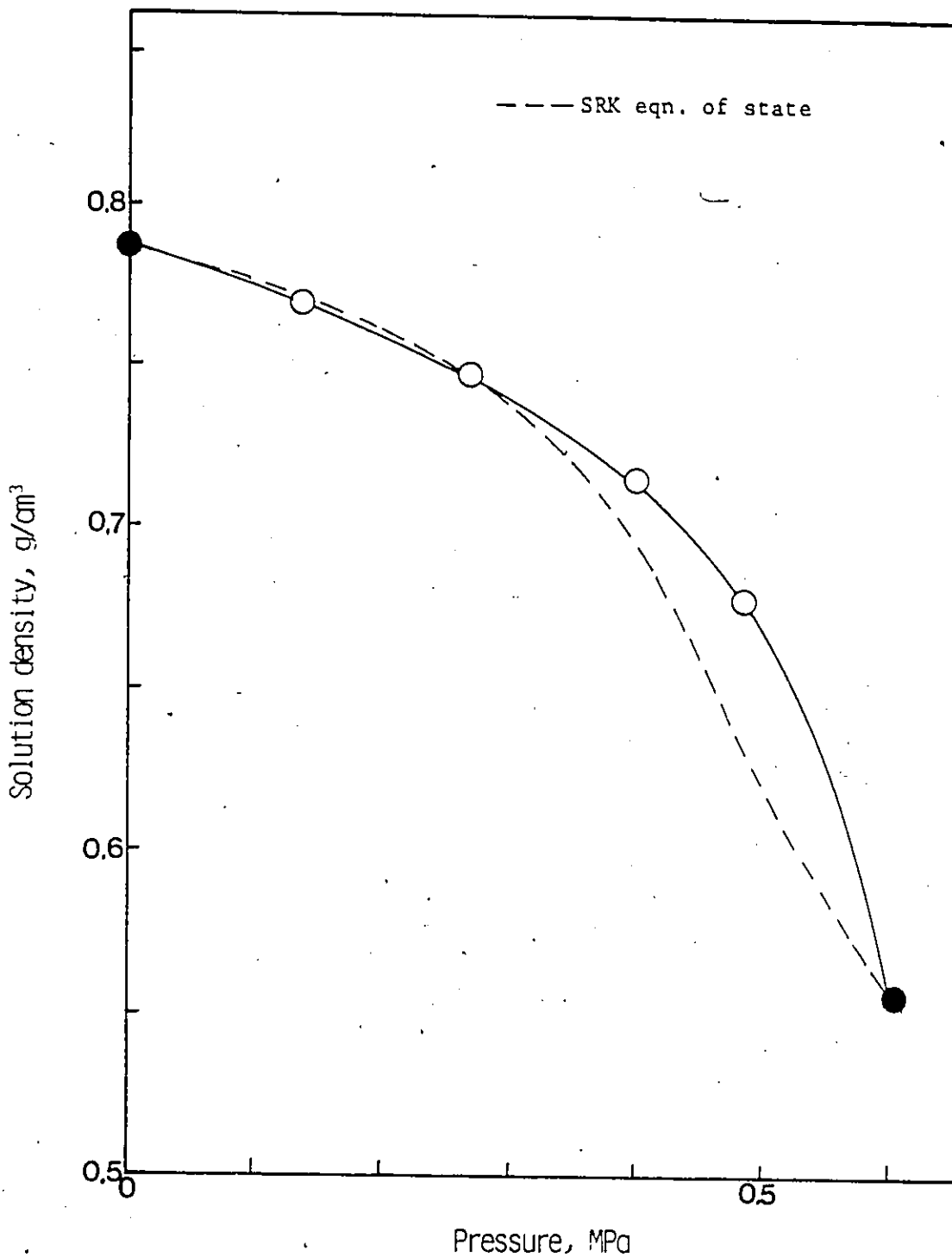


Figure C-10 Experimental and predicted densities of isobutene-saturated n-butanol solutions at 323.15 K as a function of pressure.

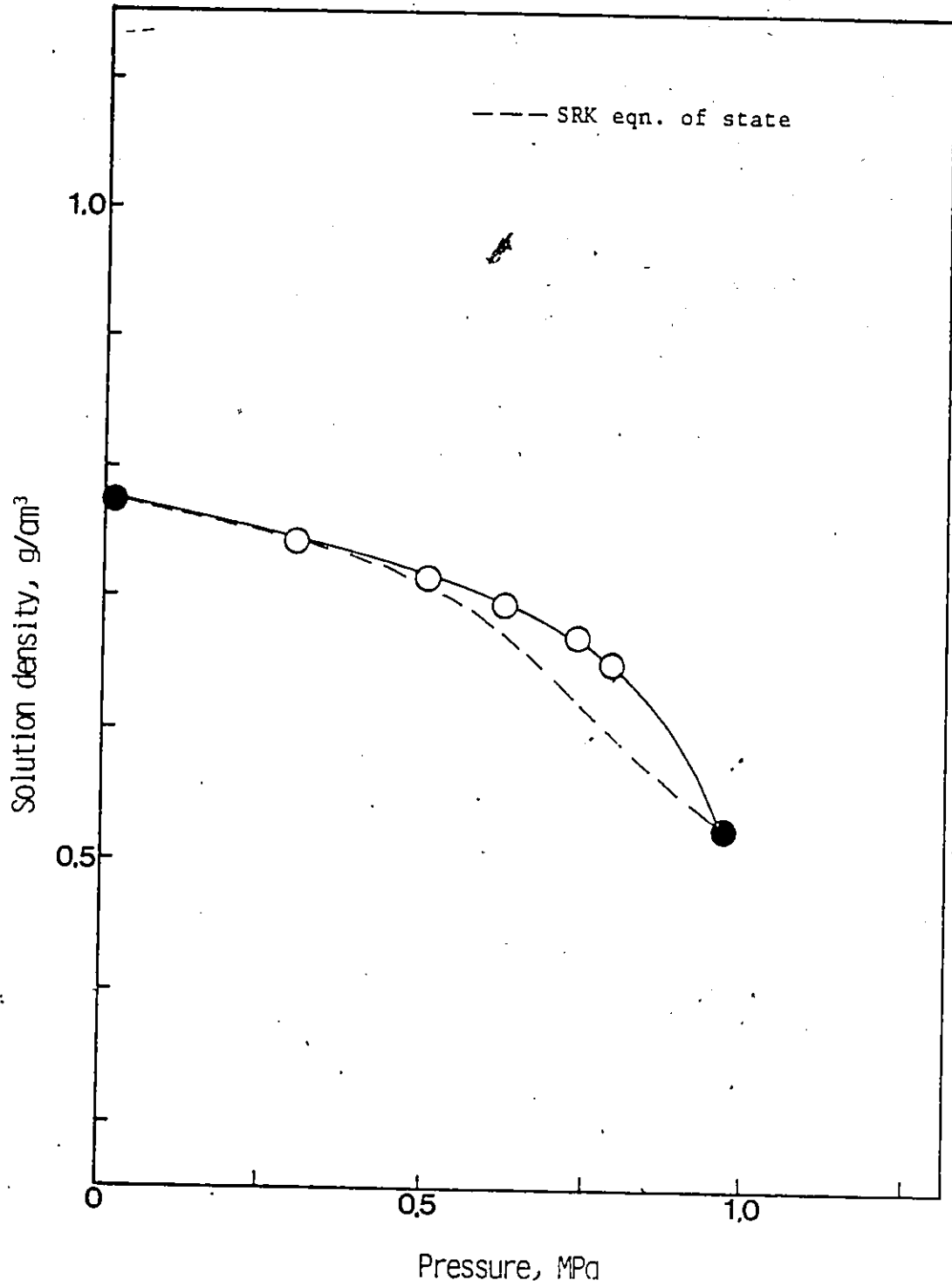


Figure C-11 Experimental and predicted densities of isobutene-saturated n-butanol solutions at 343.15 K as a function of pressure.

Appendix D

Experimental and predicted solution  
densities of gas-saturated solutions.

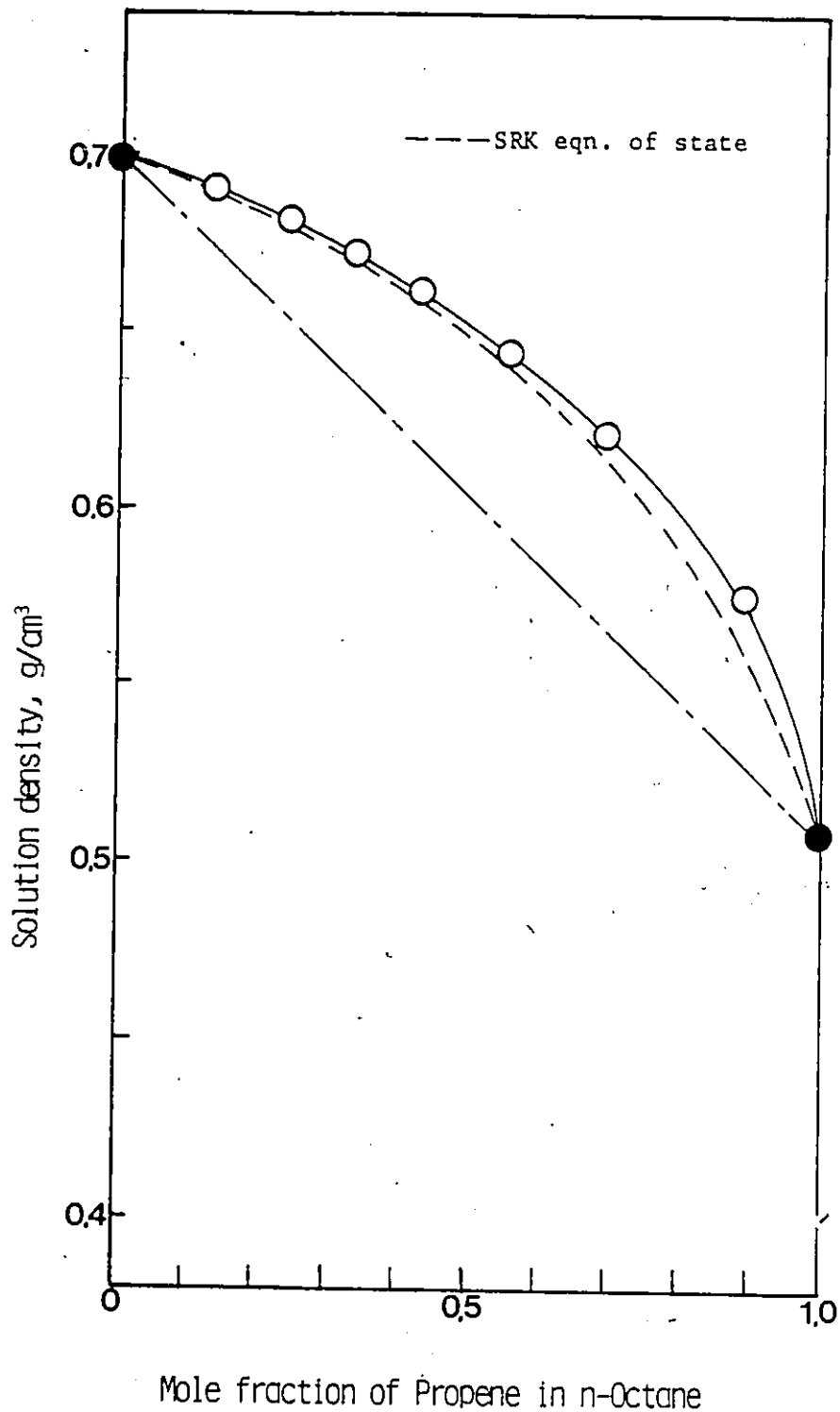


Figure D-1 Experimental and predicted densities of propene-saturated n-octane solutions at 298.15 K as a function of propene concentration in the solution.

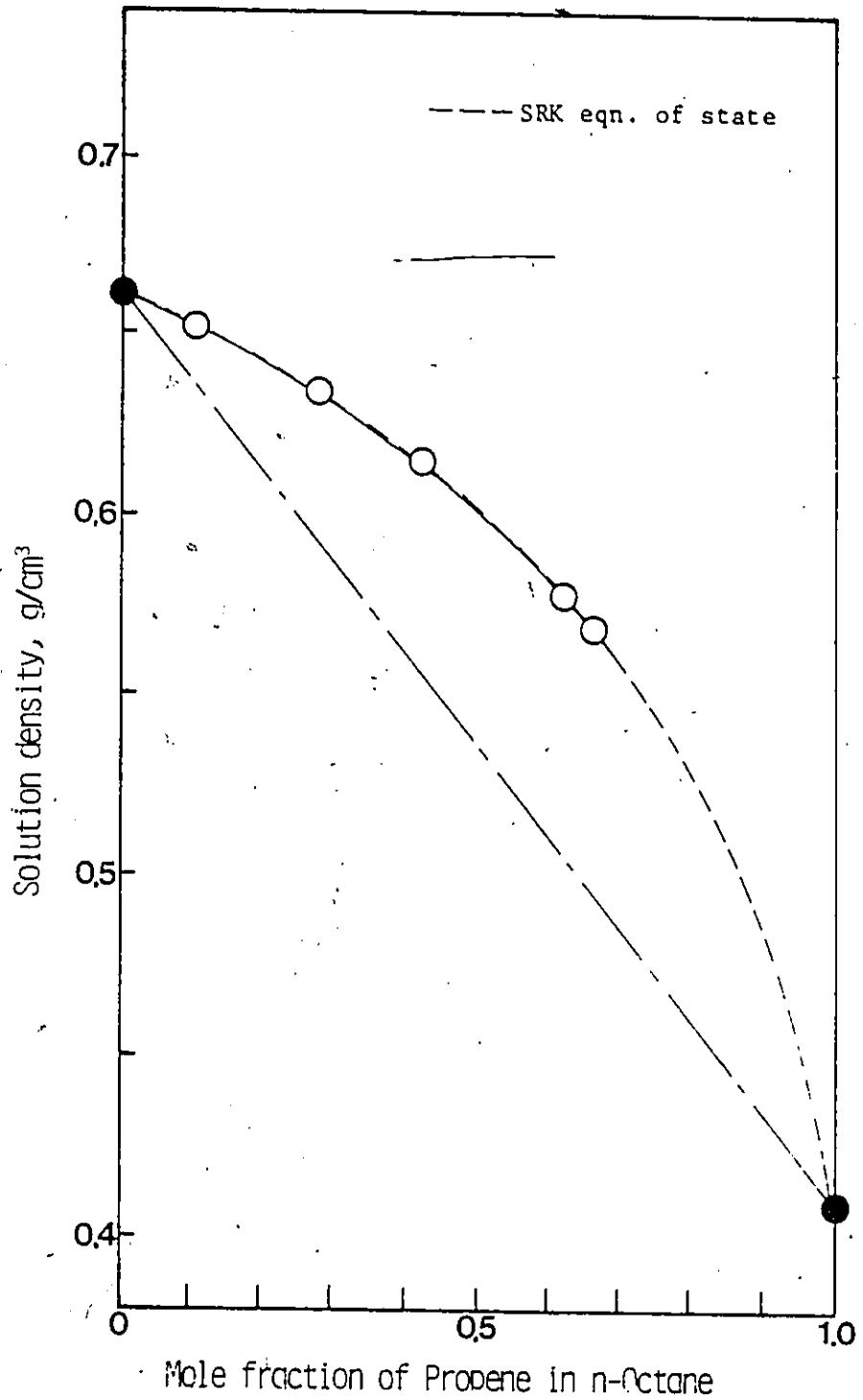


Figure D-2 Experimental and predicted densities of propene-saturated n-octane solutions at 343.15 K as a function of propene concentration in the solution.

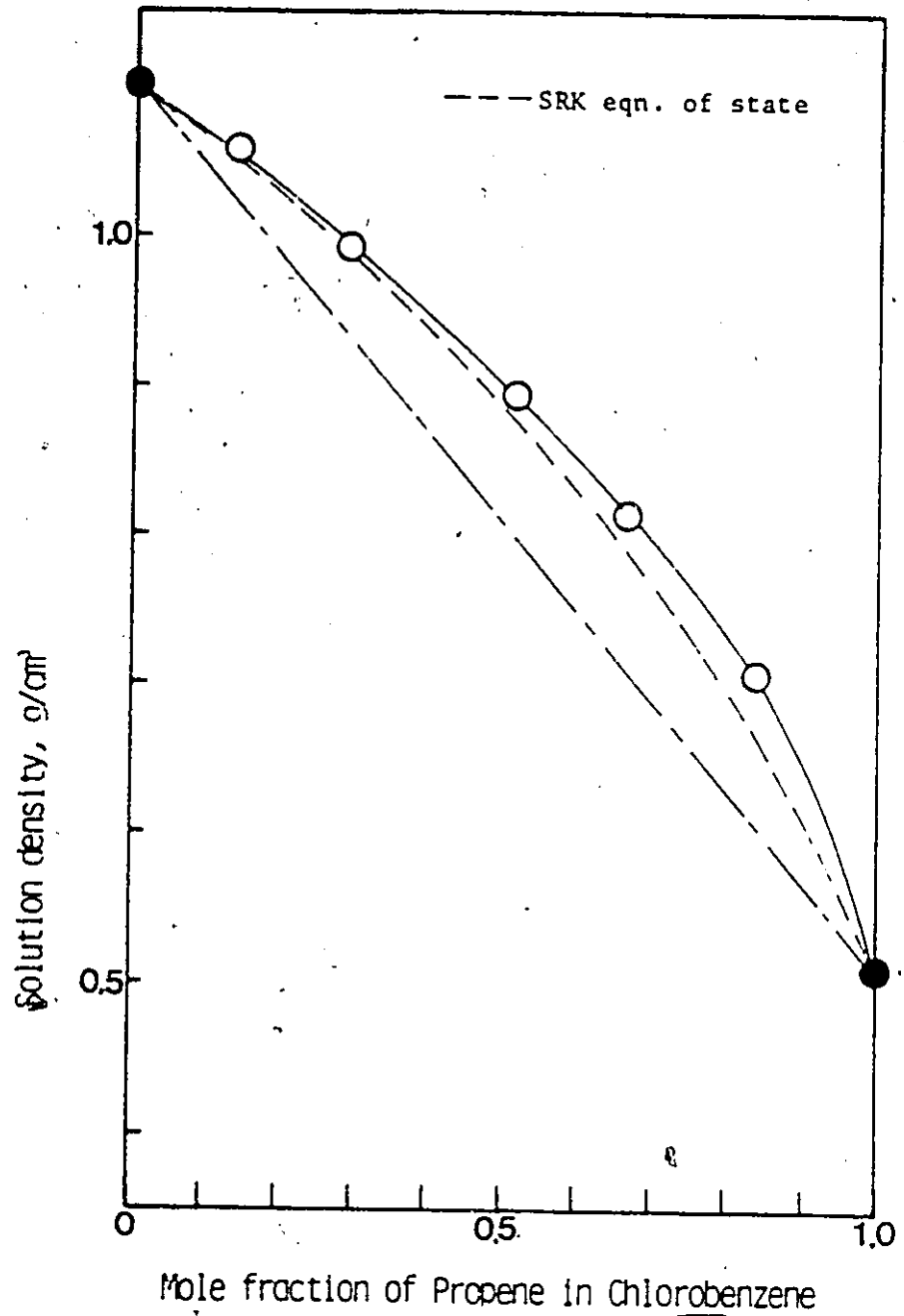


Figure D-3 Experimental and predicted densities of propene-saturated chlorobenzene solutions at 298.15 K as a function of propene concentration in the solution.

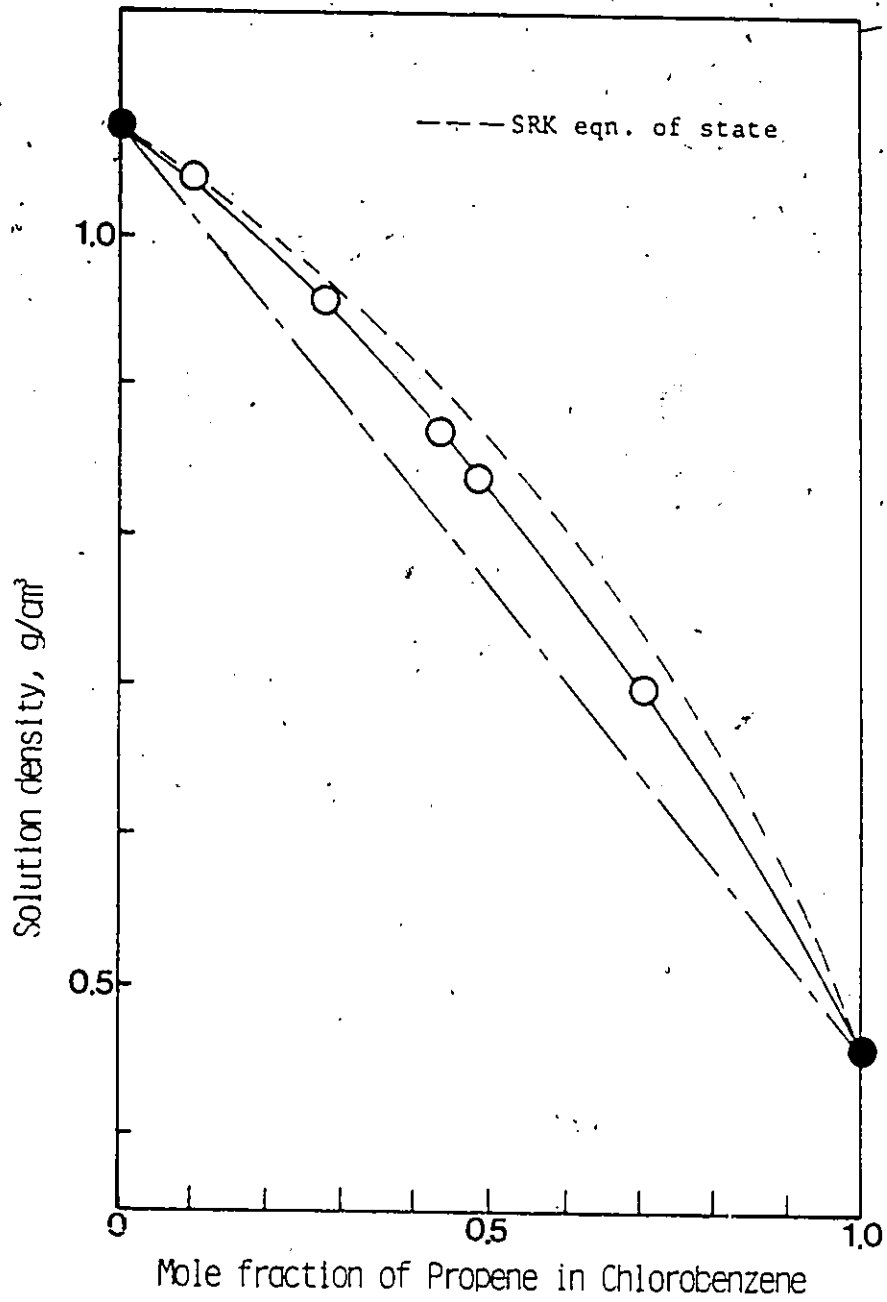


Figure D-4 Experimental and predicted densities of propene-saturated chlorobenzene solutions at 323.15 K as a function of propene concentration in the solution.

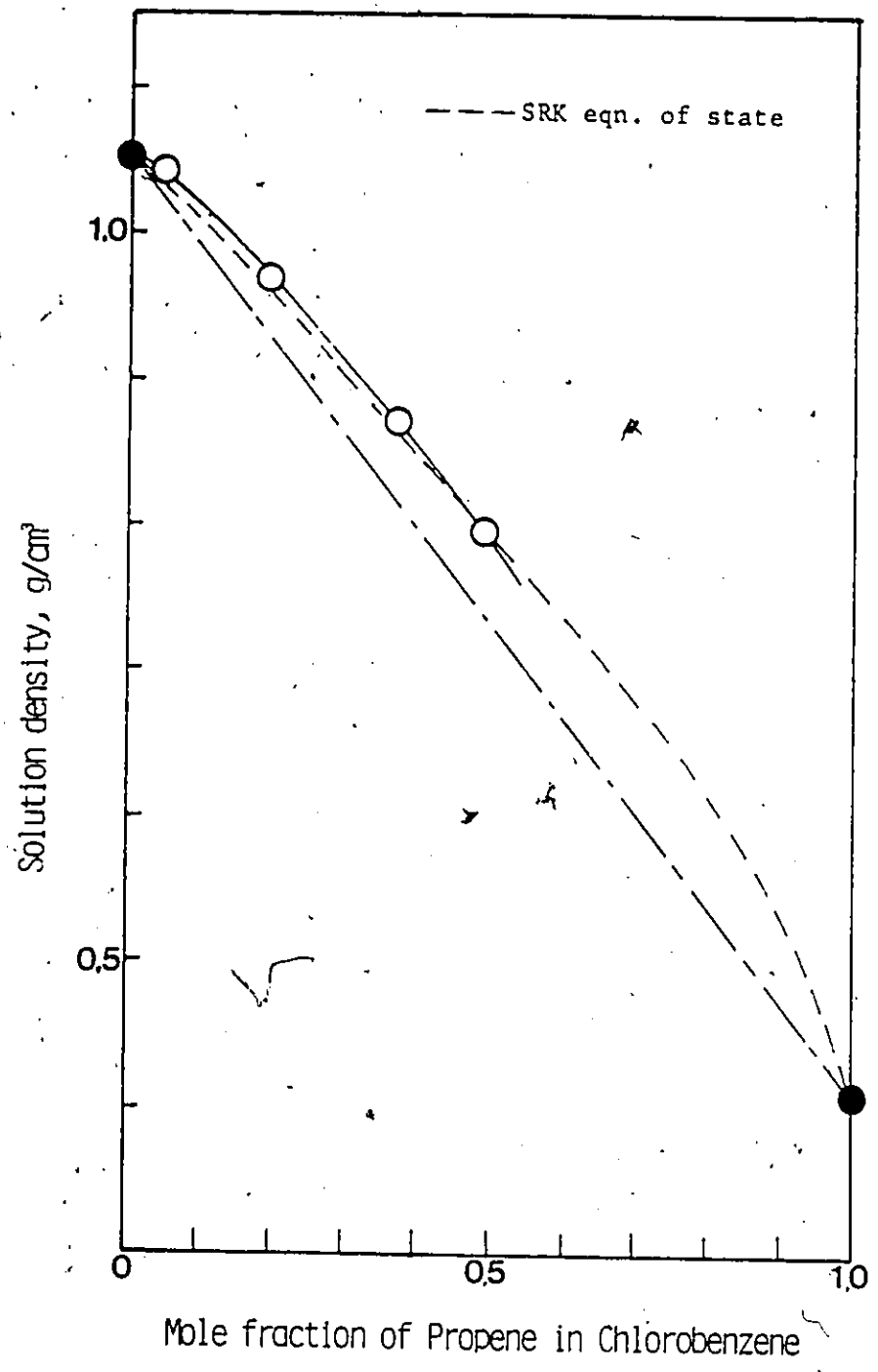


Figure D-5 Experimental and predicted densities of propene-saturated chlorobenzene solutions at 343.15 K as a function of propene concentration in the solution.

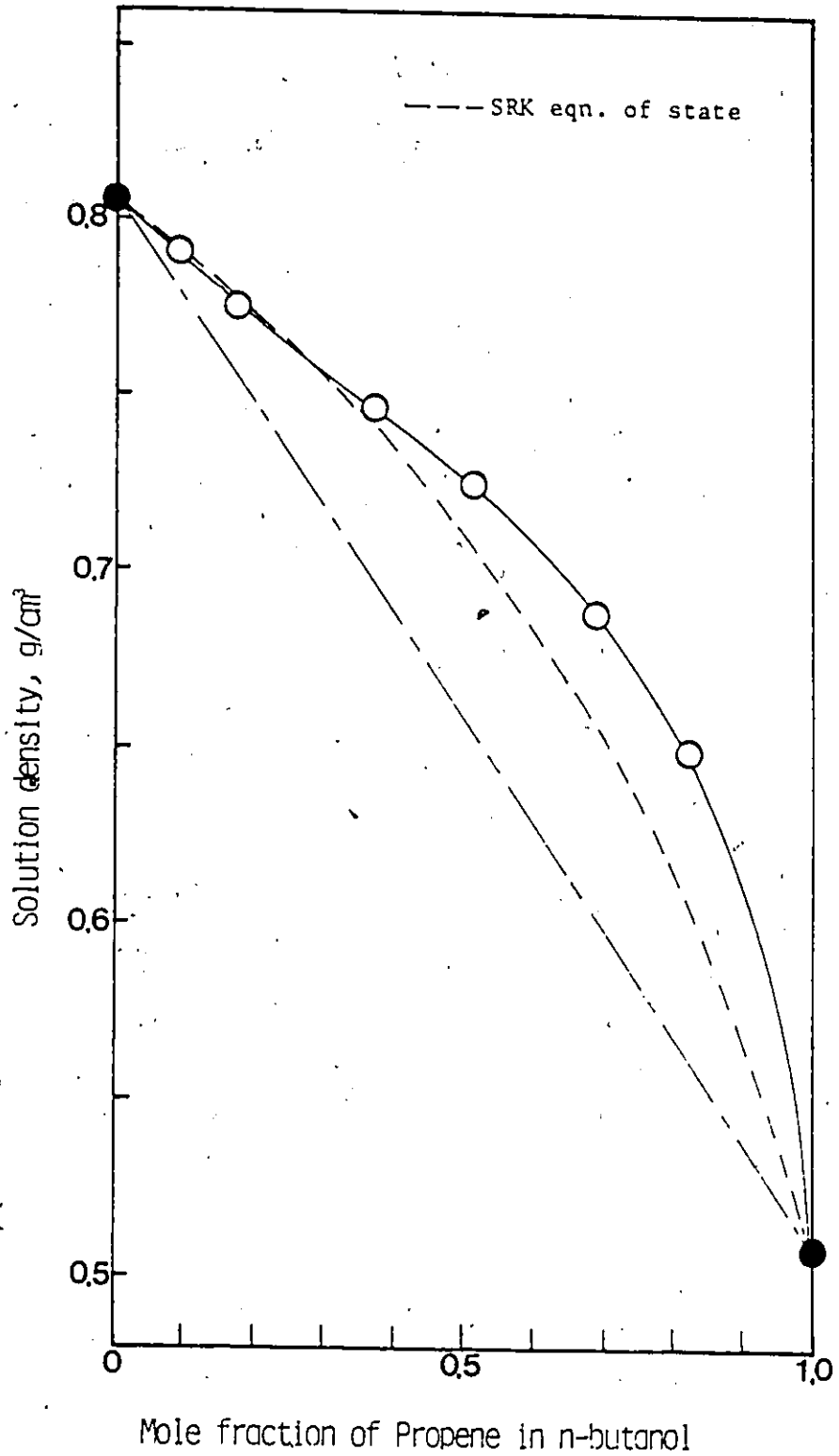


Figure D-6 Experimental and predicted densities of propene-saturated n-butanol solutions at 298.15 K as a function of propene concentration in the solution.



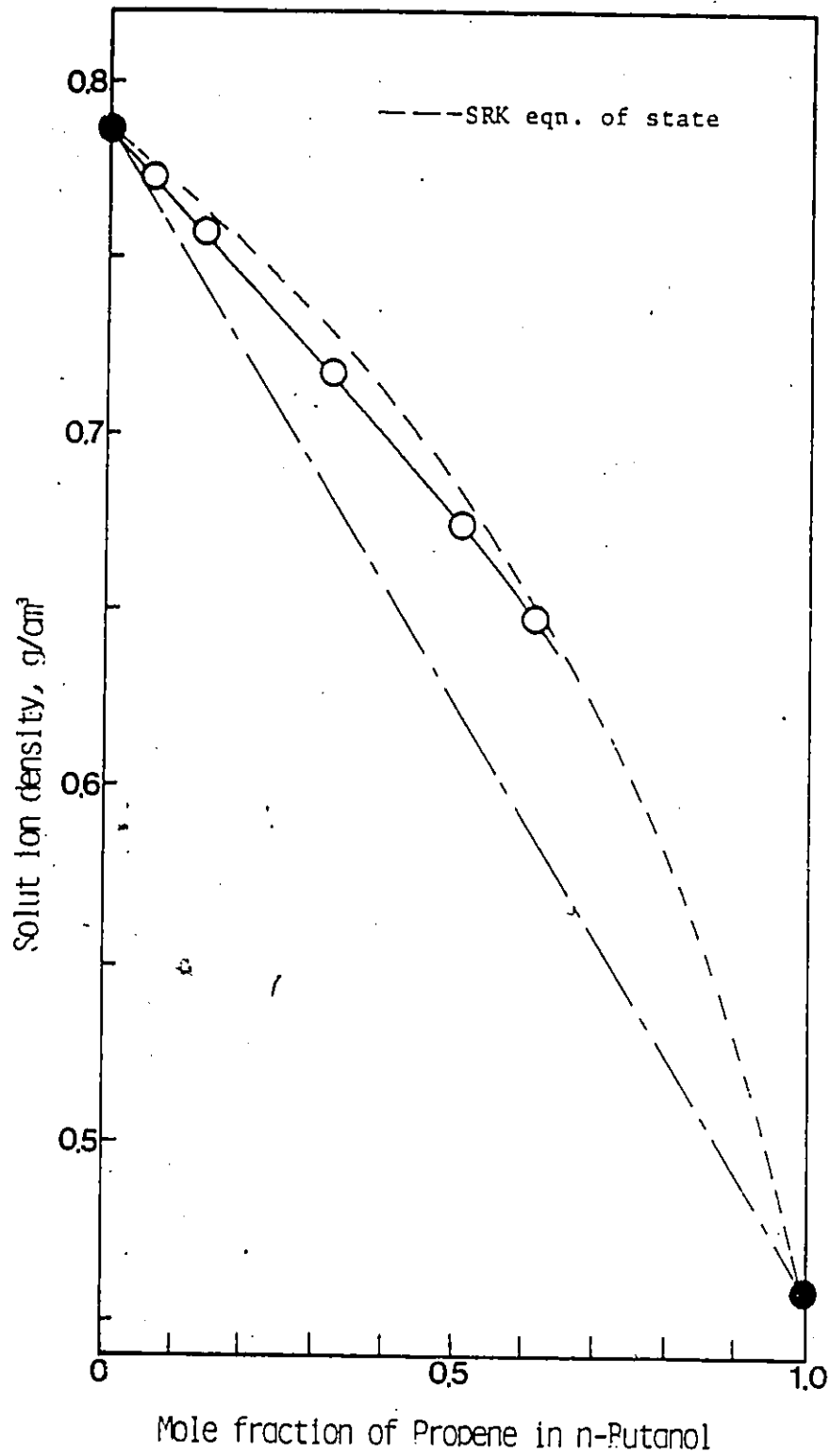


Figure D-7 Experimental and predicted densities of propene-saturated n-butanol solutions at 323.15 K as a function of propene concentration in the solution.

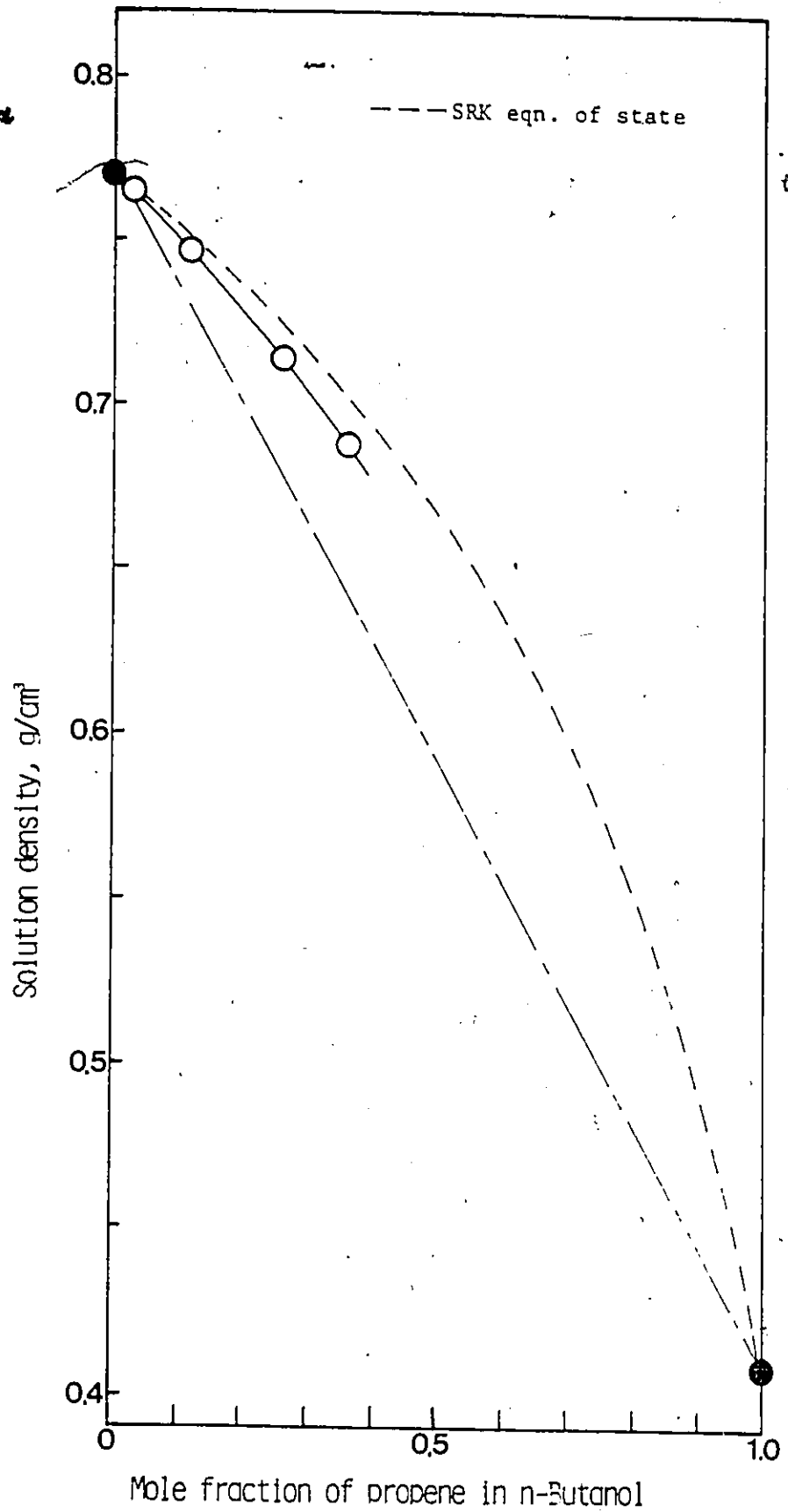


Figure D-8 Experimental and predicted densities of propene-saturated n-butanol solutions at 343.15 K as a function of propene concentration in the solution.

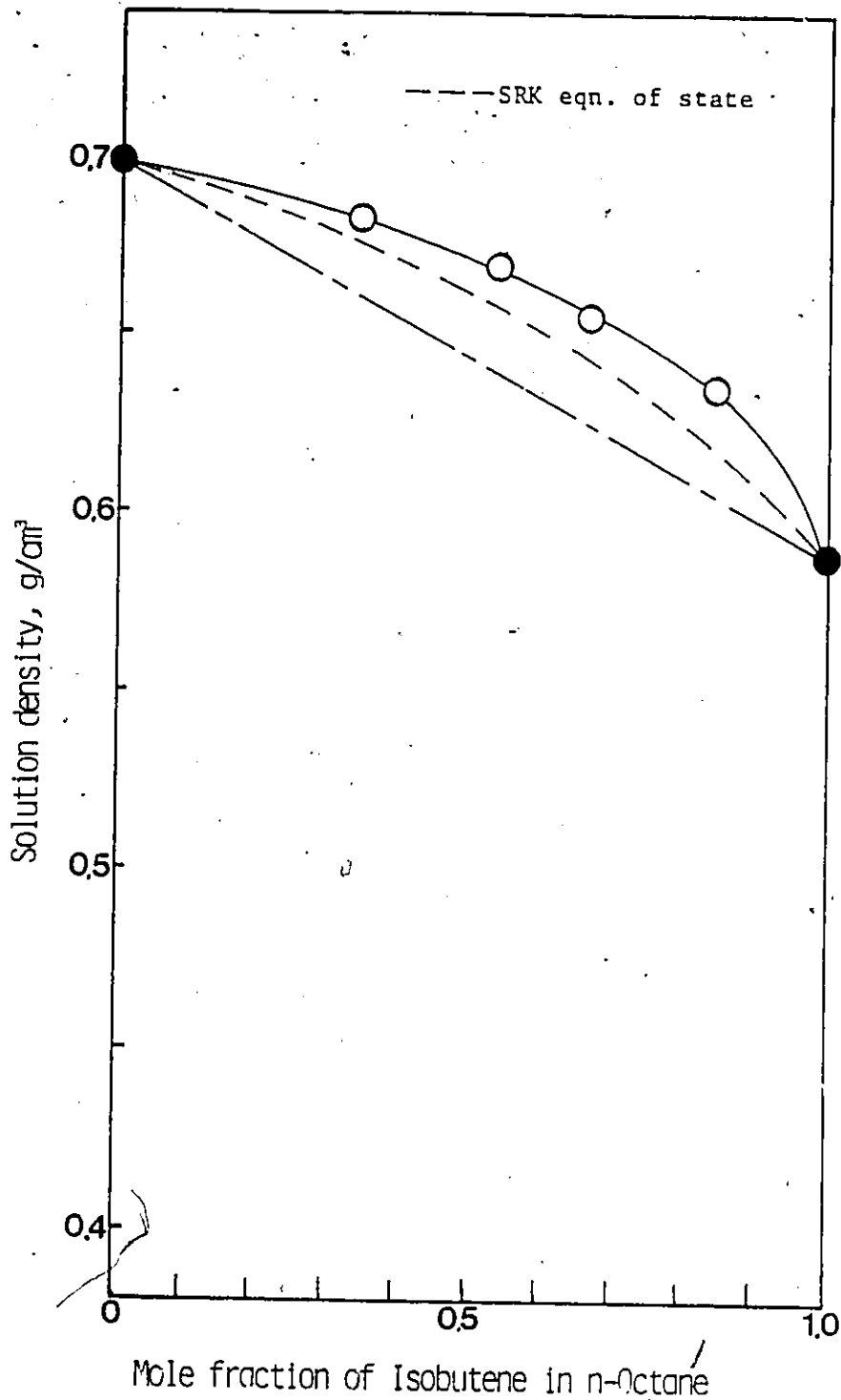


Figure D-9 Experimental and predicted densities of isobutene-saturated n-octane solutions at 298.15 K as a function of isobutene concentration in the solution.

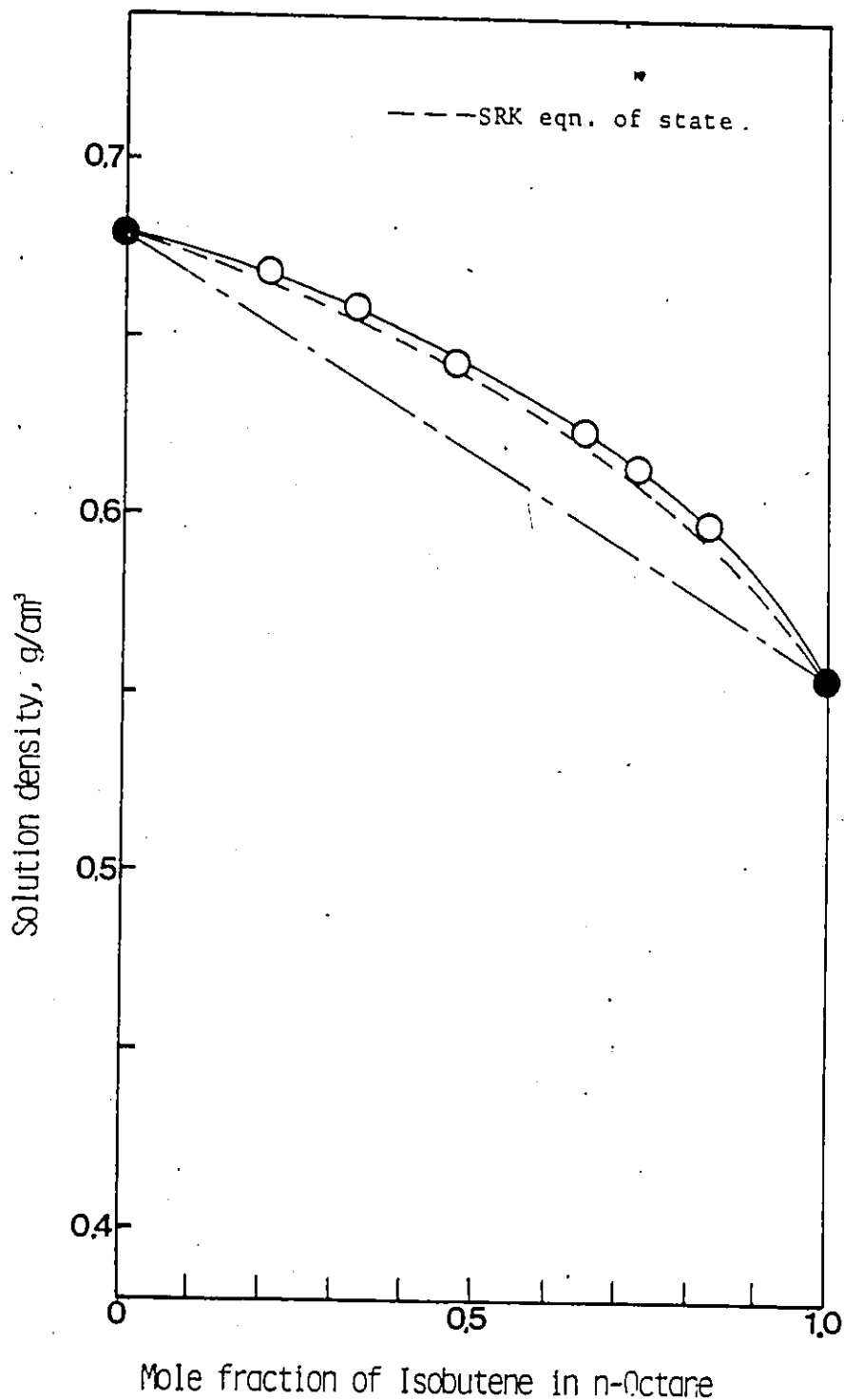


Figure D-10 Experimental and predicted densities of isobutene-saturated n-octane solutions at 323.15 K as a function of isobutene concentration in the solution.

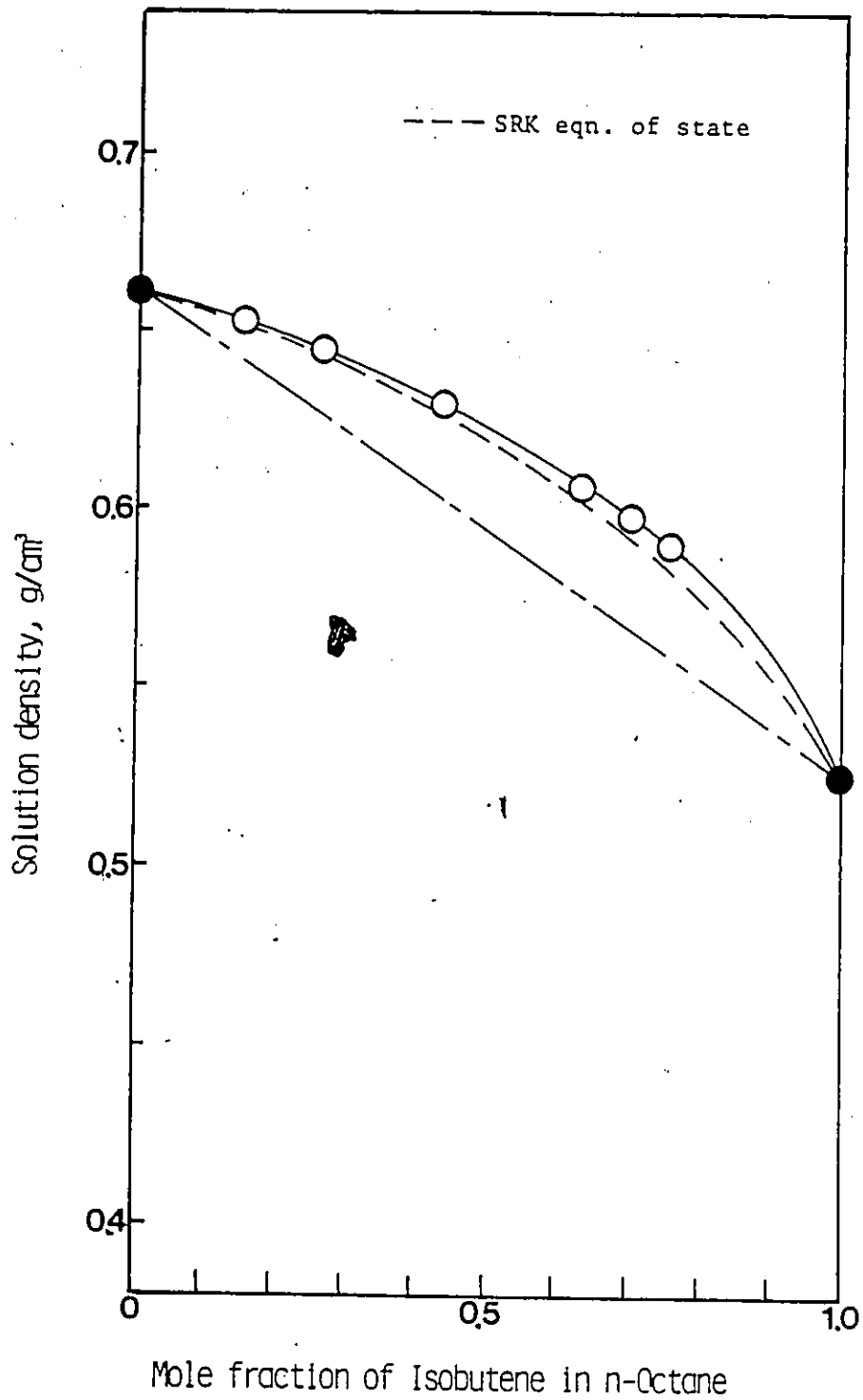


Figure D-11 Experimental and predicted densities of isobutene-saturated n-octane solutions at 343.15 K as a function of isobutene concentration in the solution.

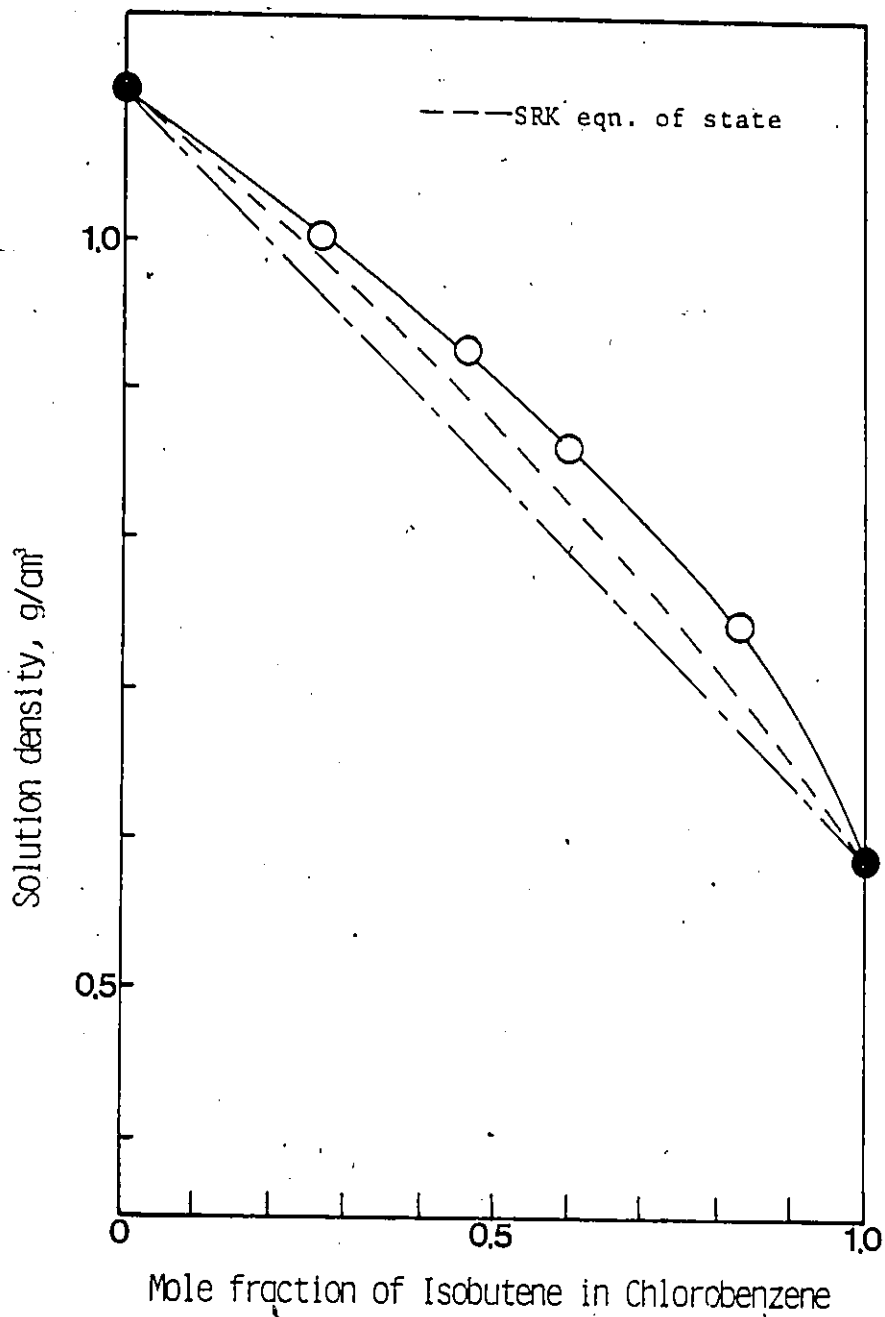


Figure D-12 Experimental and predicted densities of isobutene-saturated chlorobenzene solutions at 298.15 K as a function of isobutene concentration in the solution.

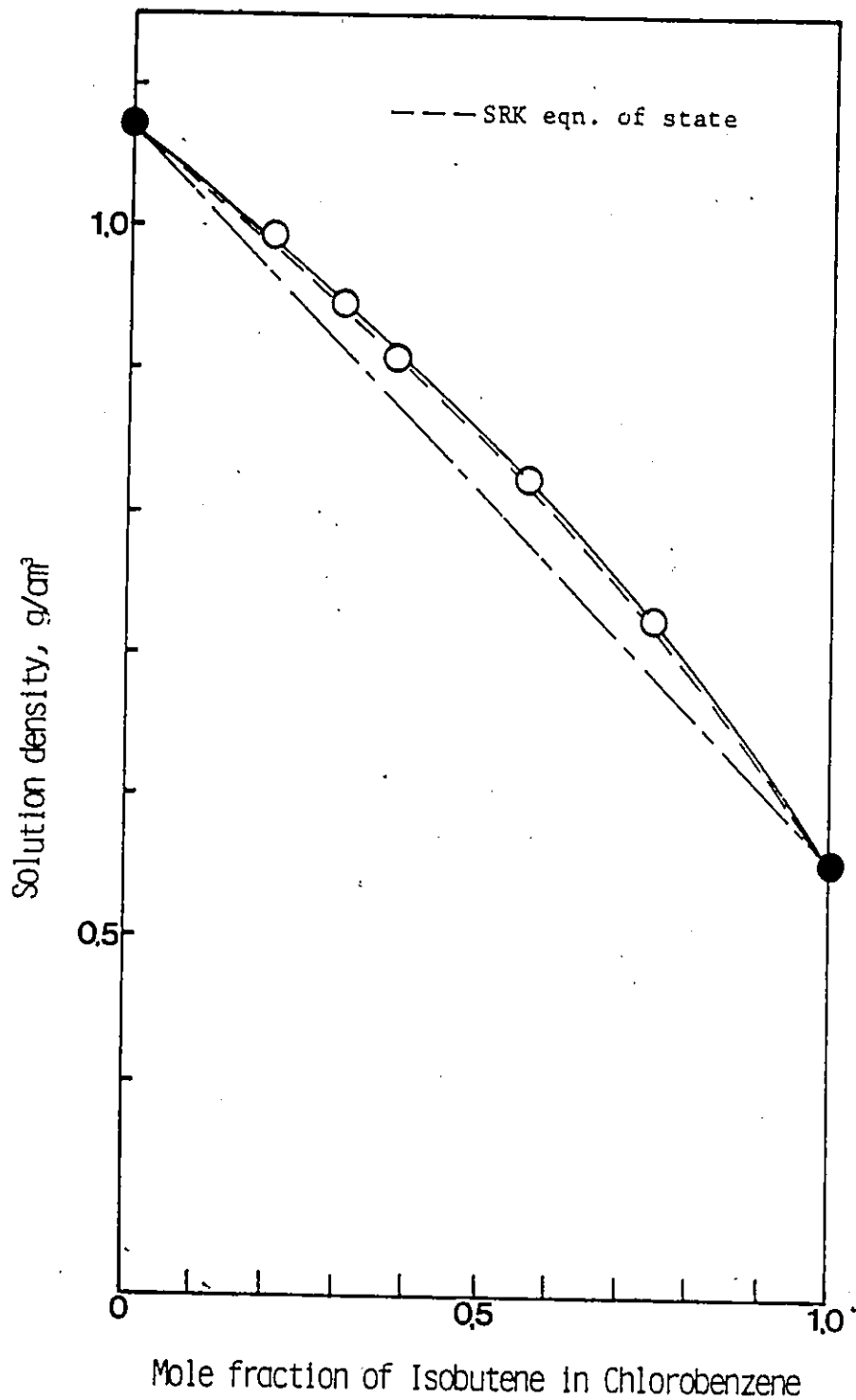


Figure D-13 Experimental and predicted densities of isobutene-saturated chlorobenzene solutions at 323.15 K as a function of isobutene concentration in the solution.

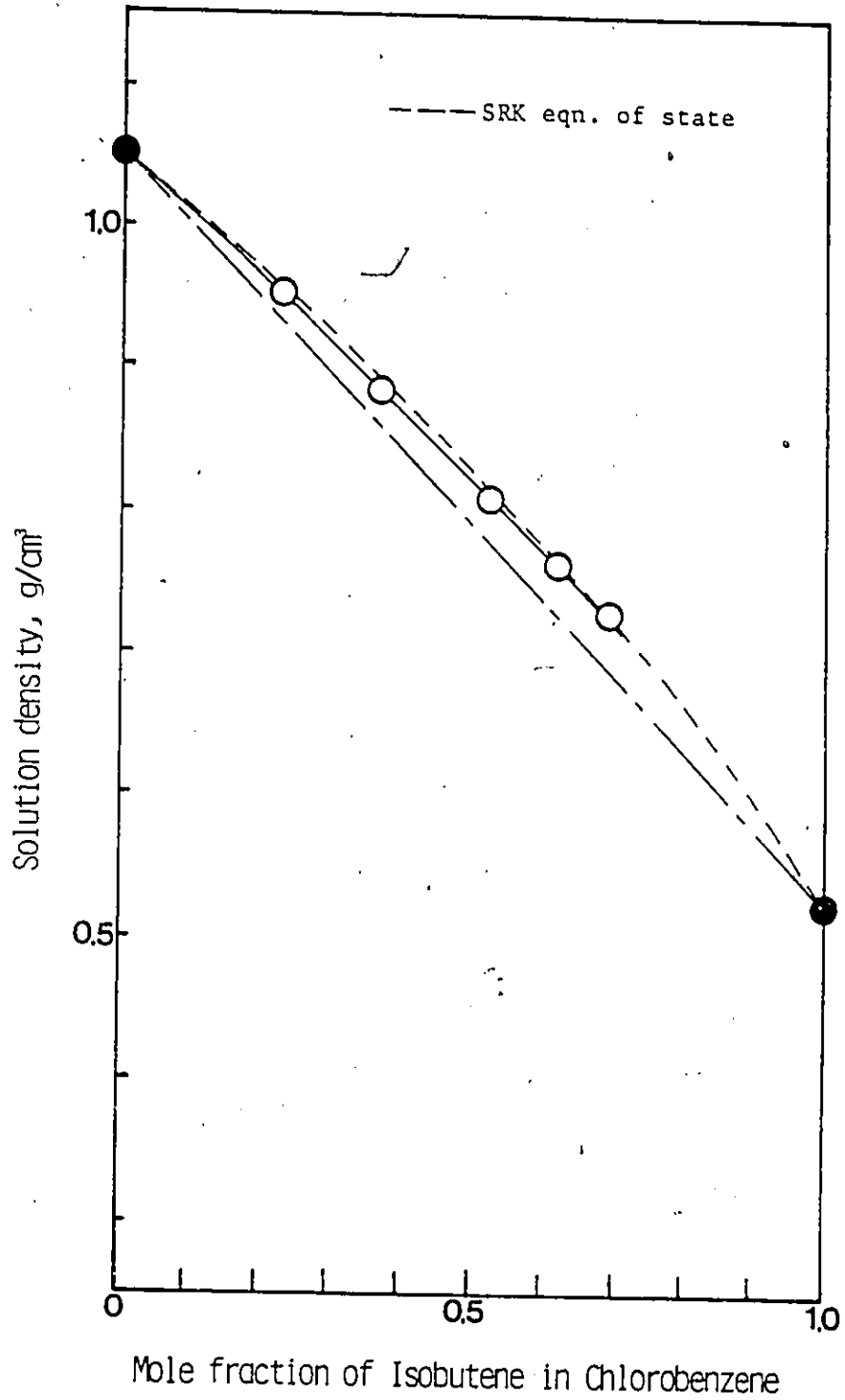


Figure D-14 Experimental and predicted densities of isobutene-saturated chlorobenzene solutions at 343.15 K as a function of isobutene concentration in the solution.

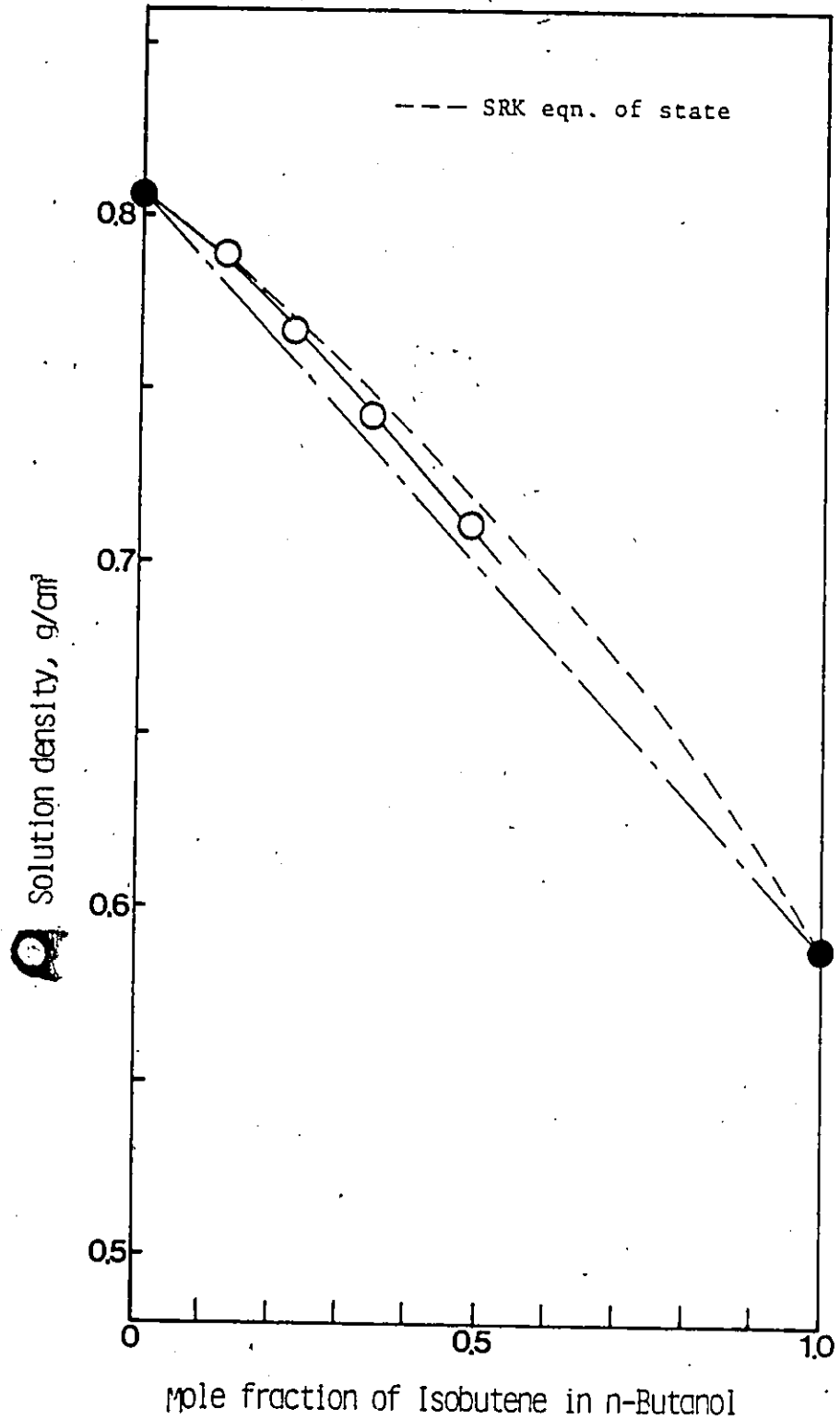


Figure D-15 Experimental and predicted densities of isobutene-saturated n-butanol solutions at 298.15 K as a function of isobutene concentration in the solution.

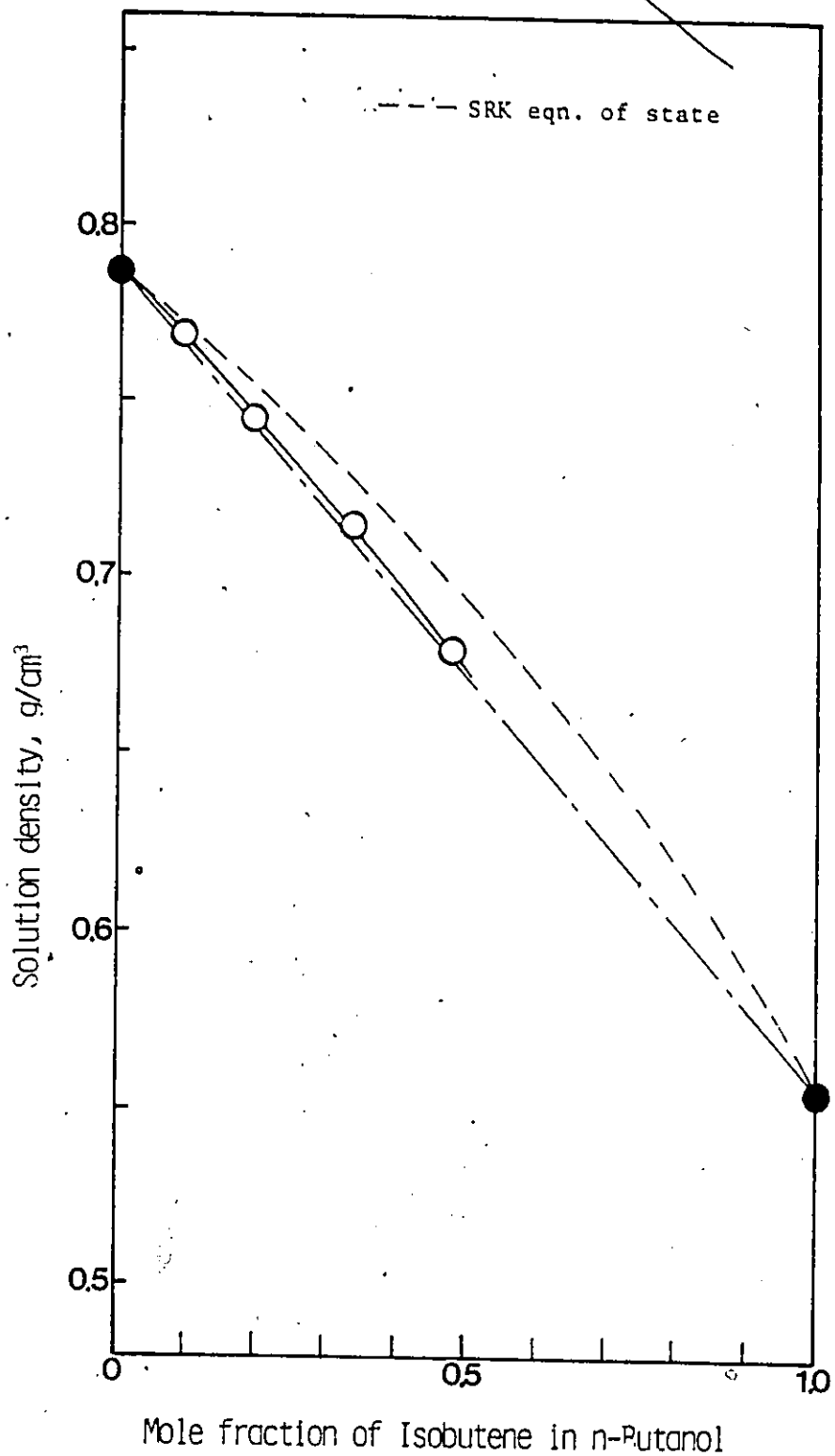


Figure D-16 Experimental and predicted densities of isobutene-saturated n-butanol solutions at 323.15 K as a function of isobutene concentration in the solution.

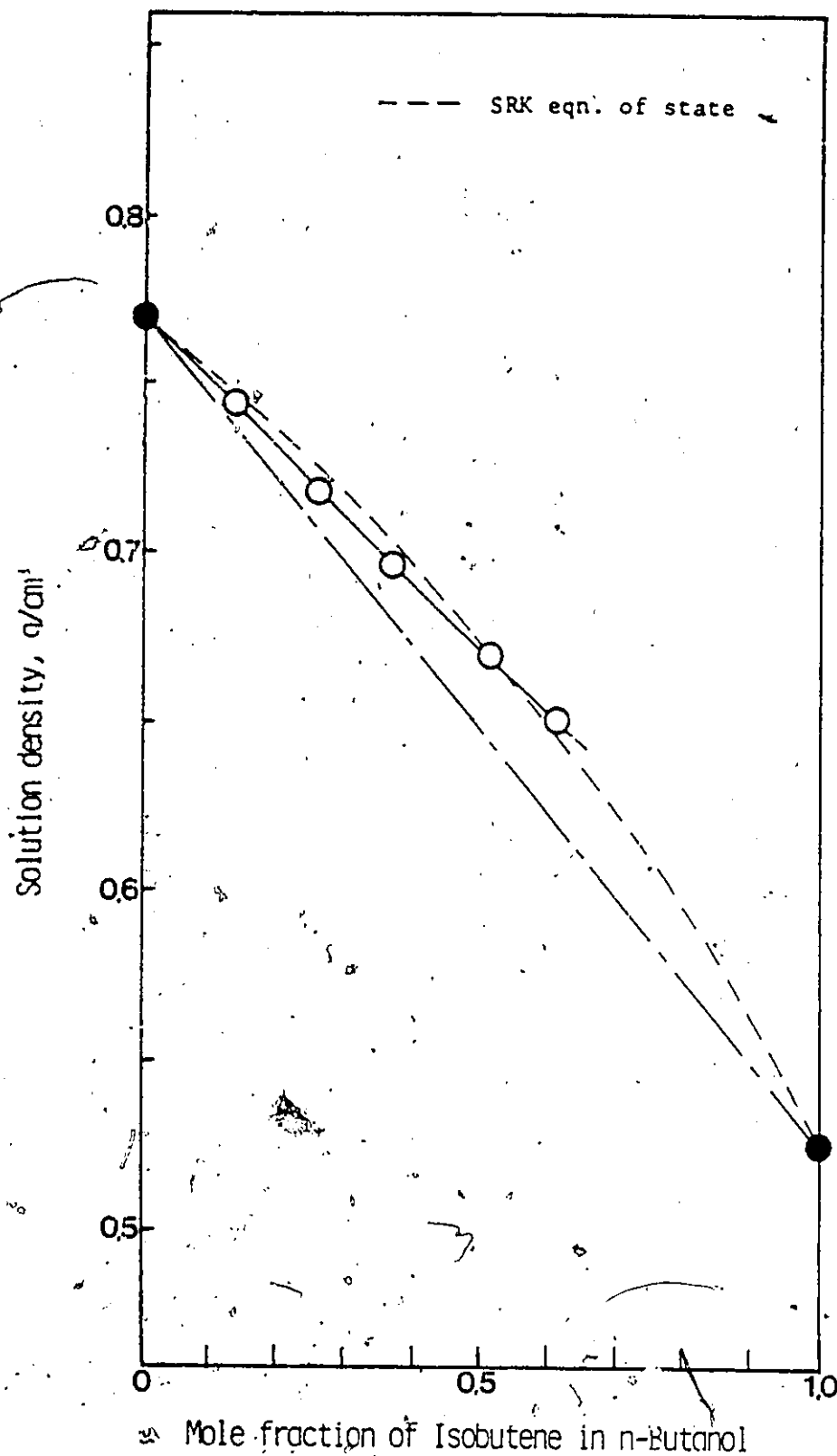


Figure D-17. Experimental and predicted densities of isobutene-saturated n-butanol solutions at 343.15 K as a function of isobutene concentration in the solution.

Appendix E

Sample calculation for the determination of gas solubility on the basis of gas chromatographic analysis of gas-saturated solutions.

Sample calculation for the gas chromatographic determination of solubility will be illustrated for the (1)n-octane-(2) propene system at 298.15 K and 1013.25 kPa.

Gas chromatographic analysis of the vaporized propene-saturated n-octane solution was repeated three times. The area ratios resulting from the three analyses are as follows:

- (1) Area ratio:  $83.06/16.94=4.903$
- (2) Area ratio:  $82.97/17.03=4.872$
- (3) Area ratio:  $83.01/16.99=4.886$

By means of the calibration line as shown in Figure 5-8, these three area ratios are immediately converted to the mole fraction ratios:

- (1) Mole frac. ratio:  $(2.054)(4.903)=10.07$
- (2) Mole frac. ratio:  $(2.054)(4.872)=10.01$
- (3) Mole frac. ratio:  $(2.054)(4.886)=10.04$

Then, by means of Equation (5-5), these mole fraction ratios are converted to the solubilities of propene in n-octane at 298.15 K and 1013.25 kPa:

- (1) Solubility: 0.9097
- (2) Solubility: 0.9091
- (3) Solubility: 0.9094

Finally, by taking the average of these three solubilities, the solubility to be obtained results in :

Solubility of propene in n-octane  
at 298.15 K and 1013.25 kPa = 0.909

Appendix F

Estimated precision for the measurements  
conducted in this investigation.

- (1) Density measurements of pure solvents at atmospheric pressure.

The precision for the density measurement at atmospheric pressure is estimated to be  $\pm 0.0002$  g/cm<sup>3</sup>. As mentioned in Chapter 6, this precision results from the fact that the densities of n-octane precisely determined by Chappelow, Winnick et al. and those of this investigation agreed within this accuracy.

- (2) Solubility measurements at atmospheric pressure.

The apparatus is designed and operated such that the factors which lead to erroneous measurement as pointed out by Cook and Hanson can be thoroughly avoided. The precision for the measurement is estimated to be 1.0% corresponding to the experimental error.

- (3) Density measurements of gas-saturated solutions at elevated pressures.

It is shown in Appendix C that when the measured densities were fitted with pressure the absolute average percent deviations of the experimental values from the smoothed lines were usually much less than 1.0%. Considering also the fact that reproducibility was always less than 0.5% the precision for the measurement is estimated to be within 2.0%.

- (4) Volumetric solubility measurements at elevated pressures.

As indicated in the data reduction for the solubility measurements at elevated pressure, the partial pressure of solvent in the vapor phase is assumed negligibly small. This assumption is justified when the measurements are performed utilizing non-volatile solvents at low temperature and high pressure. It is also indicated that the volume correction of solute gas utilizing gas-saturated solution volume is necessary. When the measurements are conducted for the systems of high solubility under appropriate experimental conditions and the volume correction is made for the solute gas volume the overall precision is estimated to be within 2.5%.

- (5) Solubility based on the gas chromatographic analysis of gas-saturated solutions.

The consistent results were obtained for the systems investigated, as shown in Tables 6-34 and 6-35. When careful sampling is made the estimated precision is 2.5%.